THE UNIVERSITY OF
SYDNEY

Enhanced metabolic engineering of lipid biosynthesis in leaves and seeds with the use of viral silencing-suppressor proteins

A thesis submitted in fulfilment of the requirements for the degree of Doctor of Philosophy in the Faculty of Science at The University of Sydney.

Fatima Naim

March 2014

Certificate of Authorship

The research described in this thesis was conducted at CSIRO Plant Industry and The University of Sydney between February 2010 and May 2013. I hereby declare that this thesis is my own work and to the best of my knowledge it does not contain material previously published or written by another person unless otherwise referenced.

Acknowledgements

The accomplishment of this PhD thesis has been the hardest and the most rewarding time of my life. I am thankful to my supervisors Craig Wood and Peter Waterhouse for their support throughout this project. Craig, you are the teacher who made it is easy for me to move into plant molecular biology. Your passion for science and easy going attitude are what made plant science fun. You are a great person and I will forever cherish our friendship. Peter and Craig, you are both masterminds and I feel so lucky to have worked with you.

I have had a great team of wonderful people behind me. Firstly I thank my family, both immediate and distant, whom I am always in contact with. Mum and Dad, you have worked hard throughout your lives so that your children could achieve their dreams and succeed in whatever they wanted in life. If it wasn't for your open-mindedness and the value you gave to education, I would have never grown out of my upbringing in the strict conditions of Kabul and Peshawar. My grandfather, my hero, I always look forward to telling you about my lab adventures and the status of my experiments. Our discussions are always very motivating and we need grandmother to bring us back to reality. My best friends – Naim, Sara, Mustafa, Asma, Louisa, Raheel, Bob, Salma and Walid – you are the joy in my life. Thank you for unconditional love and support.

The team at CSIRO Plant Industry Oils group, you were my second family in Canberra and I miss every one of you. Thank you to Cheryl for helping me throughout the project. Your tight regulation of the growth space made the lipid analyses data very reliable. Thank you to Luch, Pushkar, Xue-Rong, Srinivas, Anne, Ammu, Anu, Lijun, Qing, Fahim, Nathalie, Geraldine, Shoko and Uday for teaching me many experimental techniques over the years. Thank you to Surinder for the valuable discussions and the fun Christmas parties at your place. Thank you to Wendy and Lucy for making lab life easier. Thank you to Ben for chats and other life-related tips, Elena for teaching me so much in such a small amount of time, Kenlee and Osama for your help with bioinformatics, Nicole for being a great summer student, Alec and Alex for your help with data analysis, and CSIRO OCE for funding this project.

Finally thank you to the love of my life for being a wonderful life partner. Changing cities and writing this thesis in Brisbane was rather stress-free thanks to you by my side – looking

out for me, looking after me and building that strong support behind me. Life is wonderful with you.

Presentations and Publications

Naim, F., Belide, S., Shreshtha, P., Singh, S.P., Waterhouse, P.M. and Wood, C.C. (2014). The use of potent viral silencing-suppressor proteins to prolong and enhance transgene expression in five generations of transgenic *A.thaliana* and *B.napus*. Metabolic Engineering (to be submitted).

Naim, F., Zwart, A.B., Wood, C.C. (2014) Statistical design and analysis of large metabolite datasets generated from transient leaf assays in *N.benthamiana* leaves. Plant Methods (to be submitted).

Wood, C.C., **Naim, F.**, Singh, S.P., Okada, S. (2013) Production of dihydrosterculic acid and derivatives thereof. International Patent WO 2013/096992 A1.

Wood, C.C., **Naim, F.**, Singh, S.P. (2013) Simultaneous gene silencing and suppressing gene silencing in the same cell. International Patent WO 2013/096992 A1.

Naim, F. (2013) Successful RNAi silencing in plants 'Pure' oils in safflower for the industry, Speaker at the RNAi Science Strategy Workshop, Canberra Australia.

Naim, F., Nakasugi, K., Crowhurst, R.N., Hilario, E., Zwart, A.B., Hellens, R.P., Taylor, J.M., Waterhouse P.M., and Wood, C.C. (2012) Advanced engineering of lipid metabolism in *Nicotiana benthamiana* using a draft genome and the V2 viral silencing-suppressor protein. PLoS ONE *7*, e52717.

Naim, F., Wood, C.C., (2012) Advanced metabolic engineering of lipid pathways in *Nicotiana benthamiana* leaves using V2 and a draft genome assembly. Speaker at the International Symposium on Plant Lipids, Seville Spain.

Table of contents

List of Tables

List of Figures

Abbreviations

Abbreviation	Explanation
16:0	palmitic acid
16:2	hexadecadienoic acid
16:3	hexadecatrienoic acid
18:0	stearic acid
18:1	oleic acid
18:2	linoleic acid
18:3n3 or 18:3	linolenic acid
18:3n6 or GLA	γ-linolenic acid
18:4 or SDA	stearidonic acid
20:2n6 or EDA	eicosadienoic acid
20:3n6 or DGLA	dihomo-γ-linolenic
20:4n6 or 20:4 or AA	arachidonic acid
20:5n3 or 20:5 or EPA	ecosapentaenoic acid
22:6 or DHA	docosahexaenoic acid
2D TLC	2-dimensional thin layer chromatography
A.thaliana	*Arabidopsis thaliana*
A.tumefaciens	*Agrobacterium tumefaciens*
AA	arachidonic acid
ABC	ATP-binding cassette
acetyl-CoA	acetyl-coenzyme A
ACP	acyl carrier protein
AGO	argonuate
amiRNA	artifical miRNA
B.napus	*Brassica napus*
bp	base pair
C.elegans	*Caenorhabditis elegans*
C.tinctorius	*Carthamus tinctorius*
CaMV	*Cauliflower mosaic virus*
CHS	chalcone synthase
CMV	*Cucumber mosaic virus*
CoA	Coenzyme A
CPEFA	cyclopropenated fatty acids
CPFA	cyclopropane fatty acid
CPFAS	cyclopropane fatty acid synthase
CPT	cholinephosphotransferase
D.melanogaster	*Drosophila melanogaster*
DAG	diacylglycerol
DCL	dicer-like protein
DCM	dichloromethane
DGAT	diacylglycerol acyltransferase
DGD1	digalactosyldiacylglycerol synthase
DGDG	digalactosyldiacylglycerol
DHSA	dihydrosterculic acid or cis-9,10-methyleneoctadecanoic acid
DNA	deoxyribonucleic acid
dNTP	deoxynucleoside triphosphate
dpi	days post infiltration
DRB4	dsRNA binding protein4

dsRNA	double-stranded RNA
E.coli	*Escherichia coli*
EDTA	ethylenediamine tetra-acetic acid
EF1α	elongation factor 1-α
FAB2	fatty acid biosynthesis 2
FAD	fatty acid desaturase
FAE	fatty acid elongase
FAH	fatty acid Δ12-hydroxylase
FAME	fatty acid methyl ester
FAS	fatty acid synthase
FAT	acyl-ACP thioesterase
FP1	truncated napin promoter
G.hirsutum	*Gossypium hirsutum*
G3P	glycerol-3-phosphate
GAPDH	glyceraldehyde 3-phosphate dehydrogenase
GC	gas chromatography
GC-MS	GC-mass spectrometry
GFP	green fluorescent protein
GFiP	The ORF of GFP modified to include an intron
GLA	y-linolenic acid
GPAT	glycerol-3-phosphate acyltransferase
GUS	β-glucuronidase
GW	glycine/tryptophan
HA	hemagglutinin
Hc-Pro	helper component protease
HEN1	methyltransferase that adds a 2'-O-methyl group at the 3'-end of sRNAs
hpAtCHS	hpRNA targeting *A.thaliana* CHS
hpGFP	hpRNA against GFP
hpRNA	hairpin RNA
I.galbana	*Isochrysis galbana*
IPTG	isopropyl-β-D-thiogalactoside
IR-PTGS	inverted repeat - posttranscriptional gene silencing
KAS	ketoacyl-ACP synthase
kb	kilobase-pairs
kDa	kilo dalton
L.chinensis	*Litchi chinensis*
LACS	long-chain acyl-CoA synthetase
LB	Luria-Bertani medium
LCPUFA	long chain poly-unsaturation fatty acid
LEC	leafy cotyledon
LPA	lysophosphatidic acid
LPAAT	lysophosphatidic acid acyltransferase
LPC	lyso-PC
LPCAT	lyso-phosphatidylcholine acyltransferase
LSD	least significant difference
MAG	monoacylglycerol
MGD	monogalactosyldiacylglycerol synthase
MGDG	monogalactosyldiacylglycerol
miRNA	micro RNA
MQ	mili-Q water
mRNA	messenger RNA

MS	Murashige-Skoog medium
N.benthamiana	*Nicotiana benthamiana*
N.tabacum	*Nicotiana tabacum*
natsiRNA	naturally antisense siRNA
NOS	nopaline synthase
NPTII	neomycin phosphotransferase
nt	nucleotide
ORF	open reading frame
PA	phosphatidic acid
PAP	phosphatidate phosphatase
PC	phosphatidylcholine
PCR	polymerase chain reaction
PDAT	phospholipid:DAG acyltransferase
PDCT	PC:DAG phosphocholine transferase OR Phosphatidylcholine diacylglycerol cholinephosphotransferase
PDHC	pyruvate dehydrogenase complex
PE	phosphatidylethanolamine
pFN045	AA+GFiP+P0^{PE}
pFN046	AA+GFiP+p38
pFN047	AA+GFiP+p19
pFN048	AA+GFiP+35S:V2
pFN049	AA+GFiP+V2
pFN050	AA+GFiP
PLA	Phospholipase A
PLD	Phospholipase D
Pol IV	RNA polymerase IV
PTGS	post transcriptional gene silencing
PUFA	polyunsaturated fatty acid
qRT-PCR	quantitative real time - PCR
R.communis	*Ricinus communis*
RdDM	RNA directed DNA methylation
RDR	RNA dependant RNA polymerase
RdRP	RNA dependant RNA polymerase
RISC	RNA-induced silencing complex
RNA	ribonucleic acid
RNAi	RNA interference
RNase	ribonuclease
RNAseq	RNA sequencing
ROD1	reduced oleate desaturation 1
rpm	revolution per minute
RT	room temperature
RT-PCR	reverse transcriptase polymerase chain reaction
S.chilense	*Solanum chilense*
S.foetida	*Sterculia foetida*
S.lycopersicum	*Solanum lycopersicum*
SAD	stearoyl-ACP desaturase
S-Ado-Met	S-adenosyl-L-methionine
SDS	sodium dodecyl sulphate
SE	serrate
SED	standard error of differences
SGS3	Suppressor of gene silencing 3

siRNA	small interfering RNA
S-PTGS	sense-strand PTGS
ssDNA	single-stranded DNA
ssRNA	single-stranded RNA
TAG	triacyglyceride
TAIR	The Arabidopsis Information Resource
tasiRNA	trans-acting siRNA
TBST	*Tomato bushy stunt virus*
TCV	*Turnip crinkle virus*
T-DNA	transfer DNA
TE	Tris-EDTA
TGD	trigalactosyldiacylglycerol synthase
TGS	transcriptional gene silencing
TLC	thin layer chromatography
TLCJV-A	*Tomato leaf curl Java virus-A*
TMV	*Tobacco mosaic virus*
TRV	*Tomato ringspot virus*
TuMV	*Turnip mosaic virus*
TYLCV	*Tomato yellow leaf curl virus*
V.fordii	*Vernicia fordii*
VIGS	virus-induced gene silencing
VLCFA	very long chain fatty acids
vsiRNA	viral-induced siRNA
VSP	viral silencing-suppressor protein
X-gal	5-bromo-4-chloro-3-indoyl-β-D-galactopyranoside
ω-3	omega-3
ω-6	omega-6

Abstract

The use of transgenic pathways is a cornerstone of basic and applied research into plant biology. However, transgenes can fail over time and obtaining elite plant materials that perform well over numerous generations is an intensive process. Such failures in transgene performance are associated with the generation of small RNA (sRNA) in the host plant that trigger silencing. This mechanism is related to host defence pathways against invading nucleic acids including those from viral genomes. To counteract this silencing mechanism, plant viruses have evolved and encode for viral silencing-suppressor proteins (VSP) to block the silencing machinery of the host. This thesis tests the hypothesis that VSPs are also capable of enhancing transgene performance in stably-transformed plants. The effects of a number of VSPs on transgenic pathways were assessed transiently in *Nicotiana benthamiana* leaves and in long-term population studies spanning five and four generations in *Arabidopsis thaliana* and *Brassica napus* seeds, respectively. Overall this study shows that VSPs are able to enhance the performance of transgenic pathways in both leaves and seeds.

The transient leaf assay in *N.benthamiana* leaves is a well-established tool and allows a rapid examination of transgenic pathways in a short period of time. One limitation of the assay format is an inability to both silence endogenous pathways and permit maximal overexpression of transgenes. This study demonstrates extensive manipulation of lipid pathways in *N.benthamiana* leaves by introducing an alternative VSP, V2, which stops the co-suppression of transgenes and allows simultaneous silencing of endogenes. A combination of V2, silencing of *NbFAD2* and overexpression of *GhCPFAS* and *AtDGAT1* resulted in high levels of a novel fatty acid, dihydrosterculic acid, in leaf oil. The V2-based assay was used to silence *NbFAD7* and shunt linoleic acid into a three step transgenic pathway to synthesise arachidonic acid (AA), an ω-6 long chain polyunsaturated fatty acid (LCPUFA). Lipid head group fractionations of infiltrated leaf extracts showed that leaf cells rapidly shuffle novel fatty acids between various soluble and membrane-bound lipid pools. The assay was also used to investigate the effect of silencing a number of key lipid biosynthesis genes which included *NbSAD1*, *NbFATA*, *NbFATB*, *NbFAD3*, *NbFAD6*, *NbLPCAT*, *NbGPAT9*, *NbLPAAT4* and *NbLPAAT6* on lipid fluxes in *N.benthamiana* leaves.

Various VSPs were co-expressed with a three step transgenic pathway for the synthesis of AA in *A.thaliana* and *B.napus* seeds. The expression of the VSP was limited to oil synthesis in the seed and in *A.thaliana* the results showed that transgenic populations co-expressing V2

or p19 contained higher levels of AA. A p19 line contained 40% of AA in T3 seeds although such high levels came at the expense of oil content. Similar constructs were also transformed into *B.napus*. Unlike *A.thaliana*, *B.napus* displayed a bottleneck in AA biosynthesis at an intermediate step, indicating differences in the biochemical capacity of *B.napus* and *A.thaliana* for the production of LCPUFA.

Finally, a range of resources and experiments were designed for the characterisation of V2 protein. These resources resulted in the production and verification of a polyclonal antibody recognising V2. The experiments were aimed at quantifying V2 protein in various transgenic plant materials to assess the role of V2 in inhibiting co-suppression of transgenes however, the results were not conclusive.

Chapter 1 Literature Review

1.1 Introduction

This chapter provides a brief overview of a number of fundamental areas of plant biology that this research concerns. These areas include lipid metabolism and metabolic engineering of lipid pathways in plants, sRNA biogenesis and RNA silencing and VSPs.

Metabolic engineering of oil seed crops for food and biofuels is an expanding area of research. Lipid metabolism in plants leads to a number of end points, including energy storage and intermediates used by important cellular pathways. A thorough understanding of plant lipid biosynthesis is required to successfully manipulate lipid pathways in plants. This chapter presents an overview of plant lipid metabolism with an emphasis on the genetic engineering of plants to produce novel and LCPUFA.

sRNA metabolism is a general term used to describe many complex pathways involved in plant defence against viruses, transposons and transgenes, as well as regulation of development and maintenance of chromatin integrity. Two major failures of metabolic engineering are the gradual messenger RNA targeted degradation (post-transcriptional gene silencing) and DNA methylation (transcriptional gene silencing) of transgenes. This chapter also provides an overview of sRNA silencing pathways in plants with a focus on transgene silencing in both transient and stable systems.

1.2 Lipid metabolism in plants

Lipids are an essential component of all plant cells and play various roles in different plants. Fatty acids are a major form of carbon storage in the seeds of many plant species and are required for the synthesis of cuticular wax on the surface of many plants that provides protection against pathogen attacks, while also reducing water loss. Some fatty acids are also associated with hormone-related stress responses in plants. Therefore lipid processing enzymes are responsible for regulating a number of key cellular processes.

Triacylglycerides stored in seed oils are also an important source of fatty acids for human nutrition, therefore it is essential to understand the processes involved in the synthesis of oil in the seed in order to manipulate the pathways for increased yield.

Metabolic engineering of lipid pathways in plants for the synthesis of novel fatty acids and industrial oils is an emerging area of research as plant lipids are suitable replacements both for mineral oils and industrial feedstocks. The successful metabolic engineering of lipid pathways is dependent on an extensive understanding of the processes and enzymes involved in lipid biosynthesis and lipid trafficking between the membranes. This section provides an overview of fatty acid biosynthesis, lipid modification and transport, and the enzymes in the plant cell involved in these processes. Although lipid metabolism is a broad area of research, this section provides a brief summary of major lipid modification and transport processes. To emphasise the importance and sophistication of lipid biosynthesis, a number of novel fatty acids which are naturally synthesised in plants and micro-organisms are also reviewed.

1.2.1 Fatty acid synthesis and export out of the plastid

The processes and enzymes involved in the biosynthesis of 16 or 18 carbon-chains are relatively complex in plants when compared to other eukaryotes. Essentially all acyl chains are synthesised in the plastid and assembled on the acyl carrier protein (ACP) (Ohlrogge and Browse, 1995; Ohlrogge et al., 1979). This *de novo* synthesis is essential for membrane and storage lipids.

The building block of fatty acid synthesis is acetyl-coenzyme A (acetyl-CoA) which is generated by pyruvate dehydrogenase complex (PDHC). In the fatty acid synthase (FAS)

cycle there are four reactions catalysed by diverse enzymes (condensation, reduction, dehydration and reduction) and these reactions elongate the acyl chain by two carbons. These cycles are repeated seven times, at which point 16:0-ACP is generated as a final product. During these cycles condensation reactions are catalysed by ketoacyl-ACP synthase (KAS) III (first cycle) and KASI (remaining six cycles). Reduction, dehydration and reduction reactions are catalysed by ketoacyl-ACP reductase, hydroxyacyl-ACP dehydrase and enoyl-ACP reductase respectively. The fatty acid biosynthesis pathways result in the production of saturated fatty acids, however >75% of fatty acids found in most plant tissues are unsaturated fatty acids (Ohlrogge and Browse, 1995).

The final product of FAS (16:0-ACP) is either hydrolysed by an acyl-ACP thioesterase and released into the cytoplasm as 16:0-CoA or further elongated to 18:0-ACP by KASII which is then desaturated to 18:1-ACP by stearoyl-ACP desaturase (SAD). There are two plastidic fatty acyl-ACP thioesterases, FATA & FATB. These thioesterases hydrolyse the acyl group from acyl-ACP and free fatty acids are then available for export into the cytoplasm (Andrews and Keegstra, 1983). The roles of FATA and FATB are important in transportation of fatty acids out of the plastid – FATB is responsible for hydrolysing 16:0-ACP and 18:0-ACP whereas FATA hydrolyses 18:1-ACP. One of the possible functions of acyl thioesterases might be to maintain a balance for the incorporation of saturated and desaturated fatty acids into membranes (Bonaventure et al., 2003). The removal of the ACP from acyl-ACP results in termination of fatty acid elongation in the plastid, thus the thioesterases have many regulatory roles in the plastid (Ohlrogge and Browse, 1995).

The enzymes responsible for the formation of acyl-CoA on the outer envelope of the plastid are called long-chain acyl-CoA synthetases (LACS). There are nine *LACS* genes in *A.thaliana* and single or multiple mutations in these genes did not show a dramatic change in fatty acid biosynthesis, therefore the molecules involved in the export of fatty acids out of the plastid are yet to be unravelled (for a review of this, see Chapman and Ohlrogge 2012). There are studies which point toward ABC transporters (Koo et al., 2004), however more evidence is required to support the proposed mechanisms and the enzymes involved. Fatty acids diffuse in the cytosol with the aid of soluble carriers such as CoA.

For a summarised schematic of the fatty acid synthesis in the plastid, see Figure 1.1. For detailed descriptions of the processes and molecules involved in fatty acid synthesis and

export, see chapter “Acyl-Lipid Metabolism” in “The Arabidopsis Book” (Li-Beisson et al., 2013).

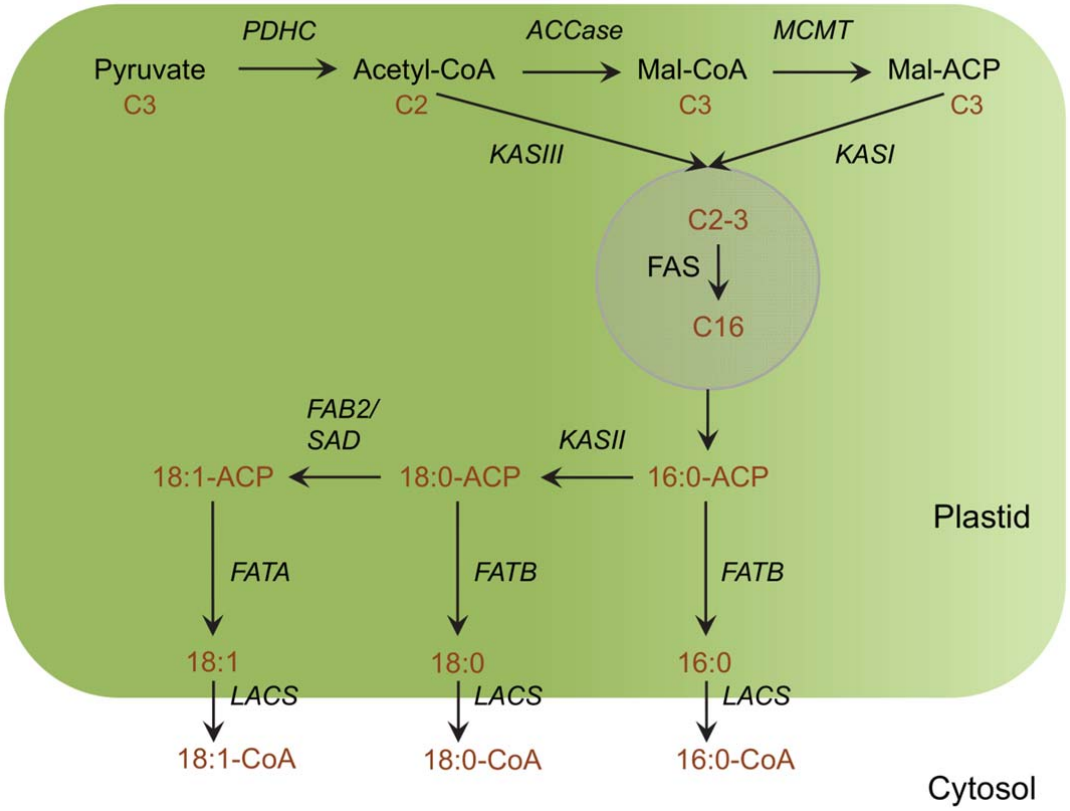

Figure 1.1. Schematic of fatty acid synthesis in the plastid and enzymes involved in the export of acyl groups out of the plastid.

This schematic is a brief representation of fatty acid synthesis cycle in the plastid.

1.2.2 Lipid trafficking between the endoplasmic reticulum and the plastid

There are two distinct pathways (prokaryotic and eukaryotic) reported for the assembly of lipids critical in chloroplast membrane synthesis (Carlson et al., 1993; Li-Beisson et al., 2013; Roughan et al., 1980; Roughan and Slack, 1982). The prokaryotic pathway refers to the synthesis of lipids in the chloroplast, whereas the eukaryotic pathway involves modification of lipids in the endoplasmic reticulum (ER) and transfer of some lipids back to the chloroplast for assembly of thylakoid membranes (Li-Beisson et al., 2013). The contributions of prokaryotic and eukaryotic pathways to lipid formation vary in different plant species, however labelling assays have revealed that they are relatively equal in *A.thaliana* (Browse et al., 1986; Mongrand et al., 1998; Xu et al., 2005).

The plant cell chloroplast accounts for approximately 70% of total cell membranes and is enclosed by two envelopes, one outer and one inner (Block et al., 1983; Dörmann and Benning, 2002). Galactoglycerolipids constitute approximately 80% of the chloroplast membranes and play an important role in photosynthesis (Block et al., 1983; Wang and Benning, 2012). The two major galactolipids in the chloroplast are MGDG (monogalactosyldiacylglycerol) and DGDG (digalactosyldiacylglycerol).

Chloroplastic lipids are assembled at the chloroplast envelope membranes and on the ER (Wang and Benning, 2012). Lipid assembly in the chloroplast involves incorporation of fatty acids into PA (phosphatidic acid) at the inner plastid envelope. Phosphatidate phosphatase (PAP) dephosphorylates PA into DAG and MGD1 (major MGDG synthase) has been shown to use DAG as a substrate to synthesise the most abundant galactolipid, MGDG, on the inner envelope of chloroplast (Muthan et al., 2013; Xu et al., 2005).

The eukaryotic pathway involves formation of PA from the fatty acids synthesised and exported out of the chloroplast, and their subsequent incorporation into phospholipids in the ER (Xu et al., 2005). These fatty acids are further modified in the ER. The fatty acids required for biosynthesis of thylakoid lipids enter the plastid from ER either as PA or PC (phosphatidylcholine). Phospholipase D (PLD) is required for conversion of PC to PA on the outer chloroplast envelope, which is followed by incorporation of PA into MGDG, similar to the prokaryotic pathway (Xu et al., 2005). MGDG is also a substrate for synthesis of DGDG on the outer chloroplast envelope by the DGD1 (major DGDG synthase) enzyme (Xu et al., 2005).

MGDG and DGDG are used for the assembly of thylakoid membrane, therefore the central metabolite and enzyme required for assembly of thylakoid lipids are PA and PAP respectively. However, the relative percentage of PA in the polar lipids is low in *A.thaliana,* suggesting that it is converted to other lipid forms rapidly (Xu et al., 2005).

Xu et al. (2005) showed that *A.thaliana* TGD1 is involved in recycling of TAG and PA for synthesis of thylakoid lipids in the chloroplast. MGDG synthesis was impaired in *tgd1* mutants due to accumulation of PA, which is incorporated into DAG for MGDG synthesis (Xu et al., 2005). The loss of TGD1 function in *A.thaliana* resulted in high incidence of embryo lethality emphasising its importance in thylakoid lipid biosynthesis. The developing seeds of *tgd1* mutants contained a relatively low amount of galactolipids and increased levels of PC when compared to wild-type developing seeds (Xu et al., 2005).

1.2.3 Oil synthesis in the seed

In eukaryotes, oil is synthesised through two major pathways: the glycerol-3-phosphate (G3P) and the monoacylglycerol (MAG) pathways. DAG is an intermediate of both these and is modified by diacylglycerol acyltransferase (DGAT) to form TAG (Parthibane et al., 2012). Addition of a third acyl group converts DAG to TAG and replacement of the head group gives rise to the different polar lipids, including galactolipids and phospholipids (Muthan et al., 2013).

Although all acyl chains are produced in the plastid, in an oilseed the majority of the lipids (>95%) are used for synthesis of glycerolipids (Ohlrogge and Browse, 1995). Free fatty acids, which are exported out of the plastid envelope and activated to acyl-CoA (Andrews and Keegstra, 1983) are then available for further modification in the ER. The acyl-CoA are preferably incorporated into the production of PC which, in comparison to other phospholipids such as PE (phosphatidylethanolamine), is found in abundance in leaves and seeds (Bonaventure et al., 2004; Slack et al., 1978).

In plants, the classical view of oil synthesis involves the biosynthesis of fatty acids in the plastid, their subsequent export into the cytosol and their assembly onto the *sn*-1, *sn*-2 and *sn*-3 positions of the glycerol molecule via the Kennedy Pathway (Vanhercke et al., 2013). In the seed TAG molecules are enclosed by oleosins into oil bodies and these oil bodies serve as energy storage for germination of the seed. These spherical intracellular organelles are

referred to as oleosomes or oil bodies (Parthibane et al., 2012). As oilseeds with high oil content generally have more oleosins, which emphasises the importance of oleosins in oil accumulation in the seed (Tzen et al., 1993).

1.2.3.1 The Kennedy pathway – de novo *assembly of TAG*

De novo assembly of TAG involves the incorporation of acyl-CoAs into G3P and this is referred to as the Kennedy pathway. The sequential esterification of G3P to synthesise TAG involves four enzymatic steps: two acylation steps by *sn*-1 glycerol-3-phosphate acyltransferase (GPAT) and *sn*-2 lysophosphatidic acid acyltransferase (LPAAT), followed by dephosphorylation of PA by PAP to form DAG, and a final acylation step by DGAT to synthesise TAG (Bates et al., 2013).

A.thaliana encodes eight *GPAT*s. While the majority of these are involved in cutin, suberin and mitochondrial membrane lipid biosynthesis and pollen development, AtGPAT9 is a strong candidate for *sn*-1 acylation of G3P for *de novo* synthesis of TAG (Gidda et al., 2009). AtGPAT9 is highly homologous to mammalian GPAT, which is involved in the formation of storage oil and therefore it was proposed that, for plants, AtGPAT9 was also involved in oil synthesis (Gidda et al., 2009). Epitope tagging experiments have shown that AtGPAT8 and AtGPAT9 are localised in the ER (Gidda et al., 2009) and therefore it is possible that these two GPATs are also involved in TAG biosynthesis.

Plant LPAATs are involved in the second step of the Kennedy pathway and are essential for the production of PA, used for the production of membrane phospholipids and TAG in developing seed (Maisonneuve et al., 2010). A number of microsomal LPAATs were identified in developing rapeseed that are possibly involved in TAG synthesis (Maisonneuve et al., 2010). Overexpression of these LPAAT isozymes in *A.thaliana* resulted in an increase in total oil in *A.thaliana* seed (Maisonneuve et al., 2010). Five *LPAAT* genes are annotated in *A.thaliana* (Chapman and Ohlrogge, 2012). Although *LPAAT1*, *LPAAT2* and *LPAAT3* remain crucial for plant development, a homolog of *LPAAT2* identified in *B.napus* was shown to increase TAG accumulation in *A.thaliana* seeds (Maisonneuve et al., 2010). Overall LPAATs are not characterised very well due to lethality observed in *lpaat* mutants (Chapman and Ohlrogge, 2012).

PA is formed as a result of esterification of G3P by GPAT and LPAAT. This intermediate is converted to DAG by PAP, which is substrate for many other pathways (including TAG synthesis). PAP was first described in mammals and yeast and is essential in controlling the levels of PA available for synthesis of membrane phospholipids and TAG (Carman and Han, 2009). The yeast homologs of genes encoding for *PAP* were found in *A.thaliana* and referred to as *PAH1* and *PAH2* (Nakamura et al., 2009). Under phosphate starvation, *pah1* and *pah2* mutants showed growth defects and were not able to re-model membrane phospholipids (Nakamura et al., 2009). The *pah1pah2* double mutant showed a major effect on the eukaryotic pathway of galactolipid biosynthesis which was similar to observations in the *tgd1-1* mutant (Nakamura et al., 2009). The double mutant contained relatively low amounts of MGDG and it was proposed that PAH1/PAH2 are involved in the synthesis of DAG, which is used as substrate for the production of galactolipids (Nakamura et al., 2009). More importantly PC content approximately doubled and TAG decreased by approximately 15% in the double mutant (Chapman and Ohlrogge, 2012; Eastmond et al., 2010). The marginal decrease in TAG content suggests that *A.thaliana* encodes for other enzymes or back-up pathways which become active in the absence of PAH1 and PAH2.

Unlike GPATs and LPAATs, the plant DGATs are well characterised. *A.thaliana* encodes two *DGAT* genes: DGAT1, involved in TAG accumulation (Routaboul et al., 1999), and DGAT2, with an unclear role in TAG synthesis (Chapman and Ohlrogge, 2012). However the activity of DGAT2 has been associated with the accumulation of unusual fatty acids in TAG: *Ricinus communis* (*R.communis*) DGAT2 is involved in the accumulation of ricinoleic acid in *R.communis* endosperm (He et al., 2004) and activity of DGAT2 is also reported in *Vernicia fordii* (*V.fordii*) seed, which contains large amounts of eleostearic acid, a conjugated fatty acid (Shockey et al., 2006). DGAT1 and DGAT2 were also localised in different sub-domains of the ER in *V.fordii* (Shockey et al., 2006). Although *A.thaliana* encodes for two *DGAT* genes, *dgat1* mutants only show a 20–40% reduction in seed oil and no oil change was observed in *dgat2* mutants (Chapman and Ohlrogge, 2012). These results suggest that there are other mechanisms involved in TAG synthesis in the absence of DGAT1 and DGAT2 in *A.thaliana*.

1.2.3.2 The alternative pathway for the production of TAG

Recent *in vitro* and *in vivo* studies have shown that TAG synthesis in a number of plants is not dependent on the utilisation of acyl-CoA by the enzymes of the Kennedy pathway, but

rather by combinations of pathways which are more complex than the oil synthesis pathways initially recognised in plants (Chapman and Ohlrogge, 2012). For example, an acyl-CoA independent transacylase pathway in yeast and plants involves PDAT (phospholipid:DAG acyltransferase), which produces TAG using PC and DAG as substrates (Dahlqvist et al., 2000) (Fig 1.2). PDAT activity was related to the presence of unusual fatty acids fatty detected in a number of plants (Dahlqvist et al., 2000).

Another enzyme involved in the conversion of PC to DAG is PDCT (PC:DAG phosphocholine transferase), encoded by *ROD1* (*reduced oleate desaturation 1*) gene in *A.thaliana*. PDCT is responsible for the presence of unsaturated fatty acids in TAG and the *A.thaliana rod1* mutant showed a 40% decrease in the level of polyunsaturated fatty acids (PUFA) in TAG.

The continuous switch between TAG and phospholipid synthesis requires the presence of complex pathways to modulate the flow of intermediates accordingly. Recent *in vivo* studies have shown that there are two distinct DAG pools synthesised for the production of TAG and PC, for the conventional and alternative pathways of TAG biosynthesis respectively (Bates et al., 2009). Overall the presence of PC fraction is important for the utilisation of specific ER bound desaturases, which use PC as a substrate to catalyse the production of novel fatty acids. Therefore the alternative routes for the production of TAG ensure that PC pools containing novel fatty acids become part of seed storage lipids.

The nature of oil synthesis and accumulation is very complex due to the number of processes involved and becomes more so due to the presence of alternate enzymes and pathways in different plants.

1.2.3.3 Enzymes involved in the remodelling of the PC lipid pool

The rapid acyl editing that occurs in the ER involves the PC and acyl-CoA lipid pools. The acyl-CoA that enter the PC acyl-editing pool are directly transferred from the plastid rather than through the Kennedy pathway (Bates et al., 2007; Williams et al., 2000). In plants, a number of enzymes are involved in the acyl editing reactions. *In vitro* assays using microsomal preparations of developing *Carthamus tinctorius* (*C.tinctorius*) cotyledons have confirmed that LPCAT (lyso-phosphatidylcholine acyltransferase) and Phospholipase A (PLA) are involved in acyl editing of PC (Stymne and Stobart, 1984). As shown in Figure 1.2, LPCAT is able to catalyse the forward and reverse acyl-editing reactions of PC. PLA catalyses the

removal of an acyl group from PC to generate free fatty acids (into the CoA pool) and lyso-PC (LPC). LPCAT was shown to be one of the most active acyltransferases during TAG synthesis in *C.tinctorius* seed (Ichihara et al., 1995).

A.thaliana encodes for two *LPCAT* genes, both of which catalyse the acylation and deacylation of PC (Lager et al., 2013). Results showed that LPCATs are responsible for the presence of PUFA and hydroxyl fatty acids synthesised on PC in the CoA pool. The double *lpcat1/lpcat2 A.thaliana* mutant did not show a major decrease in the level of PUFA in seed oil, however a triple mutant of *lpcat1/lpcat2/rod1* showed a 66% decrease (Bates et al., 2012; Wang et al., 2012). These results are indicative of the complexity of the pathways and enzymes involved in the biosynthesis of TAG.

1.2.3.4 Transcription factors responsible for the activation of enzymes during oil synthesis in the seed

There are a number of transcription factors identified in *A.thaliana* that directly control the production of fatty acids for the assembly of TAG during seed maturation. *WRINKLED1* (*WRI1*) and *LEAFY COTYLEDON* (*LEC*) genes (*LEC1*, *LEC1-LIKE*, *LEC2* and *FUS3*) have been specifically associated with oil biosynthesis in *A.thaliana*. Constitutive expression of *LEC2* has also been shown to activate seed-specific promoters in the transient leaf assay (Petrie et al., 2010). *A.thaliana lec1*, *lec2* and *fus3* single mutants have decreased protein and oil accumulation (Harada, 2001). A dramatic 80% decrease in seed oil was measured in *A.thaliana wri1* mutant (Baud and Lepiniec, 2010; Cernac and Benning, 2004). This shows that transcription factors also play an important role in the accumulation of oil in the seed.

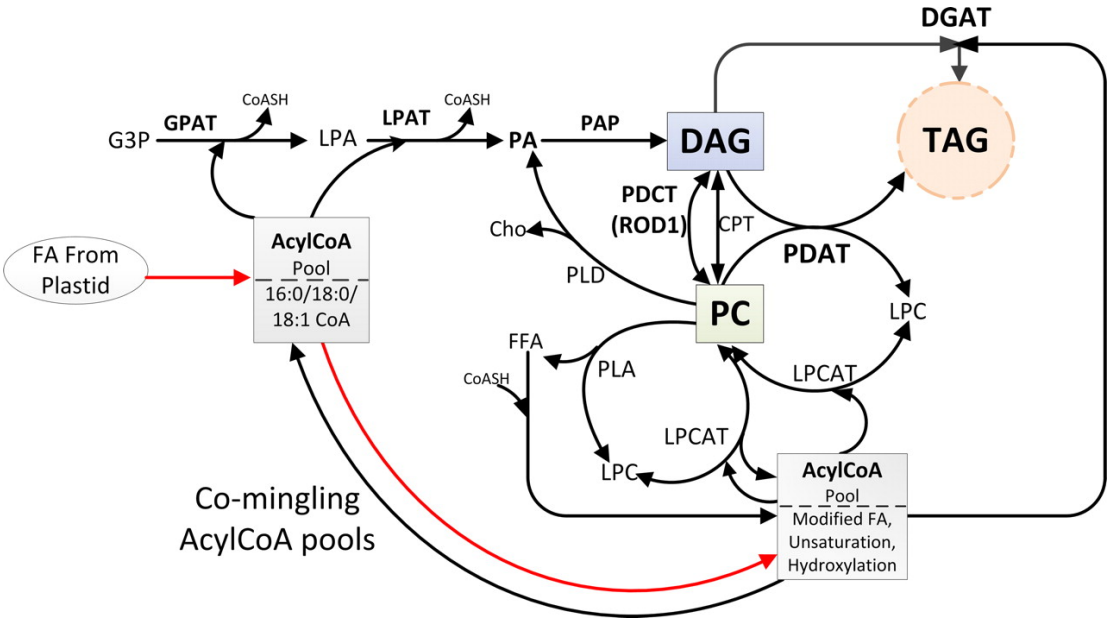

Figure 1.2. Figure adopted from Chapman and Ohlrogge (2012). A schematic of the complexity of TAG biosynthesis pathways in plants.

This schematic describes the conventional pathway for TAG biosynthesis involving acyl-CoA and G3P as starting substrates, which are modified by GPAT, LPAAT (LPAT), PAP and DGAT to synthesise LPA, PA, DAG and TAG respectively. The other unconventional pathways involve an intermediate of the Kennedy pathway, DAG, which is modified by PDCT or CPT (cholinephosphotransferase) to produce PC. PDAT modifies PC to produce TAG and LPC. Another enzyme, LPCAT, esterifies LPC with an acyl-CoA to form PC. PLD is also able to hydrolyse PC into PA which is recycled back into the Kennedy pathway. The acyl-CoA, including the unusual fatty acids that are modified in the ER, is esterified onto LPC by LPCAT to generate PC. Another enzyme, PLA is able to convert PC to LPC and release a free fatty acid. The reactions involving LPCAT, PDCT and CPT are reversible (Chapman and Ohlrogge, 2012).

1.2.4 Enzymes involved in desaturation and elongation of fatty acids

There are many other reactions which can also take place in the cytosolic compartment and plastid, including desaturation and elongation reactions. Desaturation is the enzyme catalysed reaction between an acyl group and dioxygen to generate an unsaturated acyl group and water. Monounsaturated fatty acids esterified to a glycerolipid are further desaturated by complex plant desaturases to produce PUFA. The plastidial and ER bound desaturases use monogalactosyldiacylglycerol and PC as their preferred substrates respectively. The soluble desaturases have consensus motifs comprised of carboxylates and histidine boxes. However the consensus motif found in the insoluble, membrane-bound desaturase is comprised of histidine boxes only (Shanklin and Cahoon, 1998). In the presence of diiron, the histidines coordinate the active site of the enzyme. The enzymatic functions of desaturases are reviewed in (Shanklin and Cahoon, 1998).

The five main fatty acids found in the glycerolipids of almost all plant membranes are 16:0, 16:3, 18:1, 18:2 and 18:3 (Ohlrogge and Browse, 1995). Seven classes of *A.thaliana* mutants, each lacking the activity of a specific desaturase, were studied and the observed phenotypes were associated with the lack of a particular step in lipid biosynthesis (reviewed by Wallis and Browse 2002). Membrane-bound desaturases have been difficult to extract, so mutant studies have proven to be the best way of analysing their activities. The key enzymes and their functions described include *A.thaliana* fatty acid desaturases such as AtSAD (18:0 to 18:1 desaturase), AtFAD2 and AtFAD6 (18:1 to 18:2 desaturases), AtFAD3, AtFAD7 and AtFAD8 (18:2 to 18:3 desaturases). *A.thaliana* also encodes for a number of condensing enzymes involved in fatty acid elongation, however this section will only focus on the function of *A.thaliana* FATTY ACID ELONGATION1 (FAE1), which elongates 18:1 to 20:1, 20:1 to 22:1 and 18:0 to 20:0.

1.2.4.1 Stearoyl-acyl-carrier-protein-desaturase

Stearoyl-acyl-carrier-protein-desaturase (SAD) is an enzyme, located in the plastid, which catalyses the desaturation of 18:0. It is a unique soluble desaturase, unlike other known desaturases which are found in membranes (Ohlrogge and Browse, 1995). SAD is a plastidial desaturase which introduces the first double bond to 18:0-ACP between carbon 9 and 10 to produce 18:1-ACP (Hsieh et al., 2009). This soluble enzyme is responsible for regulating the ratios of saturated and monounsaturated fatty acids (Ruxton et al., 2004) and a key

determinant of fatty acid desaturation (Hsieh et al., 2009). *A.thaliana* encodes seven SAD-like enzymes (Ruxton et al., 2004) and the original mutant discovered was referred to as *fab2* (fatty acid biosynthesis2). The function of one isozyme was not localised to the plastid (Ruxton et al., 2004).

Previous studies have shown that silencing of *AtSAD* resulted in an increase in 18:0 levels, which in turn resulted in an increased incorporation of 18:0 in membranes (Lightner et al., 1994). At normal growth temperatures, the van der Waals interactions between the saturates may have resulted in loss of membrane fluidity (Wallis and Browse, 2002). Consequently cell expansion was inhibited and the mutants were dwarfed (Lightner et al., 1994). The desaturation of 18:0 by SAD is also critical for biosynthesis of jasmonic acid, thus SAD plays a critical role in the defence-based signalling responses of the plant (Gibellini and Smith, 2010). In other cases silencing of SAD is beneficial, for example an increase in levels of stearic acid in soybean oil has been shown to be important due to its oxidative stability in oil (Clemente and Cahoon, 2009).

1.2.4.2 Fatty acid desaturases involved in desaturation of 18:1 to 18:2

Oleic acid is a major component of the monounsaturated fatty acids found in membrane glycerolipids in plants. It is a crucial component of plant lipid metabolism, yet its concentration in leaves is low, due to the high activity of FAD6 and FAD2 converting 18:1 into 18:2 (Okuley et al., 1994a). The presence of PUFA in plants is essential in maintaining plant responses against environmental factors, such as extreme temperatures and high salinity, as well as the regulation of plant defence pathways against various pathogen attacks (Browse and Somerville, 1991; Kirsch et al., 1997; Zhang et al., 2012). *A.thaliana* encodes for two 18:1 desaturases, *AtFAD2* and *AtFAD6*. A number of reports have shown, that in *A.thaliana*, oleic acid is involved in the jasmonic acid and salicylic acid related to defence mechanisms (Gibellini and Smith, 2010). The *fad2* and *fad6 A.thaliana* single mutants also lose photosynthetic ability due to the unavailability of PUFA (Wallis and Browse, 2002).

A.thaliana encodes for one plastidic *FAD6* gene (a 16:1/18:1 desaturase) and it has been shown that lipids 16:1 and 18:1 were desaturated by FAD6 to 16:2 (hexadecadienoic acid) and 18:2 respectively (Miquel and Browse, 1992; Wallis and Browse, 2002). AtFAD6 does not show specificity for acyl chain length nor the position at which it is attached in the

glycerol backbone (Wallis and Browse, 2002). The leaves of *A.thaliana fad6* mutant contained high levels of 16:1 and 18:1 and reduced levels of 16:3 and 18:3. Chloroplast development was also impaired in the *fad6* mutant at low temperatures (Wallis and Browse, 2002).

In comparison to other plant desaturases, the FAD2 gene family has been studied extensively in diverse plants. *A.thaliana* encodes for one FAD2 gene, an ER bound 16:1/18:1 desaturase. Removal of FAD2 activity in *A.thaliana* and *Nicotiana tabacum* (*N.tabacum*), by either mutagensis or hairpin RNA (hpRNA) mediated silencing, resulted in elevated levels of 18:1 in leaf lipid pools (Okuley et al., 1994a; Yang et al., 2006a). Unlike FAD6, FAD2 is highly selective for desaturating 18:1 esterified to PC lipid head group (Okuley et al., 1994a; Shanklin and Cahoon, 1998). There are also variants of FAD2 with diverse functions that catalyse the synthesis of novel fatty acids. FAD2 catalysed reactions include hydroxylation, epoxidation, acetylenation and conjugation (Cao et al., 2013). Unlike *A.thaliana*, other plant species such as soybean (Glycine max), *C.tinctorius* and *Gossypium hirsutum* (*G.hirsutum*) encode a two, eleven and four member *FAD2* gene family respectively (Cao et al., 2013; Heppard et al., 1996). The presence of large numbers of gene family members is indicative of the importance of the function of FAD2 in the synthesis of PUFA in plants. The double *fad2/fad6 A.thaliana* mutant, deficient in PUFA, was unable to grow in soil (Wallis and Browse, 2002).

1.2.4.3 Fatty acid desaturases involved in desaturation of 18:2 to 18:3

Unusually high levels of 16:3 (hexadecatrienoic acid) and 18:3 (α-linolenic acid) are measured in the chloroplast membranes of higher plants. The synthesis of PUFA is dependent on the desaturation of 16:2 and 18:2. *A.thaliana* encodes for two chloroplastic 16:2/18:2 desaturase isozymes, *AtFAD7* and *AtFAD8* (Wallis and Browse, 2002). *A.thaliana* also encodes for another 18:2 desaturase specific to the ER, *AtFAD3*. Both the chloroplastic and ER bound desaturases have highly conserved regions, indicating a possibility that both genes descended from a common ancestor (Iba et al., 1993).

The *fad7* mutant did not have any associated defects in growth or development (Iba et al., 1993). When *fad7* mutants were grown at 20^{o}C or lower the lipid profiles were similar to wild-type plants, however a difference was observed at higher temperatures (Iba et al., 1993). This difference was related to the presence of another chloroplastic desaturase

which was activated at lower temperatures. Mutating the *fad7* mutant to search for the second ω-3 chloroplastic desaturase resulted in the discovery of *AtFAD8* (McConn et al., 1994). FAD8 is involved in controlling the levels of PUFA (McConn et al., 1994). Interestingly, the leaves of *fad7* mutant did not contain 18:3 desaturated in the ER, suggesting that the majority of the 18:3 was transferred to ER from the chloroplast and that FAD7 and FAD8 were the main 18:3 desaturases (Iba et al., 1993; McConn et al., 1994). The activity of AtFAD7 is also inducible by light: the transcript level of the desaturase increased when the plants were moved from dark to white light (Park et al., 2002).

AtFAD6 and AtFAD7 have no preference for the length of the acyl chain, the position they are esterified to the glycerol backbone, or the lipid head group to which they are attached (Wallis and Browse, 2002). AtFAD2 and AtFAD3 only desaturate 18:1 and 18:2 respectively, which are esterified to PC, therefore desaturation of 16:1 and 16:2 only takes place in the glycerolipids of chloroplast (Browse and Somerville, 1991).

Although FAD3 is not as active as FAD7 in desaturating 18:2, it has been shown that *FAD3* gene product is present in *A.thaliana* root tissue and responsible for the desaturation of 18:2 in the root (Browse et al., 1993). Results also showed that FAD3 was responsible for desaturating 18:2 at an equivalent rate to FAD7, although this only occurred in leaf tissue from the emergence of *A.thaliana* until the onset of flowering (Browse et al., 1993).

1.2.4.4 Fatty acid elongation1

Very long chain fatty acids (VLCFA), such as 20:x and 22:x, are synthesised in the seeds of numerous plant species, including Brassicaceae (Kunst et al., 1992). They are primarily synthesised in the epidermal cells for their subsequent use in the synthesis of waxes. VLCFAs are not synthesised via the *de novo* pathway but rather by the addition of acetate units to the carboxyl end of 18 long carbon chains in the CoA pool (Kunst et al., 1992). The functions of elongases were studied in *A.thaliana* mutants that lacked VLCFA. All four mutants that contained altered levels of 20:1 had their mutations mapped to the *FAE1* (fatty acid elongase 1) locus (Kunst et al., 1992), confirming that the extension was dependent on the activity of FAE1. The levels of 20:0, 20:1 and 22:1 were altered in the *fae1* mutants, suggesting that the elongation system was not specific to the level of unsaturation in the 18:x acyl-CoA (Kunst et al., 1992). Therefore, *AtFAE1* encodes a condensing enzyme that catalyses the length extension of 18:x to 20:x and 22:x (Broun and Somerville, 1997; Millar

and Kunst, 1997). The activity of this microsomal elongase is limited to the seed, where it catalyses the addition of malonyl-CoA to 18:x fatty acids (Millar and Kunst, 1997). Although elongation of fatty acid chain length requires four enzymatic processes (a condensing enzyme, two reductases and one dehydrase), the ectopic expression of FAE1 yielded the same types of VLCFAs normally only made in the seeds, and the levels of FAE1 expression correlated with the levels of VLCFA products (Millar and Kunst, 1997). Based on these data you can say that FAE1 controls the chain length and amounts of the generated VLCFA products.

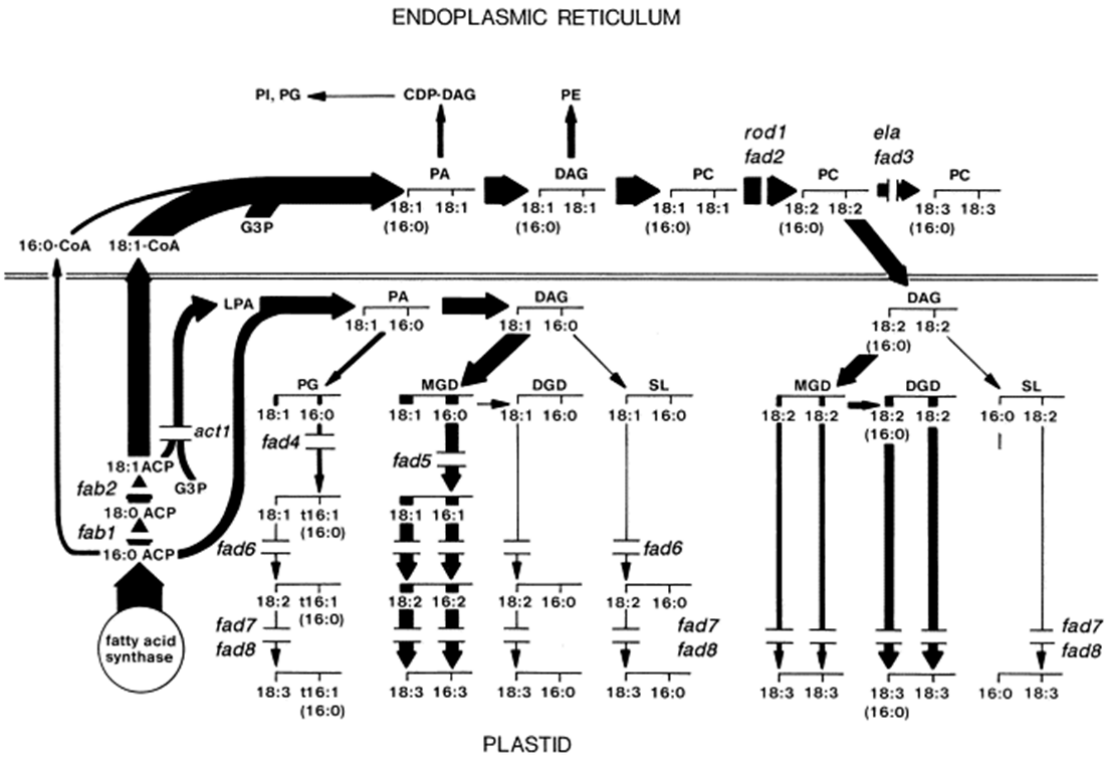

Figure 1.3. A classic schematic of the membrane glycerolipid biosynthesis.

This schematic is adopted from Browse and Somerville (1994). It shows the flow of acyl groups into either the plastidic or the ER bound desaturases. The thicknesses of the arrows are indicative of the relative fluxes. The breaks are associated with the lack of the activity of a putative enzyme in the corresponding *A.thaliana* mutant.

1.3 Metabolic engineering of lipid pathways

Metabolic engineering of crop plants to synthesise high levels of particular oils with nutritional value and/or industrial importance has been a challenge. Plant oils used for human consumption typically contain five main fatty acids: 16:0, 18:0, 18:1, 18:2 and 18:3. The modification of plant lipid metabolism for the synthesis of novel fatty acids provides alternate means for incorporating more nutritional fatty acids (otherwise obtained from other sources) and allows the synthesis of industrial fatty acids at a lower cost (otherwise sourced from petrochemicals). Examples of the metabolic engineering of lipid pathways for the accumulation of novel fatty acids are described here.

1.3.1 Novel fatty acids with value for industrial use

At least 300 different fatty acids have been found in plant lipids (Napier, 2007). Industrial oils generally contain fatty acids with an unusual functional group such as cyclopropane or cyclopropene ring(s), acetylenic or epoxy or hydroxyl groups. There are a number of plants that produce unusual fatty acids and many of these can be used for industrial purposes. However in most cases these fatty acids are not made in sufficient levels in the plant, which lowers the cost efficiency of oil extraction.

Plants that synthesise hydroxyl fatty acids are also well-studied. *R.communis* accumulates considerable amounts of ricinoleic acid in seed oil (90%) and this oil is used in industrial processes to produce plastics, surfactants, lubricants and cosmetics. However *R.communis* meal contains toxic compounds (ricin) which reduce the cost efficiency of the plant's industrial oil use. There would be great benefit from the identification of the gene responsible for the hydroxylation of oleic acid and subsequent cloning into a suitable oilseed crop: the hydroxylase responsible for the synthesis of ricinoleic acid is a microsomal enzyme that catalyses the hydroxylation of oleic acid esterified to PC (Bafor et al., 1991; Smith et al., 1992). However in *R.communis*, all rincinoleic acid was found in the TAG fraction and none in the PC, and this observation resulted in the discovery of other enzymes in *R.communis*, specialised in channelling ricinoleic acid from site of synthesis (PC) into TAG (Napier, 2007). This is a brief example of the complexity of the plant lipid metabolism involved in the synthesis of a novel fatty acid.

DHSA is another novel fatty acid and the enzyme system involved in the synthesis of DHSA-TAG has not yet been identified. DHSA is described in detail below.

1.3.1.1 Dihydrosterculic acid (DHSA): an unusual fatty acid produced from oleic acid on the sn-*1 position of PC*

It is well known that a variety of bacteria, protozoa and myripoda contain fatty acids that have a cyclopropane ring in their molecular structure (Sledzinski et al., 2013; Yu et al., 2011). Although the enzymes responsible for cyclopropanation have not been discovered in mammals, recent reports have shown that low levels of cyclopropanated fatty acids are also present in humans and mice (Sakurada et al., 1999; Sledzinski et al., 2013).

Cyclopropane fatty acids (CPFA) are identified by the presence of 3-carbon carbocyclic ring(s) in different positions of the fatty acid chain (Fig 1.4). The enzymes involved in the cyclopropanation of unsaturated fatty acids are known as cyclopropane fatty acid synthase (CPFAS) and have been identified in plants, bacteria and parasites (Yu et al., 2011). In plants, the major producers of CPFA related fatty acids include Malvaceae, Sterculiaceae, Bombaceae, Tilaceae, Gnetaceae and Sapindaceae (Badami and Patil, 1980; Ralaimanarivo et al., 1982; Vickery, 1980; Vickery et al., 1984). Seed-oil analysis of these plants revealed that a significant percentage is made up of CPFA. The highest relative percentage of CPFA was measured in *Litchi chinensis* (*L.chinensis*) seed-oil (Gaydou et al., 1993). There is high homology in the amino acid sequences of plant and bacterial enzymes involved in the synthesis of cyclopropane rings (Grogan and Cronan, 1997). The prokaryotic CPFAS have been extensively studied when compared to the equivalent enzymes encoded by plant species.

Furthermore CPFA are found in abundance in bacteria, while they are only are minor components of lipids in plants. In bacteria, the monoenoic fatty acids esterified to PE are cyclopropanated by CPFAS whereas in plants the reaction occurs on PC. The *Escherichia coli* (*E.coli*) CPFAS was the first cyclopropane ring-synthesising enzyme of known amino acid sequence to be studied (Grogan and Cronan, 1984). Characterisation of EcCPFAS revealed that the enzyme did not bind to phospholipids containing saturated fatty acids and that the saturated fatty acids were not able to stabilise the soluble cytoplasmic enzyme (Taylor and Cronan, 1979). The cytoplasm soluble EcCPFAS catalysed the addition of a methylene group from *S*-adenosyl-L-methionine (S-Ado-Met) to the *cis* double bond of an unsaturated

(monoenoic) fatty acid that was esterified to the membrane phospholipid (Grogan and Cronan, 1997). Successful cyclopropanation required the double bond to be positioned 9–11 carbons distance from the ester linkage to the glycerol backbone (Bao et al., 2003). Due to the enzyme's soluble nature, it was not clear if the enzyme was able to access its substrate in the hydrophobic region of the lipid bilayer of the membrane, or whether the removal of the acyl group from the membrane was necessary for subsequent cyclopropanation (Wang et al., 1992).

The preferable substrate for *Agrobacterium tumefaciens* (*A.tumefaciens*) CFPAS is also PC (Hildebrand and Law, 1964). Interestingly, the crystal structures of *Mycobacterium* CPFAS suggested that they preferably bind to acyl-ACP (Huang et al., 2002). In bacterial strains, the cyclopropanation generally occur at the *sn*-2 position of the phospholipid moiety (Hildebrand and Law, 1964). This observation was related to the presence of shorter chain unsaturated substrates at the *sn*-2 position and preference of CPFAS for these substrates (Grogan and Cronan, 1997). Labelling experiments in cell suspension cultures of tobacco expressing *Sterculia foetida* (*S.foetida*) *CPFAS* indicated that DHSA was exclusively associated with PC (Bao et al., 2003). These experiments have also shown that DHSA comprise 5% of PC fatty acids of which 91% are located on *sn*-1 and 9% on *sn*-2 position.

DHSA (*cis*-9,10-methyleneoctadecanoic acid) is a cyclopropane fatty acid (Fig 1.4) synthesised in a number of land plants and microorganisms. This fatty acid, which contains a mid-chain cyclopropane ring, can be processed into high value commercial products. Bao et al. (2002) first discovered that *S.foetida* CPFAS catalysed the addition of a methylene group to the double bond at Δ9 position of oleic acid (see Fig 1.4). The *SfCPFAS* is a microsomal-membrane bound enzyme, which selectively adds the methylene group to the double bond of oleic acid, esterified to the *sn*-1 position of PC (Bao et al., 2003). The highest level of DHSA (approximately 37%) was measured in *L.chinensis* seed oil (Gaydou et al., 1993).

In *S.foetida*, DHSA was mainly found at the *sn*-1 position of PC, although sterculic acid (containing a cyclopropene ring) was equally distributed between *sn*-1 and *sn*-2 positions of PC. This suggests that DHSA was removed from *sn*-1 position prior to desaturation and sterculic acid is re-incorporated into PC (Bao et al., 2003). Furthermore, analysis of the positional distribution of TAG in *S.foetida* developing seeds suggested that cyclopropenated fatty acids (CPEFA) were found at *sn*-1 or *sn*-3 positions of TAG containing one cyclopropene

fatty acid. However CPEFA were more abundantly found on the *sn*-2 position of TAG in TAG molecules containing more than one CPEFA (Bao et al., 2003). These results have indicated that the use of CPFAS may play an important role in detecting the movement of acyl groups between different lipid pools.

G.hirsutum produces a range of fatty acids that are derived from DHSA, including sterculic acid and malvalic acid, a chain shortened version of sterculic acid (Yu et al., 2011). *G.hirsutum* encodes three genes, *GhCPFAS1*, *GhCPFAS2* and *GhCPFAS3*, which are involved in the synthesis of CPFA and these were recently described and characterised by Yu et al. (2011). These isozymes contained two enzymatic domains equivalent to the *S.foetida* CPFAS: the carboxy terminus (encoded CPFAS for synthesis of dihydrosterculate) and the amino terminus (encoded for a FAD-binding oxidase domain of unknown function) (Yu et al., 2011). The amino terminus of SfCPFAS is associated with membrane anchorage (Bao et al., 2003). Although the oxidase domain is not present in the bacterial CPFAS, in *A.tumefaciens* it is located next to the CPFAS gene. Surprisingly, the oxidase domain enhanced the CPFAS activity of GhCPFAS but not the bacterial CPFAS. Although the sequence of *GhCPFAS3* contained the conserved S-Ado-Met binding domain, fatty acid and gene expression analyses indicated that this isozyme contributed the least to the CPFA production in *G.hirsutum* (Yu et al., 2011). GhCPFAS1 and GhCPFAS2 were responsible for high levels of DHSA in roots and stems of *G.hirsutum*. The gene expression analysis revealed that all three isoforms were transcribed in developing seed of *G.hirsutum* (Yu et al., 2011), however the seed-specific expression of *GhCPFAS1* in *A.thaliana* resulted in approximately 1% of DHSA and the other two isoforms did not perform well. Although the carbocyclic-ring-containing fatty acids are found at low levels in *G.hirsutum* seed oil, their elimination is crucial for human consumption (Yu et al., 2011). CPEFA are involved in the repression of fatty acid desaturases in animals and it is proposed that the consequence of feeding animals with low levels of cyclopropene fatty acids is resulting physiological disorders (Yu et al., 2011).

DHSA is a valued industrial oil and it is crucial to identify the set of enzymes involved in the synthesis and subsequent transfer of it into oil. This information is expected to assist in genetic engineering of a high oleic acid crop plant to efficiently synthesise DHSA into oil.

1.3.2 Synthesis of LCPUFA in plants

The genetic transformation of plants to accumulate LCPUFA for nutritional benefits has been one of the most successful examples of metabolic engineering. Unlike plants, humans are not able to synthesise PUFA such as 18:2 and 18:3. Humans acquire PUFA and LCPUFA through their diet: given the presence of dietary 18:2 and 18:3, humans are able to synthesise LCPUFA. Plants do not accumulate LCPUFA. The intake of ω-3 and ω-6 LCPUFA in humans assists in the development of brain and visual function. Deficiencies in LCPUFAs, such as DHA (docosahexaenoic acid), EPA (ecosapentaenoic acid) and AA (arachidonic acid) which are synthesised in micro-organisms in abundance, have been associated with increased risk of cardiovascular and inflammatory diseases. DHA and AA are important components of membrane glycerolipids and are also precursors for a range of signalling molecules, which include prostaglandins, thromboxanes and leukotrienes (Needleman et al., 1986; Spychalla et al., 1997).

The human intake of LCPUFA through consumption of fish has reduced over time. An alternative source of ω-3 and ω-6 LCPUFA may be transgenic oilseed crops, expressing transgenes to synthesise 'fish oils'. A number of microorganisms have therefore been studied extensively and the genes encoding for LCPUFA have been isolated. It has been a challenge to express the right combinations of genes in oilseed crops in order to produce considerable amounts of LCPUFA. The subsequent cloning of genes (isolated from microorganisms) into *A.thaliana* and *B.napus* has generated very low levels of LCPUFA in seed oil. These challenges arise due to the complexity of the large number of enzymes involved in the biosynthesis of LCPUFA, such as DHA.

Genes responsible for the synthesis of LCPUFA have been isolated from a large number of microorganisms. Initially, seed-specific expression of a cyanobacteria Δ6 desaturase resulted in high accumulation (~40%) of γ-linolenic acid (18:3n6, GLA) and stearidonic acid (18:4n3, SDA) in soybean (Sato et al., 2004). These results indicated that plants were able to tolerate high levels of LCPUFA unlike the previously described unusual fatty acids.

1.3.2.1 The Isochrysis galbana *Δ9 elongase*

There are a number of desaturation and elongation steps in microorganisms that use 18:2 and 18:3 as starting substrates for the synthesis of ω-3 and ω-6 LCPUFA. *Isochrysis galbana* (*I.galbana*) is a microalga that produces large amounts of LCPUFA, including EPA and DHA (Qi et al., 2002). A common pathway described for the synthesis of EPA and AA involves a Δ6

desaturase that desaturates 18:2 and 18:3, followed by an elongation step and final desaturation step (Leonard et al., 2000; Napier et al., 1999). Another pathway, referred to as the Δ8 pathway, involves an initial elongation of 18:2 and 18:3, followed by desaturation steps by Δ8 desaturase and then Δ5 desaturase (Wallis and Browse, 1999). Desaturases were extensively studied and isolated from different species, compared to their counterpart elongases required for the elongation steps of LCPUFA synthesis. Elongases involved in the synthesis of LCPUFA have been isolated from a number of organisms including humans, yeast, nematodes, fungi and algae (Qi et al., 2002), however the characterisation of elongases has been challenging and their substrate specificity in the ER has not been clearly established.

The Δ9 elongase from *I.galbana* (IgΔ9E) has been isolated and characterised. It is referred to as Δ9 elongase because of its specificity to elongating 18:x PUFAs that are desaturated at the Δ9 position. This elongase was expressed in yeast system and showed that IgΔ9E only used 18:2 and 18:3 as substrates, elongating them to 20:2 (ω-6) and 20:3 (ω-3) respectively. This system was very efficient when used to introduce an alternative elongase system that converted 45% of substrate into LCPUFA (Qi et al., 2002). Interestingly, the sequence of the last motif of the IgΔ9E is similar to one of the three conserved histidine boxes, which are found in almost all membrane bound desaturases (Qi et al., 2002; Shanklin and Cahoon, 1998). The presence of histidine boxes in desaturases depicts the active site of the enzyme, although the function of one histidine box in IgΔ9E was not investigated. Due to its specificity and conversion efficiency, IgΔ9E is used in a number of transgenic constructs designed for the stable transformation of oilseed crops for the production of LCPUFA.

1.3.2.2 Arachidonic acid (AA), an ω-6 nutritional fatty acid

Arachidonic acid is a LCPUFA that is made of a 20-carbon chain with four double bonds (Fig 1.4). It is an essential fatty acid required for brain development in infants. Commercially available infant formula is supplemented with sufficient amounts of AA as regular intake assists in visual and brain development (Koletzko et al., 2005). In adults, a deficiency of AA may result in hair loss, anaemia and reduced fertility (Petrie et al., 2012a). AA is the main molecule used as a precursor for the synthesis of a number of signalling compounds (Spychalla et al., 1997). Studies of metabolism in potato tuber have shown that AA is considerably more stable than 18:2 (AA was oxidised in potato for an onset of

hypersensitive response). These studies also showed that some of AA was converted to hydroxyl acids, while the majority was found in phospholipids and glycerolipids (Preisig and Kuć, 1988). In humans, PC is essential for the production of DAG, PA and AA, which are used for the production of other signalling molecules (Gibellini and Smith, 2010).

A number of genes have been isolated from microalgae in order to assemble transgenic pathways for the biosynthesis of AA in various oilseed crops. Recently Petrie et al. (2012a) described a transgenic pathway designed for the stable transformation of *A.thaliana* and *B.napus* for the synthesis of AA in seed oil. The pathway is dependent on the presence of sufficient levels of the starting substrate 18:2 (α-linoleic acid) and their results have shown that the enzymes of the AA pathway were able to produce considerable amounts of AA in *A.thaliana* and *B.napus* seed oil. The first enzyme of the pathway is IgΔ9E, which elongates 18:2 to EDA (eicosadienoic acid, 20:2), the second enzyme is the *Pavlova salina* Δ8 desaturase, which desaturates EDA to DGLA (dihomo-γ-linolenic acid, 20:3), and the third enzyme is the *P.salina* Δ5 desaturase, which desaturates DGLA to AA (20:4) (Petrie et al., 2012a). These genes were driven by seed-specific promoters to limit the synthesis of LCPUFA to seed lipids. Their super elite *A.thaliana* and *B.napus* transformants contained approximately 20% (T3 pooled seed data) and ~10% (T2 single seed) of AA in total seed lipids respectively. Their elite transformation events, however, were rare. The cultivar of *B.napus* also contained high levels of 18:3 and the enzymes of the pathway were able to synthesise 2.4% of EPA. Overall, their construct design and their selection of genes have shown that it is possible to generate relatively high levels of AA in oilseeds.

1.3.2.3 Docosahexaenoic acid (DHA), an ω-3 nutritional fatty acid

DHA is a very long polyunsaturated fatty acid with 6 double bonds (Fig 1.4). There are numerous health benefits of DHA, however only a very small amount of dietary 18:3 is converted to DHA in humans – recent studies have shown that the conversion of 18:3 to DHA is about 1% in infants and almost negligible in adults (Brenna et al., 2009). Therefore humans are required to supplement DHA into their daily diet.

There are a number of studies that have successfully cloned genes from microalgae and assembled pathways for the production of DHA in plants (Petrie et al., 2010; Qi et al., 2004; Robert et al., 2005; Wu et al., 2005). A patent application in 2004 was the first to report

transgenic production of DHA in soybean seeds (Cahoon et al., 2004), however there have been no reports of high levels of DHA in any oilseed crop.

A complex pathway was assembled transiently in leaves of *N.benthamiana* (Wood et al., 2009) and was later used for stable transformation of *A.thaliana*. However very low levels (2.4%) of DHA were measured in *A.thaliana* seeds (Petrie et al., 2010). A major challenge to achieving higher levels of DHA in land plants is the conversion efficiency of native plant lipid substrate into DHA, with the elimination of intermediates of the transgenic pathway (Petrie and Singh, 2011). Production of DHA in land plants requires multiple elongation and desaturation steps. The first goal is the identification of enzymes that have high conversion efficiencies in land plants. The second, to use the right combination of transgenic enzymes to fit the lipid metabolism pathways of the plant.

1.3.3 Seed-specific promoters

There are a number of seed-specific promoters used to express transgenic pathways for the modification of lipid profile in the seed.

The *B.napus* napin promoter (Stalberg et al., 1993) is commonly used for metabolic engineering of lipid metabolism in plants. The truncated promoter, referred to as FP1, has been used in many studies to limit expression of transgenes during oil synthesis in the seed (Petrie et al., 2012a; Petrie et al., 2012b; Stoutjesdijk et al., 2002). The FP1 promoter is active during storage reserve accumulation in the seed.

Another commonly used promoter is the *A.thaliana* FAE1 promoter. Petrie et al. (2012a) used the FAE1 promoter to drive the *IgΔ9E* gene in *A.thaliana* and *B.napus*.

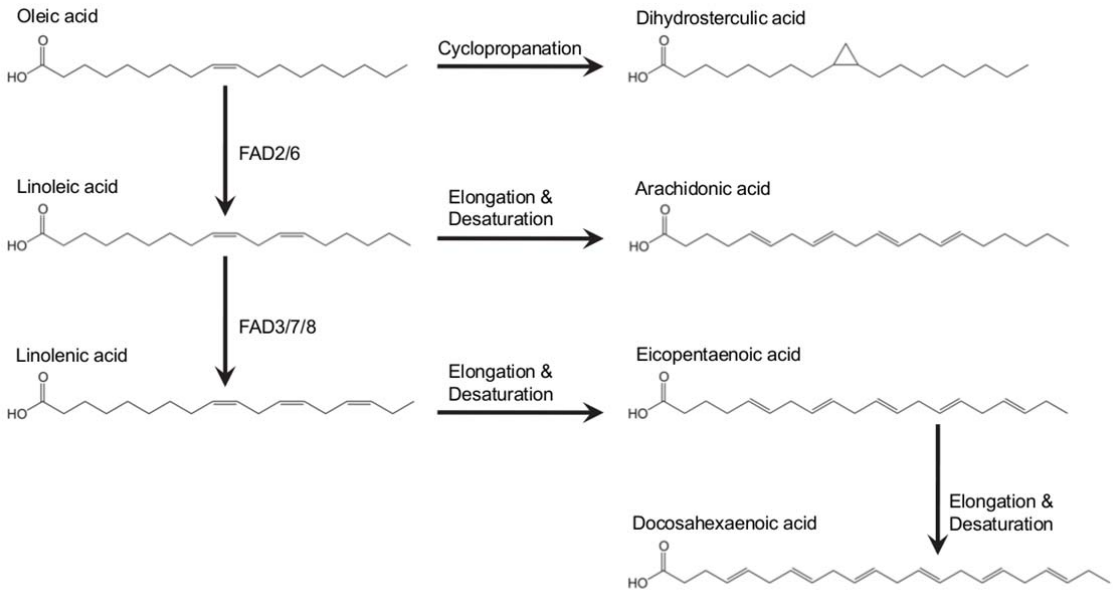

Figure 1.4. Schematic of modification of native plant fatty acids into unusual fatty acids.

Oleic acid (18:1) is converted to linoleic acid (18:2n6) by FAD6 and FAD2 in the plastid and ER respectively. Linoleic acid is desaturated to linolenic acid (18:3n3) by FAD7/8 and FAD3 in the plastid and ER respectively. Cyclopropanation of oleic acid by CPFAS enzyme generates DHSA. Arachidonic acid (20:4n6) is synthesised by elongation and desaturation of linoleic acid. Linolenic acid is used as starting substrate to generate eicosapentaenoic acid (20:5n3) and docosahexaenoic acid (22:6n3). Multiple elongation and desaturation steps are involved.

1.4 Challenges in metabolic engineering

There are many challenges in the successful engineering of transgenic traits in plants. Despite decades of research and development into the metabolic engineering of plants, there remain very few reports outlining the bottlenecks towards achieving success.

A major challenge is the generation of elite transgenic events that perform relatively well and that are taken forward into field research. In most cases, numerous independent transgenic events need to be made in order to search for a limited number of elite events. This task is both expensive and time-consuming. Another challenge is to maintain a stable expression of transgenic enzymes generation after generation – it is well-known that transgenes are silenced over time (Hagan et al., 2003). Methylation-driven silencing of transgenes is a common example of this.

Although more is known about RNA silencing pathways of the plant, it is still unclear how plants are able to silence transgenes over time. Furthermore it remains unclear how elite events that perform optimally over numerous generations, without compromising the development of the host plant, can be generated with minimal effort.

1.5 sRNA metabolism in plants

1.5.1 RNA silencing – processes and effector molecules

Plants have developed complex defence pathways for protection against foreign nucleic acids such as DNA/RNA viruses, bacterial DNA/T-DNA and transgenes, transposable elements, and viroids. The complex pathways referred to as RNA silencing, gene silencing or RNA interference (RNAi, in animals) are a set of core processes triggered by perfect or imperfect long double-stranded RNA (dsRNA). These pathways use small non-coding RNAs to direct sequence-specific inhibition of RNA and DNA. The sRNA-driven repression of gene expression is also crucial for maintenance of genome integrity and plant development (Voinnet, 2009).

The biogenesis of sRNAs involves a number of effector proteins and complex processes which are poorly understood. The molecular mechanism of RNA silencing is conserved in most eukaryotes. Although the process of RNA silencing was only discovered in the 1990s, RNAi is already known to play a crucial role in the regulation of development, genome stability, adaptive responses to both biotic and abiotic stresses, and as a primary antiviral response (Vaucheret, 2006).

RNA silencing at transcription level is called transcriptional gene silencing (TGS) and involves methylation of DNA and or histones (Jones et al., 1999). Genes can also be silenced at the post-transcription level and this is known as post-transcriptional gene silencing (PTGS) (Hamilton and Baulcombe, 1999; Vaucheret, 2006). PTGS involves sRNA-driven sequence-specific cleavage of mRNA and the subsequent repression of translation (Hamilton and Baulcombe, 1999; Vaucheret et al., 1998; Zamore et al., 2000). PTGS of a chalcone synthase (CHS) gene due to overexpression of a transgene in *Petunia hybrida* was one of the first reports of gene silencing in plants (Napoli et al., 1990). RNA silencing in plants can be divided into three stages: initiation, maintenance, and amplification of silencing signal. At the initiation stage, both TGS and PTGS are triggered by processing of long dsRNA into 19-24 nt sRNA molecules by RNaseIII-like enzymes called Dicer (in animals and insects) or Dicer-like (DCL, in plants).

Dicer is at the core of multi-step RNA silencing pathways and was originally characterised in *D.melanogaster* (Bernstein et al., 2001). The homologs were later discovered in *A.thaliana*.

There are four DCL enzymes, DCL1, DCL2, DCL3 and DCL4, encoded by *A.thaliana*, each of which plays a different role in processing of dsRNA (Baulcombe, 2004). Long dsRNA, which result from antisense transcription or the activity of RNA dependent RNA polymerases (RDRs), are diced by DCL into small interfering RNA (siRNA) (Jin, 2008). Structural and functional studies of plant DCLs have identified six functional domains, including RNaseIII-like and dsRNA binding domains (Margis et al., 2006).

The plant sRNA are classified into either micro RNA (miRNA) or siRNA. All sRNA have a similar chemical structure (contain 2 nt overhang, 5'-phosphate and 3'-hydroxyl group) however they differ in function and mode of biogenesis (Bartel, 2004; Blevins et al., 2006; Jin, 2008). siRNA are further classified into trans-acting siRNA (tasiRNA), stress-related naturally antisense siRNA (natsiRNA) and viral-induced siRNA (vsiRNA). Unlike other sRNA, miRNA and tasiRNA do not require perfect sequence complementarity to bind to their targets (Vazquez et al., 2004; Voinnet, 2009). DCL4, DCL2 and DCL3 produce 21, 22 and 24 nt siRNA respectively, whereas DCL1 is involved in production of miRNAs (Voinnet, 2009). The 21 nt miRNA have 2 nt 3' overhangs (Voinnet, 2009). Heterochromatin-associated siRNA are the 24 nt siRNA processed by DCL3, which suppress transcription (Mlotshwa et al., 2008).

After DCL processing, the 3' terminal nucleotide of the sRNA is methylated to stop degradation and oligouridylation (Yu et al., 2005). A methyltransferase (HEN1) is required to methylate the 2'-hydroxyl group on the 3' terminal nucleotide (Yang et al., 2006b; Yu et al., 2005). HEN1 was shown to selectively methylate 21–24 nt dsRNA that have 2 nt overhang and 2'- or 3'-hydroxyl on the terminal nucleotide, ensuring methylation of siRNA and miRNA only (Yang et al., 2006b).

In plants, the siRNAs are highly abundant (millions discovered in *A.thaliana*) compared to miRNAs (over 200 in *A.thaliana*), however the function of a large number of siRNA are not known (Jin, 2008). Following the processing of long dsRNA into sRNA, one strand of the sRNA duplex is incorporated into RNA-induced silencing complex (RISC) to guide sequence-specific inactivation of RNA or DNA (Incarbone and Dunoyer, 2013). Unlike siRNA, the dsRNA duplex of miRNA consists of two slightly different strands, miRNA/miRNA*. The miRNA (guide strand) is loaded onto RISC and miRNA* (passenger strand) is degraded in most cases (Manavella et al., 2012).

RISC is multi-subunit endonuclease. One strand of sRNA bound to Argonaute (AGO) protein forms its core complex (Mlotshwa et al., 2008). *A.thaliana* encodes ten AGO proteins which may be involved in RNA silencing. The function and involvement of many of the AGO proteins in RNA silencing have yet to be established (Hutvagner and Simard, 2008; Vaucheret, 2008). The 21 nt siRNA and miRNA, generated by DCL4 and DCL1 respectively, are loaded into AGO1 to direct PTGS of mRNA (Voinnet, 2009). In PTGS, mRNA is cleaved by the RNase-H activity of AGO. Recently Schott et al. (2012) reported that 21 nt plant siRNA and miRNA bind to the same effector (AGO1) unlike in *Dropsophila melanogaster* (*D.melanogaster)*, where the 21 nt siRNA and miRNA bind to different AGO proteins and binding is dependent on the dsRNA duplex structure.

In TGS, gene expression is inhibited by RNA-directed DNA methylation (RdDM), involving cytosine methylation and chromatin modification (Jones et al., 1999). Epigenetic modification at transcriptional level depends on RdDM of endogenous loci including transposable elements, repeat sequences, and complexly arranged gene arrays. It is driven by the 24 nt siRNAs products of DCL3, which are loaded into AGO4-, AGO6- and AGO9-RISC (Azevedo et al., 2010; Law and Jacobsen, 2010).

miRNA were originally discovered in humans, nematodes and *D.melanogaster* (Moss, 2002). Early studies have shown that miRNA regulate gene expression during development, for example *lin-4* gene was shown to post-transcriptionally control the expression of *lin-14*, controlling the timing of larval development in *Caenorhabditis elegans* (*C.elegans*) (Lee et al., 1993). The purposes of non-coding RNA were unknown but with the discovery of miRNA's role in regulating development it became clear that in some instances the final product of a gene can just be RNA (Voinnet, 2009). A mutation in *A.thaliana DCL1* has been shown to cause major developmental defects, which suggests that the processing of miRNAs are important for plant development and confirms the involvement of DCL1 in processing of miRNA (Jacobsen et al., 1999). miRNAs are generated from their imperfect stem-loop precursors (non-coding RNA) independent of RDRs and RNA polymerase IV (Pol IV) (Voinnet, 2009). Along with DCL1, another two proteins, Hyponastic Leaves 1 (HYL1) and Serrate (SE), are also required for processing of longer dsRNA precursors. The processing of miRNA occurs in the nucleus and stable export out of the nucleus is insured by 2'-O-methylation of the 3' ends (Voinnet, 2009). miRNAs regulate plant development through suppression of

transcription factors and transcripts which are essential for plants' metabolic and hormonal pathways (Azevedo et al., 2010). miRNAs are therefore an important class of sRNA.

Production of siRNA is also initiated by the introduction of exogenous triggers such as dsRNA, transgenes and viruses. siRNA driven from PTGS of transgenes also spread between cells locally and systemically throughout the plant, by vascular tissue (Palauqui et al., 1997; Voinnet and Baulcombe, 1997). Primary and secondary siRNA (amplifications of silencing signal) are produced to target the exogenous invaders and, in most cases, an RDR is required for conversion of primary-AGO-transcript into dsRNA (Chapman and Carrington, 2007). Secondary siRNA produced during the amplification process of silencing often originate from regions of target mRNA which were not the original target of the primary siRNA (Baulcombe, 2007). *A.thaliana* DCL2 is involved in production of primary siRNA (tasiRNA described later) and a combination of DCL4 and DCL2 are essential for the production of secondary siRNA to target transgenes and viruses (Chapman and Carrington, 2007). DCL4 is the main DCL involved in production of 21 nt secondary siRNA, which are loaded onto AGO1, containing RISC and direct PTGS of mRNA (Qu et al., 2008; Smith et al., 2007). DCL4 is the most versatile DCL because it also processes transgenic dsRNA intended for RNA interference (Blevins et al., 2006). DCL2 and DCL3 produce 22 nt and 24 nt siRNA respectively, for suppression of viral genomes, however the accumulation of these size class siRNA was observed when DCL4 function was suppressed (Ruiz-Ferrer and Voinnet, 2009). It has also been shown that products of DCL2 are loaded into AGO1 in the absence of DCL4 (Vaucheret, 2005).

1.5.2 Amplification of the silencing signal with SGS3 and RDR

Early studies of RNA silencing in *C.elegans* presented intriguing results – introduction of dsRNA triggered amplification of the silencing signal, resulting in complete degradation of target mRNA (Fire et al., 1998; Sijen et al., 2001). The silencing effect was far greater than expected and results also proved that the amplification process of silencing signal required the activity of a plant RDR, which used the primary siRNA-cleaved mRNA to synthesise new dsRNA (Sijen et al., 2001). Their experiments also showed that the population of secondary siRNAs aligned on the antisense strand of targeted mRNA (5' to 3'). The activities of two proteins, SGS3 (Suppressor of Gene Silencing 3) and RDR6, have been reported as

indispensable to plants' antiviral defence and PTGS of transgenes (Garcia-Ruiz et al., 2010; Mourrain et al., 2000; Yoshikawa et al., 2013).

SGS3 is a plant-encoded protein. It is involved in the amplification of dsRNA from cleaved single-stranded RNA (ssRNA) however its exact function is not known (Mourrain et al., 2000). *In vitro* experiments have shown that SGS3 acts as a homodimer and binds to dsRNA that have a 5' single-stranded overhang (Elmayan et al., 2009; Fukunaga and Doudna, 2009). Reports have also shown that the presence of RDR6 and SGS3 are vital for antiviral resistance (Vaucheret, 2005; Yoshikawa et al., 2013). Loss of SGS3 in *A.thaliana* results in a loss of tasiRNA production as well as accumulation of siRNA from highly transcribed sense transgenes (Mourrain et al., 2000). The *sgs3* mutants were impaired for PTGS of transgenes and were also highly susceptible to *Cucumber mosaic virus* (CMV), confirming the importance of SGS3 in PTGS of exogenous triggers (Mourrain et al., 2000). However viruses which inhibit RNA silencing at the DCL or AGO level did not show any change in level of infection in *sgs3* mutants when compared to level of infection in wild-type plants. Based on cytoplasmic replication of CMV, it was proposed that SGS3 operates in the cytoplasm and that it is not involved in the maintenance processes of RNAi at the nuclear level (Mourrain et al., 2000). It has also been suggested that SGS3 and RDR6 are involved in the systemic spread of the silencing signal, however the exact role of SGS3 in the production of secondary siRNA is not known. Other experimental reports have shown a direct interaction between *Solanum lycopersicum* (*S.lycopersicum*) encoded SGS3 and V2 (VSP encoded by *Tomato yellow leaf curl virus* (TYLCV)) in the nucleus (Glick et al., 2008). A recent study has reported interactions between AGO7 and SGS3 when both proteins were co-localised in the nucleus (Jouannet et al., 2012).

In vitro experiments have shown that SGS3 did not bind to dsRNA containing a 3' terminal phosphate and that 2'-O-methyl modification on the 3' terminal ribose of dsRNA also did not effect SGS3 binding (Fukunaga and Doudna, 2009). Recent *in vivo* experiments have demonstrated the role of SGS3 in inhibiting the degradation of 3' cleaved RNA fragments post-cleavage by miRNA–RISC (Yoshikawa et al., 2013). They have shown that SGS3 binds to the 3' cleaved site of *TAS1a* and *TAS2*, which are cleaved by miRNA173. SGS3 did not bind to cleaved products of miRNA171, a miRNA not involved in production of tasiRNA. Once the TAS2 transcript is cleaved, its 3' cleaved fragment is missing the 5' cap and is therefore

unstable. *In vitro* experiments have shown that SGS3 complexes with RISC (specifically with AGO1) only when the miRNA173-targeting *TAS2* gene is present. The 3' cleaved site of TAS2–miRNA173–RISC is stabilised by SGS3, which is then accessed by RDR6 for synthesis of dsRNA, subsequently resulting in production of tasiRNA. However their experiments also showed that SGS3 was not required to stabilise 3' cleaved sites of gene–miRNA–RISC, which are not involved in production of tasiRNA (Yoshikawa et al., 2013). In these experiments SGS3 interacted when 22 nt miRNA containing 2 nt 3' overhang that were involved in mRNA cleavage, which demonstrated its specific function. Although its exact involvement in the production of secondary siRNAs related to plant co-suppression pathways and antiviral defence are still not clear, it can be proposed that SGS3 is involved in stabilisation of transcripts that are cleaved by 21 and 22 nt primary siRNA.

Apart from SGS3, the functions of plant RDRs are also crucial in transitivity, antiviral defence and co-suppression pathways. Experiments involving delivery of dsRNA into plants and animals have shown that plants and nematodes contain RDRs (Gordon and Waterhouse, 2007). Through the function of RDRs a plant is able to amplify the antiviral- and transgene-derived silencing signal, resulting in widespread systemic immunity to viral infection (Baulcombe, 2004). RNA viruses also encode RDRs referred to as RdRPs, the importance of which will be reviewed later (Ferrer-Orta et al., 2006; Honda et al., 1986).

The function of RDRs was first detected in Chinese cabbage (Astier-Manifacier and Cornuet, 1971). The first plant RDR was extracted from *S.lycopersicum* leaves and was shown not to discriminate between single strands of RNA and DNA (Schiebel et al., 1993). In studies involving transgenic tobacco, which were expressing part of *Tobacco etch virus* genome and had become resistant to the virus, the activity of RDR was hypothesised to be related to PTGS (Lindbo et al., 1993). After RISC-mediated cleavage of mRNA (either viral or transgene related), an RDR binds to the cleaved complex and generates a new dsRNA molecule, which is then processed into secondary siRNA. Successive repeats of RDR-dependent amplification results in a large population of secondary siRNA.

There are six RDRs known in *A.thaliana*, however the functions of only three, RDR1, RDR2 and RDR6, are described. The suppression of viral infection may depend on the function of one or more of these (Garcia-Ruiz et al., 2010). *A.thaliana* RDR1 has been shown to be involved in production of siRNA against CMV and *Tobacco mosaic virus* (Diaz-Pendon et al.,

2007; Wang et al., 2010), while the functions of all three RDRs are required for the biogenesis of siRNA against *Tobacco rattle virus* (Donaire et al., 2008). Systemic infection by *Turnip mosaic virus* (TuMV) is not inhibited in *rdr6* mutants, suggesting the importance of RDR6 in production of secondary vsiRNA (Garcia-Ruiz et al., 2010). The coordination of the three RDRs in *A.thaliana* was also necessary for resistance against TuMV and the loss of function in either RDR1, 2 or 6 resulted in systemic infection of cauline leaves, however the nature of their interactions is unknown (Garcia-Ruiz et al., 2010). The *A.thaliana* RDR6 is the main RDR involved in conversion of aberrant RNA (missing cap and/or poly A tail) into dsRNA (Curaba and Chen, 2008). RDR6 can also use single-stranded DNA (ssDNA) as template, necessary for defence against ssDNA viruses (Curaba and Chen, 2008).

SGS3 and RDR6 are also involved in DNA methylation of transgenes driven by 21 nt siRNA (Jauvion et al., 2012). The chemical structure of SGS3 protein consists of XS (function not known), zinc finger and coiled-coil. Zinc finger and coiled-coil domains are hypothesised to be involved in recognition of nucleic acid and protein-protein interactions (Bateman, 2002; Fukunaga and Doudna, 2009). It has been proposed that SGS3 protects or stabilises ssRNA molecules for RDR6 reactivity (Beclin et al., 2002), however *in vitro* experiments failed to confirm interaction between SGS3 and RDR6 (Fukunaga and Doudna, 2009). RDR6 was able to convert ssRNA into dsRNA independent of SGS3 and more importantly RDR6 did not bind to dsRNA containing 5' overhang. These results suggest that there is no direct interaction between RDR6 and SGS3 (Fukunaga and Doudna, 2009).

Recently Verlaan et al. (2013) found that *TY-1* and *TY-3* expressed in wild tomato (*Solanum chilense*) contained sequence homology to *A.thaliana* RDR3/4/5. The functions of the class of RDR coded by these alleles have not been described previously, although their presence provided resistance against TYLCV. This is the first report where RDR3/4/5 have been associated with antiviral defence against begomoviruses. Further in-depth studies are needed to understand the roles of plant RDRs in resistance against viruses and in other processes involving RNA silencing of genes.

1.5.3 Transitivity and tasiRNA

Transitivity is the amplification of silencing signal by means of producing populations of primary and secondary siRNA (Baulcombe, 2007; Himber et al., 2003). During the production of secondary siRNA, the target mRNA is converted to dsRNA and processed into siRNA,

which degrade the mRNA target and increase the siRNA population (Mlotshwa et al., 2008). Transitivity can be defined as those siRNA that originate from sites immediately adjacent to the primary target site (Baulcombe, 2007). The secondary siRNA not only target genes locally but also spread the silencing signal systemically through plasmodesmata and vascular tissue (Baulcombe, 2004). Transitive silencing is an important RNA silencing pathway in plants. It is the process that drives S-PTGS (sense transgene PTGS) as well as antiviral defence (Mlotshwa et al., 2008).

An important class of siRNA are tasiRNA, which are 21 nt endogenous regulatory molecules driving hetero-silencing (silencing in *trans*). This means that the initial silencing molecule does not have any sequence resemblance to the second target (Manavella et al., 2012). The initial step of tasiRNA production requires 22 nt miRNA-programmed RISC-mediated cleavage of *TAS* transcripts (tasiRNA gene). The miRNA-driven cleavage of *TAS* genes initiates the production of secondary siRNA (tasiRNA), which silence genes in *trans*. There are eight *TAS* loci in *A.thaliana*. The main difference between tasiRNA and other endogenous siRNA is that the initiation of tasiRNA is triggered by miRNA. DCL1 processes miRNA, which are loaded to AGO1 or AGO7 for cleavage of tasiRNA precursors (Chapman and Carrington, 2007; Yoshikawa et al., 2013). However DCL4, dsRNA-binding protein 4 (DRB4), and components of co-suppression pathway (SGS3 and RDR6) are also required for direct production of 21 nt tasiRNA (Chapman and Carrington, 2007; Vazquez et al., 2004). Therefore, it It can therefore be said that all four DCLs are indirectly involved in production of siRNA.

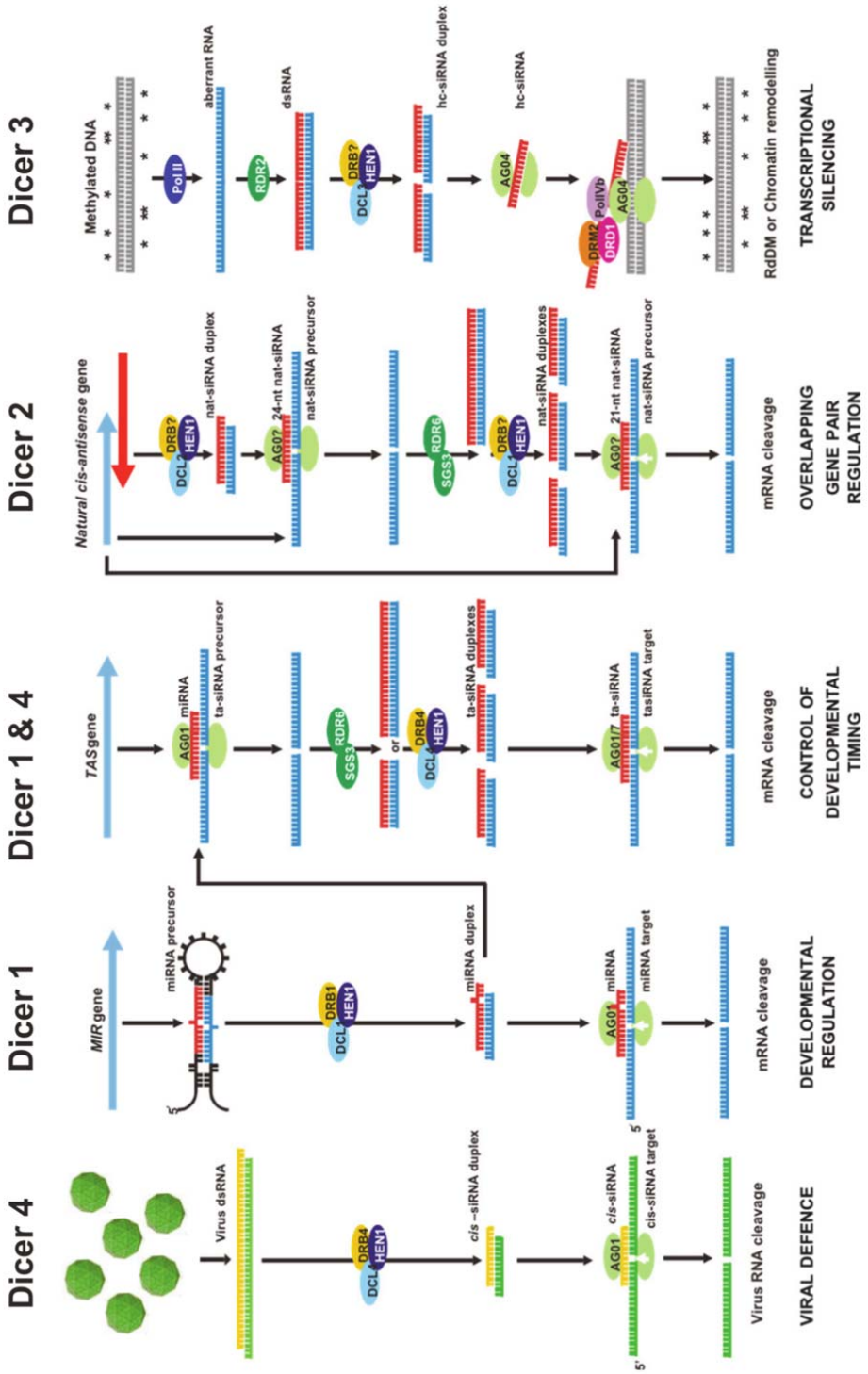

Figure 1.5. Schematic representation of parallel RNA silencing pathways in *A.thaliana*.

This schematic is adapted from Eamens et al. (2008) and updated to include more recent findings. The processes and effector molecules are described throughout in the text.

1.5.4 Viruses and the functions of their respective VSPs

Viruses are among the plant pathogens which cause yield losses in a variety of economically-important crops and result in limiting the productivity of agriculture worldwide. Although they have relatively small genomes coding for a limited number of proteins, the devastations caused by viral infections are large.

The primary plant immune system against viruses is also dependent on RNA silencing, known as viral-induced RNA silencing. Viral genomes attract RNA silencing by their intramolecular fold-back structures and dsRNA replication intermediates. Antiviral resistance in plants consists of initiation, amplification, and the systemic spread of silencing signal, and involves the use of multiple DCLs. The majority of phytoviruses have ssRNA genomes that are processed into dsRNA intermediates by RdRPs and vsiRNA are produced by DCL4. An accumulation of 21 nt vsiRNA was detected in plants infected with positive-strand RNA viruses. In other cases, DRB4 is required to assist in production of vsiRNA from RNA and DNA viruses (Incarbone and Dunoyer, 2013). DCL4 and its backup DCL2 process the dsRNA structures into 21 nt and 22 nt vsiRNAs respectively, however 22 nt vsiRNA make up less than 20% of total vsiRNA population (Ding, 2010; Garcia-Ruiz et al., 2010). Compared to 21 and 22 nt vsiRNA, a more abundant population of 24 nt vsiRNA (processed by DCL3) are produced upon infection with DNA viruses (Blevins et al., 2006).

The downstream components of virus-induced RNA silencing are not well characterised (Wang et al., 2011). The two AGO proteins which allow PTGS of endogenous and exogenous RNA are AGO1 and AGO7 (Montgomery et al., 2008). The hypomorphic *ago1* and null *ago7* mutants were shown to be hyper-susceptible to virus infection (Qu et al., 2008). The function of these two AGO proteins is therefore to provide defence against viral infection (Azevedo et al., 2010). There is no difference between endogenous siRNA and vsiRNA in terms of terminal structure, processing by DCL or incorporation into AGO effector complex (Ding, 2010).

A.thaliana also produces secondary vsiRNA for amplification and spread (to other tissue types) of the silencing signal against the virus. The primary vsiRNA bound to the cleaved RNA target is used as a primer by plant RDR (RDR1/2/6) to convert it into dsRNA, which is then processed by DCL into secondary vsiRNA, resulting in transitive silencing (Sijen et al., 2001). The essential role of secondary vsiRNA in plants' antiviral response is not as clear

(Ding, 2010). Recently the roles of secondary vsiRNA were demonstrated to efficiently silence CMV-Δ2b. The experiments showed that the activity of DCL4, RDR6 and SGS3 were crucial for production of secondary vsiRNA to silence the virus (Wang et al., 2011).

Viruses also encode for VSPs and the suppressor activities of VSPs were discovered in experiments where PTGS silencing of GFP was stopped in *N.benthamiana* leaves after infection with *Potato virus Y* and CMV (Brigneti et al., 1998). These early experiments verified that PTGS was a natural mechanism used for protection against viruses in plants and that viruses produced VSPs to counter-defend by suppressing PTGS. A number of VSPs were originally expressed in *N.tabacum* and *A.thaliana* in order to learn about sRNA metabolism in plants (Dunoyer et al., 2004). In the past 15 years, a number of VSPs have been extensively studied to uncover the nature of virus infection in plants and to further apply this knowledge in engineering defence mechanisms to stop the spread of viruses in affected plants.

It has become evident that VSPs from different viruses stop RNA silencing by interacting with different components of plants' antiviral silencing pathways (see Fig 1.6, adopted from Incarbone & Dunoyer (2013)). In many cases VSPs are multi-functional proteins and their molecular mechanism of action is poorly understood. Many VSPs are known to interact with the processing and effector steps of RNA silencing, yet their exact significance in causing viral infections have been poorly characterised (Incarbone and Dunoyer, 2013). One example is P6, encoded by the *Cauliflower mosaic virus* (CaMV), which interacts with DRB4 and therefore stops DCL4 from processing vsiRNA (Haas et al., 2008). VSPs such as p38 and p1, encoded by TCV and *Sweet potato mild mottle ipomovirus* respectively, directly interact with AGO1, resulting in inhibition of the slicing activity of AGO1 in RISC (Giner et al., 2010). P0, encoded by polerovirus *Beet western yellow virus* and enamovirus *Pea enation mosaic virus-1,* is a VSP that acts as F-Box protein, resulting in degradation of AGO protein (Bortolamiol et al., 2007; Fusaro et al., 2012). The VSP 2b, encoded by CMV, has also been shown to physically interact with AGO1 and AGO4, as well sequester sRNA in order to stop the systemic spread of silencing signal (Gonzalez et al., 2010). p19 and p21, encoded by *Tomato bushy stunt virus* (TBSV) and *Beet yellow virus* respectively, are another two VSPs which bind to sRNA to inhibit PTGS and systemic spread of silencing signal (Dunoyer et al., 2010). V2, encoded by TYLCV, inhibits the production of secondary vsiRNA by binding to

SGS3 or dsRNA structures that have a 5' overhang (Fukunaga and Doudna, 2009; Glick et al., 2008). These examples are only a brief overview of the complexity of interactions between VSPs and RNA silencing pathways in plants. In most cases VSPs disrupt the defence mechanism of the plant in more ways than one and present studies of the VSPs mentioned are not complete in characterisation of their exact mechanism of action.

1.5.5 The viral silencing-suppressor proteins of interest

VSPs such as V2 (TYLCV-Is, Israel isolate), p19 (TBSV), $P0^{PE}$ (*Pea enation mosaic virus-1*) and p38 (*Turnip crinkle virus*) are encoded by phylogenetically unrelated viruses. These VSPs suppress the silencing machinery of the plant at different points as shown in Figure 1.6 and Table 1.1. The phenotypic changes by the stable expression of the selected VSPs observed in *A.thaliana* depend on the interactions of VSP with the processes and effector molecules of the plant's silencing mechanisms.

1.5.5.1 **V2 *encoded by the* Tomato yellow leaf curl virus *(TYLCV)***

V2 is encoded by the TYLCV. Transmitted by the whitefly (*Bemisia tabaci*), it causes major devastation to *S.lycopersicum* crops in tropical and subtropical regions worldwide (Bar-Ziv et al., 2012). TYLCV is ssDNA begomovirus, falling under the Geminiviridae family of plant viruses. This family of viruses use the plant cell nucleus for replication and transcription. A number of wild varieties of *S.lycopersicum* are highly resistant to TYLCV but all domesticated varieties are susceptible (Verlaan et al., 2013).

The virus attacks the silencing machinery of the plant cell by transcribing VSPs. The mechanisms of infection and the suppression of the silencing pathways of the plant cell are also determined by the virus isolate. There are a number of different isolates of TYLCV worldwide and the Israeli isolate (TYLCV-Is) encoding V2 is well-characterised. TYLCV-Is is known to cause extensive damage to *S.lycopersicum* crops, with some instances resulting in 100% crop losses (Czosnek and Laterrot, 1997). TYLCV-Is has a bi-directional and circular ssDNA genome encoding two ORFs on viral (+) strand (V1 and V2) and four ORFs on the complimentary (–) strand (C1, C2, C3 and C4) (Kheyr-Pour et al., 1991; Navot et al., 1991).

Mutagenesis of V2 in the TYLCV resulted in loss of viral infection in *N.benthamiana* and *S.lycopersicum* (Wartig et al., 1997). It was also reported that the mutated version of V2 did not have an effect on the replication of the virus and no ssDNA accumulation was observed.

V2 was also involved in systemic movement of the virus (Wartig et al., 1997). To assess the suppressor activity of the six proteins encoded by the virus, Zrachya et al. (2007) transiently overexpressed the virus proteins, along with GFP, in *N.benthamiana* leaves. They reported that V2 was the only protein which stopped co-suppression of GFP and was therefore the VSP encoded by TYLCV-Is. Interestingly C2, encoded by the Chinese isolate of TYLCV, also acts as a VSP (Dong et al., 2003; van Wezel et al., 2002). It has been suggested that TYLCV encodes two VSPs, V2 and C2, for early- and late-onset suppression of siRNA-mediated defence of the plant (Zrachya et al., 2007).

There are a number of studies that give insight into the interactions of V2 with sRNA-driven silencing. Experiments in *N.tabacum* and *N.benthamiana* cells, using YFP and GFP fused to the N-terminus and C-terminus of V2 respectively, determined the location of V2 in the cytoplasm (Zrachya et al., 2007). The experiments by Glick et al. (2008) used cDNA libraries to report that TYLCV-Is V2 was bound to *S.lycopersicum* SGS3 (SlSGS3). The *SlSGS3* is a homolog of *A.thaliana SGS3*. Both SlSGS3 and AtSGS3 were co-localised with V2 in the cytoplasm and no cell-to-cell movement of the proteins was detected (Glick et al., 2008). Two-hybrid yeast system was used to confirm interaction between V2 and SGS3 – the media lacked leucine and positive growth can only occur if there is interaction between the expressed proteins. The positive interaction between V2 and SlSGS3 resulted in survival of yeast transformed cells on leucine dropout media (Glick et al., 2008). The direct interaction of V2 and SGS3 was proposed to disrupt the RDR6 driven production of siRNA against TYLCV (Glick et al., 2008). The phenotypic changes (i.e. developmental defects in leaf morphology) caused by TYLCV in *S.lycopersicum* plants are similar to phenotypes observed in *sgs3 S.lycopersicum* mutants (Glick et al., 2008). Based on these reports V2 has therefore proved responsible in suppression of plants' antiviral response (primary and secondary vsiRNA) as well as disrupting the endogenous pathways necessary for production of tasiRNA. More recently Fukunaga et al. (2009) reported that V2 shares RNA binding selectivity with SGS3 and that it out-competes SGS3 in binding dsRNA structures that have 5' overhangs. *In vitro* experiments demonstrated that V2 does not interact with RDR6 (Fukunaga and Doudna, 2009).

The V2 encoded by the *Tomato leaf curl Java virus*-A (TLCJV-A, Java Indonesian isolate) has been shown to be multi-functional (Sharma and Ikegami, 2010). Constitutive expression of

TLCJV-A V2 induced a hypersensitive-like response in *N.benthamiana* leaves, resulting in cell-death (Sharma and Ikegami, 2010). The TYLCV-Is V2 has also been shown to induce hypersensitive response in *N.benthamiana* but not in *S.lycopersicum* (Bar-Ziv et al., 2012). The response is not induced in *S.lycopersicum* because V2 interacts with a member of the papain-like cysteine proteases (CYP), which are involved in disease immunity (Bar-Ziv et al., 2012). Experiments involving the yeast two-hybrid system identified a positive interaction between V2 and the *S.lycopersicum* CYP and, more specifically, identified that V2 binds to the cysteine protease active site of CYP.

Verlaan et al. (2013) recently described two alleles from a wild tomato (*S.chilense*), which code for an uncharacterised class of plant RDRs. These genes, homologous to *A.thaliana RDR3/4/5*, are responsible for resistance in *S.chilense* against TYLCV. The new findings suggest a more direct interaction of V2 with an uncharacterised class of molecules RDR3/4/5. It is also another example of a virus leading to identification of a new set of molecules involved in defence mechanism of the plant. Understanding the interactions between V2 and plant RDRs may lead to a better understanding of the plant symptoms caused post- infection with TYLCV.

1.5.5.2 p19 *encoded by the* Tomato bushy stunt virus *(TBSV)*

Tombusvirus p19 is a small protein of the TBSV (a *positive-strand RNA virus*). p19 was one of the first VSPs introduced to transient leaf assay systems to stop the PTGS of transgenes (described in detail later) (Voinnet et al., 2003). This small (19 kDa) and soluble protein has been extensively studied and crystal structures of p19 bound to sRNA have shown that p19 sequesters 21 nt sRNA (Silhavy et al., 2002; Ye et al., 2003). These crystal structures in conjunction with *in vitro* and *in vivo* experiments have shown that p19 forms a homodimer specifically with 21 nt sRNA that contain a 2 nt 3' overhang (Lakatos et al., 2004; Vargason et al., 2003; Ye et al., 2003). p19 stops 21 nt sRNA produced both as the primary targets of silencing (including miRNA and siRNA) as well as the secondary targets generated for systemic spread of the silencing signal. It stops sRNA loading onto RISC but it does not suppress the activity of already activated RISC (Lakatos et al., 2004).

Constitutive expression of p19 with CaMV 35S promoter caused major developmental defects in *A.thaliana* (ecotype Col-0), including partially fertile flowers and leaf serration (rosette and cauline leaves) (Dunoyer et al., 2004). To determine the effect of p19 on the

processing of hpRNA construct targeting *A.thaliana* CHS, Col-0 stably transformed with hpAtCHS (Wesley et al., 2001) were crossed with lines expressing 35S:p19 (Dunoyer et al., 2004). In the hpAtCHS lines, silencing of CHS resulted in the reduction of anthocyanins in *A.thaliana* seed coat and the transformed seeds were white. Post crossing, constitutive expression of p19 was able to stop the siRNA generated by the hpRNA against CHS and the resulting plants had brown-coloured seed coat. A major size class of siRNA generated by the processing of hpAtCHS structures is 21 nt siRNA and p19 binds to these, thus cancelling the silencing effect of the hpRNA.

The mode of action of p19 has been well studied and it is hypothesised that p19 will inhibit the 21 nt siRNA driven S-PTGS, based on its sequestration of 21 nt siRNA. Limiting the expression of p19 to later stages of embryo development is expected to avoid disruption of miRNA-driven regulation of development.

1.5.5.3 p38 *encoded by the* Turnip crinkle virus *(TCV)*

The positive strand RNA virus carmovirus, TCV, encodes the VSP p38. Apart from its suppressor ability, p38 is also a viral capsid required for genome packaging (Azevedo et al., 2010). Preliminary results by Dunoyer et al. (2004) suggested that constitutive expression of p38 showed no noticeable developmental defects in *A.thaliana*. *In vivo* experiments have ruled out the affinity of p38 to bind siRNA directly (Schott et al., 2012) and also reported that constitutive expression of p38 in *A.thaliana* did not change the levels of DCL4 and DRB4.

In order to assess the suppressor activity of p38 on hpRNA silencing constructs, p38 was constitutively expressed in hpAtCHS (hpRNA targeting *CHS*) lines, which lead to suppression of the hpRNA against CHS resulting in an accumulation of CHS mRNA (Schott et al., 2012). The 21 nt siRNA generated by hpAtCHS were not observed, with an accumulation in 22 nt siRNA were detected instead (Deleris et al., 2006). As activities of both DCL4 and DCL2 are required for silencing of TCV, these reports suggested the p38 indirectly suppressed DCL4 activity.

Azevedo et al. (2010) reported that p38 allowed maximal overexpression of GFP in *N.benthamiana* transient leaf assay. Their experimental data suggested that p38 disrupted the function of AGO1 by mimicking the endogenous GW/WG (glycine/tryptophan GW) motif

interactions thus inhibiting RISC assembly. AGO proteins (AGO1 and AGO4) contain conserved GW motifs, which are essential for the assembly of silencing effector complexes. Two GW motifs (one in the N-terminal and one at the C-terminal) were discovered in the ORF of p38 and both of the GW motifs are necessary for AGO binding (Azevedo et al., 2010). They also reported a dramatic up-regulation of DCL1 levels, which in turn promoted down-regulation of DCL3 and DCL4. A down-regulation of DCL3 was proposed to result in reduced RdDM of endogenous loci disrupting other silencing pathways essential for regulation of genome integrity.

1.5.5.4 $P0^{PE}$ *encoded by the* Pea enation mosaic virus-1

P0 protein is encoded by poleroviruses and enamoviruses, which fall under the *Luteoviridae* family of plant viruses. Aphids transmit the virus. There are many studies suggesting that the P0 inhibits RNA silencing by degradation of AGO1 as previously described. The VSP $P0^{PE}$ is encoded by the first ORF of enamovirus *Pea enation mosaic virus-1* (PEMV-1, a *positive-strand RNA virus*). Recently Fusaro et al. (2012) reported that $P0^{PE}$ acts as an F-Box protein and constitutive expression in *A.thaliana* caused major developmental defects. These defects were similar to those seen with the P0 encoded by polerovirus *Western beet yellow virus* (Bortolamiol et al., 2007). However there were phenotypic differences between the *ago1* null mutant and *A.thaliana* expressing $P0^{PE}$, which suggests that the VSP was also inhibiting other aspects of the silencing mechanism. $P0^{PE}$ is localised in the nucleus and shares no apparent conserved regions with other known VSPs (Fusaro et al., 2012).

The VSP caused a dramatic decrease in local PTGS of transiently expressed GFP and only slight effects were observed on the systemic spread of silencing signal (Fusaro et al., 2012). In transient assay, co-agro-infiltration of $P0^{PE}$ with GFP allowed overexpression of GFP for up to 14 days post infiltration. Poleroviral P0 and enamovirus $P0^{PE}$ proteins have been shown to inhibit production of secondary siRNA through destabilisation of AGO1 (Bortolamiol et al., 2007; Fusaro et al., 2012).

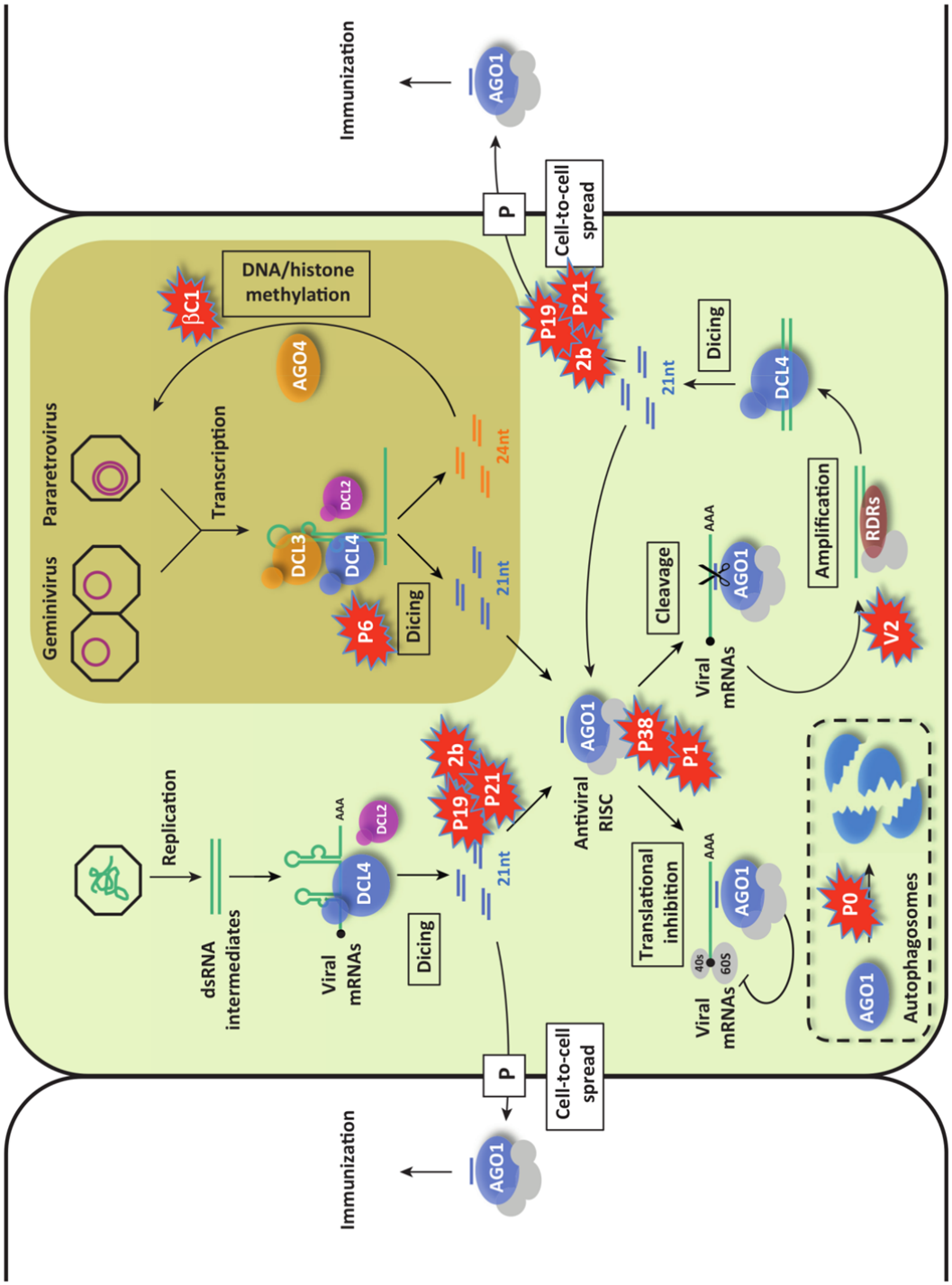

Figure 1.6. Schematic representation of characterised VSPs and their proposed interactions with the RNA silencing pathways in plant.

This schematic is adopted from Incarbone and Dunoyer (2013). The VSPs encoded by the respective viruses are described throughout the text.

VSP	Virus	Proposed function(s) of VSP
AC4	*African cassava mosaic geminivirus*	binds to single stranded miRNA
bC1	*b satellite of Tomato yellow leaf curl China begomovirus*	disruption of DNA methylation
L2	*Beet curly top virus*	disruption of DNA methylation
C2	*Beet severe curly top virus*	disruption of DNA methylation
p21	*Beet yellows virus*	binds sRNA
P6	*Cauliflower mosaic virus*	interacts with DRB4 (dsRNA binding protein) and possibly inhibits the DNA methylation of CaMV
2b	*Cucumber mosaic virus*	disrupts RISC assembly by binding to AGO1, AGO4 and siRNA
P15	*Peanut clump virus*	binds sRNA
P0	*Polerovirus/Enomovirus*	disrupts RISC assembly by binding to AGO1
P14	*Pothos latent virus*	size-independent binding to dsRNA
HC-Pro	*Potyvirus*	binds sRNA
P1	*Sweet potato mild mottle ipomovirus*	disrupts RISC assembly by binding to AGO
AL2	*Tomato golden mosaic virus*	disruption of DNA methylation
V2	*Tomato yellow leaf curl virus*	disrupts amplification of silencing signal
p19	*Tombusvirus*	binds sRNA
p38	*Turnip crinkle virus*	size-independent binding to dsRNA and AGO

Table 1.1. List of known VSPs and their proposed interactions with plant defence system.

1.5.6 Co-suppression of transgenes

Insertion of a transgene into the genome of a plant triggers siRNA-driven silencing, resulting in spontaneous silencing of the transgene. This phenomenon is referred to co-suppression and was reported by Napoli et al. (1990) in experiments involving accidental silencing of pigmentation in commercial petunia flowers. They attempted to change the pigmentation level of the flowers by increasing the expression of *CHS* in petunia, however they noticed that both the transgene and the endogene were silenced. The resulting flowers had un-pigmented white sections (Napoli et al., 1990). Introduction of a transgene encoding part or all of the coding sequence of an endogenous gene resulted in a reduction in levels of both transgene and endogenous transcribed mRNA (Napoli et al., 1990; Smith et al., 1990; van der Krol et al., 1990; Vaucheret et al., 1995). Another example of this involved co-suppression (PTGS) of an invading RNA virus genome in plants transgenically transformed with part of the RNA virus genome (Lindbo et al., 1993; Sijen et al., 1996).

The mechanisms behind siRNA-driven silencing of transgenes are not well understood, although it was observed that overexpression of a transgene with a strong promoter triggered PTGS of all homologous RNA in the cytoplasm (biochemical switch model) (Elmayan et al., 1998; Palauqui et al., 1997). Interestingly, expression of transgenes without a promoter also triggered co-suppression (*CHS* silencing in petunia) (Van Blokland et al., 1994). S-PTGS of transgenes without homology to endogenous genes of the host cell has also been reported (Hobbs et al., 1990; Hobbs et al., 1993). The results suggested that there were interactions between transgenes or between transgenes and host genes, which lead to production of aberrant RNA and subsequent S-PTGS (Van Blokland et al., 1994). While there are many reports of transgene silencing which were dependent on copy number, there are other reports where S-PTGS was independent of transgene copy number (Elmayan and Vaucheret, 1996; Hagan et al., 2003).

The plant co-suppression pathways depend on the formation of dsRNA. The discovery of SGS3 and RDR6 led to a better understanding of the importance of these proteins in mechanistic silencing of transgenes (Elmayan et al., 1998; Mourrain et al., 2000). Recent reports have shown that the function of RDR2, but not RDR6 (21 nt), is required in inverted repeat-PTGS (IR-PTGS)-related systemic spread of silencing signal (Jauvion et al., 2012; Smith et al., 2007). However both SGS3 and RDR6 were responsible for 21 nt-driven DNA

methylation of transcribed regions of sense transgenes (Himber et al., 2003). The siRNA generated by RDR2 were shown to be inefficient in S-PTGS (Jauvion et al., 2012). In addition, S-PTGS was more efficient in *rdr2* mutants compared to wild-type plants. It was proposed that RDR2 possibly antagonises activity of RDR6 by competing for the same dsRNA substrate, resulting in reduced DNA methylation of sense transgenes (Jauvion et al., 2012). The functions of different RDRs change depending on the plant species – *N.benthamiana* used for transient leaf assay has a dysfunctional RDR1 and the function of RDR6 has been shown to be important for RNA silencing (Qu et al., 2005; Schwach et al., 2005; Yang et al., 2004).

IR-PTGS is another form of induced RNA silencing in plants. The presence of inverted repeat sequences (hpRNA) in transgene loci is able to cause IR-PTGS (Waterhouse et al., 1998). This technique has many useful applications in crop biotechnology, including reduction in selected endogenous gene activity and resistance against pathogens (Stoutjesdijk et al., 2002; Wesley et al., 2001). Although the functions of RDR6 and SGS3 are crucial to synthesise dsRNA for S-PTGS, they are not required for processing of dsRNA formed from inverted repeat sequences (Beclin et al., 2002; Jauvion et al., 2012). A number of viruses (CMV, TuMV, and TCV) which were known to inhibit S-PTGS were used to challenge IR-PTGS to gain a better understanding of the processes and effector molecules involved in the two different types of transgene-induced RNA silencing (Beclin et al., 2002). The experiments confirmed that the selected viruses were able to stop IR-PTGS and that the processing of hpRNA-mediated silencing was not effected in *rdr6*, *sgs3* and *ago1* mutants (Beclin et al., 2002). These reports were the first to propose a branched pathway for transgene-induced silencing in plants.

Extensive research has shown that RNA silencing is not only the primary defence response in plants, fungi and invertebrate animals – it is also the fundamental genetic regulatory mechanism in eukaryotes. The complexity of RNA silencing in plants requires more extensive research with in-depth focus on the functions of effector molecules and processes involved in *in vivo* systems.

1.5.7 Transient assay in N.benthamiana *leaves*

N.benthamiana is widely used in the plant sciences, both in basic and applied contexts. It has become a very important and the most widely used host in which to study plant–pathogen interactions (Goodin et al., 2008). One of the 76 species in the genus *Nicotiana, N.benthamiana* is an allopolyploid containing 19 pairs of chromosomes. The species is endemic to Australia and was first discovered by Benjamin Bynoe during the final exploration voyage of the H.M.S Beagle between 1837 and 1843 (Goodin et al., 2008). *N.benthamiana* was selected to study plant–pathogen interactions due to its high susceptibly to viral infections (Goodin et al., 2008; Yang et al., 2004). There are a number of accessions available for *N.benthamiana* (The Kentucky Tobacco Research and Development Centre at the University of Kentucky holds six accessions), and the most commonly used accession by researcher groups around the world is referred to as “lab benth” or “research accession” (Goodin et al., 2008). Apart from its popularity in field of plant-pathogen studies, the advent of enhanced transient leaf assays has seen *N.benthamiana* put to many applications, including metabolic engineering (Voinnet et al., 2003; Wood et al., 2009). However a number of existing limitations are a hindrance in metabolic engineering of various pathways in the leaf.

The extensive use of *N.benthamiana* by the research community occurred over the past two decades after the advances in three techniques. The first technique, introduced and developed in the early 1990s, involves the manipulation of the plant virus system to express foreign genes in *N.benthamiana* (Chapman et al., 1992; Goodin et al., 2008). The second technique developed the virus-based vectors to exploit reverse genetics to silence different genes in the plant defence pathways by means of virus-induced gene silencing (VIGS) (Kumagai et al., 1995; Thomas et al., 2001). This technique was very powerful – it allowed biologists to study plant–pathogen interactions at a molecular level and enhance their understanding of the gene families essential for plant defence (Ding and Voinnet, 2007). The third technique revolutionised the use of *N.benthamiana* in other fields of molecular biology, including manipulation of transgenes for metabolic engineering of crops. This technique involves transient transformation of *N.benthamiana* leaves with infiltrating *A.tumefaciens*-carrying T-DNA (Petrie et al., 2010; Voinnet et al., 2003; Wood et al., 2009). The expression of transgene is assessed 2–5 days post infiltration. Since the introduction of

the transient leaf assay, there has been a mass increase in the number of research articles mentioning *Nicotiana benthamiana* and describing successes in metabolic engineering. The transient system in *N.benthamiana* has applications beyond studies of plant–pathogen interactions.

The "lab benth" is more susceptible to virus infections compared with other accessions of *N.benthamiana* because of a natural mutation occurring in the *RDR1* (*rdr1*). Plant RDRs are known to recognise aberrant RNA transcripts and process them into dsRNA for initiation and amplification of sRNA-mediated silencing pathways as described in the previous sections (Marker et al., 2010). In the case of *A.thaliana* and *N.tabacum,* RDR1 acts as a defence mechanism against virus attacks (Ying et al., 2010). In 2004 Yang et al. tested the functionality of RDR1 and they confirmed the mutation in the gene: protein analysis produced a dysfunctional protein. The reason for the mutation was a 72 nt insertion in the 5' region of the gene, generating many stop codons in the open reading frame (ORF) of RDR1 (Yang et al., 2004). Expression of RDR1 is induced by production of salicylic acid as part of the plant's hypersensitive response (Garcia-Ruiz et al., 2010; Jovel et al., 2011; Yang et al., 2004). Hypersensitive response is another form of defence mechanism against viral infection and involves cell death. The mutation has led to a loss in hypersensitivity response to most virus attacks in *N.benthamiana* (Jovel et al., 2011). For example the *Tomato ringspot virus* (TRV) induces a hypersensitive response in *N.tabacum* after infection, a response not induced in *N.benthamiana* (Jovel et al., 2011). It was also shown that TRV caused systemic infection in *N.benthamiana* whereas *N.tabacum*, which has a functional RDR1, inhibits systemic infection by the virus (Jovel et al., 2011; Jovel et al., 2007). Surprisingly, silencing of *NtRDR1* did not show an increase in systemic infection by the virus (Jovel et al., 2011). In this instance, and based on previous discussion, it can be proposed that perhaps the functions of both RDR1 and RDR6 are essential to reduce viral infection. There is no model at present showing classifications of novel accessions of *N.benthamiana* and the accessions that are carrying natural mutation in *NbRDR1* are not known.

The enhanced transient leaf assay partly relies on the use of the VSP p19 from the TBSV for interference with the host's endogenous co-suppression pathway (Voinnet et al., 2003). The use of p19 allows co-infiltrated transgenes to express at high levels for extended periods. The leaf assays permit complex multigene pathways to be assembled "in planta" from

individual T-DNA expression vectors, allowing their pathway activities to be assessed within a few days (Castilho et al., 2010; Mikkelsen et al., 2010; van Herpen et al., 2010; Wood et al., 2009). Such an assay format allows individual components of complex pathways to be readily interchanged and compared, with numerous pathways compared side-by-side on a single leaf. Such comparisons can guide the design and composition of large single-vector constructs that contain the entire optimised pathway and that may then be deployed for stable expression in plants (Petrie et al., 2010). It was also shown that, with the inclusion of a transcription factor called LEC2, genes driven by seed-specific promoters were expressed in the leaf (Petrie et al., 2010).

Beyond its use as a model system in studying plant–pathogen interactions, reports have shown that the system can produce proteins for large-scale purification (Garabagi et al., 2012; Lombardi et al., 2009). The leaves provide large tissue area, which can be agro-infiltrated with several different overexpression plasmids. The transient assay in *N.benthamiana* leaves is an essential tool in plant-related research and its application has also been adopted by other biological sciences. One of the advantages of this rapid assay includes high-level transient production of HIV-1 Nef (HIV antigen) in *N.benthamiana* leaves. Lombardi et al. (2009) were able to produce record high levels of the antigen in agro-infiltrated leaves of *N.benthamiana* with the aid of a VSP. They also reported that p19 from *Artichoke mottled crinkle virus* out-performed the p19 from TBSV in stopping PTGS of HIV-1 Nef, resulting in higher amounts of the antigen.

Although *N.benthamiana* leaf assays offer certain unique advantages for complex metabolic engineering, there is one significant constraint. The use of the VSP p19 is superior in aiding transgene overexpression but a hindrance in hpRNA-driven silencing of endogenous genes. This hindrance becomes problematic when assembly of a transgenic pathway is competing with endogenous pathways for the same substrate. The VSPs (such as p19, P0 and Hc-Pro) which are agro-infiltrated to inhibit co-suppression of transgenes also interfere with IR-PTGS. As of yet there is no reported VSP that allows simultaneous silencing of endogenes (IR-PTGS) and stops S-PTGS of transgenes.

There are two genomic tools available online representing partial assemblies of the *N.benthamiana* genome (Bombarely et al., 2012; Naim et al., 2012; Nakasugi et al., 2013). The two BLAST-searchable databases contain a draft assembly of the 3.1 Gb haploid genome

and can be accessed at www.benthgenome.com and www.solgenomics.com. The transcriptomic assembly is also available on www.benthgenome.com. These assemblies have become public in the past two years and have been a major aid for gene discovery and metabolic engineering of lipid pathways.

1.6 Scope of this thesis

Humans can greatly benefit from the genetic manipulation of plant lipid metabolism for the production of high levels of native and novel fatty acids in seed oil but due to the complexity of lipid biosynthesis pathways and plant defence systems, metabolic engineering has been a challenging task.

The experiments conducted in this thesis will directly manipulate the plant defence system in order to enhance the overexpression of a transgenic pathway for the synthesis of arachidonic acid in the seeds of *A.thaliana* and *B.napus*. This enhancement will be achieved by co-expressing a VSP with the transgenic pathway. As oil production is an important pathway at a cellular level, any changes in oil profile may provide a better indication of the effects of VSPs when expressed in the seed.

An alternative VSP will also be introduced into the *N.benthamiana* transient leaf assay to allow simultaneous overexpression of transgenes and silencing of endogenes. This approach will allow efficient assembly of transgenic pathways by shunting endogenous lipid pools into transgenic pathways. hpRNA mediated silencing of a number of key lipid handling genes in *N.benthamiana* leaves is expected to enhance our current understanding of enzymes involved in the synthesis of novel fatty acids.

Chapter 2 Understanding lipid fluxes in plant cells by developing and applying an improved transient assay system in *N.benthamiana* leaves

2.1 Introduction

N.benthamiana is widely used as a model plant for research across a number of disciplines. It has proven useful in the study of lipid handling pathways in plant cells, but due to the poor availability of substrates in the host cell, the flux of metabolites into transgenic pathways, including lipid handling pathways, is often limited. In systems that have been stably transformed, these limitations can be addressed by silencing endogenous pathways to increase the concentration of critical substrates and increase flux into transgenic pathways. This chapter investigates a new method of transient assay allowing simultaneous transgene overexpression and silencing of endogenes. This method is then applied in order to better understand the flux of lipids in *N.benthamiana* leaves.

Transient overexpression in *N.benthamiana* is dependent upon the co-infiltration of a VSP. The most popular VSP is p19, which is encoded by the *Tomato bushy stunt virus*. Although p19 has been widely used for the overexpression of transgenes in transient leaf assays, numerous studies have shown that it inhibits hpRNA-based silencing of endogenes (Lakatos et al., 2004; Voinnet et al., 2003). Chapter 1 outlined the existing literature on VSPs and suggested that V2, which is encoded by the *Tomato yellow leaf curl virus*-Is and interacts with the RNA silencing pathways of the plant in a different manner, could be an alternative to p19. The key difference between V2 and other VSPs (such as p19) is its ability to interact with sRNA biogenesis pathways at a key branch point, which may in turn allow hpRNA-derived sRNAs to function while still blocking sRNA derived from sense-strand RNA silencing (co-suppression) pathways. V2 may allow hpRNA-based silencing of endogenes at the same time as blocking co-suppression sRNA to permit transgene overexpression. A key aim of this chapter is therefore to compare and contrast the activities of p19 and V2 in various formats of the transient assay, with the goal of finding assay conditions that can support advanced metabolic engineering of lipids.

It has been suggested that assembling new transgenic pathways could assist in revealing lipid movement in the leaf and allow the engineering of novel and more efficient lipid pathways – an improved transient assay could be used to better understand the basic biology of lipid fluxes in a plant cell. The biosynthesis of non-native fatty acids in *N.benthamiana* leaves was therefore used to explore the flux of lipids throughout the leaf cell, with the aim of better understanding the role of lipid biosynthesis enzymes in the leaf.

Two different classes of transgenic enzymes are used to examine the flux of lipids in transient leaf assay: GhCPFAS, which catalyses the cyclopropanation of 18:1-PC, and IgΔ9E, which catalyses the elongation of 18:2 and 18:3 in the acyl-CoA lipid pool. These two enzymes work on different substrate head groups to produce easily identifiable products that may help in tracing their flux throughout lipid metabolism in a plant leaf cell. Based on the literature, *GhCPFAS1* and *IgΔ9E* were selected for transient overexpression in the leaf. The amino acid sequences of GhCPFAS1 and SfCPFAS group into the same clade emphasising their sequence homology (Yu et al., 2011), therefore GhCPFAS is hypothesised to perform similarly to SfCPFAS in cyclopropanating oleic acid in *N.benthamiana* leaves. The function of IgΔ9E in producing LCPUFA has been described previously (Qi et al., 2002) and transient expressions of *GhCPFAS* and *IgΔ9E* have been used as tools to probe the movement and modifications of acyl-groups in different lipid head groups in the leaf.

This chapter explores the following areas in transient leaf assays:

1. Can V2, an alternative VSP, support the overexpression of transgenes without inhibiting hpRNA-based silencing of endogenes?
2. Can a transient assay based on V2 be used to optimise the flux of lipids into newly engineered pathways?
3. Can transient leaf assays provide a better understanding of lipid fluxes in leaves?

2.2 Results

2.2.1 The suppressive behaviour of V2 compared to p19 in enhancing transgene overexpression in N.benthamiana *transient assays*

Overexpression of transgenes in transient leaf assays is prolonged and enhanced by the co-expression of a VSP such as p19 (Voinnet et al., 2003). The enhancement mediated by p19 was used as the benchmark by which to assess the effects of V2 on transgene overexpression. The coding regions of the VSPs were inserted into 35S-regulated binary expression plasmids (Fig 2.1A) and *A.tumefaciens* infiltrated in various combinations with green fluorescent protein (GFP) or fatty acid metabolic enzymes (AtFAE1 and AtDGAT1) constructs into *N.benthamiana* leaves. Visual observations of the GFP-infiltrated leaves 5 days post infiltration (dpi) showed that V2 enhanced GFP expression with an efficacy similar to that of p19 (Fig 2.1B). Leaves infiltrated with a combination of GFP, V2 or p19 were photographed for 7 days and images of one representative leaf are shown.

The suppressor activities of both VSPs were further quantified using overexpression constructs encoding the *A.thaliana* FATTY ACID ELONGATION1 (AtFAE1) and acyl-CoA:diacylglycerol acyltransferase 1 (AtDGAT1) (Fig 2.1C). These enzymes catalyse the production of modified fatty acids, including the fatty acid 20:1 (gondoic acid) and production of triacyglycerides (TAG) respectively. Infiltrated leaf tissues were harvested, freeze dried, and leaf lipids directly methylated to produce free fatty acid methyl esters (FAME). When co-infiltrated with the AtFAE1 construct, V2 and p19 respectively increased the production of 20:1 by 1.9-fold and 2-fold. With the further addition of AtDGAT1, the VSPs each raised the level of 20:1 by approximately 3.5-fold (Fig 2.1C). These results demonstrate that, although targeting different components of the plant's silencing machinery, both VSPs gave similar levels of protection against the co-suppression of transgene activities in *N.benthamiana* transient assays.

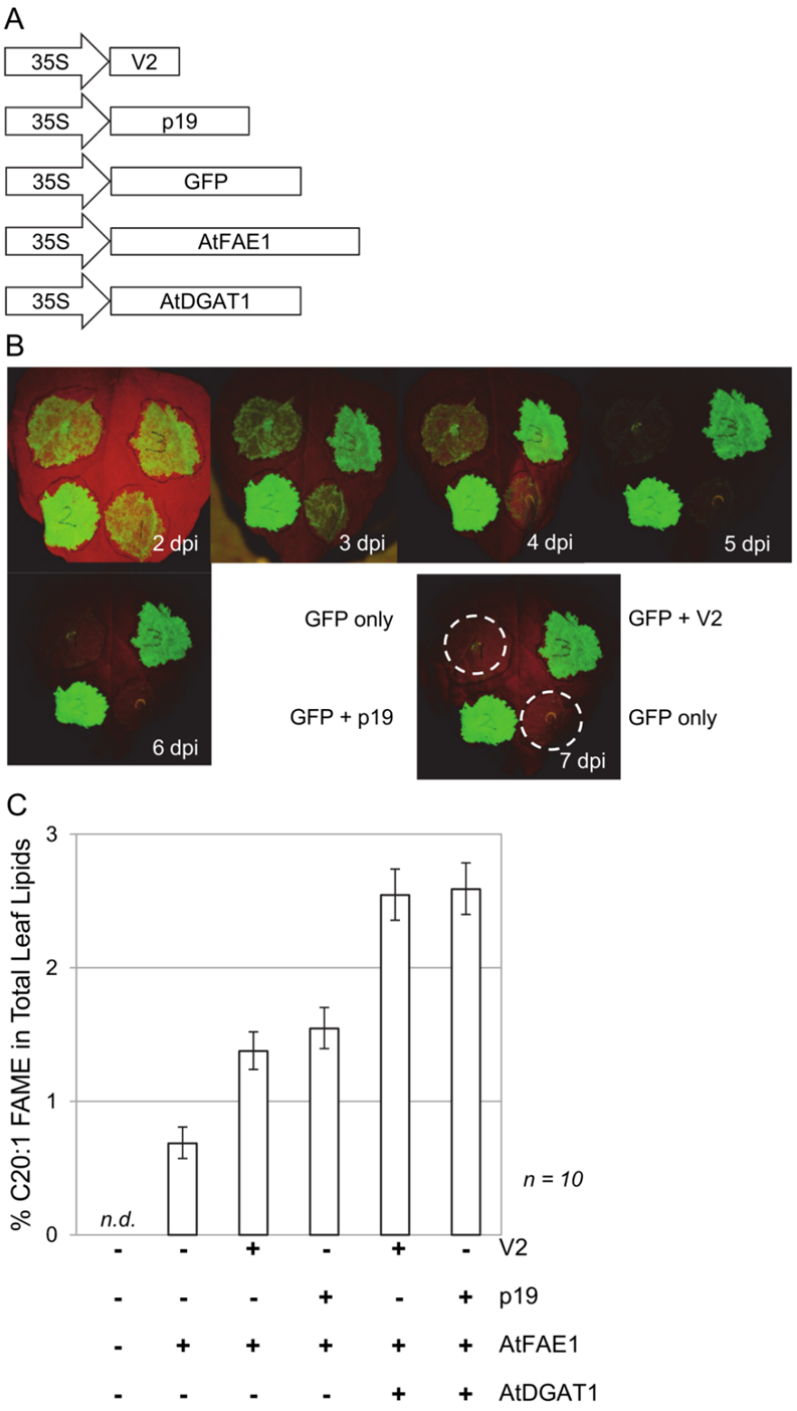

Figure 2.1. V2 supports the overexpression of multi-step transgenic pathways in transient leaf assays.

A. Schematic of T-DNA binary constructs for leaf expression of V2 and p19 and the transgenes GFP, AtFAE1 and AtDGAT1. All genes in the constructs were driven by the CaMV 35S promoter.

B. Time course of GFP expression in transient leaf assays with either no VSP or co-infiltration of V2 or p19. Images show one representative leaf photographed daily from 2–7 dpi. The last image (7 dpi) indicates the placement of infiltrations, dotted circles showing where complete co-suppression of GFP has occurred.

C. FAME extracted from leaves of *N.benthamiana* infiltrated with combinations of V2, p19, AtFAE1, and AtDGAT1. Leaves were harvested 5 dpi and relative percentage of 20:1-FAME measured. Data shown are the mean percentages and 5% LSD bars were calculated from 10 samples. When the LSD bars for two metabolites fail to overlap, the metabolite means are significantly different at the 5% level of significance. *n.d.* refers to not detectable.

2.2.2 hpRNA-mediated silencing of transiently expressed GFP in N.benthamiana *leaves*

V2 suppresses the plant's co-suppression silencing pathway by interacting either directly or indirectly with SGS3 (Fukunaga and Doudna, 2009; Glick et al., 2008) but hpRNA-mediated silencing (Wesley et al., 2001) operates effectively in *sgs3* mutant plants (Beclin et al., 2002). It therefore seemed possible that while the expression of V2 in transient assays could be used to enhance the expression of a delivered transgene, it may also permit hpRNA-mediated silencing of targeted genes where p19 could not. To test this, the efficacy of a hpRNA-targeting GFP was evaluated in transient leaf assays in the presence of either V2 or p19 (Fig 2.2A). The results were in agreement with previous reports (Fusaro et al., 2012; Voinnet et al., 2003) that silencing by a hpRNA construct is prevented by co-expression of p19 (Fig 2.2B). In contrast, the hpRNA-mediated silencing remained effective in the presence of V2 (Fig 2.2B). The difference in suppressive behaviour of the two VSPs was confirmed by immuno-blots measuring GFP protein levels (Fig 2.2C). This supports the notion that V2 can facilitate strong overexpression of transgenes in transient leaf assays yet allow concurrent hpRNA-directed silencing.

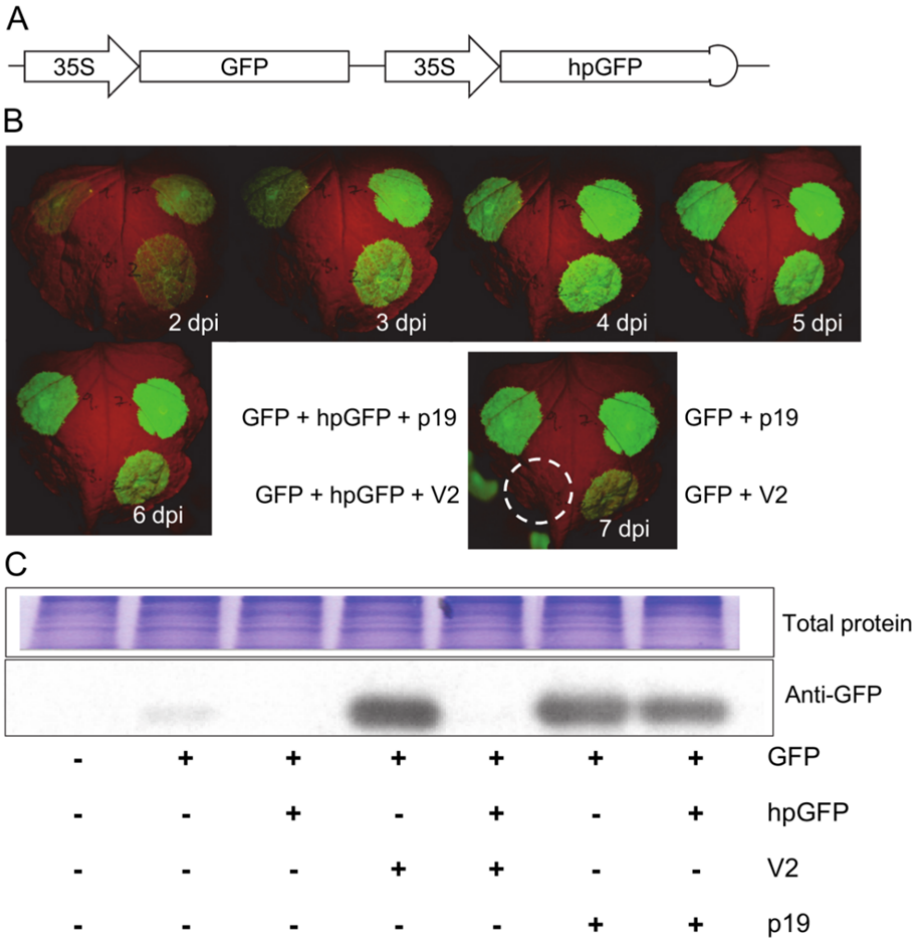

Figure 2.2. Efficient hpRNA based silencing of a co-infiltrated transgene, GFP.

A. Schematic of the T-DNA binary construct containing a GFP expression cassette and a 380 bp hpRNA directed against GFP, hpGFP.

B. Time course of GFP expression in transient leaf assays infiltrated with combinations of GFP and hpGFP with V2 or p19. Images show one representative leaf photographed daily from 2–7 dpi. The last image (7dpi) is used to indicate the placement of infiltrations, the dotted circle showing the infiltration zone that failed to express GFP.

C. Western blot analysis of GFP expression in *N.benthamiana* leaves infiltrated with combinations of GFP, hpGFP, V2 and p19 as indicated. Samples were collected 5 dpi. The upper panel shows the total protein loaded for the western blot and the lower panel shows the signal generated from an antibody recognising GFP, anti-GFP.

2.2.3 Characterisation of the FAD2 *gene family in* N.benthamiana

The first gene family assessed here was *FAD2* (*Fatty Acid Desaturase 2*) family. The availability of online genomic tools and ease of cloning techniques has made it possible to characterise the *FAD2* gene family in *N.benthamiana*. There is only one *FAD2* in *A.thaliana* and its nucleotide sequence was obtained by accessing The Arabidopsis Information Resource (TAIR) website (www.arabidopsis.org). The genome resource for *N.benthamiana* was then searched for sequences homologous to *A.thaliana FAD2*. This search revealed two *NbFAD2* genes, here named *NbFAD2.1* and *NbFAD2.2*. Both genes were subsequently cloned via PCR amplification using a DNA template and sequences verified via conventional long-read sequencing. *NbFAD2.1* and *NbFAD2.2* are 73% identical across the entire sequence and share regions of approximately 50 bp length with greater than 90% similarity at the DNA level across the histidine box motifs (Fig 2.3A). *NbFAD2.1* and *NbFAD2.2* contain the canonical histidine box motifs essential for 18:1 desaturation activity (Okuley et al., 1994b) and these are highlighted on the amino acid sequence alignment (Fig 2.3B).

The amino acid sequences of FAD2s from a number of oil-seed plant species were aligned with FAD2s from *N.benthamiana*. ClustalW (BioEdit and MEGA5 software) was used for alignments and deriving evolutionary relationships (Fig 2.3C). The FAD2s from Solanaceae family (*N.tabacum* and *Solanum commersonii*) show high similarity to *NbFAD2.1*. This limited phylogenetic analysis revealed that there were two clusters of *FAD2* genes from different plants – *FAD2*s from *N.benthamiana* to *N.tobacum*, *S.commersonii*, *Olea europaea* and *A.thaliana* formed cluster 1 and *FAD2*s from the Brassicaceae family (*Brassica juncea*, *Brassica carinata*, *Brassica rapa* and *B.napus*) formed cluster 2 (Fig 2.3C). Although *A.thaliana* is also in the Brassicaceae family, its *FAD2* is more similar to those in cluster 1. In addition to this, *AtFAD2* shares conserved regions with all of the *FAD2*s analysed, which suggests that it is the closest thing to a common ancestor. The analysis also revealed that *NbFAD2.2,* because it has the shortest branch length to *AtFAD2*, is perhaps the more conserved *FAD2* gene in *N.benthamiana* and the other *FAD2*s analysed.

To determine the gene expression levels of the two *NbFAD2s*, quantitative RT-PCR (qRT-PCR) was performed. Total RNA was extracted from large mature *N.benthamiana* leaves and used to compare the expression levels of *NbFAD2.1* and *NbFAD2.2* to those of *N.benthamiana Glyceraldehyde 3-phosphate dehydrogenase* (*NbGAPDH*). Initially the

method was optimised by testing three candidate reference genes: *Elongation factor 1-α* (*NbEF1α*), one of the more preferred reference genes (Liu et al., 2012) for qRT-PCR analysis, *Phosphatidylcholine diacylglycerol cholinephosphotransferase* (*NbPDCT*) and *NbGAPDH*. The expression levels of *EF1α* and *PDCT* were not however consistent between transiently infiltrated leaves and un-infiltrated leaves (data not shown). *NbGAPDH* was therefore used as a reference gene for the subsequent gene expression analyses throughout this chapter. See Methods (section 2.6 in this chapter) for detailed design and confirmation of primers used for this analysis. qRT-PCR analysis demonstrated that *NbFAD2.2* was expressed at approximately a 40% higher level than *NbFAD2.1* in leaves used in infiltration experiments (Fig 2.3D). A recent publication on the transcriptome of *N.benthamiana* was used to digitally assess the expression patterns of the *NbFAD2* genes (Nakasugi et al., 2013). This *in silico* analysis suggested that *NbFAD2.1* is a predominantly seed-expressed transcript and *NbFAD2.2* is a more constitutively expressed gene. This pattern of *FAD2* gene family regulation is consistent with that in other plants such as *C.tinctorius* and soybean.

The desaturase activities of NbFAD2.1 and NbFAD2.2 were assessed by cloning the ORF regions of the genes into yeast expression vector (pYES2, Invitrogen, Life Technologies) and transforming them into yeast (strain INVSc1, as part of the Invitrogen kit). The INVSc1 strain of yeast cells has been used by others to study activity of plant FAD2s (Cao et al., 2013) because of its simple lipid profile and the lack of endogenous FAD2 activity. The lipids from induced yeast clones were extracted as FAME and analysis of their fatty acid composition confirmed that NbFAD2.1 and NbFAD2.2 had catalysed the desaturation of 18:1 into 18:2 (Fig 2.3E). These desaturase activities were compared to that of AtFAD2 and the negative control (yeast cells expressing the empty pYES2 vector). All three plant desaturases were also capable of desaturating the 16:1 substrate into 16:2 (Fig 2.3F). This desaturase activity is limited to the yeast system as FAD2 in plants does not have access to 16:1 produced in the chloroplast. FAD2s from other plant species have been shown to have other roles beyond desaturating 18:1 to 18:2 (Cao et al., 2013). The chromatogram generated by the GC detector showed no other unusual fatty acid peaks when compared to the chromatogram of the yeast clone expressing the empty vector (Fig 2.3F).

A

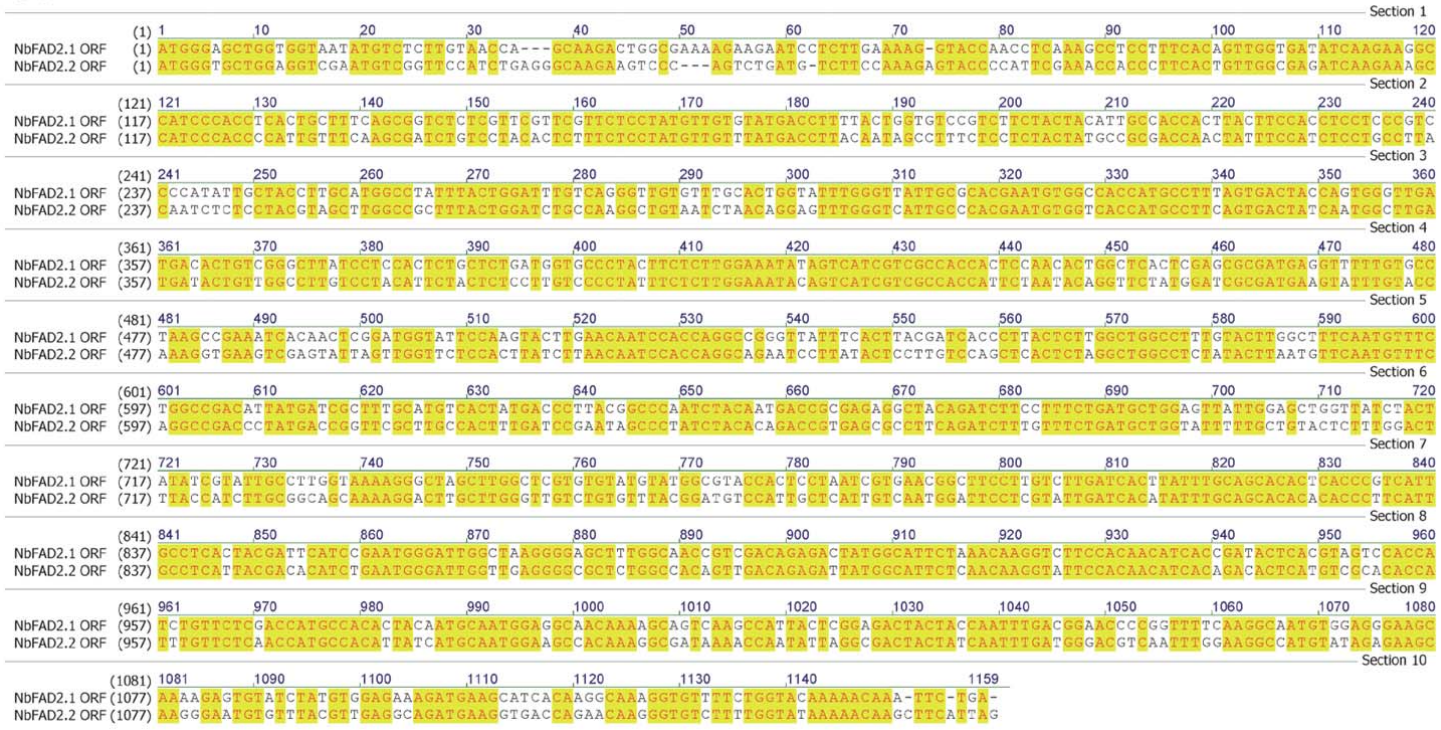
Section 1
NbFAD2.1 ORF (1) ATGGGAGCTGGTGGTAATATGTCTCTTGTAACCA---GCAAGACTGGCGAAAAGAAGAATCCTCTTGAAAAG-GTACCAACCTCAAAGCCTCCTTTCACAGTTGGTGATATCAAGAAGGC
NbFAD2.2 ORF (1) ATGGGTGCTGGAGGTCGAATGTCGGTTCCATCTGAGGGCAAGAAGTCCC---AGTCTGATG-TCTTCCAAAGAGTACCCCATTCGAAACCACCCTTCACTGTTGGCGAGATCAAGAAAGC
Section 2
NbFAD2.1 ORF (117) CATCCCACCTCACTGCTTTCAGCGGTCTCTCGTTCGTTCGTTCTCCTATGTTGTGTATGACCTTTTACTGGTGTCCGTCTTCTACTACATTGCCACCACTTACTTCCACCTCCTCCCGTC
NbFAD2.2 ORF (117) CATCCCACCCCATTGTTTCAAGCGATCTGTCCTACACTCTTTCTCCTATGTTGTTTATGACCTTACAATAGCCTTTCTCCTCTACTATGCCGCGACCAACTATTTCCATCTCCTGCCTTA
Section 3
NbFAD2.1 ORF (237) CCCATATTGCTACCTTGCATGGCCTATTTACTGGATTTGTCAGGGTTGTGTTTGCACTGGTATTTGGGTTATTGCGCACGAATGTGGCCACCATGCCTTTAGTGACTACCAGTGGGTTGA
NbFAD2.2 ORF (237) CAATCTCTCCTACGTAGCTTGGCCGCTTTACTGGATCTGCCAAGGCTGTAATCTAACAGGAGTTTGGGTCATTGCCCACGAATGTGGTCACCATGCCTTCAGTGACTATCAATGGCTTGA
Section 4
NbFAD2.1 ORF (357) TGACACTGTCGGGCTTATCCTCCACTCTGCTCTGATGGTGCCCTACTTCTCTTGGAAATATAGTCATCGTCGCCACCACTCCAACACTGGCTCACTCGAGCGCGATGAGGTTTTTGTGCC
NbFAD2.2 ORF (357) TGATACTGTTGGCCTTGTCCTACATTCTACTCTCCTTGTCCCCTATTTCTCTTGGAAATACAGTCATCGTCGCCACCATTCTAATAGAGGTTCTATGGATCGCGATGAAGTATTTGTACG
Section 5
NbFAD2.1 ORF (477) TAAGCCGAAATCACAACTCGGATGGTATTCCAAGTACTTGAACAATCCACCAGGCCGGGTTATTTCACTTACGATCACCCTTACTGTTGGCTGGCCTTTGTACTTGGCTTTCAATGTTTC
NbFAD2.2 ORF (477) AAAGGTGAAGTCGAGTATTAGTTGGTTCTCCACTTATCTTAACAATCCACCAGGGAGAATCCTTTATACTCCTTGTCCAGCTCACTCTAGGCTGGCCTCTATACTTAATGTTCAATGTTTC
Section 6
NbFAD2.1 ORF (597) TGGCCGACATTATGATCGCTTTGCATGTCACTATGACCCTTACGGCCCAATCTACAATGACCGCGAGAGGCTACAGATCTTCCTTTCTGATGCTGGAGTTATTGGAGCTGGTTATCTACT
NbFAD2.2 ORF (597) AGGCCGACCCTATGACCGGTTCGCTTGCCACTTTGATCCGAATAGCCCTATCTACACAGACCGTGAGCGCCTTCAGATCTTTGTTTCTGATGCTGGTATTTTTGCTGTACTCTTTGGACT
Section 7
NbFAD2.1 ORF (717) ATATCGTATTGCCTTGGTAAAAGGGCTAGCTTGGCTCGTGTGTATGTATGGCGTACCACTCCTAATCGTGAACGGCTTCCTTGTCTTGATCACTTATTTGCAGCACACTCACCCGTCATT
NbFAD2.2 ORF (717) TTACCATCTTGCGGCAGCAAAAGGACTTGCTTGGGTTGTCTGTGTTTACGGATGTCCATTGCTCATTGTCAATGGATTCCTCGTATTGATCACATATTTGCAGCACACACACCCTTCATT
Section 8
NbFAD2.1 ORF (837) GCCTCACTACGATTCATCCGAATGGGATTGGCTAAGGGGAGCTTTGGCAACCGTCGACAGAGACTATGGCATTCTAAACAAGGTCTTCCACAACATCACCGATACTCACGTAGTCCACCA
NbFAD2.2 ORF (837) GCCTCATTACGACACATCTGAATGGGATTGGTTGAGGGGCGCTCTGGCCACAGTTGACAGAGATTATGGCATTCTCAACAAGGTATTCCACAACATCACAGACACTCATGTCGCACACCA
Section 9
NbFAD2.1 ORF (957) TCTGTTCTCGACCATGCCACACTACAATGCAATGGAGGCAACAAAAGCAGTCAAGCCATTACTCGGAGACTACTACCAATTTGACGGAACCCCGGTTTTCAAGGGCAATGTGGAGGGAAGC
NbFAD2.2 ORF (957) TTTGTTCTCAACCATGCCACATTATCATGCAATGGAAGGCCACAAAGGCGATAAAACCAATATTAGGCGACTACTATCAATTTGATGGGACGTCAATTTGGAAGGCCATGTATAGAGAAGC
Section 10
NbFAD2.1 ORF (1077) AAAAGAGTGTATCTATGTGGAGAAAGATGAAGCATCACAAGGCAAAGGTGTTTTCTGGTACAAAAACAAA-TTC-TGA-
NbFAD2.2 ORF (1077) AAGGGAATGTGTTTACGTTGAGGCAGATGAAGGTGACCAGAACAAGGGTGTCTTTTGGTATAAAAACAAGCTTCATTAG

B

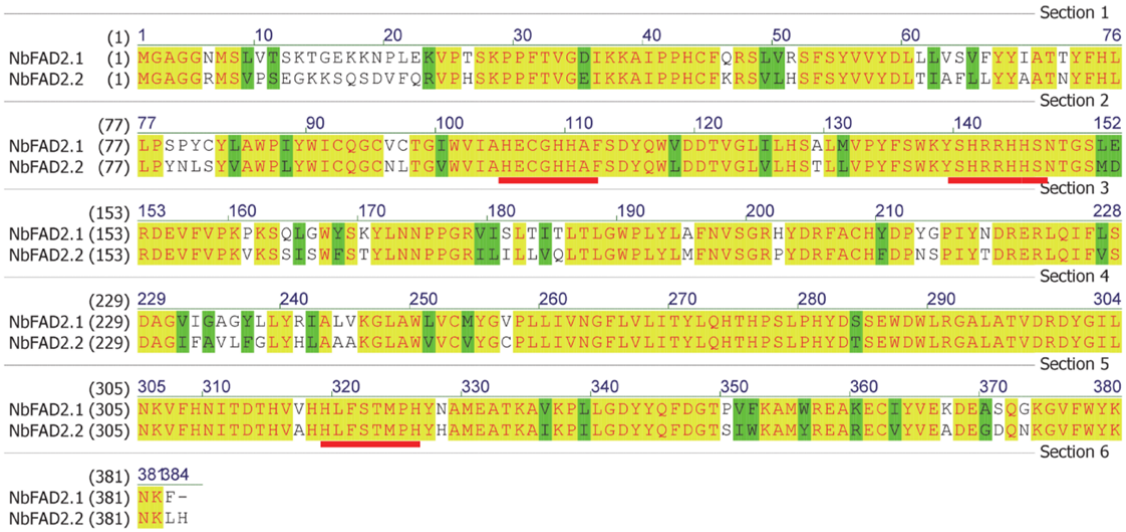
Section 1
(1) 1 10 20 30 40 50 60 76
NbFAD2.1 (1) MGAGGNMSIVTSKTGEKKNPLEKVPTSKPPFTVGDIKKAIPPHCFQRSLVRSFSYVVYDLLLVSVFYYIATTYFHL
NbFAD2.2 (1) MGAGGRMSVPSEGKKSQSDVFQRVPHSKPPFTVGEIKKAIPPHCFKRSVIHSFSYVVYDLTIAFLLYYAATNYFHL
Section 2
(77) 77 90 100 110 120 130 140 152
NbFAD2.1 (77) LPSPYCYLAWPIYWICQGCVCTGIWVIAHECGHHAFSDYQWVDDTVGLILHSALMVPYFSWKYSHRRHHSNTGSLE
NbFAD2.2 (77) LPYNLSYVAWPLYWICQGCNLTGVWVIAHECGHHAFSDYQWLDDTVGLVLHSTLLVPYFSWKYSHRRHHSNTGSMD
Section 3
(153) 153 160 170 180 190 200 210 228
NbFAD2.1 (153) RDEVFVPKPKSQLGWYSKYLNNPPGRVISLTITLTLGWPLYLAFNVSGRHYDRFACHYDPYGPIYNDRERLQIFLS
NbFAD2.2 (153) RDEVFVPKVKSSISWFSTYLNNPPGRILILLVQLTLGWPLYLMFNVSGRPYDRFACHFDPNSPIYTDRERLQIFVS
Section 4
(229) 229 240 250 260 270 280 290 304
NbFAD2.1 (229) DAGVIGAGYLLYRIALVKGLAWLVCMYGVPLLIVNGFLVLITYLQHTHPSLPHYDSSEWDWLRGALATVDRDYGIL
NbFAD2.2 (229) DAGIFAVLFGLYHLAAAKGLAWVVCVYGCPLLIVNGFLVLITYLQHTHPSLPHYDTSEWDWLRGALATVDRDYGIL
Section 5
(305) 305 310 320 330 340 350 360 370 380
NbFAD2.1 (305) NKVFHNITDTHVVHHLFSTMPHYNAMEATKAVKPLLGDYYQFDGTPVFKAMWREAKECIYVEKDEASQGKGVFWYK
NbFAD2.2 (305) NKVFHNITDTHVAHHLFSTMPHYHAMEATKAIKPILGDYYQFDGTSIWKAMYREARECVYVEADEGDQNKGVFWYK
Section 6
(381) 381384
NbFAD2.1 (381) NKF-
NbFAD2.2 (381) NKLH

C

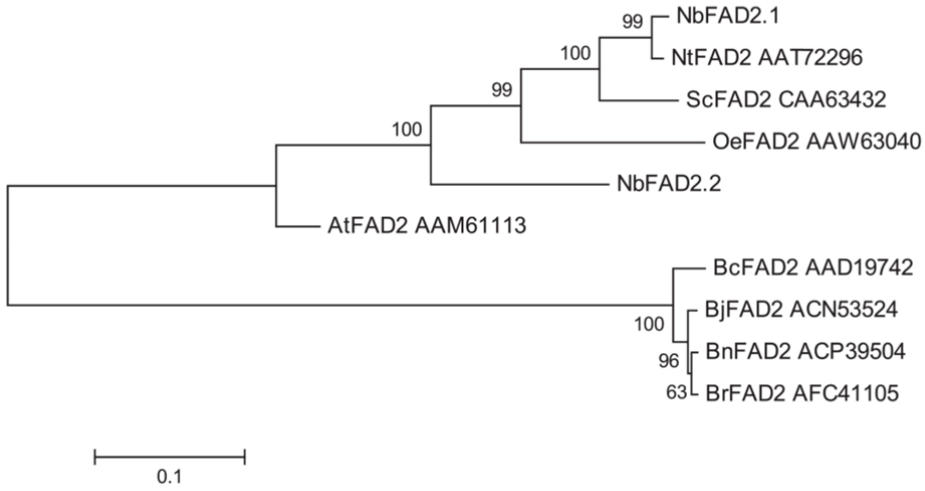
NbFAD2.1
NtFAD2 AAT72296
ScFAD2 CAA63432
OeFAD2 AAW63040
NbFAD2.2
AtFAD2 AAM61113
BcFAD2 AAD19742
BjFAD2 ACN53524
BnFAD2 ACP39504
BrFAD2 AFC41105
99
100
99
100
100
96
63
0.1

D

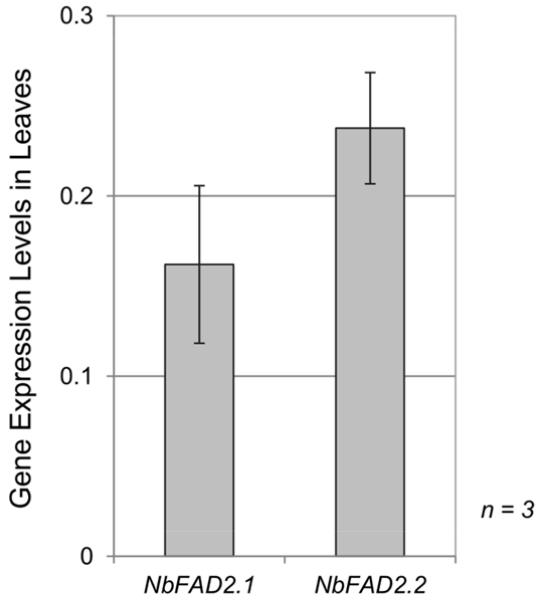
Gene Expression Levels in Leaves
0.3
0.2
0.1
0
n = 3
NbFAD2.1
NbFAD2.2

E

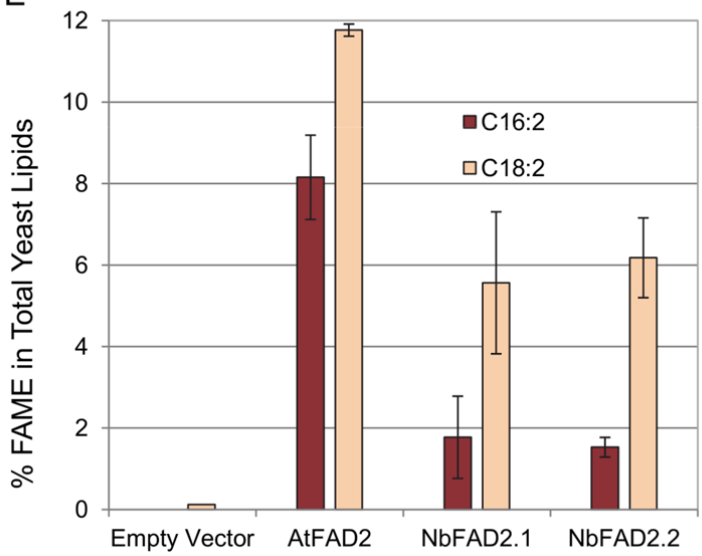
% FAME in Total Yeast Lipids
12
10
8
6
4
2
0
C16:2
C18:2
Empty Vector
AtFAD2
NbFAD2.1
NbFAD2.2

F

(i) Empty Vector

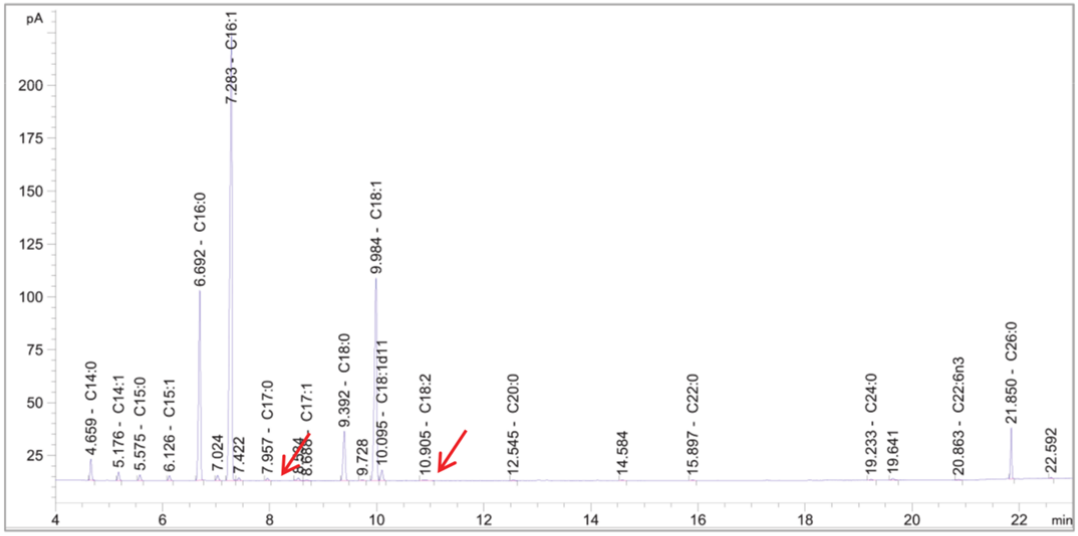

(ii) AtFAD2

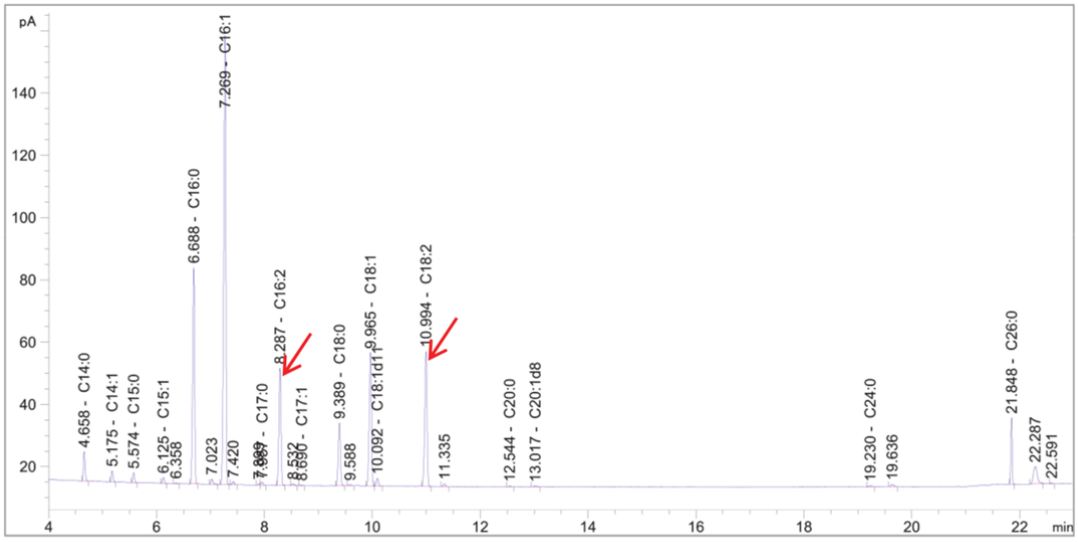

(iii) NbFAD2.1

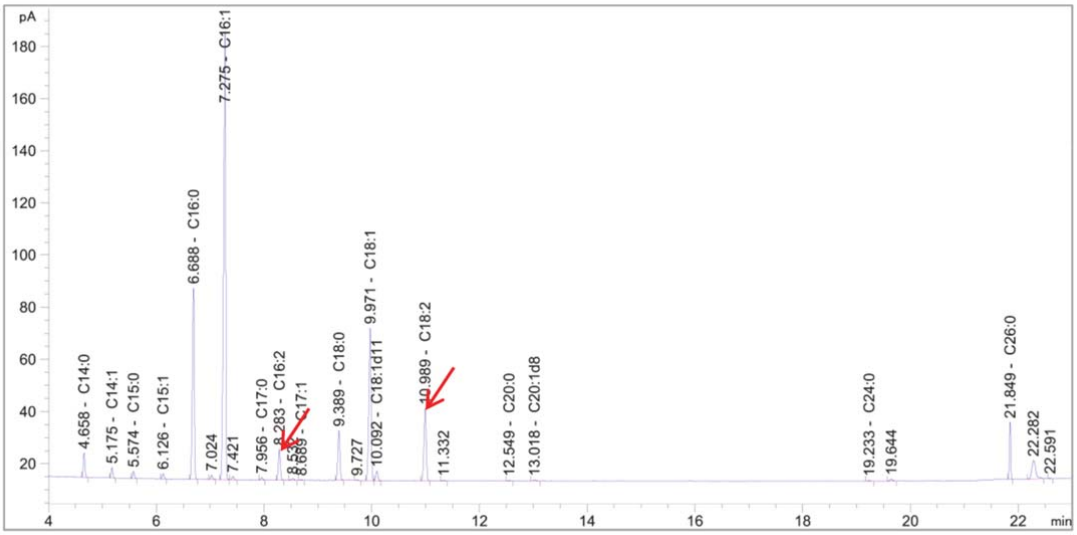

(iv) NbFAD2.2

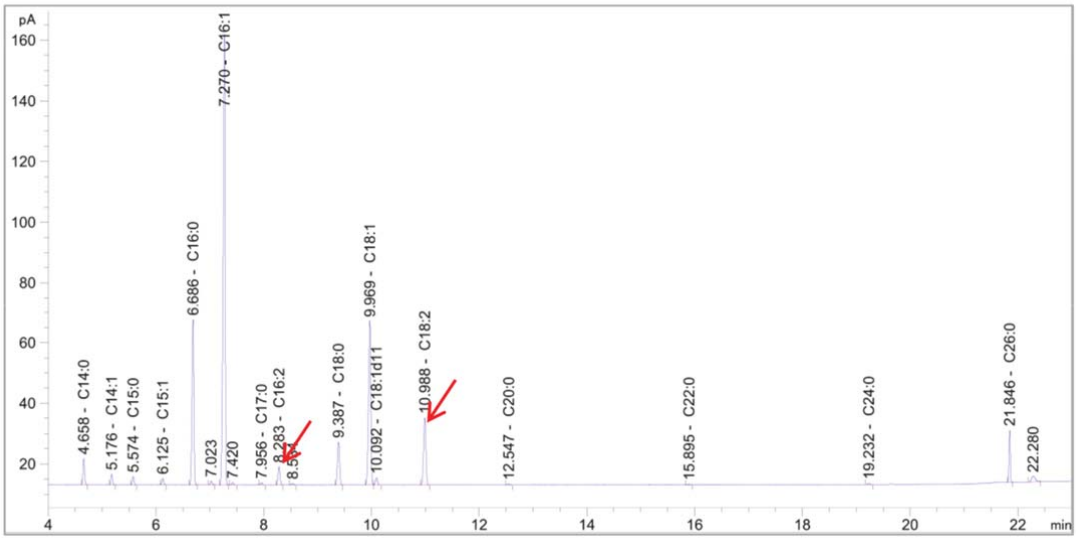

Figure 2.3. The *FAD2* gene family in *N.benthamiana*.

A. Alignment of ORFs of *NbFAD2.1* and *NbFAD2.2*.

B. Amino acid alignment of NbFAD2.1 and NbFAD2.2. Three unique histidine boxes required for desaturase activity underlined in red.

C. Phylogenetic analysis of *FAD2* genes from *N.benthamiana*, *A.thaliana* and other plant species. MEGA5 was used to analyse protein sequences and tree constructed by Neighbour joining. The bootstrap values for each node indicate percentage of bootstrap replicates that support the respective node in 1000 samples. Plants species used include the following: *Nicotiana benthamiana*, *Nicotiana tabacum*, *Solanum commersonii*, *Olea europaea*, *Arabidopsis thaliana*, *Brassica juncea*, *Brassica carinata*, *Brassica rapa* and *Brassica napus*.

D. Expression levels of *NbFAD2.1* and *NbFAD2.2* measured in mid-sized *N.benthamiana* leaves using qRT-PCR. Expression levels normalised against expression of *NbGAPDH*. Data shown are means of three biological replicates with three technical repeats for each. Error bars are the standard errors of the mean.

E. FAME extracted from yeast expressing *NbFAD2.1* and *NbFAD2.2*. Desaturase activity examined by production of 16:2 and 18:2 and compared to activity of AtFAD2.

F (i – iv). Chromatogram of FAME extracted from a representative yeast clone used for assessment of desaturase activity in **E**. Red arrows used to indicate appearance of new fatty acid peaks.

2.2.4 Efficient silencing of the endogene NbFAD2 *in* N.benthamiana *leaves*

The next area of inquiry was transient endogene silencing in *N.benthamiana*. The first gene family investigated by silencing was *NbFAD2*. FAD2 is a membrane bound Δ12-desaturase, located in the ER, which catalyses the conversion of 18:1 into 18:2 on the PC lipid head group. A 660 bp hpRNA construct (hpNbFAD2) was designed against the ORF of *NbFAD2.1* and used in infiltration assays to silence *NbFAD2* (Fig 2.4A). The sequence of the hpRNA construct covers the three conserved histidine boxes common between *NbFAD2.1* and *NbFAD2.2*. A shorter hpRNA, hpNbFAD2-300, was designed against a central portion of *NbFAD2.1*, which is more divergent in sequence from *NbFAD2.2* (Fig 2.4A). Both hpNbFAD2 and hpNbFAD2-300 were infiltrated in leaves and qRT-PCR analysis revealed that both *NbFAD2.1* and *NbFAD2.2* were silenced by infiltration of hpNbFAD2 (Fig 2.4B). The shorter hpNbFAD2-300 silenced *NbFAD2.1* gene expression to the same degree as the longer hpRNA, but was much more specific against *NbFAD2.1*, being only partially active in silencing *NbFAD2.2* gene expression (Fig 2.4B).

The leaves infiltrated with hpNbFAD2 and hpNbFAD2-300 were also assessed for changes in their fatty acid profiles. Total leaf lipids were extracted from infiltrated leaves and the changes in the level of 18:1 suggest that hpNbFAD2 is more effective in increasing 18:1, an increase from 2.3% in 'mock' control leaves to 13.8% in leaves infiltrated with hpNbFAD2. hpNbFAD2-300 partially silences NbFAD2 activities, increasing 18:1 to 5.6%, a result consistent with the qRT-PCR results. FAME analysis also revealed that infiltration of *A.tumefaciens* alone also had an effect on the lipid profile of the leaf – the relative percentage of 18:2 increased from ~10% in un-infiltrated leaf tissue to ~12% in leaves infiltrated with *A.tumefaciens* (data not shown). The basis of this lipid profile change was not investigated further, although leaf tissues infiltrated with *A.tumefaciens* ('mock') were used as controls instead of wild-type un-infiltrated leaf tissue throughout the study.

The effects of V2 and p19 on the processing of hpNbFAD2 were assessed by measuring the levels of 18:1 on the PC fraction. Leaves infiltrated with combinations of hpNbFAD2 and either V2 or p19 were harvested 5 dpi (Fig 2.4D). Total leaf lipids were extracted from dry leaf tissue using the protocol described by Bligh & Dyer (1959) and the PC fraction was extracted using a two-dimensional (2D) TLC system (Wood et al., 2009). The 2D TLC system ensures an ideal separation of polar lipids (such as PC, MGDG and DGDG) from other polar

and non-polar lipids. The combination of hpNbFAD2 and V2 increased the 18:1 content on PC to over 25%, while the combination of p19 and hpNbFAD2 increased 18:1 content to ~17%. The increase in 18:1 content is mostly reflected in a decrease in 18:2-PC, and the other major fatty acids (16:0 and 18:3) were largely unaffected. DGDG fraction is a group of polar lipids found in the chloroplast – it was also extracted from the lipid samples used for PC analysis (Fig 2.4E) and no significant changes were observed in its the fatty acid profile. The FAME profile of DGDG confirmed that the activity of NbFAD2 is limited to modification of 18:1 on PC and its silencing does not affect the fatty acid profile of DGDG, a fraction dominated by 18:3.

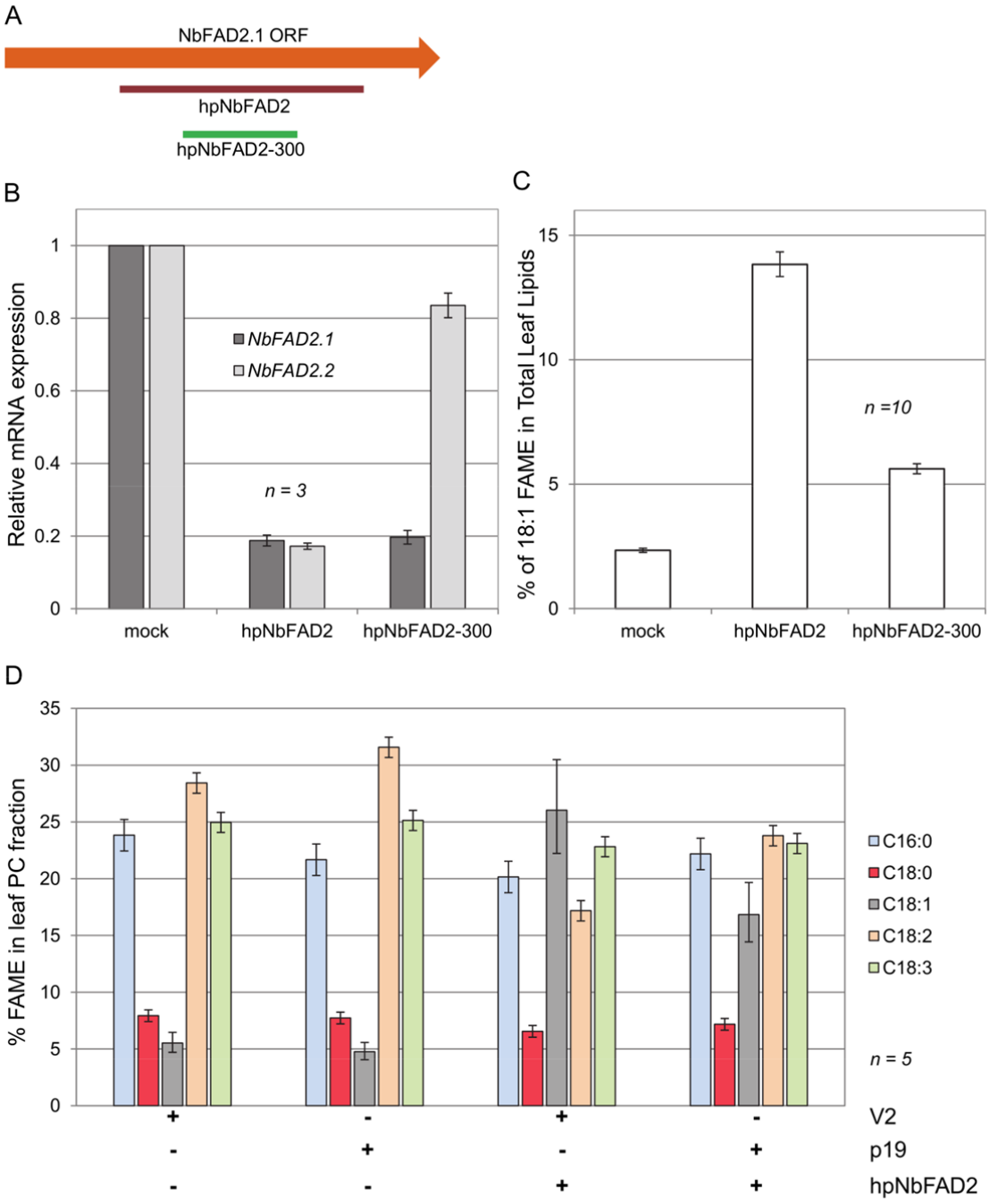
A
NbFAD2.1 ORF
hpNbFAD2
hpNbFAD2-300
B
Relative mRNA expression
NbFAD2.1
NbFAD2.2
n = 3
mock
hpNbFAD2
hpNbFAD2-300
C
% of 18:1 FAME in Total Leaf Lipids
n =10
mock
hpNbFAD2
hpNbFAD2-300
D
% FAME in leaf PC fraction
C16:0
C18:0
C18:1
C18:2
C18:3
n = 5
V2
p19
hpNbFAD2

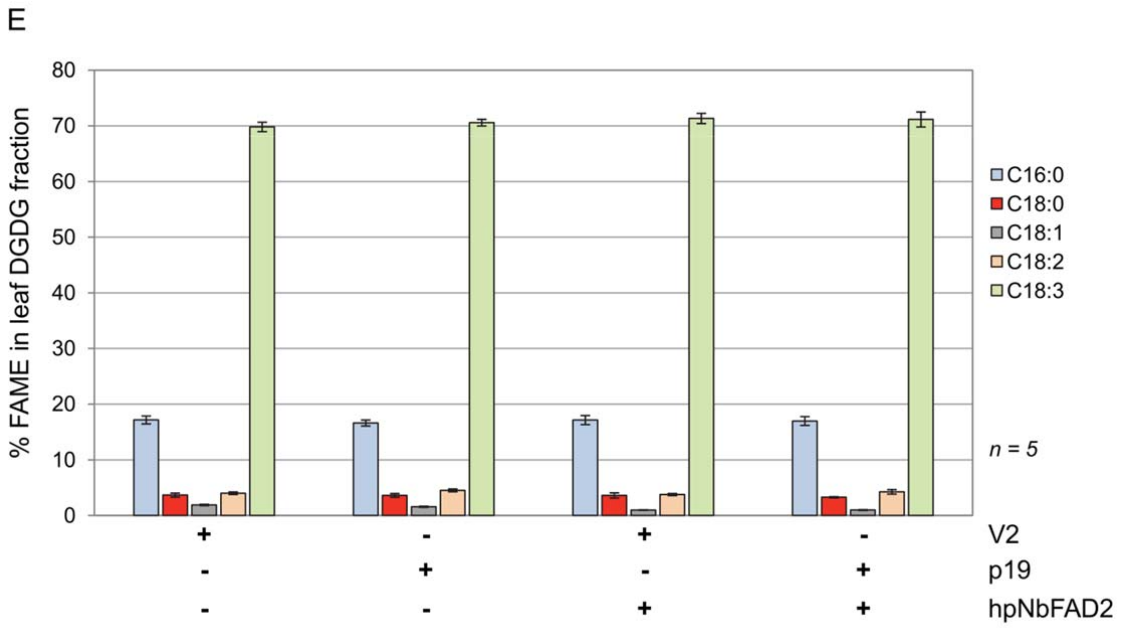

Figure 2.4. Effective silencing of the *FAD2* gene family in *N.benthamiana* leaves.

A. Relative position and length of the 660 bp hpRNA (hpNbFAD2) and the 300 bp hpRNA (hpNbFAD2-300) against *NbFAD2.1*.

B. Reduction in expression levels of *NbFAD2.1* and *NbFAD2.2* when silenced using hpNbFAD2 and hpNbFAD2-300 hpRNA constructs. Total RNA extracted from leaves infiltrated with the different hpRNA constructs and expression levels of *NbFAD2.1* and *NbFAD2.2* were analysed by qRT-PCR, 4 dpi. Mock represents RNA extracted from leaf tissue infiltrated with *A.tumefaciens* only. Data shown are means of three biological replicates with three technical repeats for each. Error bars are the standard errors of the mean.

C. The total leaf lipids of leaves infiltrated with either hpNbFAD2 or hpNbFAD2-300 were analysed. FAME extracted 4 dpi and the data shown are the mean and 5% LSD bars calculated from ten independent leaf infiltrations per treatment. When the LSD bars for two metabolites fail to overlap, the metabolite means may be regarded as significantly different at the 5% level of significance. Mock refers to leaves infiltrated with *A.tumefaciens* only.

D. Fatty acid profile of PC fraction extracted from leaves infiltrated with combinations of V2, p19 and hpNbFAD2. Data shown are the mean and 5% LSD bars calculated from at least five infiltrations. When the LSD bars for two metabolites fail to overlap, the treatments may be regarded as significantly different at the 5% level of significance.

E. The fatty acid profile of the leaf DGDG fraction extracted from the infiltrated leaf samples used for PC analysis in **D**. Data shown are the mean and standard error of the mean.

2.2.5 Deep sequencing analysis of the sRNA population generated by hpNbFAD2 against NbFAD2.1 *and* NbFAD2.2

The sRNAs generated by the 660 bp hpNbFAD2 in the transient leaf assay system were analysed by 'deep' sequencing approaches (Fig 2.5). sRNA library was generated using the Illumina TruSeq kit and deep sequencing was performed on the GLX platform using 36 base reads (see methods for details). This revealed that sRNA populations generated from the transient overexpression of the 660 bp hpRNA were exclusively confined to the region of the hpRNA, with no sRNA reads mapping to *NbFAD2.1* outside of the primary target region (Fig 2.5A). The sRNA populations mapped unevenly across the target region of the hpRNA and the distribution and abundance of the reads were different for each size class (20-24 nt). Another study has also described the uneven distrubtion of hpRNA generated sRNA across a target region (Zhao and Song). The 21 and 22 nt size classes dominated the overall profile in each orientation (Fig 2.5B) and respectively accounted for approximately 42% (2299484) and 33% (1809853) of the population analysed.

It was surprising that very few sRNA aligned to the *NbFAD2.2* sequence, given that hpNbFAD2 reduces the transcript of *NbFAD2.2* drastically. However a significant number of sRNA aligned on the forward and reverse strands of *NbFAD2.2* when 3-mismatch flexibility was allowed between the alignments (Fig 2.5C). The plot revealed that when there were 3-mismatches, a higher number of sRNA aligned on the forward and reverse strands of *NbFAD2.1* as well (around 10 times more). sRNA-driven silencing does not have to follow a stringent sequence match with the target genes and there are rules described for up to 6-mismatches (Horn and Waterhouse, 2010). Appendix Table A contains absolute numbers of sRNA aligning to *NbFAD2.1* and *NbFAD2.2* with 0- and 3-mismatches.

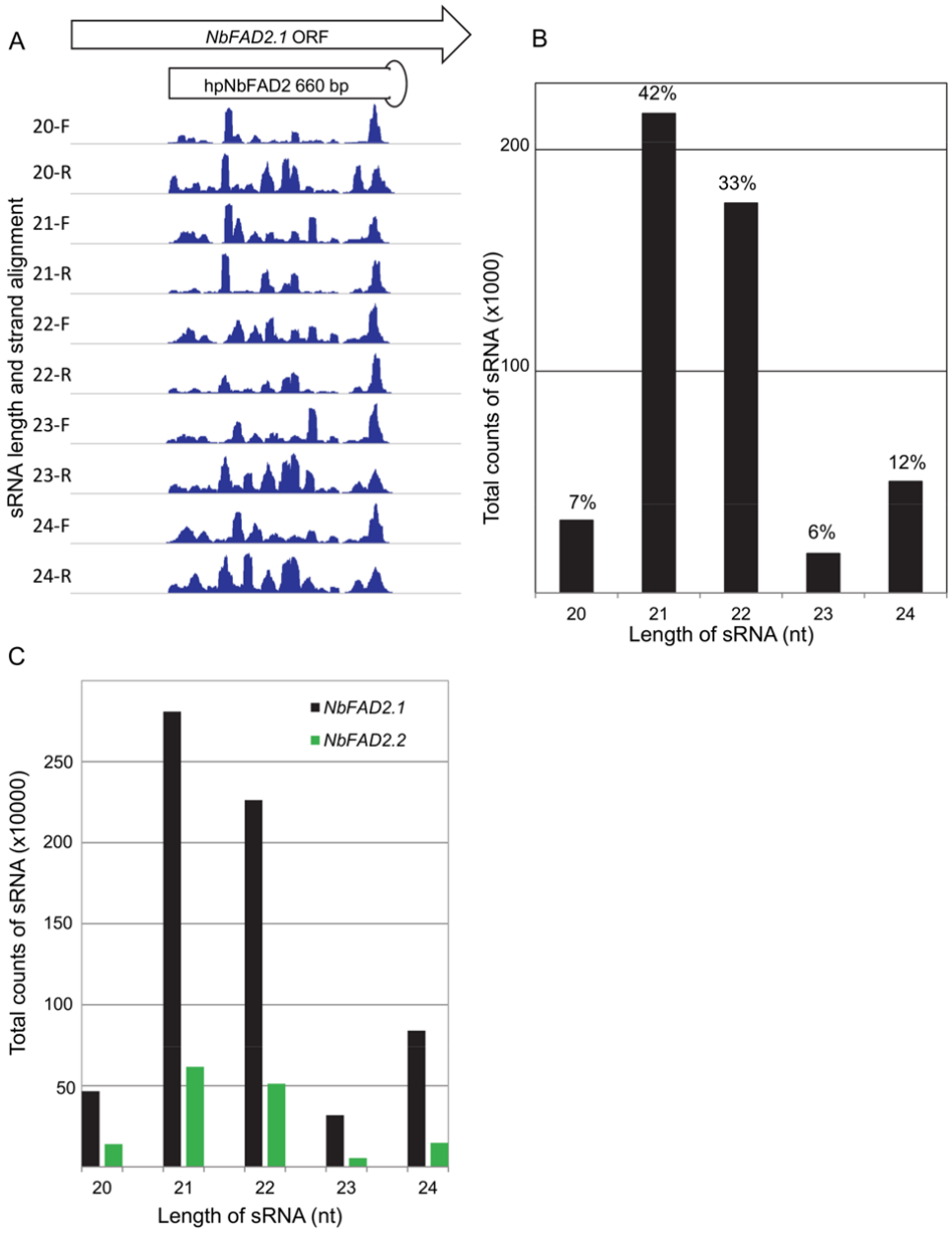

Figure 2.5. sRNA population generated by hpRNA, hpNbFAD2, targeting the endogene *NbFAD2*.

A. The ORF of *NbFAD2.1* portrayed indicating the region used to generate hpNbFAD2. Total RNA was extracted from leaves infiltrated with hpNbFAD2, 4 dpi. The size and distribution of the dominant classes of sRNAs on the forward (F) and reverse (R) strand of the *NbFAD2.1* is illustrated. Absolute read coverage was normalised for each track.

B. Absolute numbers and relative percentages of the dominant sRNA size classes generated by hpNbFAD2.

C. The number of sRNA aligned to the forward and reverse strands of *NbFAD2.1* and *NbFAD2.2* with 3-mismatches between the nucleotide sequences of target gene and sRNA.

2.2.6 Engineering N.benthamiana *leaf lipid pathways with silencing of endogenes and overexpression of transgenes*

2.2.6.1 Changes in total leaf TAG amount and in the composition of leaf TAG

An example of metabolic engineering is outlined in Figure 2.6A & 2.6B – in that example, the steady-state flux of lipids in the host plant is shunted into a transgene-engineered pathway by the concomitant silencing of an endogene. The hpNbFAD2 construct was used to reduce NbFAD2 activity in infiltrated *N.benthamiana* leaves to elevate 18:1 levels for downstream modification by AtFAE1 and AtDGAT1. Combinations of the hpNbFAD2 and overexpression constructs AtFAE1, AtDGAT1, p19 and/or V2 were *A.tumefaciens*-infiltrated into *N.benthamiana* leaves and the production of leaf oils and their composition analysed (Fig 2.6C). Leaf oil was measured by extracting the fatty acids found in the TAG fraction of total leaf lipids. The composition of the leaf oils is a reflection of the AtFAE1 activity and the amount of leaf oil is dependent upon the activity of the AtDGAT1.

In this study 'mock' refers to leaves infiltrated with *A.tumefaciens* only. In mock control leaves, 18:1 comprised only 1.1% of the leaf oils and there were no detectable levels of 20:1 (Fig 2.6C, upper panel; Table 2.1 for a complete range of fatty acids detected in the extracts). Co-infiltration of AtFAE1 and AtDGAT1 constructs without any VSP or hpRNA resulted in 2.2% 18:1 and 1.7% 20:1, indicating that some overexpression of *AtFAE1* is possible without any VSP added. The inclusion of hpNbFAD2 in combination with AtFAE1 and AtDGAT1 resulted in an increase to 15.4% of 18:1 in the total fatty acid profile and 10.2% of 20:1 in leaf oils. The inclusion of p19 in combination with hpNbFAD2, AtFAE1 and AtDGAT1 resulted in only 8% 18:1, almost half of the oleic acid composition of the hpRNA alone. Using V2 in combination with hpNbFAD2, AtFAE1 and AtDGAT1 resulted in 14.4% 18:1 and 13% 20:1 in leaf oils. This level of 20:1 is approximately 40% higher than that obtained using p19. It is surprising that hpNbFAD2 alone, with no VSP added, was also able to enhance shunting of lipids into new metabolites (Fig 2.6C) although the total elongated products (20:1 and 22:1) are no greater than those resulting from the use of p19 (Table 2.1). The largest increase in leaf oil content (Fig 2.6C, lower panel) was using the combination of V2, hpNbFAD2, AtDGAT1 and AtFAE1 – this produced 14.1 μg/6 mg dry leaf tissue compared to assays with only the combination of AtFAE1 and AtDGAT1, which produced 4.4 μg/6 mg

dry leaf tissue. The combination of p19, hpNbFAD2, AtDGAT1 and AtFAE1 produced an oil content of 11.1 µg/6 mg dry leaf tissue and the combination of hpNbFAD2, AtDGAT1 and AtFAE1 produced 9.5 µg/6 mg dry leaf tissue.

2.2.6.2 Changes in the fatty acid profile of total leaf lipids

Direct methylation of infiltrated leaf tissue is a simpler method to determine the changes in lipid metabolism in transient assays. *N.benthamiana* leaves infiltrated with combinations of hpNbFAD2, AtDGAT1, AtFAE1, V2 and p19 were harvested 5 dpi and dry leaf tissues methylated to produce FAME (Fig 2.6D). The figure shows that a VSP is not required for effective silencing of *NbFAD2* – the increase in the level of 18:1 from 1.4% to ~13% in leaf tissue infiltrated with hpNbFAD2 and AtDGAT1 is the same as that seen with the combination of V2, hpNbFAD2 and AtDGAT1. The statistical analysis of data reinforces that a VSP is not required for efficient silencing of endogene *NbFAD2*. It also shows that V2 does not interfere with the processing of hpRNA construct and allows for better overexpression of other transgenes – for example, 4.5% 20:1 produced in the leaf tissues infiltrated with hpNbFAD2 and AtFAE1 increases to 5.3% with the addition of V2. This dataset is in agreement with the previously described leaf PC and TAG analysis, showing that p19 is not the ideal choice of VSP for simultaneous silencing (8.5% 18:1) and overexpression assays (3.8% 20:1) (Fig 2.6D). These results indicate overall that the use of p19 in transient leaf assays only allows partial silencing of endogenous *NbFAD2*, approximately 66% of the level attained with the use of V2.

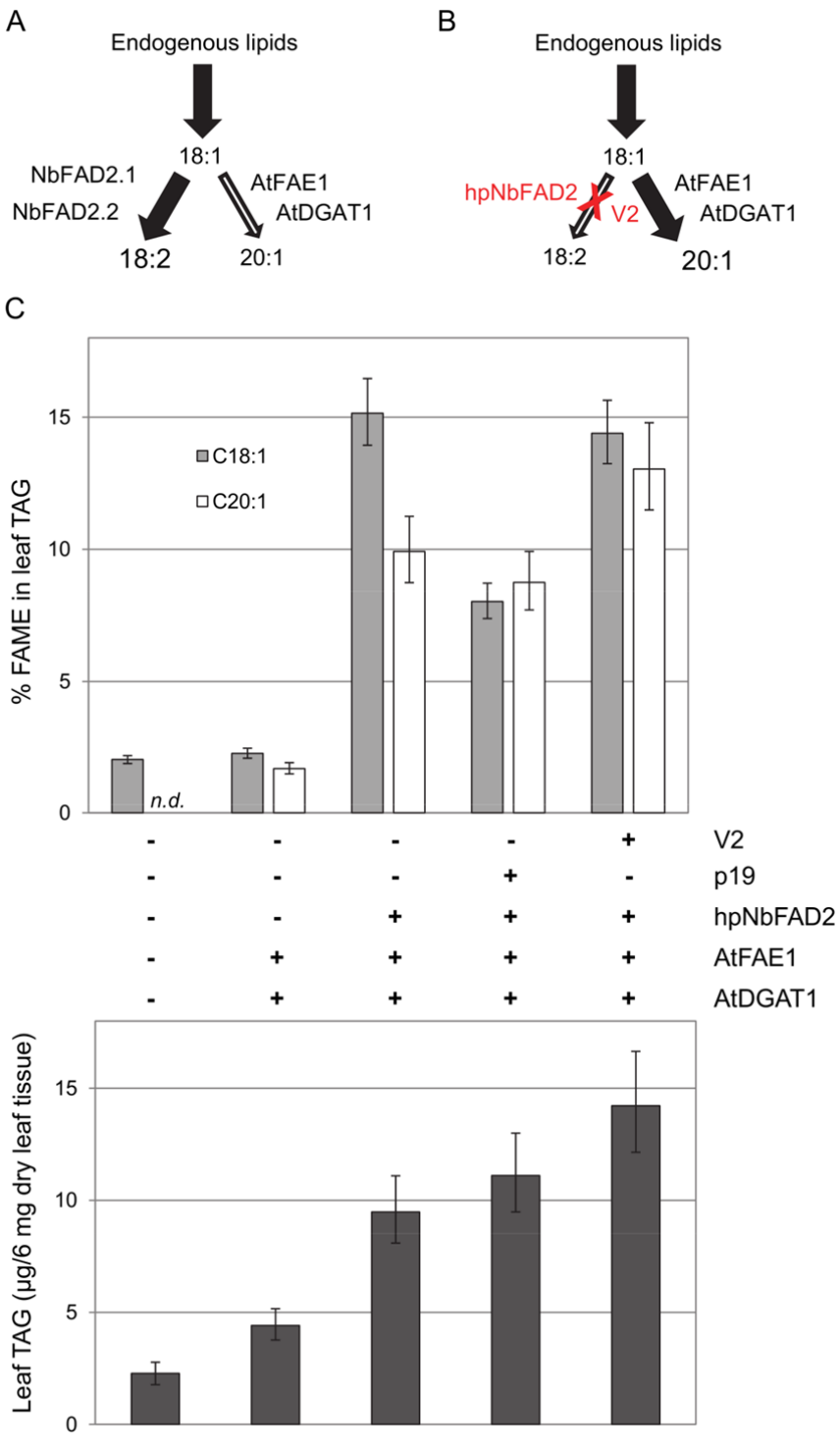
A
Endogenous lipids
18:1
NbFAD2.1
NbFAD2.2
AtFAE1
AtDGAT1
18:2
20:1
B
Endogenous lipids
18:1
hpNbFAD2
V2
AtFAE1
AtDGAT1
18:2
20:1
C
% FAME in leaf TAG
C18:1
C20:1
n.d.
V2
p19
hpNbFAD2
AtFAE1
AtDGAT1
Leaf TAG (µg/6 mg dry leaf tissue)

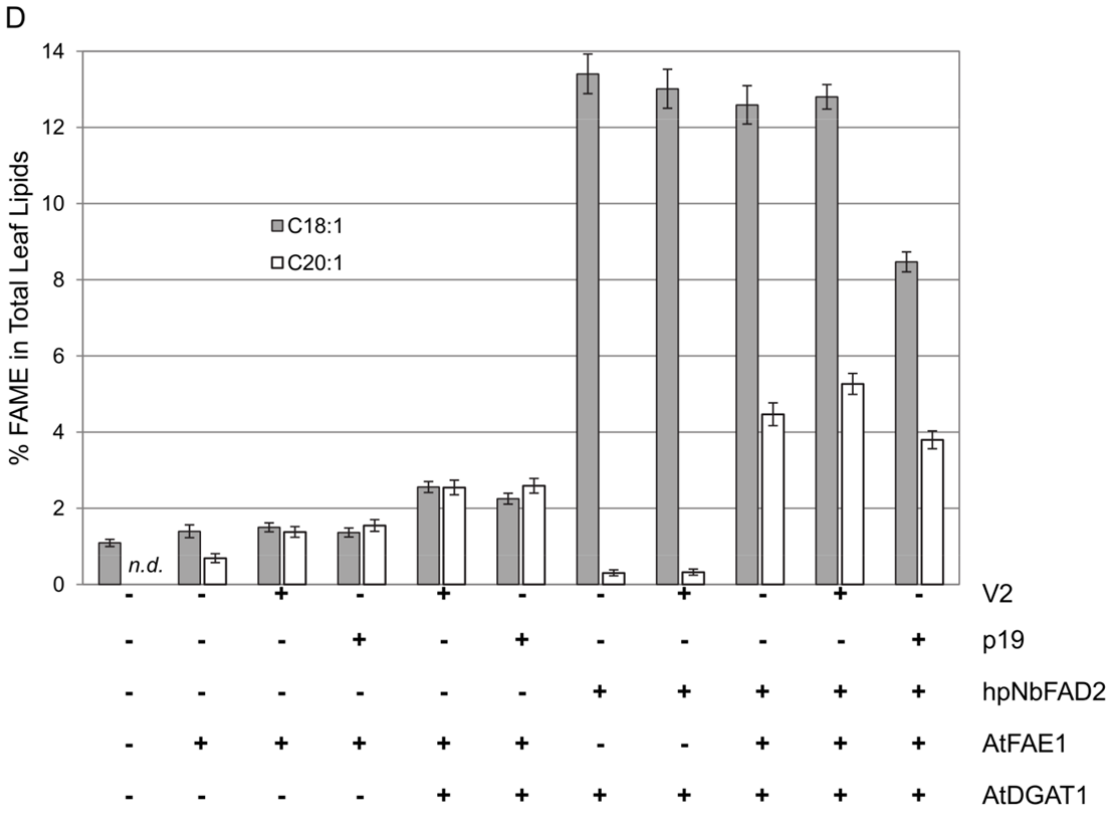

Figure 2.6. Shunting a metabolite into a transgenic pathway by silencing an endogene.

A. Diagram outlining the flux of lipid metabolites from 18:1 to 18:2, via endogene NbFAD2, limiting the availability of 18:1 to enter into transgenic pathways, such as that catalysed by AtFAE1 and AtDGAT1 to produce 20:1.

B. Diagram outlining the efficient hpRNA driven (hpNbFAD2) silencing of endogene NbFAD2 to increase the flux of 18:1 into the engineered pathway to produce 20:1, where both silencing and transgene overexpression are supported with the addition of V2.

C. Combinations of hpNbFAD2, V2 or p19, and a two-step metabolic pathway (AtFAE1 and AtDGAT1), used for the production of oil (lower panel), and the weight percentage of 18:1 and 20:1 in the total FAME in the oil (upper panel). Data shown are the mean and 5% LSD bars calculated from 4–6 infiltrations per treatment. When the LSD bars for two metabolites fail to overlap, the metabolite means may be regarded as significantly different at the 5% level of significance.

D. FAME of total leaf lipids extracted from leaves infiltrated with combinations of hpNbFAD2, AtFAE1, AtDGAT1, p19 and V2. Leaves were harvested 5 dpi. The relative percentages of 18:1 and 20:1 are plotted. Data shown are the mean and 5% LSD bars calculated from 4–10 infiltrations per treatment. When the LSD bars for two metabolites fail to overlap, the metabolite means may be regarded as significantly different at the 5% level of significance.

	% FAME in leaf TAG fraction									
T-DNA constructs	**16:0**	**16:3$^{\Delta 9,12,15}$**	**18:0**	**18:1$^{\Delta 9}$**	**18:2$^{\Delta 9,12}$**	**18:3$^{\Delta 9,12,15}$**	**20:0**	**20:1**	**22:0**	**22:1**
AtFAE1/AtDGAT1	23.3 ± 1.5	3.9 ± 0.2	8.6 ± 0.6	2.2 ± 0.2	19.1 ± 0.2	34.7 ± 1.4	4.5 ± 0.2	1.7 ± 0.2	0.4 ± 0.2	0.7 ± 0.4
AtFAE1/DGAT1/hpNbFAD2	17.8 ± 1.0	2.0 ± 0.4	7.8 ± 0.6	15.4 ± 0.8	9.4 ± 0.4	24.1 ± 1.6	6.5 ± 0.5	10.2 ± 1.0	0.9 ± 0.1	4.2 ± 0.8
AtFAE1/DGAT1/hpNbFAD2/p19	15.4 ± 0.7	1.6 ± 0.3	6.0 ± 0.4	8.1 ± 0.2	16.2 ± 0.3	23.0 ± 1.5	10.2 ± 0.7	8.7 ± 0.4	1.3 ± 0.1	6.2 ± 0.4
AtFAE1/DGAT1/hpNbFAD2/V2	14.4 ± 0.8	1.2 ± 0.1	5.5 ± 0.2	14.5 ± 0.8	10.4 ± 0.4	21.2 ± 0.6	8.9 ± 0.4	13.1 ± 0.9	1.0 ± 0.1	7.4 ± 0.2

Table 2.1. The complete fatty acid profile of TAG fraction extracted from infiltrated *N.benthamiana* leaves.

Leaves infiltrated with combinations of hpNbFAD2, V2 or p19, and a two-step metabolic pathway (AtFAE1 and AtDGAT1) for production of modified oils. The table outlines the changes in endogenous metabolite levels and the production of elongated products due to expression of *AtFAE1*. Standard error of the mean was also calculated, p = 0.05%.

2.2.6.3 High levels of 18:1 shunted to production of dihydrosterculic acid and elongated dihydrosterculic acid in N.benthamiana leaves

Cyclopropane fatty acid synthases (CPFAS) are a class of enzymes that use 18:1 as a substrate (Bao et al., 2002), therefore CPFAS activity may benefit from shunting of 18:1. CPFAS catalyse the cyclopropanation of 18:1 on the *sn*-1 position of PC to produce dihydrosterculic acid (DHSA). The *CPFAS* from *Gossypium hirsutum* (*GhCPFAS*), previously described by Yu et al. (2011) as *GhCPS1*, was overexpressed to produce DHSA in *N.benthamiana* leaves (Fig 2.7B). The possibility of elongating DHSA into elongated DHSA (eDHSA) was also assessed by infiltrating GhCPFAS with AtFAE1 (Fig 2.7A). The double bond at the Δ9 position of oleic acid is cyclopropanated by GhCPFAS (Fig 2.7A).

A 35S-driven binary construct of GhCPFAS was used in subsequent infiltrations. *N.benthamiana* leaves were infiltrated with combinations of GhCPFAS, V2, hpNbFAD2, AtDGAT1 and AtFAE1 and leaves were harvested 5 dpi. AtOleosin (*A.thaliana* Oleosin) and AtDGAT1 were both infiltrated to produce oil bodies in the leaf. Oleosins have been shown to stabilise oil bodies and increase leaf oil content (Siloto et al., 2006; Winichayakul et al., 2013), however preliminary results (data not shown) suggested that the addition of AtOleosin in this instance did not have an observable effect on the oil profile and was therefore not included in the subsequent infiltrations.

Total leaf lipids were extracted from ~10 mg of dry leaf tissue as described previously (Bligh and Dyer, 1959). An extract equivalent to 4 mg of dry leaf tissue was subjected to basic methylation and FAMEs extracted in hexane. Sodium methoxide in anhydrous methanol was used for transesterification of leaf lipids – this solution has been reported to be the most efficient in methyl esterification of CPFA, however it is not suitable for esterification of free fatty acids (Grogan and Cronan, 1997). The FAME profile of total leaf lipids revealed that 1.5% of 18:1 was utilised by GhCPFAS to produce 1.0% of DHSA (Fig 2.7B). The addition of hpNbFAD2 increased levels to 8.9% of 18:1 resulting in the production of 5.3% of DHSA (Fig 2.7B). The addition of AtDGAT1 saw an increase in both 18:1 to 9.5% and DHSA to 6.2%. The efficiency of GhCPFAS in cyclopropanating 18:1 was 40%, 44% and 43% in leaves infiltrated with GhCPFAS/V2, GhCPFAS/V2/hpNbFAD2 and GhCPFAS/V2/hpNbFAD2/AtDGAT respectively.

Previous studies have monitored the appearance of fatty acids in the CoA pool using elongases and fatty acid reductases that work exclusively in it (Doan et al., 2012). The AtFAE1 enzyme is well known to elongate saturated and 18:1 substrates as previously described (Fig 2.1C, 2.6C & 2.7B), so the ability of AtFAE1 to elongate DHSA in the CoA pool and generate an elongated DHSA product (eDHSA) was assessed (Fig 2.7A). The FAME of total leaf lipids showed that DHSA was elongated by AtFAE1 in the CoA pool, which resulted in 0.4% eDHSA (Fig 2.7B). The structure of eDHSA was confirmed using GC-MS techniques (chromatogram not shown, validated by Kath Damcevski, Division of Ecosystem Sciences, CSIRO). 1.0% 20:1 was also measured in the same infiltrated leaf tissue. Addition of AtDGAT1 did not change the relative percentage of eDHSA, however 20:1 increased to 1.8% (Fig 2.7B).

The PC fraction of the total leaf lipid extracts were isolated using 2-D TLC system as previously described. 5.0% DHSA was detected on PC in leaves infiltrated with V2 and GhCPFAS and the addition of hpNbFAD2 increased DHSA to 24.8% (Fig 2.7C). The combination of V2, hpNbFAD2, GhCPFAS and AtFAE1 resulted in a decrease in the relative percentage of DHSA to 19.6% due to the appearance of the elongated products of AtFAE1 detected on PC, 3.6% 20:1 and 1.4% eDHSA (Fig 2.7C).

The TAG fraction of total leaf lipids infiltrated with combinations of GhCPFAS, hpNbFAD2, V2 and AtDGAT1 was extracted using a two-phase TLC system. The FAME profile of leaf TAG revealed that leaves infiltrated with V2, AtDGAT1 and GhCPFAS contained 5.5% 18:1 and 6.2% DHSA in leaf oil (Fig 2.7D). The addition of hpNbFAD2 to the combination increased levels to 14.0% 18:1 and 14.5% DHSA (Fig 2.7D).

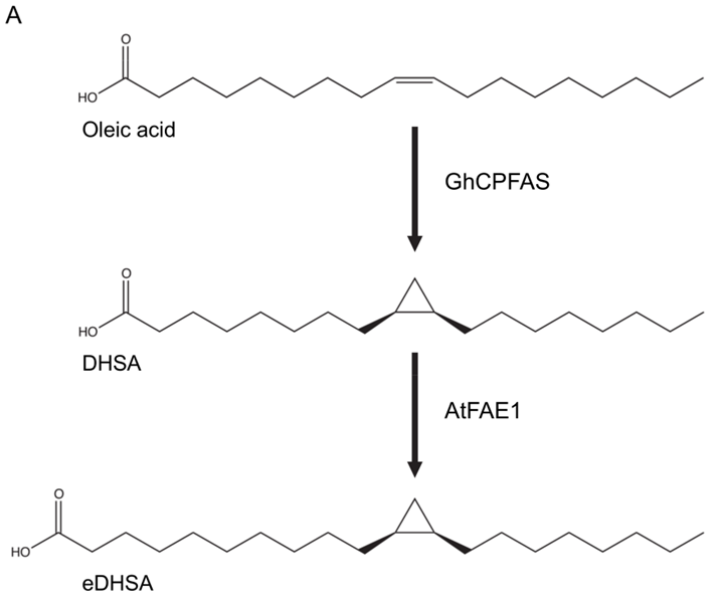
A
Oleic acid
GhCPFAS
DHSA
AtFAE1
eDHSA

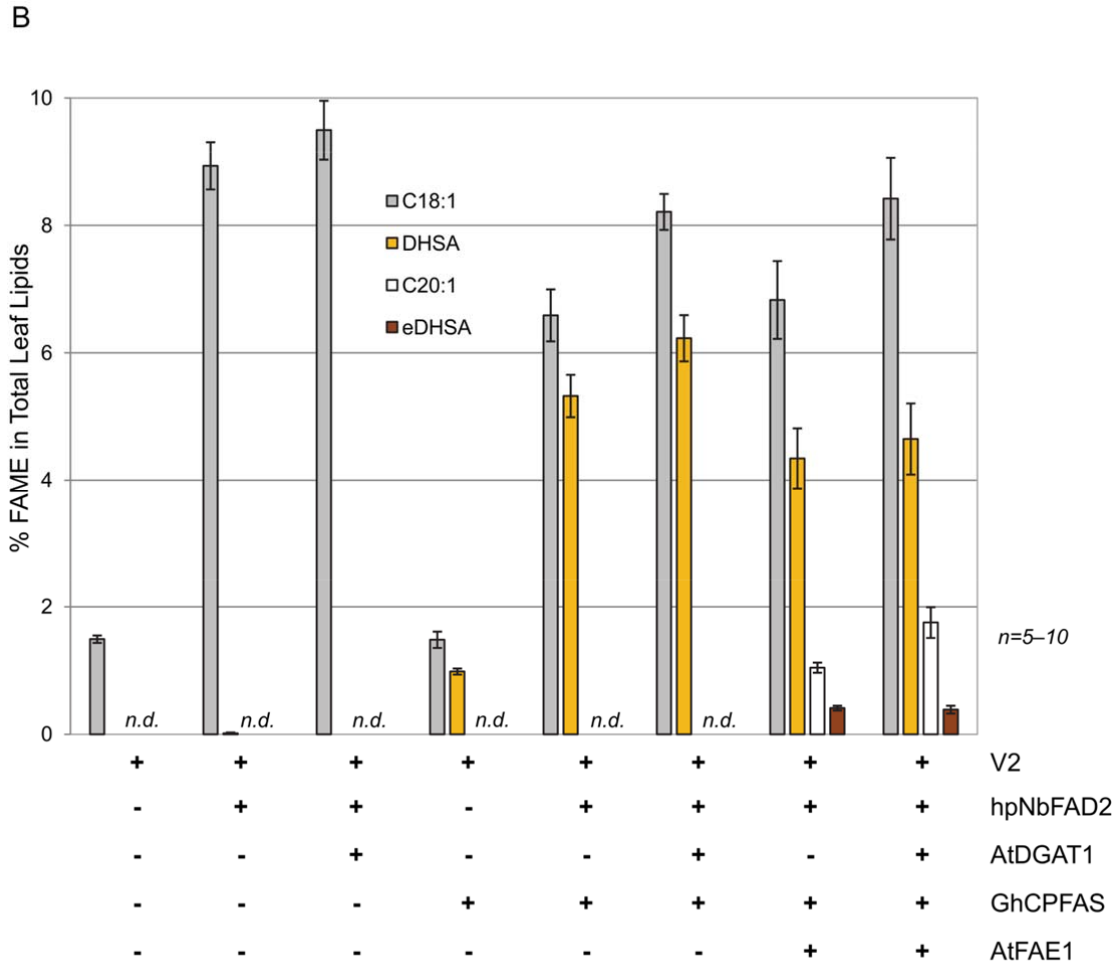
B
% FAME in Total Leaf Lipids
C18:1
DHSA
C20:1
eDHSA
n.d.
n=5–10
V2
hpNbFAD2
AtDGAT1
GhCPFAS
AtFAE1

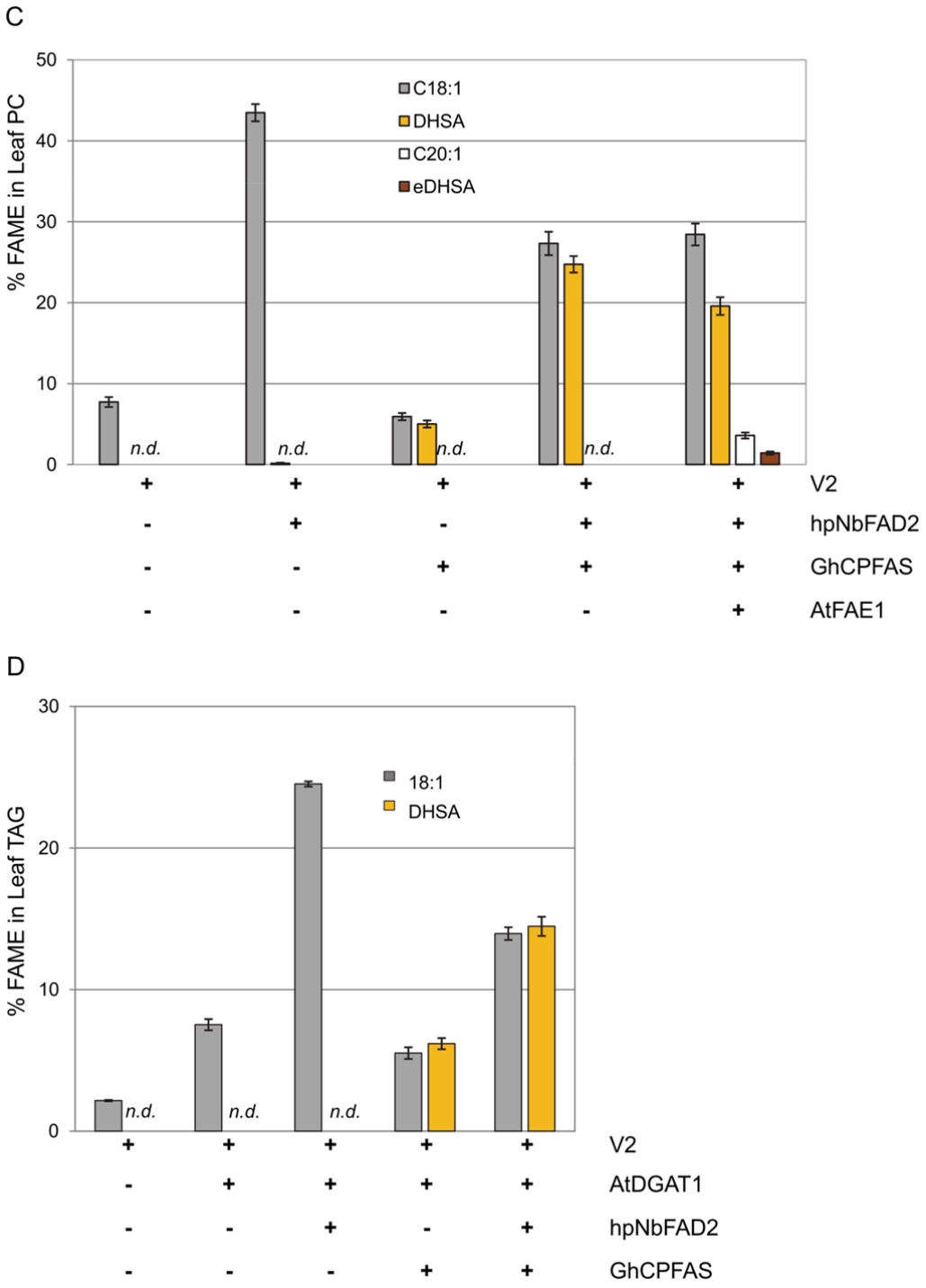

Figure 2.7. *N.benthamiana* leaves engineered to produce significant amounts of DHSA and eDHSA.

A. Schematic of conversion of 18:1 to DHSA. The double bond at Δ9 position of 18:1 is cyclopropanated by the GhCPFAS. Addition of a second enzyme, AtFAE1, elongates DHSA to eDHSA.

B. Total FAME extracted from leaves infiltrated with combinations of V2, hpNbFAD2, GhCPFAS, AtDGAT1 and AtFAE1. Leaves were harvested 5 dpi. Data shown are the means and standard errors calculated for 5–10 samples per treatment.

C. FAME of leaf PC and extracted from leaves described in **B**. Treatments that had AtDGAT1 were excluded from PC analysis.

D. Total oil extracted from leaves infiltrated with combinations of V2, AtDGAT1, hpNbFAD2 and GhCPFAS. Leaves were harvested 5 dpi. Data shown are the means and standard errors calculated for 5–8 samples per treatment.

2.2.7 Silencing of NbFAD2 *with different size hpRNA constructs targeting different regions of* NbFAD2

hpNbFAD2, which targets 660 bp fragment of *NbFAD2* and covers a central portion of the endogene, was effective in raising 18:1 levels in transient assay formats. The genome databases of *N.benthamiana* indicated that at least two different *FAD2* genes are expressed in *N.benthamiana* leaves, *NbFAD2.1* and *NbFAD2.2,* which were also shown to be targeted by hpNbFAD2. It was therefore of interest to specifically target different regions of *NbFAD2.1* as well as the 3'UTR regions of *NbFAD2.1* and *NbFAD2.2* to gauge their contribution to 18:1 desaturation in *N.benthamiana* leaves. HpRNA constructs targeting various different regions of *NbFAD2.1* were designed to explore the effectiveness of shorter hpRNAs in the silencing of endogenes in transient assay formats. The 660 bp hpRNA was compared to five shorter hpRNAs spanning 300 bp regions on *NbFAD2.1,* including the intron positioned within the 5'UTR (300a), three different regions of the ORF (300b, hpNbFAD2-300 and 300d) and the 3'UTR (300e) (Fig 2.8A, upper panel). The hpRNA constructs against *NbFAD2.1* were co-infiltrated with V2 and AtDGAT1 and the composition of the leaf lipids then measured to assess the ability of hpRNA molecules to silence the *NbFAD2* gene family (Fig 2.8A). Infiltrated leaf tissues were harvested 4 dpi and freeze-dried overnight. Leaf lipids were extracted as FAME and analysed using GC. In this study 'mock' refers to leaves infiltrated with V2 and AtDGAT1 only. Changes in the percentage composition of 18:1 content of infiltrated leaves were analysed and the results are reported in Figure 2.8A.

The results demonstrate that 300 bp hpRNAs targeting different positions along the ORF and the 3'UTR of *NbFAD2.1* were only partially effective when compared to hpNbFAD2. Two of the shorter fragments were less effective in silencing – the 18:1 levels were increased from 2.3% in mock to 5.6% in hpNbFAD2-300 and 5.1% in 300e. More effective silencing was achieved by 300b and 300d, increasing 18:1 levels from 2.3% in mock to 7.8% and 7.5% respectively. Furthermore the 300 bp hpRNA (300a), targeting the intronic region of *NbFAD2*, showed no significant changes in levels of 18:1 FAME when compared to mock (2.9% vs 2.3%). The most effective silencing construct was hpNbFAD2, which increased 18:1 from 2.3% (mock) to 13.8%. This analysis indicated that longer hpRNA constructs which

cover a significant proportion of the target gene are likely to be more effective in transient silencing assays.

It must be noted that hpNbFAD2 targets the three unique histidine boxes common to all *FAD2* genes and it may effectively reduce all FAD2 activity in the leaf. hpNbFAD2-300, 300b and 300d were aligned against their homologous regions on *NbFAD2.2* to assess whether high similarity was associated to better cross-silencing of *NbFAD2.2* and the higher increase in levels of 18:1 that was observed. Vector NTI (Life Technologies) was used for alignments. The percentage consensus between the two sequences calculated was not consistent with the changes in the level of 18:1 (data not shown). It was expected that sequences of 300b and 300d would be very similar to *NbFAD2.2*, however the analysis revealed that 300d had the highest level of amino acid sequence identity to *NbFAD2.2* at 77%, while 300b and hpNbFAD2-300 had approximately 67%. The level of silencing achieved with short hpRNAs (300b, hpNbFAD2-300 and 300d) and cross-silencing of *NbFAD2.2* did not correlate consistently with the degree of sequence consensus between the hpRNA sequences and *NbFAD2.2*.

To explore the selective silencing of gene members of *NbFAD2* family, hpRNA constructs were designed to target the 3'UTR regions of *NbFAD2.1* (hpNbFAD2.1 3'UTR (300e)) and *NbFAD2.2* (hpNbFAD2.2 3'UTR). *N.benthamiana* leaves were infiltrated with combinations of AtDGAT1, hpNbFAD2, hpNbFAD2.1 3'UTR and hpNbFAD2.2 3'UTR. Leaves were harvested 4 dpi, freeze-dried overnight and total FAME analysed (Fig 2.8B). The change in the relative percentage of 18:1 was assessed. The most effective silencing was achieved by hpNbFAD2, which increased 18:1 from 2.3% (mock) to 12.5%. No significant changes were observed in the levels of 18:1 between mock and leaves infiltrated with hpNbFAD2.2 3'UTR. These results indicated that NbFAD2.2 might not be the main Δ-12 desaturase in the leaf. The silencing construct against the 3'UTR of *NbFAD2.1* increased the level of 18:1 to 4.0%. When the 3'UTR of *NbFAD2.1* and *NbFAD2.2* were silenced together, levels of 18:1 increased from 2.3% to 7.9%. Silencing of the *FAD2* gene family with hpNbFAD2 remained the most effective silencing construct. The results also indicated the presence of a third FAD2 in the leaf, which was silenced by hpNbFAD2, yet remained active when *NbFAD2.1* and *NbFAD2.2* were targeted specifically. Vector NTI (Life Technologies) software was again used to align the 300 bp sequences of the silencing constructs used to target the 3'UTR regions of

NbFAD2.1 and *NbFAD2.2* (Fig 2.8C). *In silico* analysis of similarity reinforced that the homology between the two 3'UTR target regions was not sufficient for cross silencing.

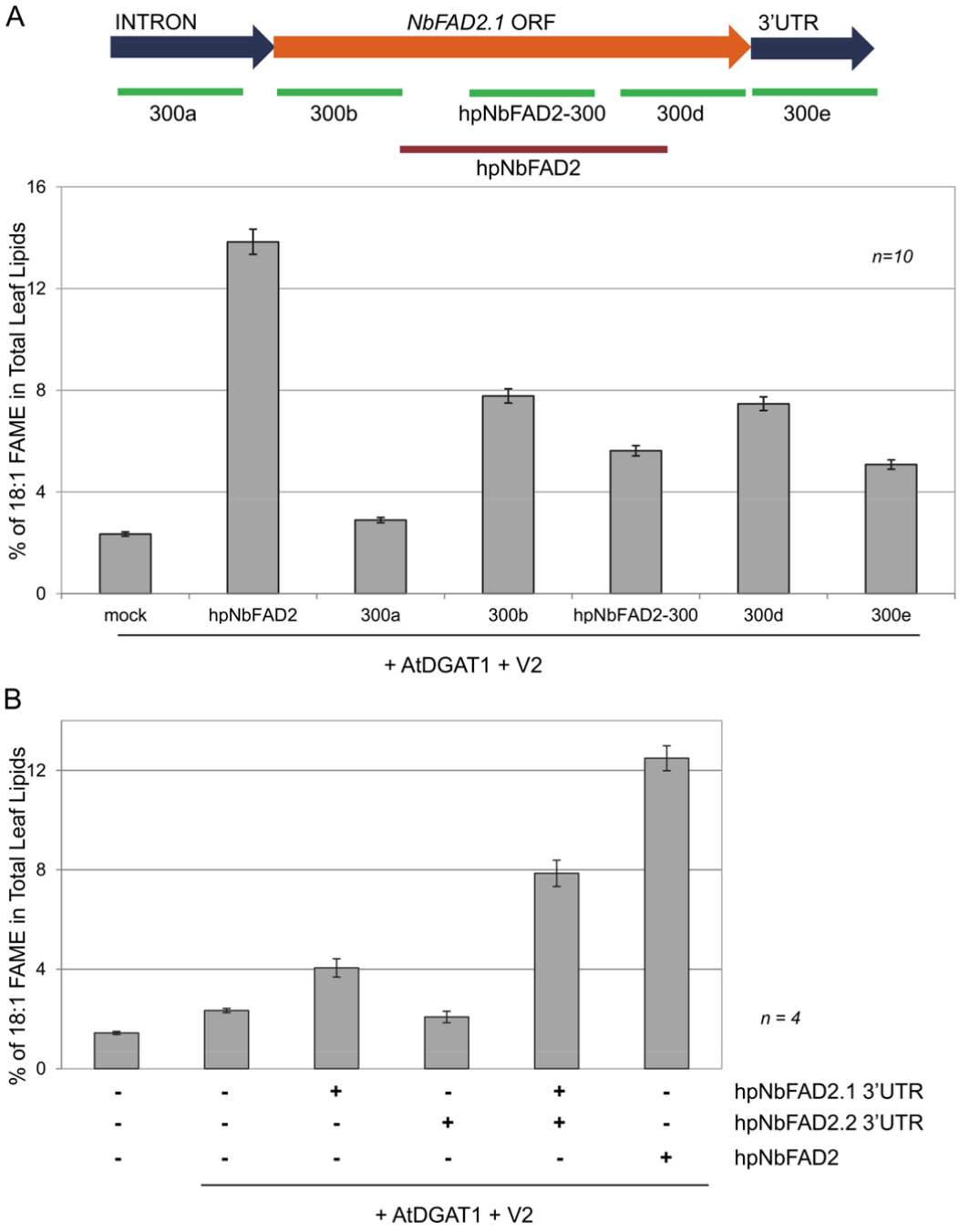
A
INTRON
NbFAD2.1 ORF
3'UTR
300a
300b
hpNbFAD2-300
300d
300e
hpNbFAD2
% of 18:1 FAME in Total Leaf Lipids
16
12
8
4
0
n=10
mock
hpNbFAD2
300a
300b
hpNbFAD2-300
300d
300e
+ AtDGAT1 + V2
B
% of 18:1 FAME in Total Leaf Lipids
12
8
4
0
n = 4
- - + - + - hpNbFAD2.1 3'UTR
- - - + + - hpNbFAD2.2 3'UTR
- - - - - + hpNbFAD2
+ AtDGAT1 + V2

C

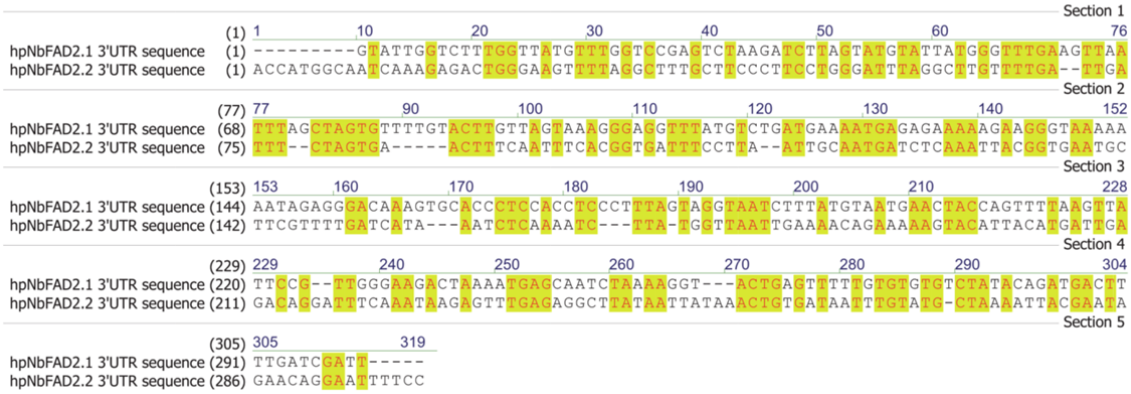

Figure 2.8. Comparison of length and location of hpRNA in silencing FAD2 activity in *N.benthamiana* leaves.

A. Combinations of V2, AtDGAT1 and the various hpRNA molecules targeting *NbFAD2.1* (as indicated in the upper panel) were infiltrated and the level of 18:1 FAME analysed 4 dpi. Data shown are the mean and 5% LSD bars calculated from 10 independent leaf infiltrations per treatment. When the LSD bars for two metabolites fail to overlap, the metabolite means may be regarded as significantly different at the 5% level of significance. Mock refers to leaves infiltrated with V2 and AtDGAT1.

B. Leaves infiltrated with a combination of AtDGAT1, hpNbFAD2, hpRNA targeting the 3'UTR region of *NbFAD2.1* (hpNbFAD2.1 3'UTR (300e)) and hpRNA targeting the 3'UTR region of *NbFAD2.2* (hpNbFAD2.2 3'UTR). Leaves were harvested 4 dpi and FAME extracted. The change in relative percentage of 18:1 FAME was measured. Data shown are the means and standard errors calculated for 10 samples per infiltration treatment.

C. Sequence alignment of fragments used for silencing of 3'UTR regions of *NbFAD2.1* and *NbFAD2.2*.

2.2.8 The effect of V2 on the processing of various different hpRNA constructs

VSPs are known to interact with sRNA silencing pathways of plants and the aim was to design a detailed statistical analysis assessing the effect of V2 on the processing of hpRNA constructs. Statistical analyses require generating large datasets. The dataset that was used for analysis of the effect of different hpRNA constructs on silencing of NbFAD2 was also designed to determine the effect of V2 on the processing of various hpRNAs. The statistical analysis involved a two-way factorial design to determine the effect of V2 on the hpRNAs. *N.benthamiana* leaves were infiltrated with a combination of GFP, AtDGAT1, and hpRNA constructs (Fig 2.8A, upper panel), with or without V2. Leaves were harvested 4 dpi and total leaf lipids analysed. A leaf spot not infiltrated by these was also harvested from each leaf and referred to as wild type, WT. A representative leaf was photographed prior to harvest and the positions of various different infiltration treatments are indicated on the image (Fig 2.9A). GFP was overexpressed in all of the infiltration treatments and not dependent upon the addition of V2.

The means for each treatment were obtained from 10 individual infiltrated leaf tissue samples and mean values were $\log_{10}$ transformed to ensure an even distribution of residual values. GenStat software was then used to determine a combined standard error of differences (SED) in the $\log_{10}$ scale and a linear mixed model was also applied to the data. The SED added to each mean value (upper border) and subtracted from each mean value (lower border). The mean, lower range and upper range were then back-transformed to the original scale.

The statistical analysis indicated that the addition of V2 did not have a biologically significant effect on the performance of other transgenes (Fig 2.9B). The measured levels of 18:1 suggested that V2 did have a statistically significant effect on the processing of 300a, 300b, hpNbFAD2-300 and 300d. The relative percentage of 18:1 measured in leaves infiltrated with 300a, 300b, hpNbFAD2-300 and 300d with V2 were 2.9%, 7.8%, 5.6% and 7.5% respectively (Fig 2.9B). The same hpRNA infiltrated without V2 resulted in 18:1 at 2.3%, 7.0%, 5.0% and 8.6% respectively. The SED for levels of 18:1 for the mentioned treatments, with and without V2, did not overlap, although these differences were not regarded as biologically significant.

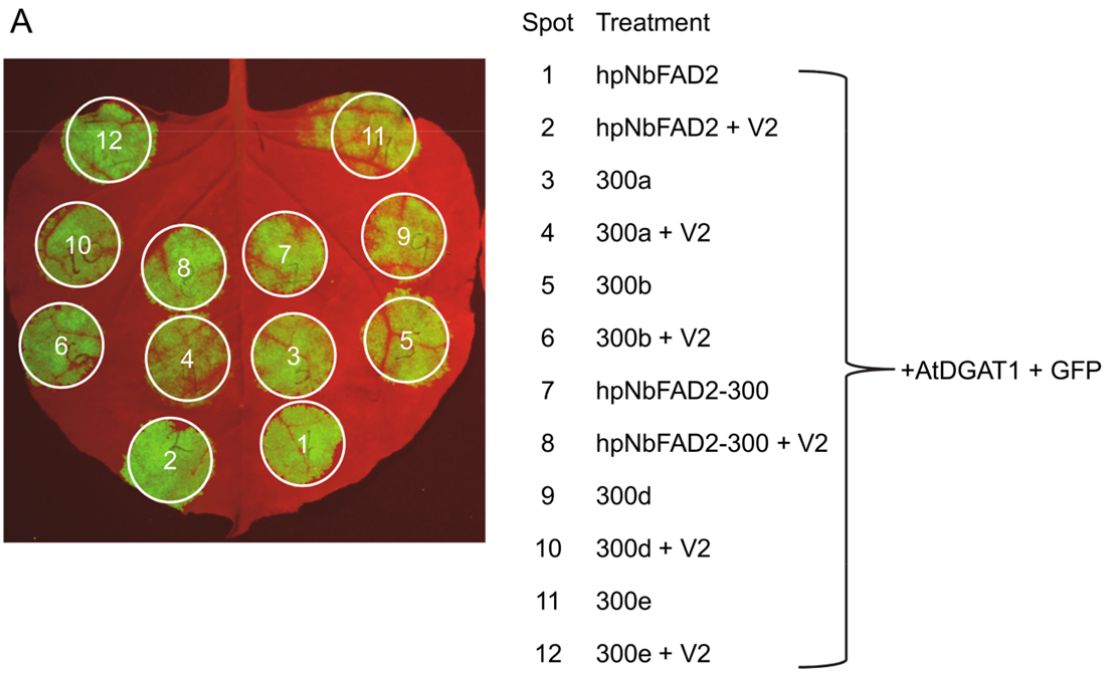

Spot labels refer to figure 2.9A

Figure 2.9. The effect of V2 on processing of several different hpRNA constructs targeting *NbFAD2*.

A. *N.benthamiana* leaves infiltrated with combinations of hpRNAs (Fig 2.8A, upper panel), AtDGAT1 and GFP, with or without V2. The infiltrated spots on the leaf are indicative of a two-way factorial design in determining the effect of V2 on the processing of hpRNA constructs targeting *NbFAD2*.

B. Relative percentage of 18:1 FAME extracted from leaves described in **A**, 4 dpi. Data shown are the mean and 5% LSD bars calculated from 10 independent leaf infiltrations per treatment. When the LSD bars for two

metabolites fail to overlap, the metabolite means may be regarded as significantly different at the 5% level of significance. WT (wild type) refers to FAME extracted from un-infiltrated leaf tissue.

2.2.9 Assessment of the effect of a non-specific hpRNA construct on the overexpression of AtDGAT1 *in infiltrated* N.benthamiana *leaves*

Previous results showed that a silencing construct targeting *NbFAD2* was able to allow overexpression of other transgenes in transient leaf assay (Fig 2.6). This result suggested that the generation of sRNA from hpRNA could potentially block host cells from silencing transgenes. This notion was investigated further by infiltrating *N.benthamiana* leaves with a hpRNA completely unrelated to lipid metabolism. Leaves were infiltrated with combinations of hpGFP (hpRNA against GFP), AtDGAT1, V2, and *A.tumefaciens* (strain GV3101) – the hpGFP was the non-specific hpRNA, which was hypothesised to allow maximal overexpression of *AtDGAT1*. The leaves were infiltrated with a final $OD_{600\ nm}$ of 0.25 for each *A.tumefaciens* culture carrying a T-DNA construct. GV3101 culture not carrying a T-DNA construct was added to treatments to ensure that all infiltration treatments contained an equal concentration of *A.tumefaciens* cells. Infiltrated leaves were harvested 4 dpi for oil analysis and 5 dpi for RNA extraction. The mRNA levels of *AtDGAT1* was measured by qRT-PCR and expression levels compared to *NbGAPDH* (Fig 2.10A). The results indicated that the highest level of expression of *AtDGAT1* was achieved with the addition of V2, 4.5 times and 8.7 times greater than the infiltration treatments of AtDGAT1 with GV3101 and hpGFP respectively. Surprisingly, the addition of GV3101 (to equalise the final concentration of *A.tumefaciens* in each infiltration treatment) enhanced the overexpression of *AtDGAT1* more than hpGFP. Total leaf lipids were extracted from freeze-dried leaf samples as described previously (Bligh and Dyer, 1959) and TAG fraction extracted using a one-phase TLC system (Fig 2.10B) (Wood et al., 2009). The highest amount of oil was extracted from leaf tissues infiltrated with AtDGAT1 and V2, 12.9 µg/6 mg dry leaf tissue. Addition of GV3101 produced 9.3 µg/6 mg dry leaf tissue and hpGFP 9.8 µg/6 mg dry leaf tissue. All infiltration treatments were able to raise the amount of leaf oil significantly from the 3.6 µg/6 mg in dry leaf tissue infiltrated with just GV3101. The presence of V2 allowed the highest accumulation of oil which confirmed the qRT-PCR results.

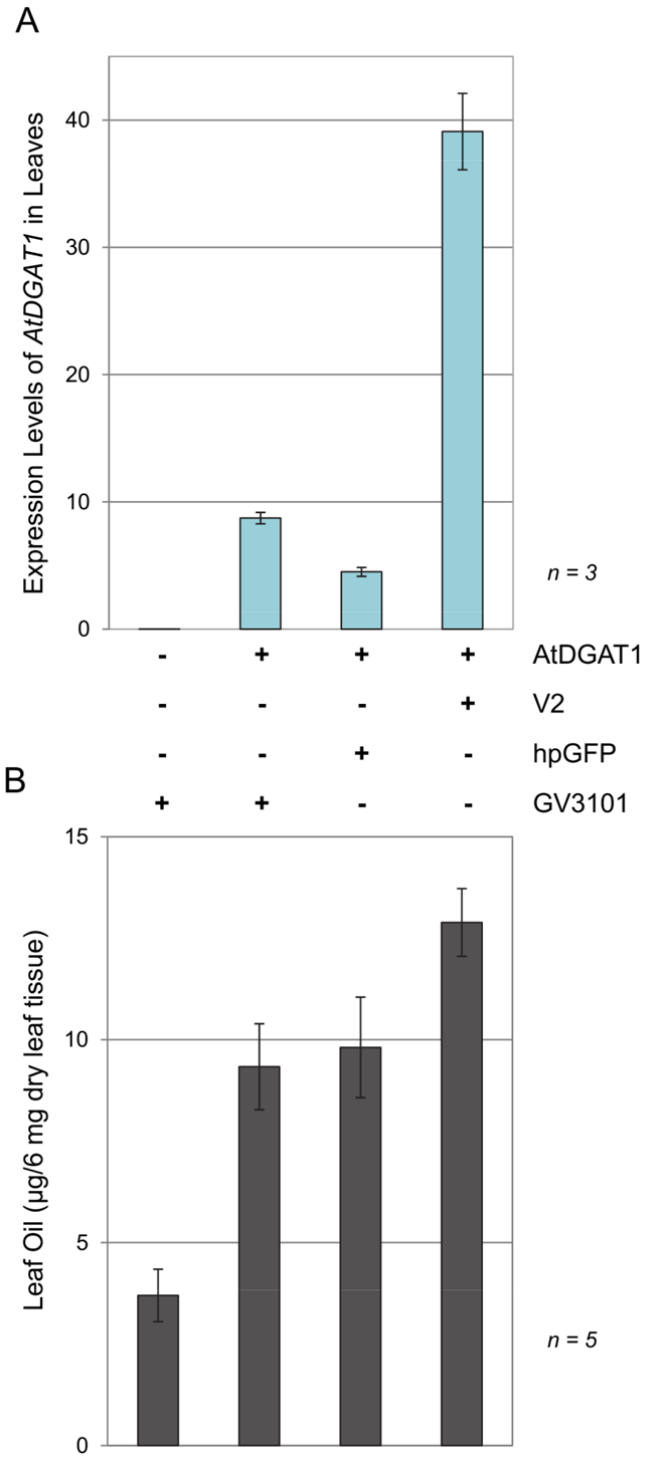

Figure 2.10. The effect of overexpression of a non-specific hpRNA on the accumulation of oil mediated by co-infiltration of *AtDGAT1* in *N.benthamiana* leaves.

A. Quantitative RT-PCR analysis of *AtDGAT1* when overexpressed in *N.benthamiana* leaves. Total RNA extracted from leaves infiltrated with combinations of AtDGAT1, V2 and non-specific hpRNA against GFP (hpGFP) 4 dpi. Mock represents RNA extracted from leaf tissue infiltrated with *A.tumefaciens* only. Data shown

are means of 3 biological replicates with 3 technical repeats for each. Error bars are the standard errors of the mean.

B. Total oil extracted from leaf tissues infiltrated with combinations of AtDGAT1, V2 and non-specific hpRNA against GFP, leaves harvested 4 dpi. Data shown are the means and standard errors calculated for 5 samples per treatment.

2.2.10 Silencing of a transgene and an endogene with varied concentrations of hpRNA constructs in transient leaf assay

One feature of metabolic engineering in transient assays is that numerous different transgenes can be infiltrated from individual *A.tumefaciens* cultures, with each contributing a single transgenic component to the pathway of interest (Wood et al., 2009). The transient leaf assay system however does not tolerate infiltration mixes with a combined *A.tumefaciens* concentration in the range of $OD_{600\ nm}$ of 2 or above (data not shown) – this results in cell death. It has been established that overexpression constructs need to be infiltrated at $OD_{600\ nm}$ 0.15–0.20 to generate a maximum activity in the transient assay system (Wood et al., 2009). Previous results in this chapter established that hpRNA silencing is effective in endogene and transgene silencing in transient leaf assay. The concentration of *A.tumefaciens* required for maximal silencing of both endogene (*NbFAD2* family) and transgene (*GFP*) was investigated for this section.

N.benthamiana leaves were infiltrated with GFP, hpGFP and V2 to determine the lowest possible concentration of *A.tumefaciens* carrying the hpGFP required for effective silencing of GFP. The overexpression constructs GFP and V2 were infiltrated at a final $OD_{600\ nm}$ of 0.2. Leaves were infiltrated with combinations of GFP, V2 and various different concentrations of hpGFP (hpRNA against GFP). Silencing of GFP was observed for up to 5 dpi, at which point one representative leaf was photographed (Fig 2.11A). The leaf image showed that GFP was silenced effectively with concentrations of hpGFP ranging from 0.05–0.2.

Efficient silencing of the *NbFAD2* gene family was assessed by infiltrating leaves with combinations of AtDGAT1, V2 and various different concentrations of hpNbFAD2 (Fig 2.11B). AtDGAT1 and V2 were infiltrated at a final $OD_{600\ nm}$ of 0.1 and 0.2 respectively. 'WT' refers to un-infiltrated leaf tissue and 'mock' refers to leaf tissue infiltrated with V2 and AtDGAT1 only. Where required, *A.tumefaciens* cells were added to treatments to maintain an equal final concentration in every treatment. Leaves were harvested 4 dpi, freeze-dried and total FAME was analysed. The changes in relative percentages of metabolites (18:1 and 18:2) showed that NbFAD2 activity was silenced effectively with infiltrated concentrations of hpNbFAD2 ranging between 0.05–0.2. The concentration of hpNbFAD2 was 0 in WT and mock leaf tissue. $OD_{600\ nm}$ of 0.01 and 0.02 hpNbFAD2 increased 18:1 levels from 2.2% (mock) to 5.8% and 7.2% respectively. Furthermore the concentrations of hpNbFAD2

ranging between 0.05–0.2 increased 18:1 levels to 8.5–9.0%. As the levels of 18:1 increased with greater concentrations of hpNbFAD2, a consequent decrease was observed in the levels of 18:2 (Fig 2.11B). The results also indicated that effective silencing was achieved with hpRNA constructs infiltrated at a concentration of 0.05.

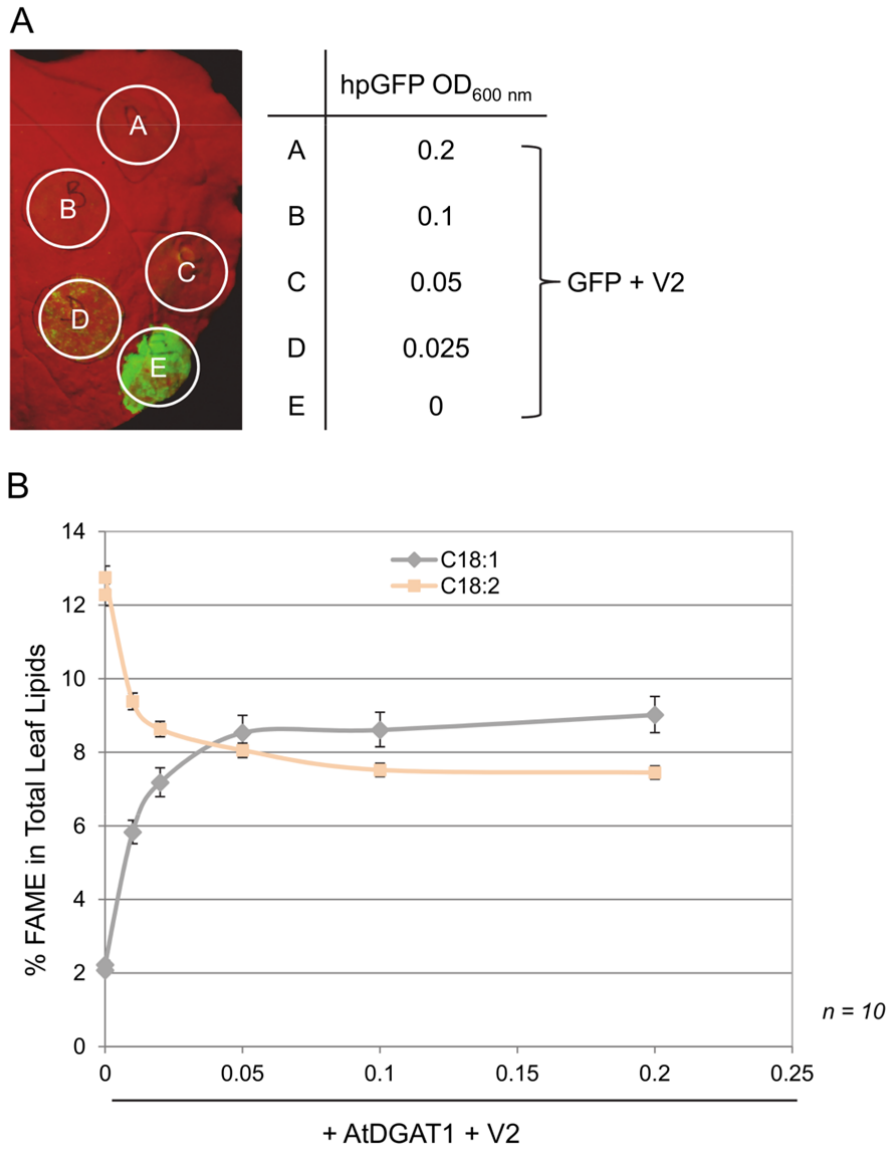

Figure 2.11. Efficient silencing of *GFP* and *NbFAD2* in transient leaf assay with varied concentrations of the hpRNA constructs.

A. A representative *N.benthamiana* leaf infiltrated with combinations of GFP, hpGFP (hpRNA against GFP) and V2 was photographed 4 dpi. Optical density of *A.tumefaciens* carrying the transgenes measured at 600 nm ($OD_{600\ nm}$). V2 and GFP infiltrated at a final concentration of $OD_{600\ nm}$ 0.2 in all treatments with varied concentrations of hpGFP ranging from 0.025 to 0.2.

B. Relative percentage of 18:1 FAME of *N.benthamiana* leaves infiltrated with hpNbFAD2, V2 and AtDGAT1 and harvested 4 dpi. V2 and AtDGAT1 infiltrated at an $OD_{600\ nm}$ of 0.2 with varied concentrations of the hpNbFAD2 ranging from 0.02 to 0.2. Data shown are the mean and 5% LSD bars calculated from ten infiltrations per treatment. When the LSD bars for two metabolites fail to overlap, the metabolite means may be regarded as significantly different at the 5% level of significance.

2.2.11 Successful transient silencing of individual lipid handling genes in **N.benthamiana** *leaves*

The results thus far suggest optimised protocols for the assembly of pathways that require transient silencing of endogene and overexpression of transgenes. This enhanced assay system was used to explore the possibility of silencing genes involved in lipid biosynthesis and transport. A simplified schematic of enzymes involved in lipid handling in plants was shown in Chapter 1 (Fig 1.2, Fig 1.3).

The purpose of designing hpRNA constructs against genes involved in lipid handling pathways was to confirm the roles of the respective genes. The TAIR website was initially searched for genes of interest, then the *N.benthamiana* transcriptome database was searched for transcripts homologous to *AtFAD3*, *AtFAD6*, *AtFAD7*, *AtFATA*, *AtFATB* and *AtSAD1*. In *A.thaliana* there are two chloroplastic enzymes, AtFAD7 and AtFAD8, which desaturate 18:2 to 18:3, however the BLAST search revealed only one gene in *N.benthamiana* with high homology to *AtFAD7* and *AtFAD8* – this gene is referred to *NbFAD7* throughout the chapter. The BLAST search revealed one gene homologous to *AtFAD6, NbFAD6*. *A.thaliana* has two *FATA* and one *FATB* genes and the BLAST search also revealed two *FATA* genes and one *FATB* gene in *N.benthamiana*. The silencing construct designed against *NbFATA* targeted the most conserved region between the two *FATA* sequences. There was one *NbSAD1*, which aligned against *AtSAD1* gene.

An approximate 600 bp fragment was amplified from each candidate gene for cloning into hpRNA constructs (see Methods, section 2.6 of this chapter, for the accurate size of hpRNA sequence and primers used for amplification). AtDGAT1 was infiltrated with combinations of hpRNA constructs hpNbFAD2, hpNbFAD3, hpNbFAD6 and hpNbFAD7. In this experiment, hpNbFAD2 was infiltrated as a positive control. Leaves were harvested 5 dpi and FAME of total leaf lipids analysed. Changes in the relative percentages of FAME were compared to leaves infiltrated with AtDGAT1 only (Fig 2.12A). The other hpRNA constructs, hpNbFATA, hpNbFATB and hpNbSAD1, were infiltrated with the addition of V2. The control leaf tissue was infiltrated with V2 only (Fig 2.12B, Fig 2.12C). HpRNA constructs and overexpression constructs were infiltrated at a final $OD_{600\ nm}$ of 0.15 and 0.1 respectively.

The silencing abilities of the constructs were initially assessed by measuring the lipid profiles of leaves 5 dpi. Individual silencing of *NbFAD2* and *NbFAD6* increased the level of 18:1 FAME

from 1.8% to 13.0% and 6.5% respectively. This result suggested that activity of NbFAD2 is higher than NbFAD6 in desaturating 18:1 to 18:2. Silencing of *NbFAD3* did not change levels of 18:2 and 18:3, but hpNbFAD7 increased 18:2 from 12.4% to 30.2% and decreased 18:3 from 55% to 38% (data not shown).

Figure 2.12B and 2.12C present the effect of silencing *NbFATA*, *NbFATB* and *NbSAD1* on the levels of 16:0, 18:0 and 18:1. Silencing of *NbFATB* decreased leaf 16:0 from 15.0% to 13.3% and 18:0 from 2.2% to 2.0% (Fig 2.12B). The relative percentage of 18:1 FAME decreased from 1.5% to 0.5% in leaves infiltrated with hpNbFATA. Comparatively hpNbSAD1 showed a more drastic effect on the relative percentage of 18:0, with an increase from 2% to 11% (Fig 2.12C), while there was a consequent decrease in levels of 18:2 from 11.8% to 7.4% and 18:3 from 54.9% to 48.3%. A leaf discolouring (bleaching effect) was also obvious 5 dpi in hpNbSAD1-infiltrated leaf tissue (Fig 2.12D). This same leaf was also infiltrated with hpNbFATA and V2 and no discolouring was observed.

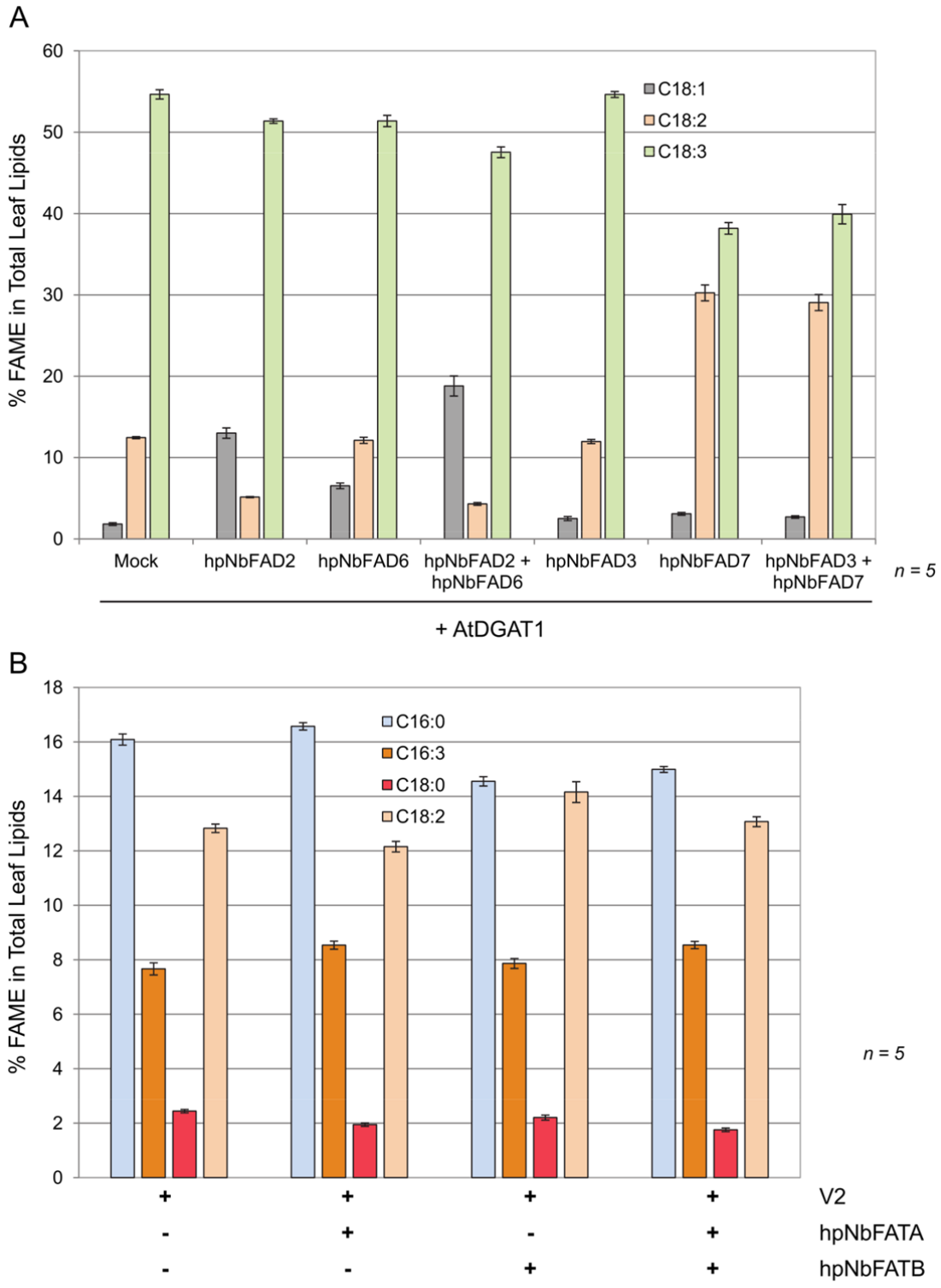
A
% FAME in Total Leaf Lipids
60
50
40
30
20
10
0
C18:1
C18:2
C18:3
Mock
hpNbFAD2
hpNbFAD6
hpNbFAD2 + hpNbFAD6
hpNbFAD3
hpNbFAD7
hpNbFAD3 + hpNbFAD7
n = 5
+ AtDGAT1
B
% FAME in Total Leaf Lipids
18
16
14
12
10
8
6
4
2
0
C16:0
C16:3
C18:0
C18:2
n = 5
+ + + + V2
- + - + hpNbFATA
- - + + hpNbFATB

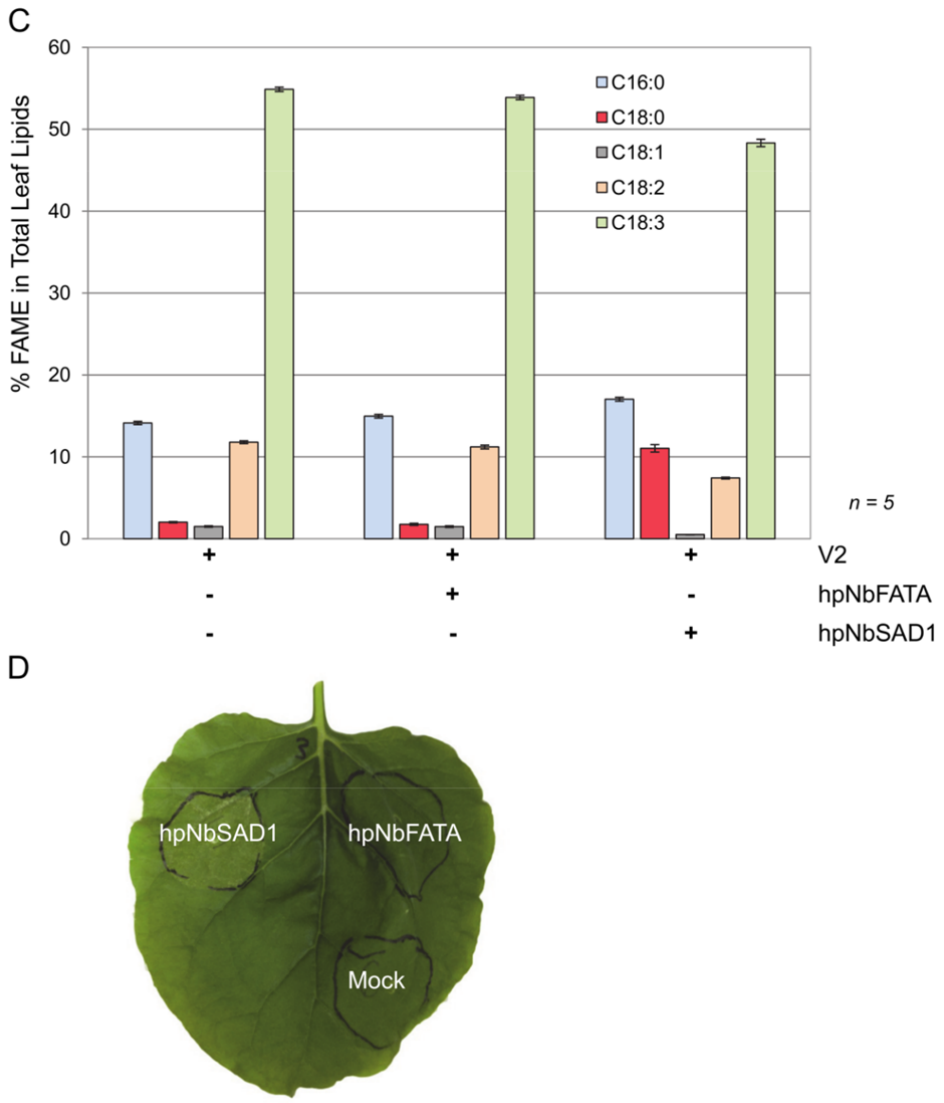

Figure 2.12. Silencing the endogenes *NbFAD2*, *NbFAD6*, *NbFAD3*, *NbFAD7*, *NbFATA*, *NbFATB* and *NbSAD1*.

A. Relative percentages of 18:1, 18:2 and 18:3 FAME extracted from leaves infiltrated with AtDGAT1 and combinations of silencing constructs targeting the endogenes *NbFAD2*, *NbFAD6*, *NbFAD3* and *NbFAD7*.

B. Relative percentages of 16:0, 16:3, 18:0 and 18:2-FAME extracted from leaves infiltrated with combinations of V2, hpNbFATA and hpNbFATB.

C. Relative percentages of 16:0, 18:0, 18:1, 18:2 and 18:3 FAME extracted from leaves infiltrated with V2 and combinations of silencing constructs against endogenes *NbFATA* and *NbSAD1*.

D. A representative *N.benthamiana* leaf used for analysis in **C** photographed prior to harvest to indicate phenotypic changes brought by silencing of *NbSAD1*. Infiltrated regions are circled in black.

Data shown in **A**, **B** and **C** are the means for each infiltration treatment. Error bars are the standard errors of the mean calculated for 5 leaf samples per treatment. Leaves were harvested 5 dpi.

2.2.12 Targeted silencing of multiple endogenes in one infiltration treatment

Silencing multiple genes can be beneficial in increasing substrate levels for the assembly of transgenic pathways as well as allowing detailed investigations into plant physiology. After the successful silencing of single genes in *N.benthamiana* leaves, the aim was to combine independent hpRNA constructs in one infiltration treatment and assess the possibility of silencing multiple genes. hpRNA constructs against either *NbFAD2* or *NbFAD6* are effective in elevating 18:1 levels in leaf assays (Figure 2.12A) and therefore provide a method to assess if combinations of both hpRNA were effective in further increasing 18:1 levels. The addition of hpNbFAD2 and hpNbFAD6 increased 18:1-FAME levels from 1.8% to 18.8%, a ten-fold increase compared to the mock treatment (Fig 2.12A). The increase in 18:1 level was higher than that measured in leaves where NbFAD2 and NbFAD6 were silenced individually. The combinative silencing of *NbFAD3* and *NbFAD7* was also assessed to elevate 18:2 levels higher than levels achieved with hpNbFAD7 alone, although failed to increase 18:2 levels any further, confirming that the desaturating ability of NbFAD3 was not high in leaves used for transient assay.

2.2.13 Assessment of lipid movement across different compartments of the cell by shunting endogenous metabolites into a transgenic IgΔ9E pathway

Efficient silencing of *NbFAD7* was combined with the overexpression of a transgenic pathway utilising 18:2 as substrate. The *Isochrysis galbana* Δ9-Elongase (IgΔ9E) has been used in assembling pathways for the production of ω-3 and ω-6 long chain polyunsaturated fatty acids in plants (Petrie et al., 2012a; Qi et al., 2002). It is accepted that the elongation of fatty acids takes place exclusively on CoA substrates and not on membrane-bound lipid head groups such as PC, MGDG and DGDG (see Chapter 1). Therefore elongase-based reactions may assist in investigating the fluxes of lipids through the CoA pool in leaf assays.

The *IgΔ9E* gene was driven by the CaMV 35S promoter and it was infiltrated into *N.benthamiana* leaves with combinations of hpNbFAD3, hpNbFAD7 and V2. Silencing and overexpression constructs were infiltrated at a final $OD_{600\ nm}$ of 0.15 and 0.2 respectively. Leaves were harvested 5 dpi and FAME extracted from total leaf lipids. For fractionation of polar lipids, total leaf lipids were extracted using the protocol described by Bligh and Dyer (1959) and leaf lipids were separated using the 2D TLC system as described previously.

IgΔ9E is more selective in elongating 18:2 to produce 20:2, the ω-6 pathway (Fig 2.13A) (Petrie et al., 2012a), but given the presence of 18:3, a parallel pathway occurs in which 18:3 is elongated to 20:3, the ω-3 pathway (Petrie et al., 2012a) (Fig 2.13A). *N.benthamiana* leaves have very high levels of 18:3 and the aim was to reduce levels of 18:3 and increase substrate for the ω-6 pathway by silencing *NbFAD3* and *NbFAD7*. The total FAME analysis of total leaf lipids indicated that 13.3% 20:2 and 9.0% 20:3 were produced in leaf tissue infiltrated with V2 and IgΔ9E constructs (Fig 2.13B). Silencing of *NbFAD7* increased 20:2 to 16.1% and decreased 20:3 to 7.8%. There were no significant differences in relative percentages of elongated products with silencing of *NbFAD3*, similar to previous results in this chapter.

Following the successful shunting of 18:2 into a transgenic pathway, the aim was to assess the presence of elongated fatty acids on the PC fraction. Fractionation of major polar leaf lipids revealed that approximately 42% of the native PC was replaced by the transgenic metabolites (Fig 2.13C). There was a reduction in relative percentages of 16:0, 18:2 and 18:3 at an expense on PC of 29.7% of 20:2 and 12.7% of 20:3. Silencing of *NbFAD7* reduced 20:3 to 9.4% and increased levels of 18:1 from 7.9% to 11.0%. When *NbFAD3* was silenced and *IgΔ9E* was overexpressed, the levels of 18:1 increased from 7.9% to 10.1% while levels of 18:2 decreased 16.0% to 14.2%. Silencing *NbFAD3* did not have a significant effect on the relative percentages of the native fatty acids and the elongated products on PC (Fig 2.13C). The PC lipid profiles (Fig 2.13C) were in agreement with the total FAME results (Fig 2.13B). The PC results also confirmed the previous results (Fig 2.12A) that indicated the activity of NbFAD3 in *N.benthamiana* leaves to be very low.

The two major polar lipid classes found in the plastids are the MGDG and DGDG pools and these were also extracted using the 2D TLC system. These lipids were taken from the same leaf lipid extracts used for PC extraction. The primary purpose of extracting these lipid pools was to demonstrate that silencing of *NbFAD7* greatly affects the chloroplastic levels of 18:2 and 18:3. Next the analysis was used to confirm that the elongated products were not transported into the chloroplast. The results have indicated that the combination of silencing *NbFAD7* and overexpression of *IgΔ9E* reduced 18:3-MGDG from 74% to 51% (Fig 2.13D, upper plot). It was interesting that overexpression of *IgΔ9E* alone increased levels of 16:3-MGDG from 15.6% to 19.3%, while 16:3 levels dropped to 13.9% when *NbFAD7* was co-

silenced. The lipid profiles also confirmed that MGDG is a fraction dominated by 18:3 and 16:3 fatty acids, whereas DGDG contained high levels of 18:3 and 16:0. In the DGDG fraction, silencing of *NbFAD7* also increased 18:2 levels (3.7% to 11.0%) and decreased 18:3 levels (57.7% to 48.8%) (Fig 2.13D, lower plot). Surprisingly, elongated products of IgΔ9E pathway (20:2 and 20:3) were transported to the chloroplast, which constituted 6% of MGDG and 7% of DGDG.

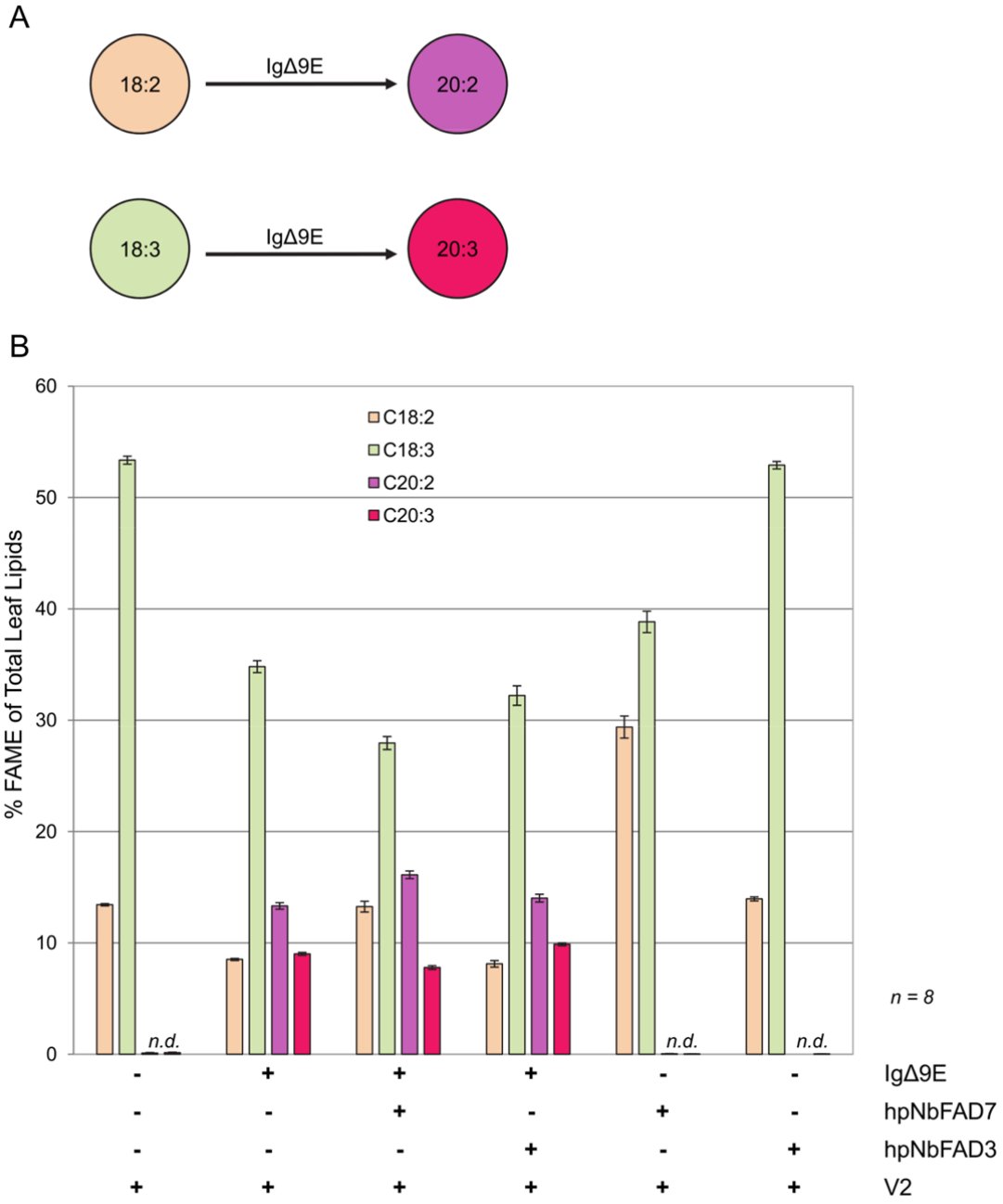
A
18:2
IgΔ9E
20:2
18:3
IgΔ9E
20:3
B
% FAME of Total Leaf Lipids
C18:2
C18:3
C20:2
C20:3
n.d.
n.d.
n.d.
n = 8
IgΔ9E
hpNbFAD7
hpNbFAD3
V2

C

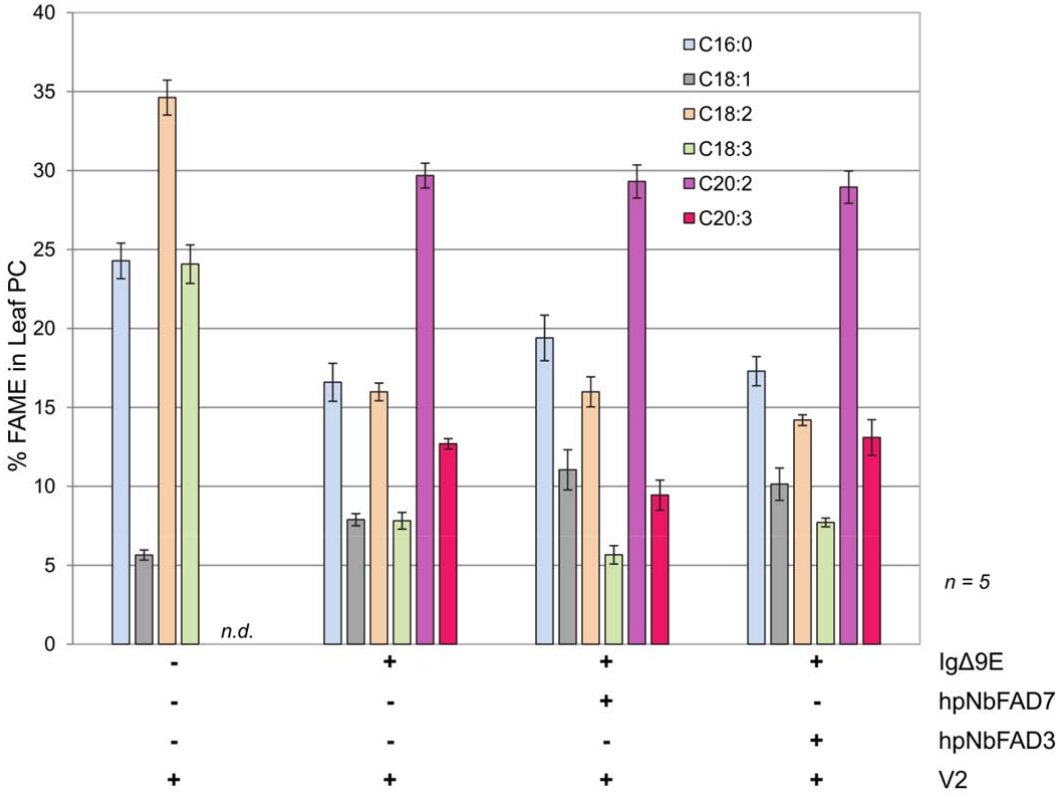
40
35
30
25
20
15
10
5
0
% FAME in Leaf PC
C16:0
C18:1
C18:2
C18:3
C20:2
C20:3
n.d.
n = 5
-
+
+
+
IgΔ9E
-
-
+
-
hpNbFAD7
-
-
-
+
hpNbFAD3
+
+
+
+
V2

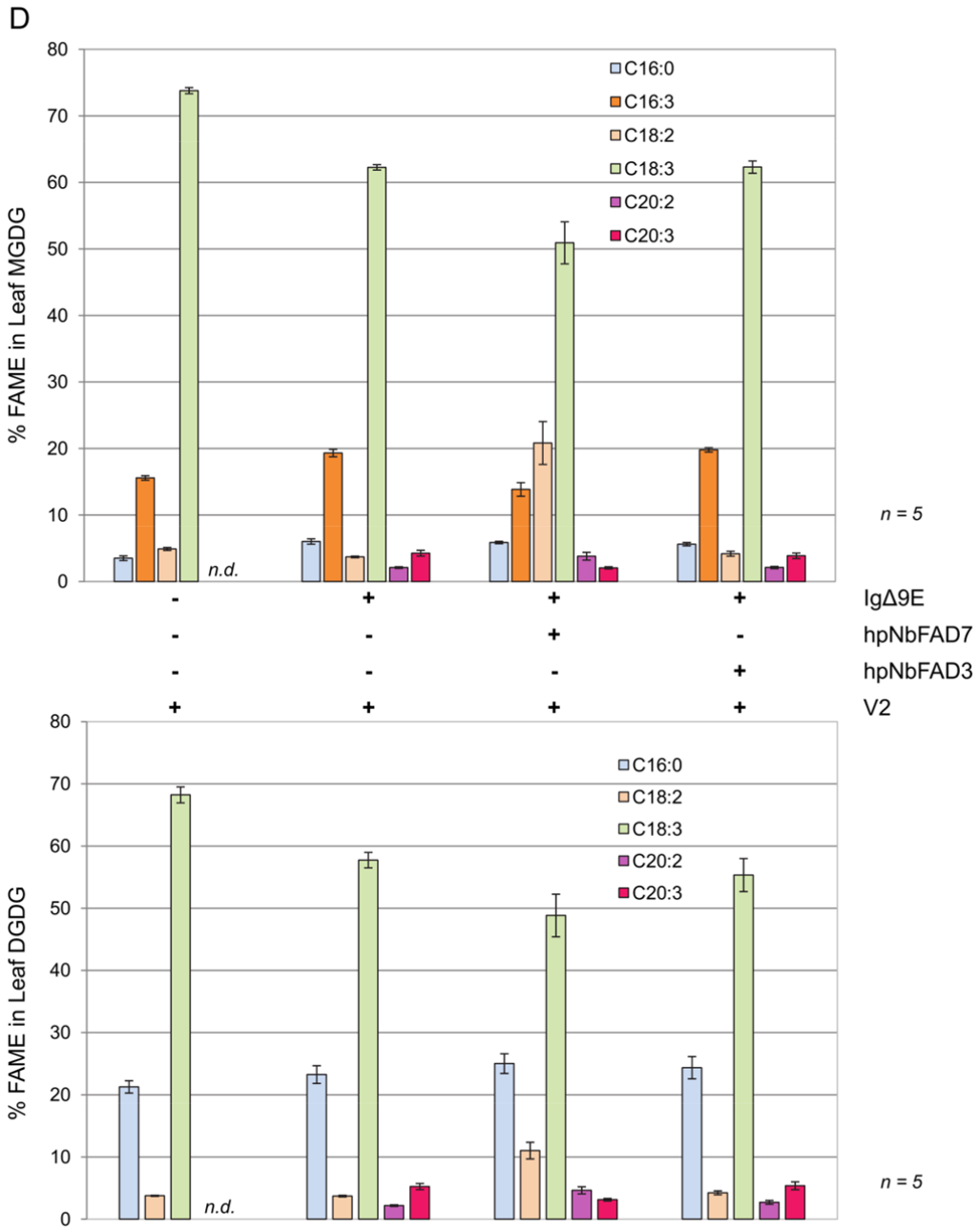

Figure 2.13. Assessment of lipid movement across different compartments of the cell: Shunting endogenous lipid pools into new transgenic pathway.

A. Schematic of IgΔ9E converting 18:2 to 20:2 and 18:3 to 20:3.

B–D. Total leaf lipids were extracted from leaves infiltrated with combinations of V2, IgΔ9E and hpRNA constructs targeting *NbFAD3* (hpNbFAD3) and *NbFAD7* (hpNbFAD7). Leaves were harvested 4 dpi. Relative percentage of FAME of total lipids (**B**), PC (**C**), MGDG (**D**), DGDG were measured. Means for each infiltration treatment were calculated. Error bars are the standard errors of the mean calculated for 8 leaf samples in the total FAME analysis and for 5 leaf samples in PC, MGDG and DGDG FAME analysis.

2.2.14 The effect of transient silencing of **NbLPCAT** *on the profile of total leaf lipids and PC lipids*

We next investigated the mechanisms by which elongated products of IgΔ9E pathway were finishing on the PC fraction. One of the candidate enzymes for exchanging head groups between CoA and PC is lysophosphatidylcholine acyl-transferase (LPCAT). The *N.benthamiana* online genome tool was searched for sequences homologous to *AtLPCAT1* and *AtLPCAT2*. The search returned two *N.benthamiana LPCAT* sequences. The most conserved region between the two genes was used to design a long hpRNA molecule, hpNbLPCAT, for efficient silencing of both genes. Leaves were infiltrated with combinations of hpNbLPCAT, IgΔ9E and V2 and then harvested 5 dpi. Infiltrated leaf tissues were then used for FAME analysis of total leaf lipids and total lipid extraction for fractionation of polar lipids.

The FAME profile of total leaf lipids indicated that silencing of *NbLPCAT* did not have a major effect on the production of elongated fatty acids by IgΔ9E (Fig 2.14, upper plot). In leaves infiltrated with IgΔ9E and hpNbLPCAT, the relative percentage of 20:2 decreased from 13.3% to 11.2% while 20:3 increased from 8.1% to 8.4%. This change was also observed in leaf PC lipid profile – 20:2-PC decreased from 32.1% to 29.6% and 20:3-PC increased from 12.6% to 14.8% (Fig 2.14, lower plot). These results indicate that NbLPCAT does not play a major role in exchange of acyl-CoA to PC and it is also known that NbLPCATs prefer loading of acyl groups with two double bonds or three double bonds. The leaf PC profile has shown that levels of 18:2 (36%) on PC were higher than 18:3 (28%). The profiles of leaf MGDG and DGDG were also analysed to assess the effect of *NbLPCAT* silencing on the elongated products previously detected in the chloroplastic lipid pools, however no significant differences were measured in the relative percentages of 20:2 and 20:3 found on the MGDG and DGDG in leaves infiltrated with IgΔ9E when compared to leaves infiltrated with hpNbLPCAT and IgΔ9E (data not shown). These results were not sufficient to address the mechanism by which the elongated products were found on PC.

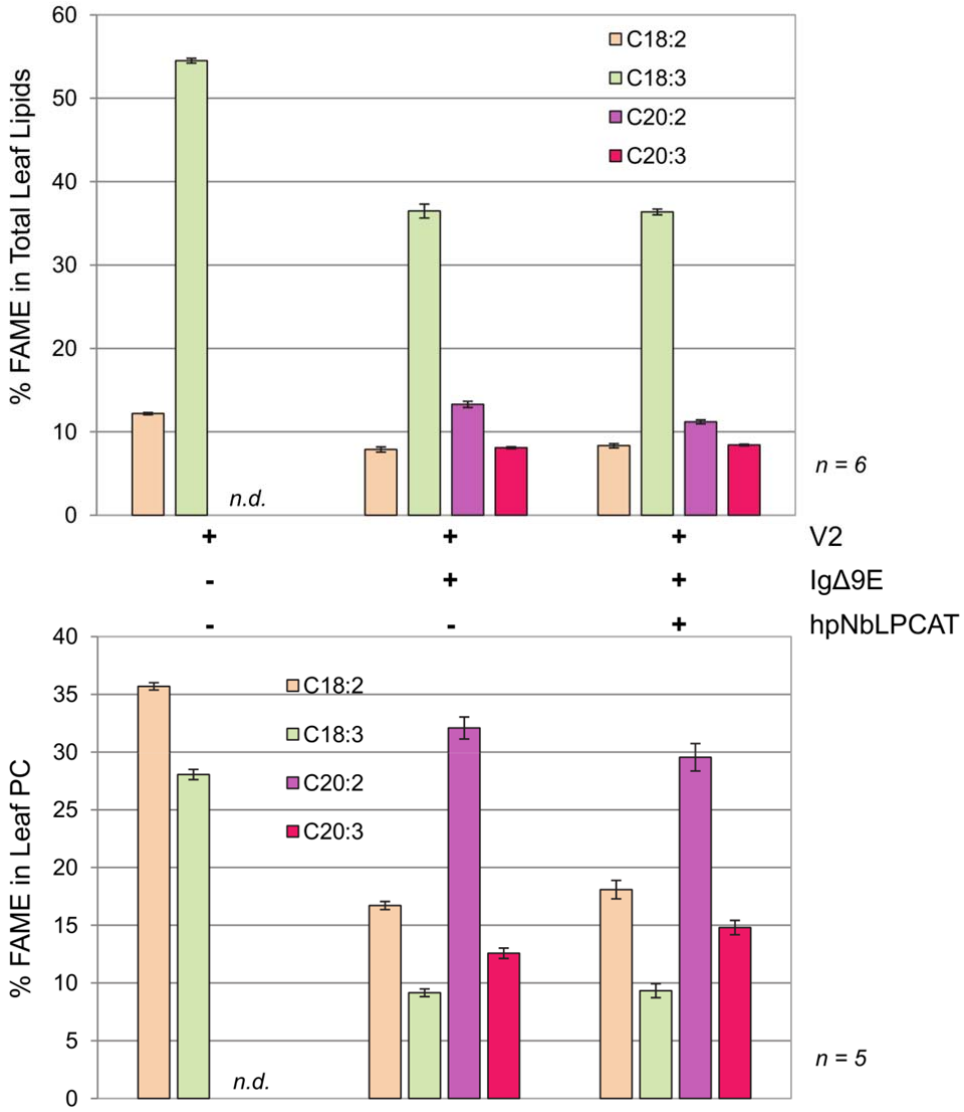

Figure 2.14. Transient silencing of *NbLPCAT* and overexpression of *IgΔ9E*.

FAME of total leaf lipids and PC lipids were extracted from leaves infiltrated with combinations of V2, IgΔ9E and silencing construct against *NbLPCAT* (hpNbLPCAT). Leaves were harvested 5 dpi. Means for each infiltration treatment were calculated. Error bars are the standard errors of the mean calculated for 6 leaf samples in the total FAME analysis and for 5 leaf samples in PC FAME analysis.

2.2.15 Assessing the effect of silencing NbTGD1*,* NbGPAT9*,* NbLPAAT4 *and* NbLPAAT6 *on total leaf lipid profile*

Following the inconclusive results obtained from silencing of NbLPCAT, we next disrupted putative candidate genes involved in the Kennedy Pathway by silencing *N.benthamiana* GPAT (glycerol-3-phosphate acyltransferase) and LPAATs (lysophosphatidyl acyltransferases). Another enzyme, TGD1 (a permease-like protein of inner chloroplast envelope, proposed to be involved in recycling of TAG and PA for synthesis of chloroplast membrane lipids (Xu et al., 2005)) was also silenced. The *N.benthamiana* transcriptome data was searched and sequences were found homologous to *A.thaliana* GPAT9, LPAAT4, LPAAT6 and TGD1.

Leaves were infiltrated with combinations of V2, IgΔ9E, hpNbTGD1, hpNbGPAT9, hpNbLPAAT4 and hpNbLPAAT6. The final $OD_{600\ nm}$ for each *A.tumefaciens* culture-carrying T-DNA construct was reduced to 0.1 and leaves were harvested 5 dpi. Total leaf lipids were extracted as FAME. There were no statistically significant differences detected between the leaf lipid profile of leaves infiltrated with IgΔ9E only and leaves infiltrated with either of the hpRNA constructs and IgΔ9E (Fig 2.15).

The total FAME profile of leaves silenced for *NbTGD1* were relatively similar to leaves infiltrated with V2 only (data not shown). The total FAME extracted from *NbTGD1*-silenced leaves were compared to leaves infiltrated with V2 in order to investigate the effect of hpNbTGD1 on the amount of total leaf lipids (results not shown). It was expected that silencing of TGD1 would result in drastic reduction of galactolipids, which in turn would affect the amount of total leaf lipids extracted from infiltrated leaf tissue. However no significant changes were detected in the amount of total leaf lipids (data not shown). The same leaf samples were also used for TAG quantification. It was expected that TAG amounts should be relatively higher in leaves infiltrated with hpNbTGD1 and V2 than in leaves infiltrated with V2 only, however this was not observed (data not shown). It is possible that the techniques used for TAG quantification are not sufficiently sensitive to detect subtle changes in low amounts of oil in the leaf.

The silencing of *N.benthamiana TGD1*, *GPAT9*, *LPAAT4* and *LPAAT6* similarly did not have a significant effect on the production of elongated products by the IgΔ9E (Fig 2.15). Based on

the insignificant differences measured in total FAME profile, it was decided to not assess the changes on the PC and galactolipid pools.

Leaves were also infiltrated with three hpRNAs against *NbGPAT9*, *NbLPAAT4* and *NbLPAAT6* in one treatment in order to assess the effect of silencing the first and second steps of *de novo* DAG synthesis. The relative percentages of 20:2 and 20:3 decreased from 9.2% to 8.5% and 6.4% to 5.8% respectively (Fig 2.15). These results have shown that the silencing of key enzymes in the Kennedy pathway (as discussed in Chapter 1) did not have a major effect on the total fatty acid profile of the leaf.

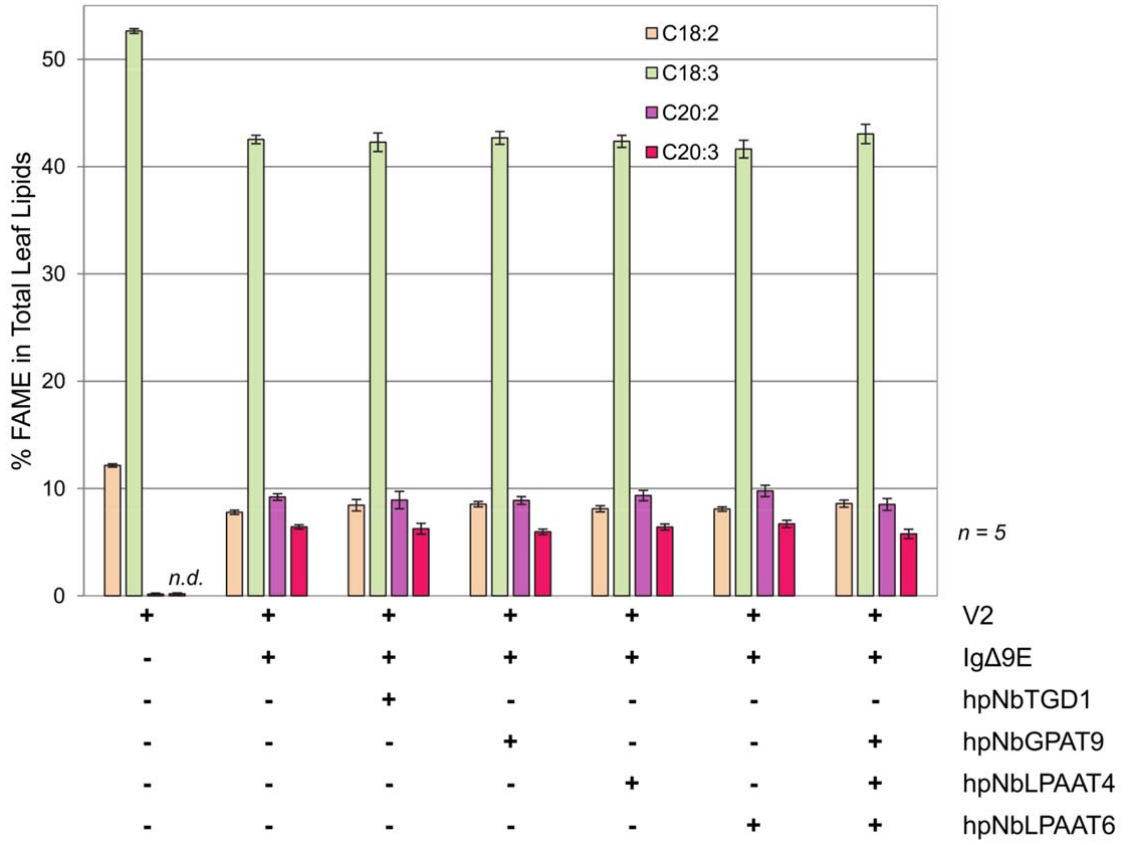

Figure 2.15. Transient silencing of *NbTGD1*, *NbGPAT9*, *NbLPAAT4* and *NbLPAAT6* combined with overexpression of the *IgΔ9E*.

The relative percentage FAME extracted from leaves infiltrated with combinations of V2, IgΔ9E and hpNbTGD1, hpNbGPAT9, hpNbLPAAT4 and hpNbLPAAT6. Leaves were harvested 5 dpi. Means for each infiltration treatment were calculated and error bars are the standard errors of the mean calculated for 5 leaf samples per treatment.

2.3 Discussion

This chapter has introduced new tools for the design and expression of complex metabolic engineering pathways in *N.benthamiana* leaves. These tools have been used to enhance our current understanding of genes involved in lipid metabolism and to probe the remodelling of fatty acids between different lipid pools in the leaf. The availability of genomic online tools and the ability to use V2, an alternative VSP, made it possible to manipulate the lipid metabolism pathways of *N.benthamiana* leaves.

2.3.1 Introduction of V2 and optimisation of the transient leaf assay for metabolic engineering of lipid pathways in the leaf

A key component of the transient leaf assays introduced in this chapter is the alternative VSP, V2, which outperformed p19 in transient engineering of plant lipid metabolism. It is well documented that different plant viruses use their respective VSPs to target different components of the host silencing apparatus (Ding and Voinnet, 2007). V2, encoded by the TYLCV-Is, is a VSP which disrupts the SGS3/RDR6 driven silencing pathways of the plant. The results in this chapter supported the hypothesis that V2 inhibited co-suppression of transgenes while allowing effective hpRNA-directed silencing of endogenes. This feature provided a distinct advantage over assays using p19, which binds to a major size class of sRNA generated by hpRNA molecules (Fig 2.2, Fig 4, Fig 6). Deep sequence analysis of a sRNA population generated by a hpRNA construct revealed that 42% of sRNA were 21 nt, a size class bound by p19 and thus rendered inactive in targeting endogenes. V2 is proposed to inhibit sense-strand co-suppression pathways as well as the formation of secondary siRNA for amplification of silencing signal. It was shown that V2 enhanced transgene overexpression to the same extent as p19, indicating that V2 blocks the co-suppression pathway generated from sense-strand RNA. Furthermore V2 supported maximal silencing of endogenes in contrast to the use of p19, which only partially inhibited silencing of endogenes (and transgenes). Therefore, V2-based assays allowed a rapid examination of transgenic pathways with optimised substrate pools by shunting endogenous metabolites into transgenic engineered pathways. Although lipid metabolism is the focus of this chapter, the principles of this approach could also be expected to result in wider applications of the transient leaf assay in both basic and applied areas of plant research.

The design of transgenic strategies for the silencing of endogenes is an important aspect of advanced metabolic engineering (Eamens et al., 2008; Wesley et al., 2001). This chapter used the silencing of FAD2, a microsomal oleate desaturase, as a test system to monitor the efficacy of hpRNA-based silencing of endogenes. The *FAD2* gene family in *N.benthamiana* was characterised using the newly developed range of genomic tools made available for this model plant. The expression analysis, activity and silencing of *NbFAD2* genes were extensively studied to establish guidelines for studying other enzymes involved in lipid handling pathways. The gene expression analysis revealed that *NbGAPDH* is an ideal internal control gene for gene expression analysis of infiltrated *N.benthamiana* leaves. The two *NbFAD2* genes were also expressed in yeast and their desaturase activity was monitored – results revealed that both FAD2s in *N.benthamiana* are 18:1 to 18:2 desaturases.

The results presented in this chapter establish the general guidelines for silencing both single genes as well as entire gene families. This investigation involved assessing the size of the hpRNA required for efficient silencing of the target gene(s). Long hpRNAs around 1100 bp (Stoutjesdijk et al., 2002) and micro RNA as short as 21 nt (Belide et al., 2012) targeting *AtFAD2* have been shown to effectively silence *AtFAD2* in stable systems. In transient systems though, a longer hpRNA targeting the most conserved region of a gene family was found to be more effective. The results have also demonstrated that a specific member of a gene family was silenced by targeting the 3'UTR region – previous reports had suggested that a 300 bp hpRNA molecule targeting the ORF or the 3'UTR region was sufficient in efficient silencing of the respective gene (Helliwell and Waterhouse, 2003). Several hpRNA molecules were designed to target different regions of *NbFAD2.1* and were useful in building a more extensive knowledge in designing silencing molecules. The results indicated that both 660 and 300 bp hpRNA fragments were capable of effective silencing of the target gene, *NbFAD2.1*. The longer hpRNA however spanned regions of high homology with a second gene, *NbFAD2.2*, and caused cross-silencing that was evident from the reduction of both mRNA abundance and biochemical activities. This indicates that single and multiple genes sharing sequence homology can be accurately silenced depending on the design of the hpRNA molecule.

It was also shown that the 3'UTR regions of the *NbFAD2* gene family can be targeted via hpRNA silencing in order to reduce the activity of individual members of a larger gene family

more specifically. It was of interest that the silencing ability of the shorter hpRNAs varied in silencing *NbFAD2* – 300 bp hpRNA targeting the intronic region of *NbFAD2.1* had no effect on the levels of 18:1, while the 300 bp hpRNA targeting the middle region of *NbFAD2.1* ORF resulted in only a very small increase in 18:1. Given that the hpRNA molecule targeting regions of high homology between the *NbFAD2* family members increased the level of 18:1 more than the combination of specific hpRNA targeting *NbFAD2.1* and *NbFAD2.2*, it seems possible that there are other undiscovered *NbFAD2* genes expressed in *N.benthamiana* leaves that were also silenced by the conserved homology construct (hpNbFAD2).

The addition of more than one silencing construct in a single infiltration treatment was optimised by assessing the lowest concentration of *A.tumefaciens* carrying the hpRNAs required for efficient silencing of the targeted genes. The infiltration experiments revealed that only a very low concentration of *A.tumefaciens* was required for effective silencing and this assisted the ability to use multiple hpRNA constructs in one infiltration treatment.

These technical advances in silencing more than one gene were further demonstrated by the co-silencing of two biochemical pathways for the desaturation of oleic acid (18:1) to linoleic acid (18:2). The silencing of *NbFAD2* and *NbFAD6* in the same infiltrated leaf tissue confirmed that more than one gene could be silenced in order to increase the flow of substrates into other pathways of interest.

Gene expression studies revealed that *NbFAD2.2* is more highly expressed than *NbFAD2.1* in *N.benthamiana* leaves, although silencing targeted to the 3'UTR region of *NbFAD2.2* did not change 18:1 levels (Fig 2.8B). This suggested that the levels of mRNA abundance for *NbFAD2.2* may not be related to its biochemical activity. Another possibility is that although mRNA is silenced via hpRNA, the NbFAD2.2 protein is long-lived and its activity does not diminish during the relatively short time frame of the transient assays. A further possibility is that the reduction in NbFAD2.2 activity or transcript abundance is counterbalanced by an improved activity in NbFAD2.1. It is worth noting that specific silencing of *NbFAD2.1* via targeting the 3'UTR region was capable of increasing 18:1 levels in transient assays, suggesting that reduction in NbFAD2.1 activity is not offset by increased NbFAD2.2 activity.

One unexpected observation in the optimisation of transient assay was the enhancement of transgene overexpression in the presence of a non-specific hpRNA and in the absence of a VSP. Overexpression of a non-specific hpRNA (hpRNA against GFP) allowed overexpression

of transgenes (*AtDGAT1*) in the absence of a VSP (Fig 2.6C). The levels of oil in leaf tissue infiltrated with AtDGAT1 and GV3101 were similar to those in leaf tissue infiltrated with AtDGAT1 and non-specific hpRNA. Intriguingly, both non-specific hpRNA and blank *A.tumefaciens* cells were able to allow overexpression of AtDGAT1. These results suggested that the production of sRNAs from the non-specific hpRNA may have saturated the endogenous silencing apparatus of the infiltrated leaf tissue, therefore the infiltrated leaf had little capacity for mounting the co-suppression response against *AtDGAT1*. Although leaf tissue infiltrated with AtDGAT1 and V2 contained slightly higher levels of oil, gene expression analysis revealed that V2 allowed the highest level of transgene overexpression (Fig 2.10B).

As oil is stable once produced in the leaf, measuring the changes in total oil may not have been an ideal method for measuring the level of overexpression of a transgene in transient systems. Measuring levels of long-lived proteins such as GFP and GUS (β-glucuronidase) (Worley et al., 1998) in similar cases were also expected to be misleading. It is also plausible that translational inhibition driven by sRNA may also affect the gene expression analysis – in this case, metabolite analysis may have been a more suitable method for measuring end-point products.

Collectively, the results presented in this chapter were able to support the use of a non-specific hpRNA to allow overexpression of transgenes. Although V2 provided maximal oil synthesis and gene expression, it is plausible that the use of a non-specific hpRNA may assist in transient assays where the use of a VSP imposes negative effect on the assay parameters.

In addition to the optimisation of the transient assay using V2, the results have shown that effective silencing was achieved in 4–5 days. Previous reports have shown that *N.tabaccum* was stably transformed with a hpRNA targeting FAD2 which resulted in an increase in the levels of 18:1 in the leaf (Belide et al., 2011) – the results in this chapter have shown that the transient silencing of *NbFAD2* is achieved in a relatively short time frame, with similar results as previously described, using stable transformation.

The findings therefore assisted in the optimisation of the transient leaf assay, allowing optimal endogene silencing to shunt endogenous metabolites into the assembly of transgenic pathways in order to synthesise LCPUFA and oil in the leaf. The results also confirmed that the hpRNA used in the infiltration experiments were very effective in gene

silencing, regardless of the size of the hpRNA. Furthermore the protocols used for characterisation of *NbFAD2* gene family served to become the basis for exploring the effect of silencing other critical enzymes involved in lipid biosynthesis.

2.3.2 Biosynthesis of novel fatty acids in the leaf to probe native lipid movement

It is a challenging task to manipulate endogenous lipid pools and then track minute changes in fatty acid profile of different lipid pools. This chapter explored an alternate approach, where novel fatty acids were traced from their site of synthesis to other lipid pools. Unusual fatty acids are relatively easy to monitor during their movements on lipid head groups and various fatty acid elongases and cyclopropanation reactions (CPFAS) were here used to probe lipid metabolism. The lipid metabolite 18:1 is a key intermediate substrate for a range of endogenous and transgenic reactions. V2 and endogene silencing were used to shunt 18:1 into production of novel fatty acids while 18:2 levels were also shunted into a new transgenic pathway. This system revealed unexpected lipid transport from the ER into the plastid.

2.3.2.1 Biosynthesis of DHSA in the leaf to probe lipid modification in different lipid pools

The results in this chapter report the engineering of DHSA, a novel fatty acid, in leaves at levels not seen previously (up to 15% in leaf oil) and are the first to demonstrate the synthesis of high levels of DHSA in plant oils. Transgenic *A.thaliana* seeds expressing GhCPFAS have been shown to contain 60% oleic acid and 1% DHSA (Yu et al., 2011), while studies in this chapter used silencing of *NbFAD2* to generate oleic acid levels at approximately 10% of total fatty acid, which was readily available for the production of DHSA at 6% in total leaf lipids and 15% in leaf oil. These experiments have shown that the enzymes involved in the handling of DHSA in *N.benthamiana* leaves are likely to be very different from in *A.thaliana* seeds – it would be of interest to systematically silence various lipid-handling pathways in *N.benthamiana* leaves to determine which steps are required for DHSA accumulation in leaves. Identifying the precise mechanisms for the accumulation of DHSA in leaf oils could help alleviate the bottlenecks for DHSA production in oilseeds.

The studies presented in this chapter used GhCPFAS to probe the lipid movement between different lipid pools and to assess the effect of shunting endogenous metabolites into a

transgenic pathway. Based on SfCPFAS and recent characterisation of *G.hirsutum* CPFAS, it is known that GhCPFAS catalyses the cyclopropanation of 18:1 esterified to the *sn*-1 position of PC (Fig 2.16) (Bao et al., 2003; Yu et al., 2011). The results here have shown that DHSA produced at the *sn*-1 position of PC readily moved to other lipid head groups for further modification (Fig 2.7 & Fig 2.16). Investigations into the movement of DHSA from the PC lipid pool (that is, the site of synthesis) into other lipid pools in the plant cell had not been previously reported. The assembly of transgenic pathways consisting of two acyl-CoA (AtDGAT1, AtFAE1) and PC pool (GhCPFAS) modifying enzymes showed that lipid movement between the PC and CoA lipid pools occurs readily (Fig 2.7). The results indicated that DHSA which was esterified to the *sn*-1 position of PC was transferred to the CoA pool, where AtFAE1 elongated DHSA to produce eDHSA (Fig 2.7). Furthermore AtDGAT1 was shown to selectively transfer DHSA and eDHSA into leaf oil, confirming that DHSA is readily assembled into TAG via AtDGAT1 and suggesting that DHSA and oleic acid have structurally similar acyl chains (Fig 2.7). The ability of AtDGAT1 to incorporate DHSA into TAG molecules provides some evidence for DHSA movement from the PC lipid pool into the CoA lipid pool, although other pathways for oil accumulation do exist. It remains unclear which pathway is used for the movement of specific chains from the PC fraction into the CoA pool, although two possible routes are the reverse reaction of LPCAT and the combined activity of PLA and ACS (Maisonneuve et al., 2010).

Biochemical analyses of eDHSA also indicated the movement of eDHSA from the CoA into the PC pool. Low levels of eDHSA were detected in the PC pool (Fig 2.7), indicating that lipids are readily transferred between the CoA and PC lipid pools in the ER. Previous reports have shown that the activity of SfCPFAS does not increase with the addition of oleoyl-CoA, which eliminates the use of acyl-CoA as substrate (Bao et al., 2003). The reverse reactions of NbLPCAT and NbPLA1 are possibly involved in the deacylation of PC, in turn releasing DHSA into the CoA pool (Fig 2.16). Furthermore, 18:1-CoA and DHSA-CoA are elongated by AtFAE1 to produce 20:1-CoA and eDHSA (Fig 2.7). The presence of 20:1 and eDHSA in the PC pool also indicates that enzymes in *N.benthamiana* have the ability to move this class of unusual fatty acids between the CoA pool and membrane-bound PC head groups.

Silencing of *NbFAD2* increased 18:1 in the leaf, resulting in an increase in DHSA. Other silencing data showed that the highest level of 18:1 measured in the leaf was the result of

combinatorial silencing of *NbFAD2* and *NbFAD6*. A small difference in the conversion efficiency of GhCPFAS was measured in leaves infiltrated with GhCPFAS alone compared to leaves infiltrated with both GhCPFAS and hpNbFAD2, suggesting that GhCPFAS performs efficiently in *N.benthamiana* leaves and a possibility that a further increase in 18:1 levels would result in higher levels of DHSA in the leaf. It is therefore plausible to combine the silencing of *NbFAD2* and *NbFAD6* with the overexpression of *GhCPFAS* in order to synthesise higher levels of DHSA in *N.benthamiana* leaves.

A very low percentage of DHSA (~1%) was also detected on the DGDG fraction, although these results were not reported due to potential contamination of the DGDG fraction with neutral lipids. It is possible that the contamination occurred during the separation of the polar lipids on the TLC plate, however this was not confirmed.

The *SfCPFAS* was reported not to contain a plastid targeting sequence (Bao et al., 2003) which eliminated the possibility of GhCPFAS using acyl-ACP as substrate. Recent work indicates that there may be significant mixing of chloroplast membranes and ER membranes in plant leaves (Mehrshahi et al., 2013), although lipids do move between the membrane and plastid, so it is plausible that more sensitive forms of lipid analysis (such as Liquid Chromatography techniques) may allow better characterisation of the galactolipid pools.

The results presented in this chapter have shown the use of GhCPFAS as a tool to remodel oleic acid esterified to the *sn*-1 position of PC. The presence of novel fatty acids (DHSA and eDHSA) were traced in different lipid pools in the leaf and it was shown that relatively high levels of DHSA were accumulated in leaf PC and TAG pools.

A schematic summarising the movement and modification of 18:1 by the enzymes described here is presented in Figure 2.16. Based on the FAME extracted from infiltrated *N.benthamiana* leaves, this figure proposes that: GhCPFAS cyclopropanates 18:1-PC into DHSA-PC; the activity of NbLPCAT and NbPLA1 may be involved in the removal of DHSA from the *sn*-1 position of PC to form LPC and to release DHSA as CoA; AtFAE1 further elongates DHSA-CoA into eDHSA-CoA; AtDGAT1 is more competitive than AtFAE1 in the CoA pool, resulting in higher incorporation of DHSA into TAG; and a final reaction by NbLPCAT incorporates eDHSA-CoA into LPC to synthesise PC. The positions of DHSA and eDHSA in the TAG and PC molecules were not investigated. The figure also illustrates the main fatty acids

found in the MGDG (18:3 and 16:3) and DGDG (18:3 and 16:0) lipid pools in the leaf. It is possible that NbTGD1 recycled leaf TAG containing DHSA into the plastid. Other mechanisms of transportation of DHSA into the plastid may depend on the roles of ABC transporters.

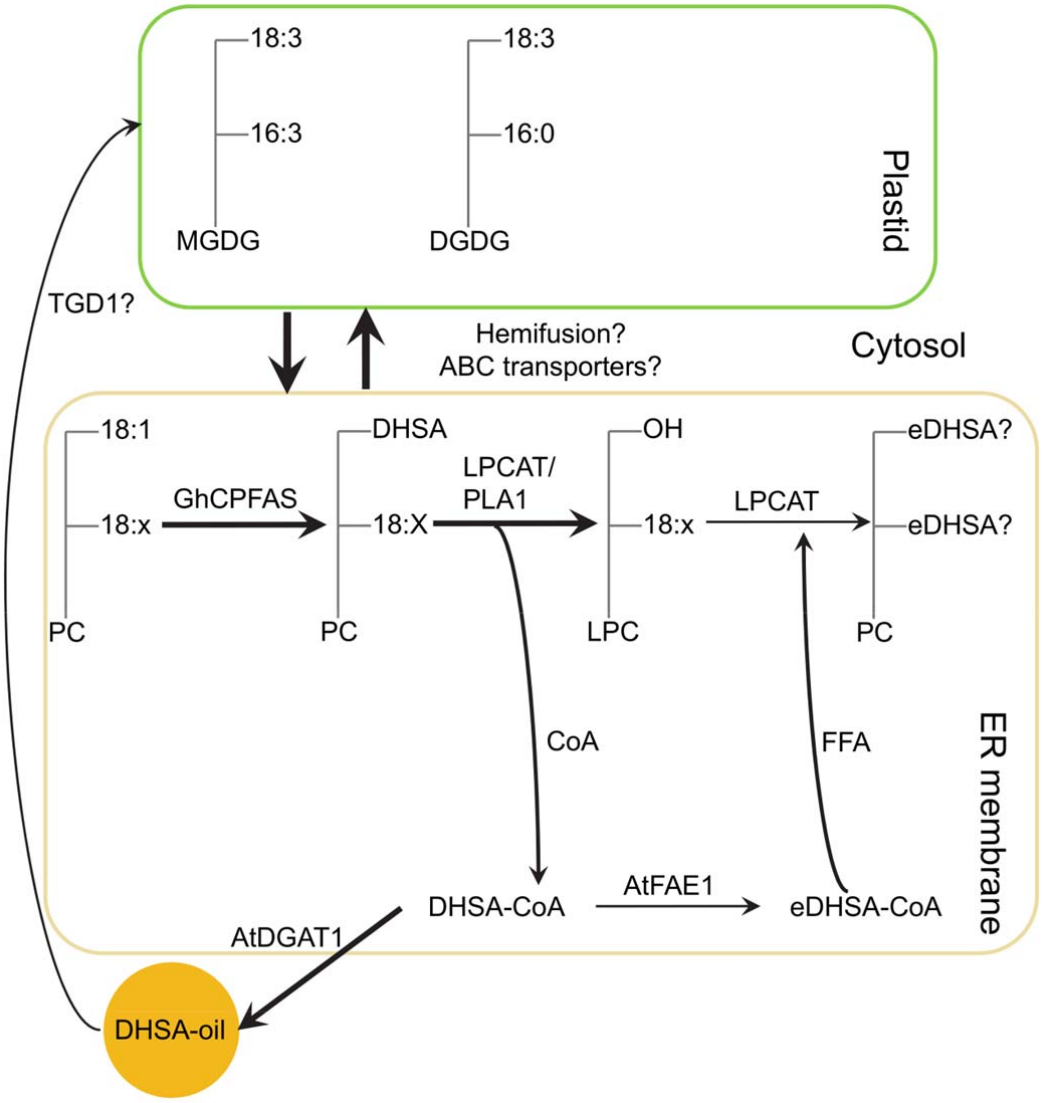

Figure 2.16. Proposed schematic of the synthesis and movement of DHSA between the PC and CoA and plastid lipid pools.

The proposed modification of lipids in *N.benthamiana* leaves overexpressing *GhCPFAS*, *AtFAE1* and *AtDGAT1*. This proposed model is based on the presence of transgenic metabolites measured in different lipid pools. The schematic also shows the main fatty acids found in the MGDG and DGDG lipid pools in the plastid.

2.3.2.2 Biosynthesis of elongated products to probe lipid movement in different lipid pools

Previous reports have shown that elongases catalyse the sequential addition of two C2 moieties to an acyl chain in the CoA pool (Broun and Somerville, 1997). Elongases *AtFAE1* and *IgΔ9E*, from two different species, were transiently expressed in *N.benthamiana* leaves to synthesise elongated products (20:1, 22:0, 22:1, 20:2 and 20:3) in total leaf lipids.

The combined silencing of *NbFAD2* and overexpression of *AtFAE1* resulted in higher levels of 20:1 in the leaf. A range of other elongated fatty acids, including 20:0, 22:0 and 22:1, were also measured in leaf oil (Table 2.1). As previously mentioned, overexpression of *AtDGAT1* in the same mix resulted in 20:1 in leaf oil. These results provided another example of metabolic engineering in the leaf dependent on maximal transgene overexpression and endogene silencing. This system may allow rapid testing of the abilities of various different enzymes to incorporate elongated and novel products into leaf oil.

The overexpression of *IgΔ9E* was coupled with the silencing of *NbFAD3* and *NbFAD7*. This system revealed that NbFAD3 did not make a major contribution to the desaturation of 18:2 to 18:3 in the leaf and IgΔ9E was able to elongate 18:2 to 20:2 and 18:3 to 20:3 (Fig 2.13A). The silencing of *NbFAD7* resulted in high levels of 18:2, which coupled with overexpression of *IgΔ9E* favoured the production of 20:2 over 20:3 (Fig 2.13B). The PC metabolite data obtained from leaves overexpressing *IgΔ9E* showed that lipids modified in the CoA pool were rapidly moved into the PC pool (Fig 2.13C). Around 42% of native PC lipids were replaced by the elongated products, suggesting that *N.benthamiana* leaves express active enzymes that are involved in transport of LCPUFA from the CoA pool into the PC lipid pool. These steps may be combined with the overexpression of desaturases and elongases to synthesise nutritional oils such as ω-3 and ω-6 LCPUFA in *N.benthamiana* leaves. The discovery of enzymes involved in handling of LCPUFA in *N.benthamiana* leaves may furthermore facilitate cloning of the respective genes into oil-seed crops, which could result in the synthesis of high levels of ω-3 and ω-6 LCPUFA in seed oils.

A significant percentage of MGDG and DGDG were also comprised of IgΔ9E products. These results suggested an active exchange between lipids modified in the ER and the chloroplast. It is also a possibility that the polar lipids were contaminated on the TLC plate with neutral lipids containing IgΔ9E products, although this possibility was not confirmed and more

sensitive assays are required to confirm presence of LCPUFA in different lipid pools in the leaf. The percentages of LCPUFA detected in galactolipid pools were higher than the levels of DHSA. It is also possible that there was a direct transfer of LCPUFA from the PC into the chloroplast, as a large portion of native PC was replaced by the LCPUFA. Labelling experiments have shown that ER-derived PC lipids were found on the outer envelope of the plastid, direct evidence of lipid movement between the two compartments (Dorne et al., 1985). There is growing evidence to support the physical contact between the membranes, however the exact process of lipid transfer between the contact sites is not clear (Mehrshahi et al., 2013).

Proteomic and bioinformatic analysis of 102 transporter candidate genes in the chloroplast envelope revealed that only one was recognised as transporter of non-polar metabolites (Mehrshahi et al., 2013). It is well-known that a large number of fatty acids are synthesised in the chloroplast (see Chapter 1) and it is highly unlikely that one transporter is sufficient for the bidirectional transfer of lipids between the plastid and the ER. Mehrshahi et al. (2013) proposed that the lack of non-polar metabolite transports may have been due to the hemifusion of membranes – during hemifusion the outer leaflet of plastid mixes with the ER and non-polar molecules are able to move between the two membranes. However, to control the movement of non-polar compounds, the hemifused sites may depend on the activity of fatty acid-specific transporters in the membrane envelope, which have not been characterised yet. Characterising the components of the hemifused sites involved in lipid transfer between the ER and the plastid using the overexpression of *IgΔ9E* in *N.benthamiana* leaves and tracing the elongated products is a promising approach.

A schematic summarising the movement of lipids between different lipids pools, based on the results of IgΔ9E experiments, is presented in Figure 2.17. This figure uses 18:3 as an example to illustrate the modifications and movements of lipids in leaves infiltrated with *IgΔ9E*. Silencing of *NbFAD3* and results on PC showed that NbFAD3 is not very active in the leaf, therefore 18:3 found on PC must directly flow from the chloroplast. 18:3 found as CoA in the membrane is elongated to 20:3 and this product is used to acylate LPC for synthesis of PC, possibly by the action of LPCAT. 20:3-PC is transferred to the chloroplast by either the action of an unknown enzyme or transporter, or simply by physical contact between the ER and the plastid.

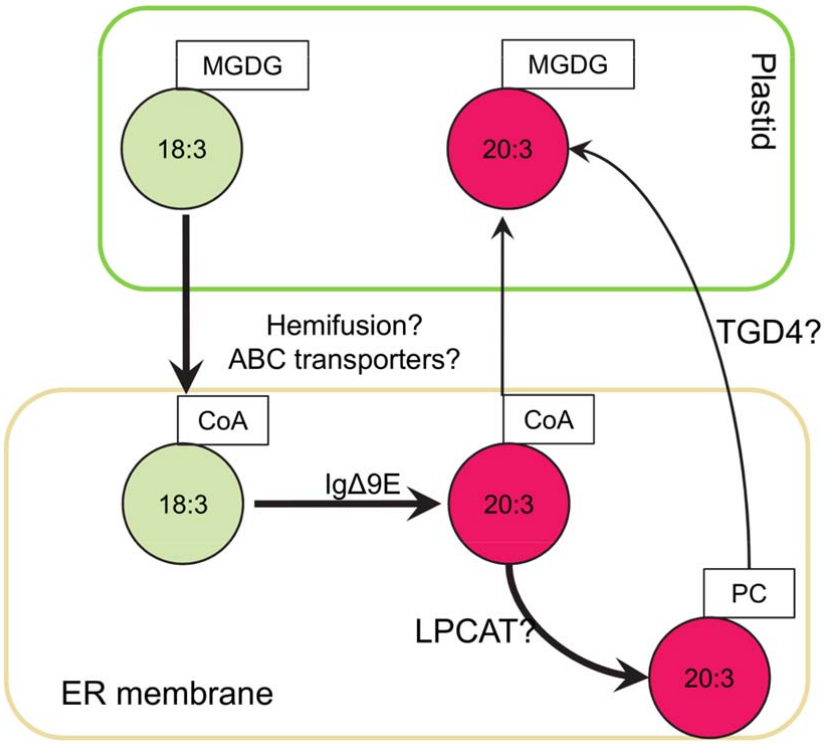

Figure 2.17. Proposed schematic of lipid transfer between the ER and the plastid – the LCPUFA example.

The proposed model based on the silencing of *NbFAD3*, *NbFAD7* and overexpression of the *IgΔ9E* to probe the modification of 18:3 in the CoA pool.

2.3.3 Targeted survey of lipid handling genes in N.benthamiana *leaves*

This chapter also sought to understand the flux of lipids through leaf cells through a targeted survey of lipid handling and modification steps. The optimised assay conditions and online genomic tool were used to explore the influence of silencing numerous lipid modification enzymes. A number of genes considered critical to lipid handling pathways, whose silencing in stable systems was found to be lethal, were silenced transiently in *N.benthamiana* leaves and their effects on metabolite levels were analysed. These enzymes included the *N.benthamiana* SAD1, FAD2, FAD3, FAD6 and FAD7, FATA and FATB. The roles of a number of enzymes involved in lipid trafficking between the ER compartments and between ER and the chloroplast, including *N.benthamiana* LPCAT, TGD1, GPAT and LPAAT, were also silenced. The combined silencing of a number of lipid-handling genes was also investigated to probe the consequence of multiple gene silencing on lipid fluxes.

2.3.3.1 Silencing of candidate enzymes involved in modification of lipids

A key step in the biosynthesis of membrane lipids involves the desaturation of 18:0 in the chloroplast catalysed by SAD1 enzyme. The transcriptome data of *N.benthamiana* revealed one candidate gene that closely matched *AtSAD1*. The resulting silencing construct hpNbSAD1 increased 18:0 levels from 2% to 11% in infiltrated leaves (Fig 2.12C) which closely matches *A.thaliana* mutant leaves (containing 14% of 18:0) (Wallis and Browse, 2002). Previous reports also suggested that the profiles of membrane lipids were not highly affected in the *sad1* mutant leaves as the mutation was in one of several genes that encode 18:0-ACP desaturase (Gibellini and Smith, 2010; Wallis and Browse, 2002). Interestingly it is the presence of other 18:0-ACP desaturases in *sad1* mutant which ensures 80% of 18:0-ACP is desaturated (Wallis and Browse, 2002), although a slight reduction in desaturation of 18:0-ACP, possibly combined with the increase in 18:0 levels incorporated into membrane glycerolipids, results in dwarfed plants (Lightner et al., 1994; Wallis and Browse, 2002). The silencing of *NbSAD1,* unlike other desaturases, resulted in leaf bleaching (Fig 2.12D) – the change in the phenotype of infiltrated tissue suggested that the increased incorporation of 18:0 into membrane lipids may have resulted in the discolouration of the infiltrated leaf tissue. This phenotype was not investigated any further.

A number of enzymatic steps take place after the desaturation of stearic acid in the plastid, releasing the acyl chain for assembly into glycerolipids in both there and in the ER. In both

locations the second desaturation step is carried out by membrane-bound desaturases, converting 18:1 to 18:2. Silencing constructs were designed against 18:1 desaturases NbFAD6, present in the plastid, and NbFAD2, found in the ER. The single mutants of *Atfad2* and *Atfad6* contained 21% and 16% of 18:1 compared to 3% measured in wild-type leaves (Wallis and Browse, 2002). The silencing experiments revealed that NbFAD2 and NbFAD6 were highly active in *N.benthamiana* leaves, however the contribution of NbFAD2 was higher than NbFAD6 in desaturating 18:1 (Fig 2.12A). These results suggest that NbFAD2 activity is very high in the ER in comparison with the activity of NbFAD6 in the chloroplast. They are also in agreement with the *A.thaliana* single mutant results. It is of interest that co-infiltration of silencing constructs against *NbFAD2* and *NbFAD6* in one target leaf tissue produced the highest level of 18:1 – this discovery confirmed the possibility of stacking multiple hpRNA constructs in order to efficiently silence multiple endogenes using one infiltration mix. Surprisingly, the combined silencing resulted in 13% reduction in 18:3 levels (Fig 2.12A) indicating, firstly, the presence of other 18:1 desaturases that were not silenced with hpNbFAD2 and hpNbFAD6. The *fad2 fad6* double mutant of *A.thaliana* contained 60% of 18:1, very low levels of 18:2 and no 16:3 and 18:3 in total leaf lipids (Wallis and Browse, 2002). The analysis of the *FAD2* gene family in *N.benthamiana* revealed the presence of at least 2 gene family members. As previously mentioned, it is possible that more isozymes of NbFAD2 and NbFAD6 are active in leaves which were not cross-silenced using hpNbFAD2 and hpNbFAD6. The galactolipid pools were not extracted to investigate the effect of NbFAD6 silencing on 18:3 levels. Silencing of *NbFAD2* showed no effect on the DGDG lipid profile (Fig 2.4E).

The results thus far have shown that hpRNAs are highly effective in silencing endogenes in *N.benthamiana* leaf assays. The FAME profiles of infiltrated leaves are also indicative of the contribution of particular enzymes in catalysing their respective reaction(s).

The next desaturation step, to convert 18:2 to 18:3, takes place in the ER by NbFAD3 and the plastid by NbFAD7. The triple *fad3 fad7 fad8 A.thaliana* mutant contained no 18:3 in leaf lipids (Wallis and Browse, 2002). The transcriptome data revealed that *N.benthamiana* contained one gene encoding for each NbFAD3 and NbFAD7 and both genes were successfully silenced in leaves. One *N.benthamiana* gene aligned to *AtFAD7* and *AtFAD8* and it is referred to NbFAD7. The leaf lipid profile of *Atfad8* mutant was similar to that of the

wild-type leaf (Wallis and Browse, 2002). The silencing experiments revealed that most of the 18:3 found on PC is synthesised in the chloroplast. Initial analysis of PC revealed no change in the level of 18:3 when *NbFAD2* was silenced (Fig 2.4E), suggesting that 18:3-PC is transported from the plastid and not synthesised on PC. Further analysis of PC in leaves infiltrated with hpNbFAD3 revealed that 18:2 and 18:3 levels did not change (Fig 2.13C). These results confirmed that NbFAD3 is not highly active in *N.benthamiana* leaves. Silencing of *NbFAD7* reduced 18:3 levels dramatically, which confirmed that majority of 18:3 is synthesised in the chloroplast. Although silencing of *NbFAD7* was not able to reduce 18:3 levels below ~30% in total leaf lipids (Fig 2.12A), it is possible both that NbFAD7 protein is long-lived and 18:3 levels would drop further if the infiltrated leaves were harvested 7–8 dpi and that other isozymes of FAD7 are present in *N.benthamiana* that were not silenced. Furthermore, 18:3 decreased by 18% and 15% in the MGDG and DGDG lipid fractions of leaves infiltrated with both hpNbFAD7 and IgΔ9E (Fig 2.13D), confirming that high levels of 18:3 remained in the plastid. 18:3 is a crucial fatty acid required for a number of processes in the thylakoid membranes and it is possible that the leaf has a number of back mechanisms that are activated after the disruption of NbFAD7. Further analyses are required to uncover the enzymes involved in biosynthesis of 18:3 and to understand the enzymes responsible for efficient transfer of 18:3 from the plastid into the ER.

A schematic summarising the activities of the desaturases silenced in *N.benthamiana* leaves is presented in Figure 2.18.

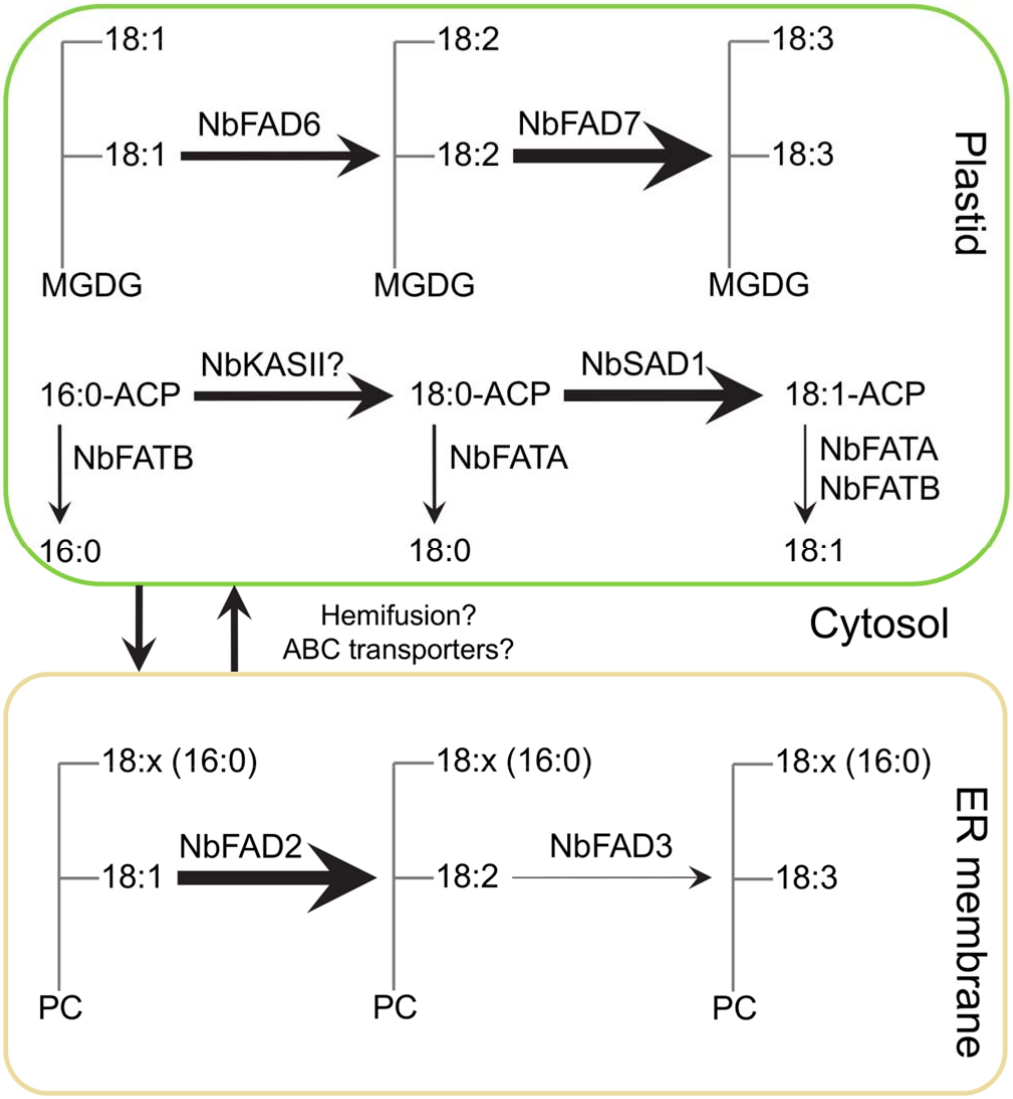

Figure 2.18. Proposed schematic of fatty acid modification in the plastid and the ER.

A simplified view of lipid modification in the plastid and ER, based on the silencing of genes in *N.benthamiana* leaves. The thickness of the arrow indicates the activity of the respective enzymes in modifying the fatty acids.

2.3.3.2 Silencing of candidate enzymes involved in modification of lipid head groups

NbFATA and NbFATB hydrolyse unsaturates (18:1-ACP) and saturates (16:0-ACP and 18:0-ACP) in the chloroplast. Both of the corresponding genes were silenced transiently in *N.benthamiana* leaves. *NbFATB* was initially silenced using a ~200 bp hpRNA targeting the middle region of the ORF (data not shown), however leaves infiltrated with this silencing construct did not show the large change in the levels of 16:0 that had been expected. A longer hpRNA construct was therefore prepared, but no difference was detected between the FAME profile of leaves infiltrated with the short and long hpRNAs. These analyses also confirmed that 200 bp hpRNA constructs are effective in silencing endogenes in transient leaf assay. The changes in the FAME profile of leaves silenced for NbFATA and NbFATB activities further indicated that both of the silencing constructs were effective in silencing their respective genes.

Previous reports have shown that a *fatb* knockout in *A.thaliana* reduced 16:0 in leaves by 42% (Bonaventure et al., 2003). Silencing of *NbFATB* resulted in 9% decrease in 16:0 levels in the leaf while 18:2 levels increased, suggesting that more of 16:0 remained in the chloroplast for downstream modifications. A significant change was measured in levels of 16:3 and 18:0 in leaves silenced for *NbFATA*, which may have been the consequence of reduced levels of 18:1 coming out of the chloroplast. Surprisingly, silencing of *NbFATA* and *NbFATB* resulted in 20% and 10% decrease in 18:0 levels respectively. These results suggested that the contribution of NbFATA is more than NbFATB in hydrolysis of 18:0-ACP and that silencing of *NbFATB* results in an increase in 16:0-ACP which remains in the chloroplast longer for downstream desaturation to 18:0. The combinatorial silencing of *NbFATA* and *NbFATB* resulted in a 28% decrease in 18:0 levels. Although the silencing experiments indicated that NbFATA and NbFATB are involved in modification of lipids in the leaf, the changes in levels of 16:0, 18:0 and 18:1 in the leaf did not match the results previously achieved in stable systems. It is therefore possible that other enzymes were involved in the active export of 16:0, 18:0 and 18:1 out of the chloroplast. It is also plausible that silencing of *NbFATA* and *NbFATB* may have had a major effect on the profile of galactolipids, however the two major galactolipid pools containing MGDG and DGDG were not analysed. It is expected that silencing of *NbFATB* will have significant effect on the levels of 16:0 in the DGDG fraction.

The overexpression of *IgΔ9E* was used to assess the function of a number of enzymes involved in the movement of lipids between the different lipid head groups. The disruption of the activities of NbLPCAT, NbGPAT9, NbLPAATs and NbTGD1 were combined with the overexpression of *IgΔ9E*, presenting a number of unexpected results.

This chapter investigated the effect on leaf lipid profile of silencing *NbTGD1* (trigalactosyldiacylglycerol1), an enzyme involved in recycling of TAG and PA from the ER into the chloroplast (Fig 2.16) (Xu et al., 2005). The silencing of *NbTGD1* is beneficial to engineering leaves for biosynthesis of oil, however no change was observed in the leaf oil (results not shown) or the FAME profile of total leaf lipids. This indicated that other enzyme(s) may become active in the absence of NbTGD1. Mutation of *TGD1* in *A.thaliana* has been shown to effect the PA lipid pool (Xu et al., 2005) – further analysis should include isolation of the PA from total leaf lipids extracted from infiltrated *N.benthamiana* leaves. TAG is similarly not easily detected in *N.benthamiana* leaves and subtle changes in leaf TAG may require alternative and more sensitive techniques of analysis. It is also expected that minor changes may be detectable in the total amount of galactolipid pools extracted from the chloroplast. Overall, the results of *NbTGD1* silencing were not as expected and as a consequence the enzymes involved in transport and recycling of ER lipids in *N.benthamiana* are yet to be uncovered.

Recent reports have shown that *A.thaliana* contains nine uncharacterised ABC transporters (Mehrshahi et al., 2013). Seven of these are expressed in the leaf and it is proposed that they may be involved in fatty acid and membrane lipid synthesis (Mehrshahi et al., 2013). The ABC transporter selective for movement of non-polar compounds into the chloroplast binds to PA (Benning, 2009). The characterisation of these transporters has been challenging and the reason, as proposed by Mehrshahi et al. (2013), is their broad selectivity for a range of non-polar substrates for transportation between the chloroplast envelope and the ER. Furthermore, it has been proposed that physical contact between the plastid-associated and ER membranes results in bidirectional access to non-polar molecules (Mehrshahi et al., 2013).

In vitro assays have demonstrated that NbLPCAT is capable of transferring an acyl group from acyl-CoA to PC (Wang et al., 2012). *N.benthamiana* leaves infiltrated with hpRNA targeting *NbLPCAT* showed no significant changes in total leaf lipids while a subtle change

was observed in the profile of PC in leaves infiltrated with hpNbLPCAT. Previous studies have shown that the forward reaction (acylation of lysophosphatidylcholine, LPC) of LPCAT is much more favoured than the reverse reaction (deacylation of *sn*-2 PC) and is selectivity reduced with increased desaturation (Stymne and Stobart, 1984). Silencing of *NbLPCAT* when combined with the overexpression of *IgΔ9E* did not show significant changes on the profile of total leaf lipids. Applying this information to the *N.benthamiana* system, it was expected that the addition of 20:2 on LPC would be more efficient compared to the loading of 20:3. A higher amount of 20:2 was found on PC compared to 20:3 levels while a reduction was observed in levels of 20:2-PC in leaves silenced for *NbLPCAT*, which confirmed that NbLPCAT is involved in acylation of LPC. There are also many other endogenous routes, which become active when one critical enzyme is silenced – the activities of enzymes such as PDCT, CPT and PLC have been shown to substitute for the lack of LPCAT activity (Li-Beisson et al., 2013; Wang et al., 2012). To further probe the activity of NbLPCAT, experiments may require preparing leaf microsomes from leaves infiltrated both with and without hpNbLPCAT. This system may reveal the forward and reverse reactions of NbLPCAT by feeding labelled LPC and PC, respectively.

Another enzyme, NbPLA2, involved in removal of acyl groups from the *sn*-2 position of PC resulting in production of LPC, was also silenced although no change was detected in the profile of total and PC leaf lipids (data not shown). The double *lpcat1*/*lpcat2* mutant of *A.thaliana* showed up regulation of *PLA*s (Wang et al., 2012) – analysis revealed an accumulation of LPC, which was due to lack of PC reacylation by LPCAT and accelerated deacylation by PLA. Future experiments could involve combined silencing of *NbLPCAT* and *NbPLA* with the overexpression of *IgΔ9E* in order to generate changes in PC lipid profile.

The Kennedy Pathway (Li-Beisson et al., 2013) is another possible route by which the products of IgΔ9E could enter PC. The first and second steps of this route involve the acylation of G3P by GPAT to produce LPA and LPAAT and to produce PA. It was hypothesised that the silencing of *NbGPAT9* would disrupt the Kennedy pathway, therefore not requiring the downstream reactions by LPAATs, however silencing of *NbGPAT9*, *NbLPAAT4* and *NbLPAAT6* did not change the total leaf lipid profile. The silencing of these genes was coupled with the overexpression of *IgΔ9E*, however no significant changes were detected in the levels of 20:2 and 20:3. The most significant change in levels of 20:2 and 20:3 was

measured when the three genes were silenced together, although this change was not significant and suggests that the contribution of Kennedy pathway to the PC lipid pool is very limited. Although the PC fraction was not isolated from these leaf infiltrations, the PC is a large fraction of total lipids and major changes in the profile of PC are mirrored in the profile of total leaf lipids.

Figure 2.19 summarises the possible routes of acyl transfer between the CoA and the PC lipid pool. The silencing and overexpression experiments in transient leaf assay have shown that the Kennedy pathway and LPCAT are not the major routes for transfer of LCPUFA from the CoA into the PC lipid pool – an unknown pathway via which an efficient transfer of LCPUFA occurs is therefore proposed. This unknown pathway may also be responsible for efficient transfer of DHSA into the CoA pool and for the transfer of eDHSA from the CoA into the PC pool.

The techniques used and the results presented in this chapter have been useful in improving current understanding, and providing an alternative approach towards the mechanisms, of lipid biosynthesis in *N.benthamiana* leaves. The rapid assay assisted in studying the roles of enzymes involved in desaturation of membrane glycerolipids. Finally, because of the advantages of the online genomic tool, this chapter has revealed many applications of *N.benthamiana* that assisted in manipulation of lipid pathways. This model plant is ideal for molecular biology and biochemistry-based studies of lipid metabolism in plants and shows an advantage over thousands of mutant screens that have been previously performed in *A.thaliana*.

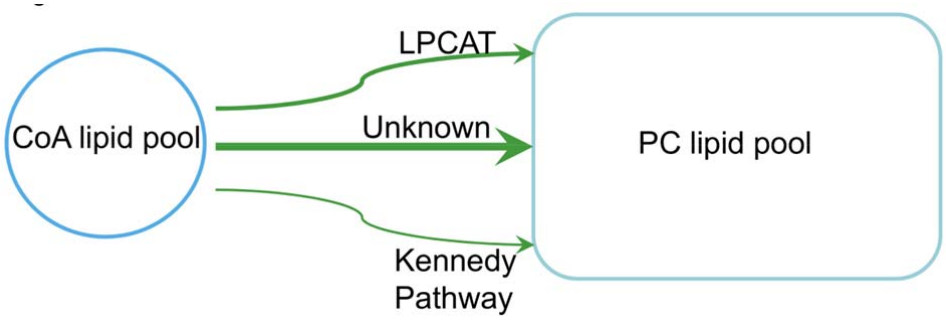

Figure 2.19. A schematic presenting routes for the flow of acyl-CoA into the PC pool in *N.benthamiana* leaves.

A proposed model showing the movement of fatty acids between the CoA and PC lipid pools. The sizes of the arrows are based on the results of silencing *NbLPCAT* and members of the Kennedy pathway.

2.4 Conclusions

The results presented in this chapter have provided an extensive source of knowledge in techniques which can enhance the metabolic engineering of lipid pathways in *N.benthamiana* leaves. The main conclusions are that:

- V2 is an alternative VSP which allows hpRNA-mediated silencing of genes and maximal overexpression of transgenes
- It is possible to infiltrate *N.benthamiana* leaves with multiple hpRNA constructs to efficiently silence several genes
- The biochemistry of *N.benthamiana* leaves is ideal for the production of novel fatty acids such as DHSA
- Lipids are actively transported between the plastid, the CoA and the ER in *N.benthamiana* leaves. Leaf lipid metabolism may be significantly different to seed lipid metabolism.

2.5 Future work

The results presented in this chapter have raised a number of questions that may be clarified with future work. This chapter targeted a range of lipid handling and editing enzymes for silencing, although not all of these endogenes generated discernible differences in lipid biochemistry. A range of changes in lipid profiles when single and multiple endogenes are silenced could be further investigated using the improvements in lipid analysis as outlined here. Furthermore, unusual fatty acids could be used in combination with silencing of endogenes and lipidomic approaches to trace the flux of lipids in transient leaf assays. It is likely that the combination of these approaches will be able to precisely pinpoint the enzymes involved in the transport and editing of lipids in plant cells.

The emerging techniques in shotgun lipidomics and the manipulation of lipid pathways in transient leaf assay may assist in rapid analysis of various pathways and critical enzymes. The combination of lipidomics and transient leaf assay will allow a better assessment of the relative contribution of the key steps of lipid metabolism to the phenotypes observed in *N.benthamiana* leaves. The possibility of multiple-gene silencing in *N.benthamiana* leaves has also welcomed a refined study of changes in phenotypes and metabolite profiles.

The metabolic engineering of the leaf for synthesis of DHSA in leaf oil was an important discovery. The discovery of enzymes involved in the handling of DHSA in *N.benthamiana* leaves may provide insight into successful engineering of seeds with high levels of DHSA. Previous studies have shown that *E.coli* CPFAS modified unsaturated fatty acids at the *sn*-2 position of phospholipids (Grogan and Cronan, 1997) – based on the GhCPFAS results, it would be interesting to investigate the overexpression of *EcCPFAS* in *N.benthamiana* leaves and assess the *sn*-2 remodelling of phospholipids. A combination of overexpressed *EcCPFAS* and *GhCPFAS* in the leaf may result in higher levels of DHSA due to their substrate preferences, including the cyclopropanation of unsaturated fatty acids in PE and PC lipid pools. The efficiency of GhCPFAS in cyclopropanating 18:1 remains unchanged with the silencing of NbFAD2. Based on these results, future studies may include stacked silencing of NbFAD2 and NbFAD6 to provide higher levels of 18:1 for cyclopropanation. It is possible that silencing of NbFAD2 and NbFAD6, when combined with the overexpression of GhCPFAS and EcCPFAS, may result in high levels of DHSA in the leaf.

Engineering leaves and seeds with reduced FAD2 and high GhCPFAS activities is of high industrial interest for downstream production of isostearic acid, which is used in cosmetics. It is plausible that stable transformation of *N.benthamiana* with GhCPFAS, AtDGAT1 and hpNbFAD2 may result in production of high levels of DHSA that can be used for industrial purposes.

Due to inconclusive results obtained from silencing of *NbTGD1*, it would be interesting to silence a number of other genes involved in transport of lipids between the ER and the chloroplast, such as NbTGD4. Previous studies have shown that *A.thaliana* TGD4 protein (trigalactosyldiacylglycerol4) is a candidate enzyme responsible for the transport of lipids with PC head group into the plastid (Xu et al., 2008). It is expected that the assessment of changes in the lipid profile of MGDG and DGDG fractions in leaves silenced for *NbTGD4*, coupled with the overexpression of *IgΔ9E*, would enhance the existing understanding of enzymes responsible for transport of lipids from the ER into the plastid.

The sRNA population generated by hpNbFAD2 was aligned against *NbFAD2.1* and no sRNAs were detected outside of the target region, which suggests that the silencing signal was not amplified. However sRNAs were extracted from leaf samples infiltrated with V2 and hpNbFAD2 and no control sample infiltrated with the hpNbFAD2 was tested. The function of V2 in suppressing the RNA silencing pathways may be better understood if future comparison of the plant can involve sRNAs generated by the hpNbFAD2 in *N.benthamiana* leaves with the exclusion of V2 from the infiltration mix. The silencing signal of hpRNA targeting endogenes is not amplified (Dong et al., 2011; Himber et al., 2003; Vaistij et al., 2002) but V2 would have inhibited the production of secondary siRNA.

2.6 Methods

2.6.1 Plasmid constructs for transient expression

Binary vectors were prepared by cloning the coding region of the gene into a modified version of the pORE04 binary vector, 35S-pORE04 – as described by Coutu et al. (2007), the CaMV 35S promoter is cloned into the SfoI site to yield 35S-pORE04. The coding sequences of p19 (Voinnet et al., 2003) and V2 (Glick et al., 2008) were chemically synthesised and cloned into 35S-pORE4 to yield pCW196 and pCW197 respectively. The *AtFAE1* gene was chemically synthesised but this ORF was impossible to clone directly into 35S-pORE4 – it is expressed in bacteria at low levels and is lethal. The catalase-1 intron was therefore included in the 5'UTR during a sub-cloning step before ligation into a 35S expression vector to yield pCW483. The 35S binary expression construct for *AtDGAT1* and *AtOleosin* were used as described in Wood et al. (2009). The CaMV 35S expression constructs of GFP and hpGFP, a hpRNA against GFP, were described in Brosnan et al. (2007a). The hpGFP construct was confirmed to include a 380 bp inverted repeat fragment targeting the first 380 bp of the GFP ORF. The binary expression vector driving a truncated version of GhCPFAS with a 35S promoter was prepared by Dr Qing Liu. A 35S expression vector driving the *IgΔ9E* gene was obtained from James Petrie (Petrie et al., 2012a). The coding sequence of *IgΔ9E* was cloned into 35S-pORE4 to yield pJP2062.

A 660 bp fragment of *NbFAD2* was cloned by RT-PCR from leaf total RNA using primers designed against a DNA contig assembly containing *NbFAD2* namely NbFAD2F1 5' TAGAACAGATGGTGCACGACGT and NbFAD2R1 5' TTATTGCGCACGAATGTGGCCA. The 660 bp *NbFAD2* gene fragment was subsequently ligated into pENTR/D-TOPO (Invitrogen™ life technologies) and recombined into the pHellsgate12 vector (Helliwell et al., 2002), using standard LR Clonase II Enzyme Mix (Invitrogen™ life technologies), to generate pFN033, a 35S-driven hpRNA directed against *NbFAD2*, hpNbFAD2. TOPO vectors were used according to manufacturer's instructions. Most Forward 5' primers were designed to contain CACC sequence to facilitate directional cloning. DNA fragments were amplified using proofreader enzyme, *PfuUltra* II Fusion HS DNA polymerase (Agilent Technologies, Inc.), to prevent 5' A overhangs. The other hpRNA constructs were generated in the same manner. The primer sets used to amplify fragments for hpRNA constructs are listed in Table 2.2.

Plasmid/Length	hpRNA	Sense primer	Antisense primer
pFN033/660 bp	hpNbFAD2	TAGAACAGATGGTGCACGACGT	TTATTGCGCACGAATGTGGCCA
pFN070/300 bp	300a	TTTTGTTTCTGTATTTGAGT	GATATGATATAATCTATAGG
pFN071/300 bp	300b	GGAGCTGGTGGTAATATGTCTCTTG	CCCAAATACCAGTGCAAACACAA
pFN072/300 bp	hpNbFAD2-300	CCTAAGCCGAAATCACAACTCG	TGGTACGCCATACATACACACGA
pFN073/300 bp	300d	TCACTACGATTCATCCGAAT	TGTTTTTGTACCAGAAAACACC
pCW609/300 bp	hpNbFAD2.1 3'UTR (300e)	CACCGTATTGGTCTTTGGTTATG	GGAAGAATCGATCAAAAGT
pFN078/370 bp	hpNbFAD2.2 3'UTR	ACCATGGCAATCAAAGAGACTGGGA	GTGTCCAGAAGTTTGATCATTTGATCC
pFN083/689 bp	hpNbFAD3	CACCGACATGACTGTGGACATG	GTTTCACCGCTTTAGTCGCTTCG
pFN084/647 bp	hpNbFAD7	CACCGTGTTGTTGGACATATCCT	CTTCCCTAATACTGGCTTAG
pFN085/652 bp	hpNbFATB	CACCGCTGCCATCACAACTATC	CATCTAAGTCACTCCATCTTGG
pFN043/679 bp	hpPetuniaFAD2	CACTAGTGATTATTGCGCAC	AATTCGATTAGCACATGAT
pFN088/1152 bp	NbFAD2.1 ORF in yeast	TTTATGGGAGCTGGTGGTAATATGT	CCCTCAGAATTTGTTTTTGTACCAGAAA
pFN089/1203 bp	NbFAD2.2 ORF in yeast	CATTGCAGGTTACTGAACAATGGGT	TGCCATGGTATTACATTCTATGAGAGA
pFN091/677 bp	hpNbFAD6	CACCATCTACTTCCCCTGGCCTG	TCTGGGGGATATGTGGTGGG
pFN094/841 bp	hpNbFATA	CACCAAGGAGAAGTTTATTGTTAGA	TCTTTCTCCATTCAGTTCGACA
pFN095/700 bp	hpNbSAD1	CACCGAAACCAGTGGAAAAATG	ACGCTGAGCAACTGCTGAG
hpNbLPCAT/637 bp	hpNbLPCAT	ATGGAATCAATGGCGTCGGC	CAGCTTGAAGAAGAGCCCTTAAAG
pFN101/502 bp	hpNbGPAT3	CACCAATTTTAGAAGGTGTTGGAT	AGCACTGATTCTGCAAAAT
pFN102/400 bp	hpNbLPAAT1	CACCCCACAATTGACTGCTAGCAA	TGCACAAGCATGACCACGAA
pFN103/491 bp	hpNbLPAAT2	CACCTGTGGATTGTTGATTGGTGG	GCTGGAACAAATGAGCGCAT
pFN104/400 bp	hpNbLPAAT4	CACCGGCGCGCCTGCATGTTTGGAA ATATTAAGGAG	GGCGCGCCAACCTACATATATTTTGAA C
pFN105/400 bp	hpNbLPAAT6	CACCATTTTTATGCCCTTGCGAGG	CCCATGGGCCTAAGCCTCTGACAA

Table 2.2. The list of primers and plasmids used during this study.

2.6.2 Cloning of the full-length NbFAD2.1 *and* NbFAD2.2 *sequences from genomic DNA*

Based on deep sequencing data and related alignments, the ORFs of *NbFAD2* sequence was PCR amplified from a genomic DNA template. *NbFAD2.1* was amplified using primers Forward 5' TTTATGGGAGCTGGTGGTAATATGT and Reverse 5' CCCTCAGAATTTGTTTTTGTACCAGAAA, while *NbFAD2.2* was amplified using primers Forward 5' TTTATGGGTGCTGGAGGTCGAA and Reverse 5' CCCCTAATGAAGCTTGTTTTTATACC. The fragments were amplified using *PfuUltra* II Fusion HS DNA polymerase (Agilent Technologies, Inc.), A-tailed and ligated into pGEM®-T Easy (Promega). The amplicon was subsequently sequenced using BigDye chemistry and verified to match the sequence obtained from BLAST search.

2.6.3 Preparation of yeast expression vectors and lipid analysis

The ORF regions of *NbFAD2.1* and *NbFAD2.2* were amplified using PCR and inserted into pGEM®-T Easy Vector System (Promega). The confirmed clones and yeast expression vector (pYES2) were digested with EcoRI. The fragment containing the gene of interest was then ligated into the EcoRI region of pYES2. Positive clones were confirmed using directional PCR (GAL1 Forward primer and gene specific Reverse primer) and sequencing. Consequently two yeast expression vectors were prepared, pFN088 containing *NbFAD2.1* and pFN089 containing *NbFAD2.2*. The pYES2 vector kit contains yeast competent cells, INVSc1, which were transformed with pFN088, pFN089, pYES2 (negative control) and yeast vector containing the gene AtFAD2 (positive control). Positive yeast clones were confirmed using PCR. The genes are driven by the *GAL1* promoter, which is repressed in the presence of glucose. The cells multiplied in glucose media for 30 hours, after which they were washed with water and transferred to media containing galactose, which de-represses the *GAL1* promoter, and protein expression begins. This transformation and induction protocol is described in the pYES2 manual (Invitrogen, Life Technologies).

After being induced for 48 hours, the cells were washed twice with water and freeze-dried overnight. The lipids were extracted in the form of FAME by heating the cells in 750 µl of MeOH/HCl/CH_2Cl_2 (10/1/1 by volume) at 80^{o}C for 3 hours. After cooling to room temperature, 300 µl of 0.9% NaCl solution and 400 µl of hexane were added to each sample.

Hexane phase was extracted, dried under N_2 gas and lipids re-eluted in 150 µl of hexane for GC analysis.

2.6.4 GFP fluorescence imaging

GFP images were captured on a digital SLR camera (Nikon D60; 55-200 mm lens or Nikon D700; 34-77 mm lens with an attached Hoya 77mm 0 (G) filter) using a Dark Reader Hand Lamp HL32T (9V DC 1.0 A, Clear Chemical Research). A fluorescent light and filter set (NightSea) were used to visualise GFP on leaves before taking photographs. Infiltrated leaves that were still intact with the whole plant were photographed daily for 7 days.

2.6.5 Lipid analyses

Lipids were analysed essentially as described previously (Wood et al., 2009). For oil analysis, lipids were extracted from 6–10 mg dry weight (freeze-dried overnight) of infiltrated leaf tissue using the method described by Bligh and Dyer (Bligh and Dyer, 1959). For total lipid analysis, the equivalent of 2 mg of dry weight leaf material was transmethylated using a solution of methanol/HCl/dichloromethane (10/1/1 by volume) at 80°C for 2 hours to produce fatty acid methyl esters (FAME). The FAME were extracted in hexane, concentrated to near-dryness under a stream of N_2 gas and quickly reconstituted in hexane prior to analysis by GC. TAG fractions were separated using a 1-phase TLC system on pre-coated silica gel plates (Silica gel 60, Merck). A sample equivalent to 6 mg dry weight of leaf tissue was first run using hexane/diethyl ether/acetic acid (70/30/1 by volume). The lipid spots and appropriate standards were visualised by brief exposures to iodine vapour, collected into vials and transmethylated to produce FAME for GC analysis as described above. Analysis of the leaf polar lipids, including PC, MGDG and DGDG fractions, were performed as previously described (Wood et al., 2009) using a two-dimensional TLC system – see Figure 2.20 for an illustration of the separation of leaf polar lipids using TLC.

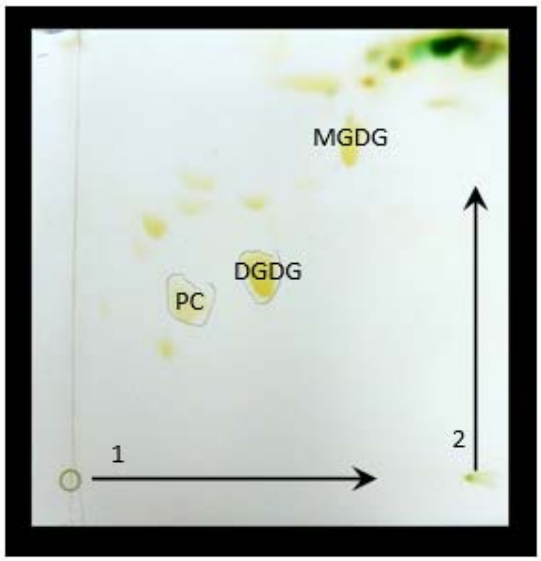

Figure 2.20. Image of 2D TLC plate used for separation of polar lipids.

2.6.6 RNA extraction and quantitative real-time PCR analysis

Prior to RNA extraction, the work area and equipment were cleaned with RNase*Zap*® (RNase decontamination solution, life technologies) to remove RNase. Total RNA was extracted from infiltrated leaf tissue using Qiagen RNeasy Plant Mini Kit according to the manufacturer's protocol, including DNase treatment. The RQ1 RNase-free DNase (Promega) was used per supplier's instructions. The RNA pellet was dissolved in 20 µL of diethylpyrocabonate (DEPC)-treated RNase-free water. The RNA concentration was measured by NanoDrop spectrophotometry.

For gene expression analysis, 360 ng of extracted total RNA was reverse-transcribed using SuperScript™ III First-Strand Synthesis System for RT-PCR (Invitrogen, Life Technologies). The primers used for the amplification of the 205 bp fragment of *NbFAD2.1* were Forward 5' CACACTACAATGCAATGGAGG and Reverse 5' CCAAAGACCAATACCAAATTCC. The primers used for the amplification of the 148 bp fragment of *NbFAD2.2* were Forward 5' AGAGAAGCAAGGGAATGTGTTTAC and Reverse 5' AGCAAAGCCTAAAACTTCCCAG. *NbGAPDH* was selected as the reference gene and was amplified using Forward 5' CACTACCAACTGCCTTGCAC and Reverse 5' ATGAAGCAGCTCTTCCACCT. qRT-PCR was performed in a 96-well format in the BIO-RAD CFX96 Real-Time System (BioRad Laboratories). The thermal profile of the qRT-PCR procedure was set to 95°C for 3 min, followed by 39 repeated cycles of 10 s at 95°C, 30 s at 60°C and 30 s at 68°C.. Melting curves were used to validate product specificity and melt curve analysis was performed from incubation at 65°C up to 95°C at a 0.5°C incremental ramp. All samples were amplified in triplicates from the same total RNA preparation and the mean value was used for further analysis. Primer efficiencies were also determined for each gene and each primer pair was found to be 99.9–100% efficient.

EF1α and *PDCT* were also tested as candidate reference genes, however their expression levels varied in leaves used for infiltrations. The primers used for amplification of the 192 bp fragment of *EF1α* were Forward 5' TGGACACAGGGACTTTATCAAG and Reverse 5' TGCTGCTGTAACAAGATGGATGC. The primers used for amplification of the 157 bp fragment of *PDCT* were Forward 5' CAAACCCGCTCTCAACACTATT and Reverse 5' AGCATACCCAAGAATACCTCTGAA.

2.6.7 Experimental design and statistical analysis of leaf assays

Leaf assays for metabolic engineering of lipid profiles were conducted on a minimum of 3 and maximum of 10 leaves, with a minimum of 4 and maximum of 12 independent infiltration zones. Preliminary experiments determined that all regions of leaves performed at similar levels in metabolic engineering scenarios, except for a ~1cm wide band across the very tip of each leaf – this region was avoided in subsequent infiltrations (data not shown). The location of spots on leaves and plants were recorded and data were analysed using a linear mixed model in GenStat™ (not all datasets), accounting for possible random plant-to-plant and leaf-to-leaf effects. All data were transformed (square root) prior to analysis to provide an even spread of residuals, so that all means, standard errors and least significant differences (LSDs) would correspond to the transformed data. In the figures, the means and (5%) LSD bar limits were directly back-transformed, therefore error bars for each metabolite that are not overlapping are significantly different at the p=0.05 level. In some instances the datasets were not analysed using the linear mixed model and the error bars given are the standard error of the mean. Figures are clearly labelled to state the type of analysis performed.

2.6.8 RNA extraction and sRNA deep sequencing analysis

Prior to RNA extraction, the work area and equipment were cleaned with RNase*Zap*® (RNase decontamination solution, life technologies) to remove RNase. About 100 mg of infiltrated leaf tissue was harvested for RNA extraction. The plant tissue was ground to a fine powder under liquid nitrogen using a mortar and pestle. The frozen ground tissue was transferred to a clean tube and 1.0 mL of TRIzol reagent (Invitrogen, Life Technologies) added and mixed thoroughly. The mixture was then incubated for 5 mins at room temperature. 0.2 mL of chloroform was added to the mixture, which was then vortexed vigorously and incubated at room temperature for 15 mins. The sample was centrifuged at maximum speed for 15 mins at 4°C. The top aqueous phase was removed and placed into a clean tube. 0.2 mL of chloroform was added to the clear phase to further remove all precipitated proteins. The sample was then centrifuged at maximum speed for 10 mins at 4°C. The aqueous phase was transferred to a clean tube, combined with one volume of cold 100% isopropanol and incubated at -20^{o}C overnight, then centrifuged at maximum speed for 15 mins at 4°C. The supernatant was removed and the pellet was carefully washed with 70% ethanol and

centrifuged for 5 mins at 7500 *g*. Supernatant was discarded and the RNA pellet was air dried for 10 mins. The RNA pellet was then dissolved in 100 µL of diethylpyrocabonate (DEPC)-treated RNase-free water. The AMBION DNase Turbo Kit was used to remove DNA from the sample and instructions were followed according to kit protocol. The RNA concentration was measured by NanoDrop spectrophotometry.

Dr Kaiman Peng prepared the sRNA libraries at the John Curtin School of Medical Research (JCSMR ANU, Canberra). The Illumina TruSeq Small RNA sample kit was used for the preparation of sRNA library. The following primers and adapters were used:

RNA 5' Adapter (RA5), part # 15013205

5' GUUCAGAGUUCUACAGUCCGACGAUC

RNA 3' Adapter (RA3), part # 15013207

5' TGGAATTCTCGGGTGCCAAGG

RNA RT Primer (RTP), part # 15013981

5' GCCTTGGCACCCGAGAATTCCA

RNA PCR Primer (RP1), part # 15005505

5' AATGATACGGCGACCACCGAGATCTACACGTTCAGAGTTCTACAGTCCGA

RNA PCR Primer, Index 3 (RPI3)

CAAGCAGAAGACGGCATACGAGATGCCTAAGTGACTGGAGTTCCTTGGCACCCGAGAATTCCA

Dr Kenlee Nakasugi assisted with the data analysis. The data analysis platforms were set up on a computer running Ubuntu 64-bit OS. PHRED/Solexa scores were used for determining the quality of the data. Conversion of the supplied fastq data to fasta format was performed using the fq_all2std script, available at the Maq (Mapping and Assembly with Qualities) project (http://maq.sourceforge.net/index.shtml). Adaptor sequences and sequences shorter than 18 nt were trimmed using the fastx_clipper from the FASTX-Toolkit (http://hannonlab.cshl.edu/fastx_toolkit). Size classes were separated out by parsing individual size classes using a custom perl script written by Dr Nakasugi. Alignments were performed using Bowtie 0.12.7 against *NbFAD2* (http://bowtie-bio.sourceforge.net).

Samtools was used to convert the resulting sam files to bam format and to subsequently sort and index the file (http://samtools.sourceforge.net/samtools.shtml). Alignments were viewed in IGV (http://www.broadinstitute.org/igv/) and figures were exported as images.

Chapter 3 The effect of seed-specific expression of V2 and p19 on transgene performance in oilseeds

3.1 Introduction

The previous chapter introduced an alternative VSP, V2, which assisted in enhancement of metabolic engineering of lipid pathways in *N.benthamiana* leaves. It has been shown both in this thesis and by previously published studies that the sustained overexpression of transgenes in the transient leaf assay is dependent on the expression of a VSP to inhibit sRNA-driven silencing of co-infiltrated transgenes. This chapter investigates the notion that the expression of VSPs may also promote and sustain the overexpression of transgenes in stably-transformed plants. To study this hypothesis, a well-studied three-gene pathway was introduced into *A.thaliana* seeds and co-expressed with various selected VSPs. This chapter explores the effect of the selected VSPs on the performance of the transgenic pathway over five generations.

As previously described in the literature review, metabolic engineering of plants requires a high number of independent transgenic events due to the high rate at which transgenic pathways fail over subsequent generations. The factors leading to failures in metabolic engineering are not precisely known, however in a number of cases the failures are due to sRNA-driven silencing pathways of the plant (Hagan et al., 2003). Stable transformation of plants is dependent upon the transfer of foreign nucleic acids into the genome of the plant. Numerous studies have shown that sRNA play a pivotal role in how plants detect and defend themselves against foreign nucleic acid. It is therefore expected that plants are able to detect integration of foreign nucleic acid and this mechanism may result in triggering of sRNA-related silencing of the transgenes. The decrease observed in transgene activity due to transgene copy number has also been associated with an increase in sRNA population targeting the transgene (Schubert et al., 2004).

The health benefits of ω-3 and ω-6 LCPUFAs (Ruxton et al., 2004) traditionally sourced from dwindling fish supplies has encouraged alternative production of DHA, EPA and AA in land-based oilseed crops (Petrie et al., 2012a; Petrie et al., 2012b), but this synthesis requires transformation of plants with multi-step pathways that need to perform at maximal levels over numerous generations to be commercially viable. Petrie et al. (2012a) have demonstrated the transformation of *A.thaliana* and *B.napus* with a three-gene pathway to produce arachidonic acid (AA) in seed oil. The design of this construct has been very successful in producing high levels of AA in the seed, although the transformation produced

very few elite events and metabolite data presented was limited to two generations of transgenic *A.thaliana* and one generation of transgenic *B.napus* (Petrie et al., 2012a). Their results have shown that metabolic engineering of *A.thaliana* and *B.napus* to produce LCPUFA in seed oil is a challenging task.

Viruses encode VSPs to interfere with the processes and effector molecules of RNA silencing in plants (Burgyan and Havelda, 2011). The constitutive expression of several VSPs in *A.thaliana* have been shown to cause developmental defects (Dunoyer et al., 2004). A major developmental difference investigated in this chapter involved the seed-specific expression of VSPs during oil biosynthesis. Various seed-specific promoters that confine transgene expression to oil synthesis in the seed are well characterised in oilseed research. It is well known that the majority of oil synthesis occurs after embryogenesis in the seed. It was therefore hypothesised that the expression of VSPs during oil synthesis would avoid disruption of developmental regulation dependent on sRNAs.

The results of the studies presented in this chapter show the effects of seed-specific expression of several different VSPs in *A.thaliana*. The seed-specific expression of VSPs was also combined with a multi-gene transgenic pathway for the production of AA in *A.thaliana* and *B.napus* seeds.

The results in this chapter address the following research questions:

1. Does the seed-specific expression of a number of potent VSPs cause major developmental abnormalities in *A.thaliana*?
2. Are the VSPs able to improve the performance of multi-gene transgenic pathways targeted to the seed of *A.thaliana*?
    a. What phenotypic changes are observed?
    b. How do the transgenes perform over five generations?
    c. Which transgenes are silenced over time?
3. Are the VSPs able to improve the performance of multi-gene transgenic pathways targeted to the seed of *B.napus*?
    a. Do VSPs cause developmental defects in *B.napus*?
    b. How do the transgenes perform over four generations?

3.2 Results

3.2.1 Phenotypic analysis of seed-specific expression of various VSPs in A.thaliana

The VSPs selected for this study included p19 (*Tomato bushy stunt virus*), V2 (*Tomato yellow leaf curl virus*), p38 (*Turnip crinkle virus*) and $P0^{PE}$ (*Pea enation mosaic virus*-1). These VSPs are considered to have different modes of action in sRNA biogenesis (Incarbone and Dunoyer, 2013) and may therefore generate a range of phenotypes in *A.thaliana*. A number of binary constructs were designed as outlined in Fig 3.1A. The VSPs were expressed using the truncated napin promoter FP1 (Stalberg et al., 1993). This seed-specific expression promoter is widely used to drive expression of transgenes during oil synthesis in seeds (Belide et al., 2012; Petrie et al., 2012a). To assess the effect of constitutive expression of V2 in *A.thaliana*, another construct was designed containing V2 driven by the CaMV 35S promoter.

A.thaliana ecotype Columbia (Col-0) was transformed with binary constructs corresponding to each of the three VSPs (p19, $P0^{PE}$ and V2) under the control of FP1 promoter, as well as with V2 under the control of 35S promoter, outlined in Figure 3.1A. A large population of transformed *A.thaliana* T2 events were selected based on kanamycin resistance, although only five independent T2 events for each construct were taken to T3 and T4, where phenotypic changes were observed (Fig 3.1B-D). The shape of cotyledons of $P0^{PE}$ ('ballerina-like') and p19 ('dog ears-like') plants were equivalent to the shape of cotyledons observed in 35S:$P0^{PE}$ and 35S:p19 plants (Fig 3.1B) (personal communication with Professor Peter Waterhouse, 2010) (Dunoyer et al., 2004). There were no visual differences between the cotyledons of GFiP (ORF of GFP modified to include an intron) plants and V2 and 35S:V2 plants (Fig 3.1B), which suggests that expression of V2 does not correlate with the occurrence of developmental defects in *A.thaliana*. Moreover, a higher number of p19, V2 and 35S:V2 transformants germinated and survived compared to $P0^{PE}$ transformants, suggesting that seed-specific expression of $P0^{PE}$ is lethal and not tolerated in *A.thaliana*.

A root phenotype was obvious in Col-0 plants expressing V2 and 35S:V2 (Fig 3.1C). The roots of these plants grew at a relatively slower rate compared to GFiP plants but did not have an effect on the rate of maturation of the plants. No further analysis was conducted to investigate the cause behind the short roots. A number of $P0^{PE}$ lines also showed defective

root growth, however no root phenotype was observed in the p19 plants. The short root phenotype is not previously described.

A number of plants expressing the constructs described in Fig 3.1A were photographed at a more mature stage and a representative plant from each group is shown in Figure 3.1D. Overall, ten independent events were observed throughout development and no major visual differences were observed.

A

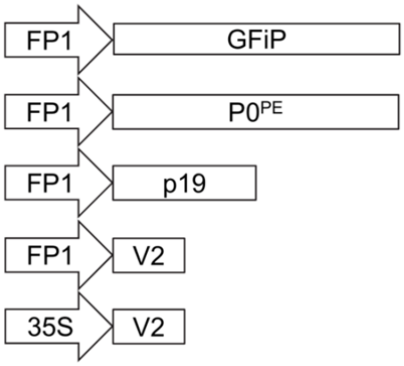
FP1
GFiP
FP1
P0PE
FP1
p19
FP1
V2
35S
V2

B

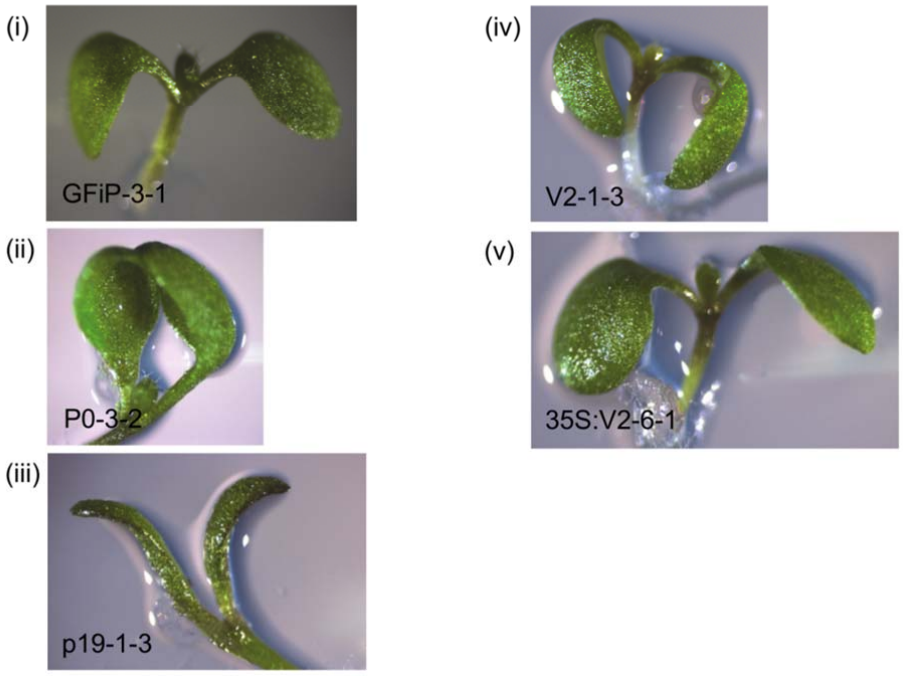
(i)
GFiP-3-1
(ii)
P0-3-2
(iii)
p19-1-3
(iv)
V2-1-3
(v)
35S:V2-6-1

C

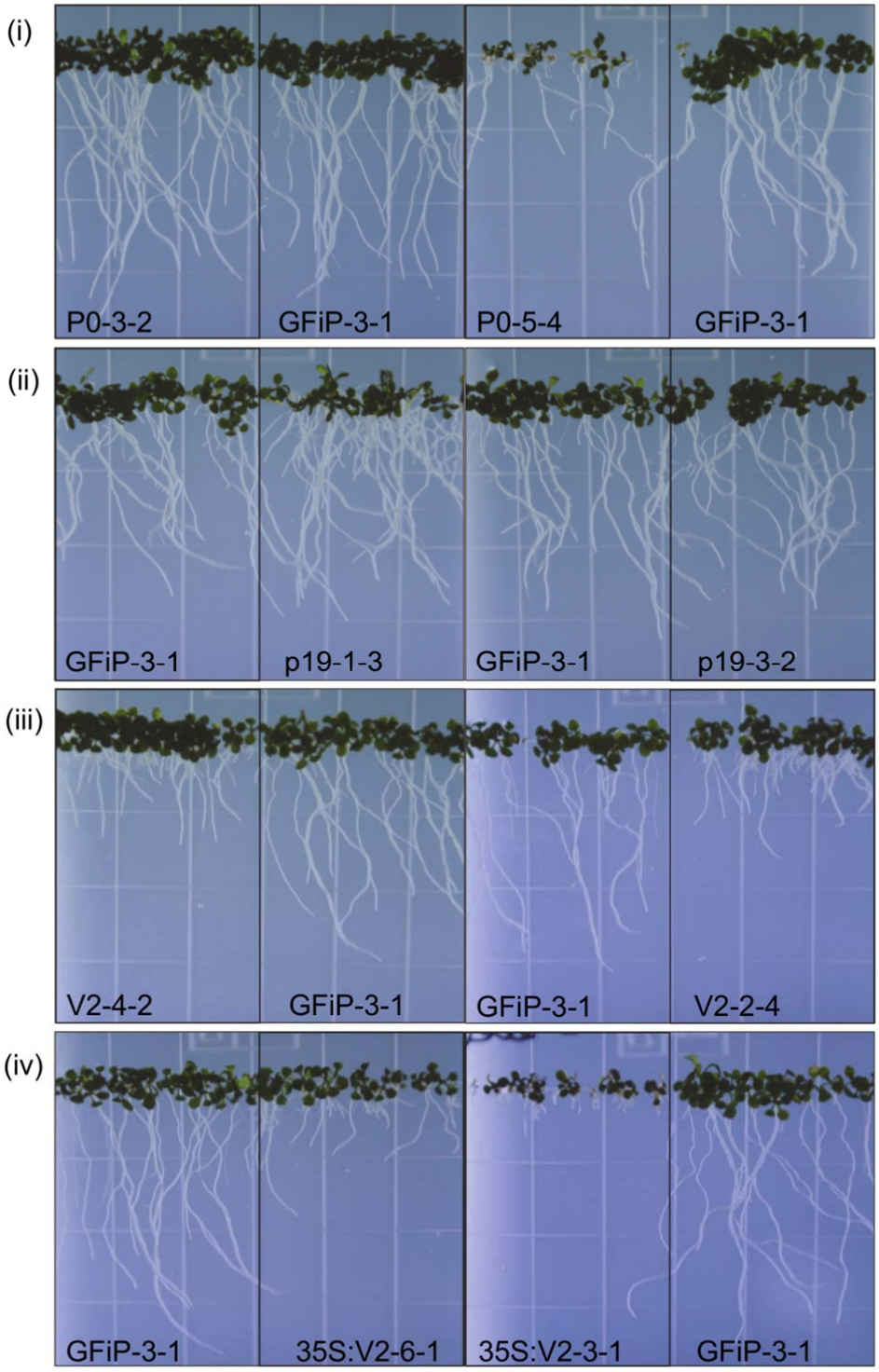
(i)
P0-3-2
GFiP-3-1
P0-5-4
GFiP-3-1
(ii)
GFiP-3-1
p19-1-3
GFiP-3-1
p19-3-2
(iii)
V2-4-2
GFiP-3-1
GFiP-3-1
V2-2-4
(iv)
GFiP-3-1
35S:V2-6-1
35S:V2-3-1
GFiP-3-1

D

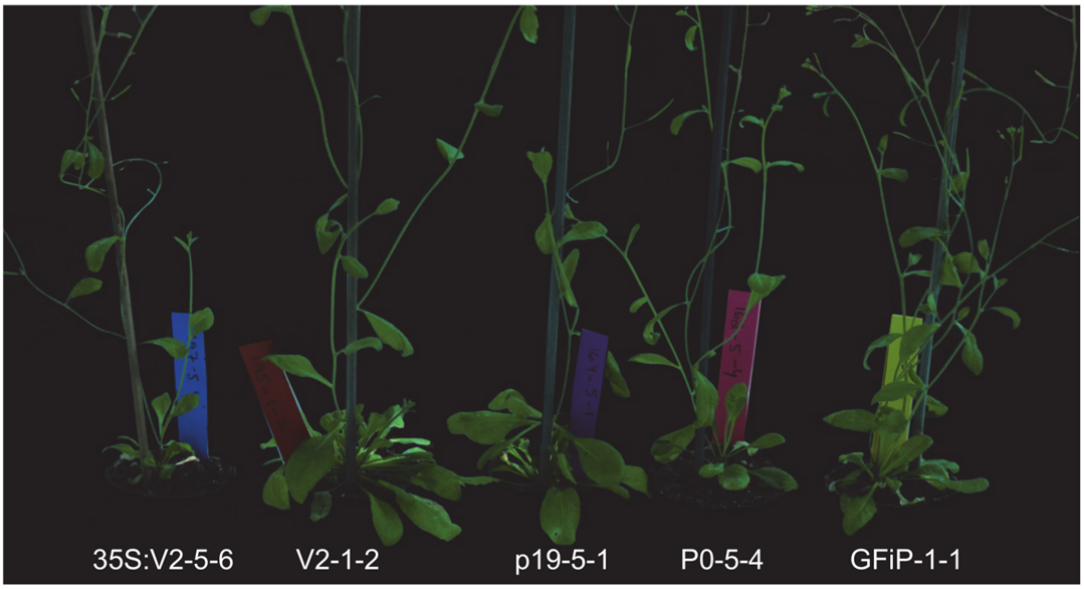

Figure 3.1. Phenotypic changes observed in *A.thaliana* transformed with selected VSPs.

A. Schematic of T-DNA binary constructs designed for stable expression of GFiP (GFP with an intron) and the VSPs ($P0^{PE}$, V2 and p19) in *A.thaliana*. Genes driven by the *B.napus* truncated napin FP1 promoter and the CaMV 35S promoter as indicated. For comparison purposes, a control construct encoding GFiP driven by the FP1 promoter was also designed.

B. The phenotypic changes in cotyledons of *A.thaliana* stably transformed with constructs outlined in **A**.

C. The phenotypic changes observed in root morphology of *A.thaliana* stably transformed with constructs outlined in **A**.

D. Representative mature plants expressing the respective constructs outlined in **A**.

B, C & D. All of the VSP, except those marked with 35S, are expressed using the FP1 promoter. Images presented are of stably-transformed *A.thaliana* in the third generation, is indicated by the numbering, e.g. GFiP-3-1 (GFiP-T2 event-T3 progeny) refers to a T3 control line.

3.2.2 Total lipid and fatty acid profile of wild-type Col-0 seeds and transgenic Col-0 expressing various VSP constructs

The total oil and fatty acid profile of *A.thaliana* seeds transformed with the constructs outlined in Figure 3.1A were compared to wild-type Col-0 seeds. Total seed lipids were extracted as FAME from approximately 50 T3 seeds of *A.thaliana*. Three individual events for each construct were selected for total lipids and FAME profile analyses. The lines selected for the analyses were grown and harvested in a single batch within the same glasshouse facility – these precautions were employed to attempt to reduce differences in oil content and oil profile due to changes in the environment.

A slight reduction in total lipids was observed in GFiP, $P0^{PE}$, V2 and 35S:V2 seeds (Fig 3.2A). The reduction in total lipid content was relatively similar in all transgenic plants, suggesting that the reduction was due to genetic transformation and not specifically due to expression of VSPs in the seed. The reduction in total lipids observed in p19 plants was more than the reduction in GFiP plants, which suggests that the expression of p19 may have a minor adverse effect on oil biosynthesis in the seed.

Minor differences were also measured in the relative percentages of the major fatty acids in VSP expressing plants (Fig 3.2B). A ~4% decrease was measured in 18:1 levels in GFiP, p19, V2 and 35:V2 plants, while a relative increase of ~6% was observed in 18:2 levels of GFiP, V2 and 35S:V2 plants. The 18:2 levels in $P0^{PE}$ and p19 plants increased by ~4%, which is consistent with the increase measured in infiltrated *N.benthamiana* leaves (Fig 2.6). The relative percentage of 18:3-FAME decreased by ~2% in all transgenic lines, which could be due to the increase in 18:2 levels (Fig 3.2B).

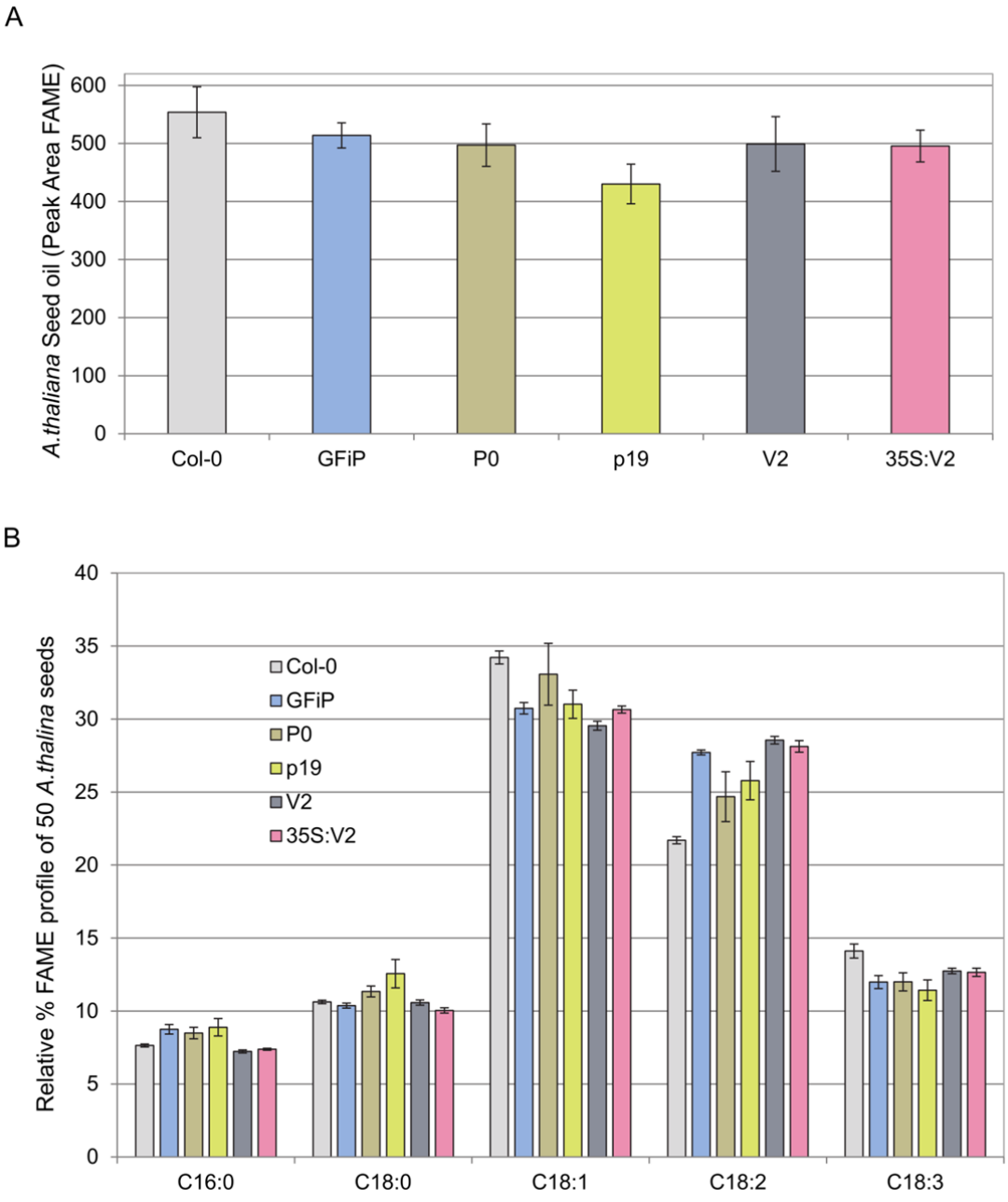

Figure 3.2. The changes measured in seed oil profile of *A.thaliana* post stable transformation with the selected VSPs.

Total oil (**A**) and relative percentages of the major fatty acids extracted as FAME (**B**) from seeds of T3 transgenic *A.thaliana*. Data presented is from 3 independent events for each construct described in Fig 3.1A. Error bars are the standard error of the mean.

3.2.3 Detection of GFiP driven by the FP1 promoter in various tissues types of **A.thaliana**

Western blot analysis of total protein extracted from different tissue types of GFiP and V2 plants confirmed that FP1 is only active in the seed tissue. The immuno-blots measuring GFP protein levels in roots, cotyledons, true leaves, meristem and seeds of plants expressing GFiP and V2 have shown that GFP protein was present in the seed tissue of GFP-expressing plants. Proteins extracted from V2 plants were used as negative control and no signal for GFP was detectable in extended exposures. These results confirmed that activity of the FP1 promoter is limited to the seed.

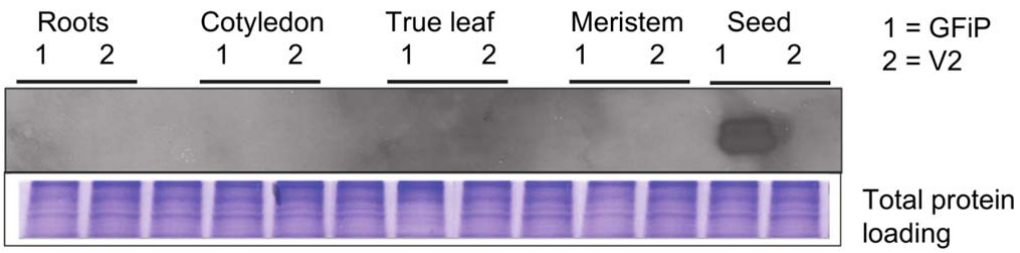

Figure 3.3. Activity of FP1 promoter measured in different tissues of *A.thaliana*.

Western blot analysis of GFP expression in roots, cotyledons, true leaves, meristem and seeds of transgenic *A.thaliana* expressing FP1:GFiP. The lower panel shows total protein loading and the upper panel shows signal generated by an antibody recognising GFP, anti-GFP.

3.2.4 A multi-gene pathway for biosynthesis of DHA in the seed of A.thaliana

The seed-specific expression of the selected VSPs and 35S:V2 showed mild developmental abnormalities (short roots), including in the seed-oil profile in *A.thaliana*. The next step was to combine the expression of the selected VSPs with a multi-gene transgenic pathway to produce DHA in seed oil. The production of DHA and EPA in land plants has been a major target of recent metabolic engineering (Petrie et al., 2012b). The transgenic pathway to produce DHA uses 18:3 as starting substrate (Fig 3.4A) involving five sequential elongation and desaturation steps. The five fatty acid synthesis genes, as outlined in Figure 3.4A and 3.4B, were under the control of the FP1 promoter. The original DHA construct (pJP3057, a T-DNA spanning 17022 bp) was designed by Petrie et al. (2010). This construct was transiently expressed in *N.benthamiana* leaves and the seed-specific promoters were activated with the addition of 35S:LEC2 (Petrie et al., 2010). This addition of transcription factor *LEC2*, driven by the CaMV 35S promoter, activated seed-specific promoters in the leaf (Petrie et al., 2010). The system produced 2.4% of DHA in total leaf lipids (Petrie et al., 2010). pJP3057 was modified to contain 35S:V2 and FP1:GFiP expression cassettes, giving rise to pFN012 (21333 bp, Fig 3.4B). Two additional constructs named pFN016 and pFN014 were also prepared, containing FP1:V2/FP1:GFiP and FP1:p19/FP1GFiP expression cassettes (Fig 3.4B). The new constructs were transiently expressed in *N.benthamiana* leaves and the levels of DHA measured were in agreement with the results published by Petrie et al. (2010).

In this present work only a limited number of transgenic events were produced by the genetic transformation of *A.thaliana* with pJP3057, pFN012, pFN014 and pFN016 using floral dipping techniques (Clough and Bent, 1998). A very low amount of DHA (<1%) was detected in the seeds of plants expressing pFN012, pFN014 and pFN016 (data not shown). The limited numbers of transgenic events were not investigated any further.

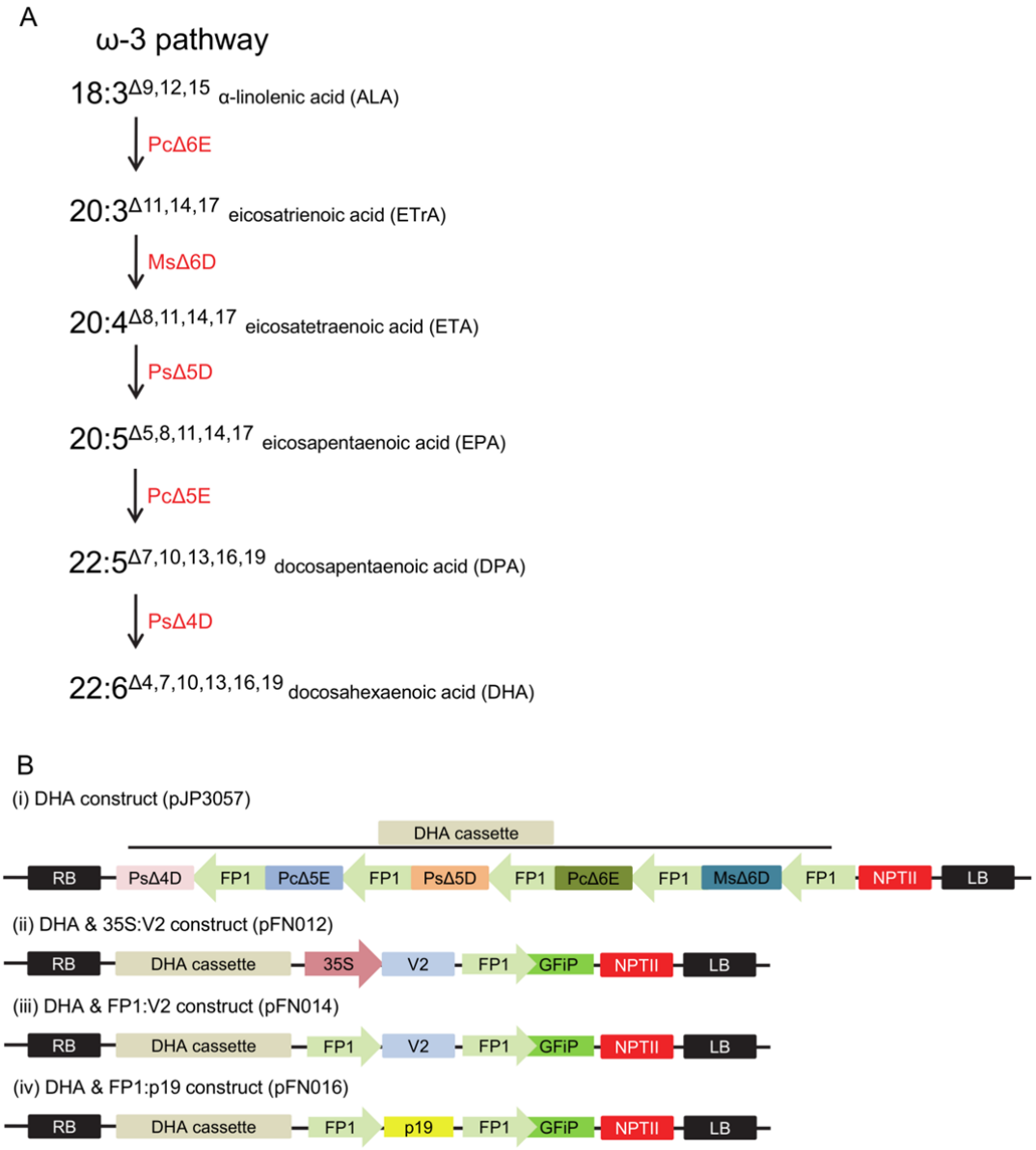

Figure 3.4. Design of constructs containing a five-gene pathway for biosynthesis of DHA (22:6) in seed oil.

A. A schematic of enzymes involved in the biosynthesis of DHA via the ω-3 pathway, using 18:3 (ALA) as the starting substrate.

B. The intra-border binary construct maps designed for stable transformation of *A.thaliana* in this study. **(i)** The original DHA construct (pJP3057) consisted of the *PcΔ6E*, *MsΔ6D*, *PsΔ5D*, *PcΔ5E* and *PsΔ4D* driven by FP1 promoters. **(ii)** The addition of 35S:V2 and FP1:GFiP to the DHA construct generated a second construct (pFN012). **(iii)** The addition of FP1:V2 and FP1:GFiP to the DHA construct generated pFN014. **(iv)** The addition of FP1:p19 and FP1:GFiP to the DHA construct generated pFN016. Abbreviations are: RB, right border; PsΔ4D, *Pavlova salina* Δ4-desaturase; PcΔ5E, *Pyramimonas cordata* Δ5-elongase; PsΔ5D, *Pavlova salina* Δ5-desaturase; PcΔ6E, *Pyramimonas cordata* Δ6-elongase; MsΔ6D, *Micromonas pusilla* Δ6-desaturase; NPTII, neomycin phosphotransferase II selectable marker; LB, left border.

3.2.5 A multi-gene pathway for biosynthesis of AA in the seed of A.thaliana

AA is an important LCPUFA and a target for oilseed metabolic engineering (Petrie et al., 2012a). A metabolic pathway to produce AA requires three transgenes starting from 18:2 substrates, rather than the five transgenes required for synthesis of DHA. The metabolic engineering of AA was therefore expected to be less complicated than that required for the DHA biosynthesis. Petrie et al. (2012a) have previously produced *A.thaliana* and *B.napus* transgenic lines that contain high levels of AA in seed oil and this pathway was made available for this doctoral study.

A three-gene transgenic pathway for the synthesis of AA (20:4) was used to monitor the effect of seed-specific expression of a VSP on the performance of transgenes in the seed. The control genetic construct included the set of fatty acid biosynthesis genes for production of 20:4 from 18:2 (Fig 3.5A). The AA construct (pJP3010, 13991 bp original three-gene construct, modified to pJP3025, 17298 bp for transformation of *A.thaliana* and *B.napus*) was kindly donated by Dr James Petrie (2010). The construct design is described in detail by Petrie et al. (2012a). The genes to synthesise AA were cloned from micro-algae, including the *Isochrysis galbana* Δ9-elongase (IgΔ9E, elongates 18:2 to 20:2) and the *Pavlova salina* Δ8-desaturase (PsΔ8D) and Δ5-desaturase (PsΔ5D) (desaturate 20:2 to 20:3 and 20:4, respectively) (Petrie et al., 2012a). This construct avoided the use of the FP1 promoters to drive all three genes – *IgΔ9E* is driven by the *A.thaliana* FAE1 promoter and *PsΔ8D* and *PsΔ5D* are driven by the napin truncated FP1 promoter. The placement of the gene cassettes in a linear design was also avoided (Fig 3.5B).

The GFiP was added to pJP3025 to operate as a visual seed-specific marker, allowing simple and non-destructive identification and thereby selection of transgenic seed. The gene encoding for GFiP contains an intron in the open reading frame (obtained from the Waterhouse laboratory) and the final protein includes a secretory peptide sequence that forces GFP to the apoplast of the plant cell, resulting in easier visualisation of fluorescence in mature seed (Wood laboratory, unpublished results). The base AA+GFiP binary construct and subsequent transformed lines are referred to as 'No VSP' or pFN050. The addition of the selected VSPs generated another five binary constructs referred to as pFN045 or '$P0^{PE}$' (AA+GFiP+$P0^{PE}$), pFN046 or 'p38' (AA+GFiP+p38), pFN047 or 'p19' (AA+GFiP+p19), pFN048 or '35S:V2' (AA+GFiP+35S:V2) and pFN049 or 'V2' (AA+GFiP+V2) (Fig 3.5B). The VSPs were

under the control of the FP1 promoter and OCS transcription termination signal, however the construct pFN048 contained V2 coding region, which was driven by the CaMV 35S promoter. The results reported in this chapter refer to the various AA constructs by the presence or absence of the various VSPs as well as their respective construct number.

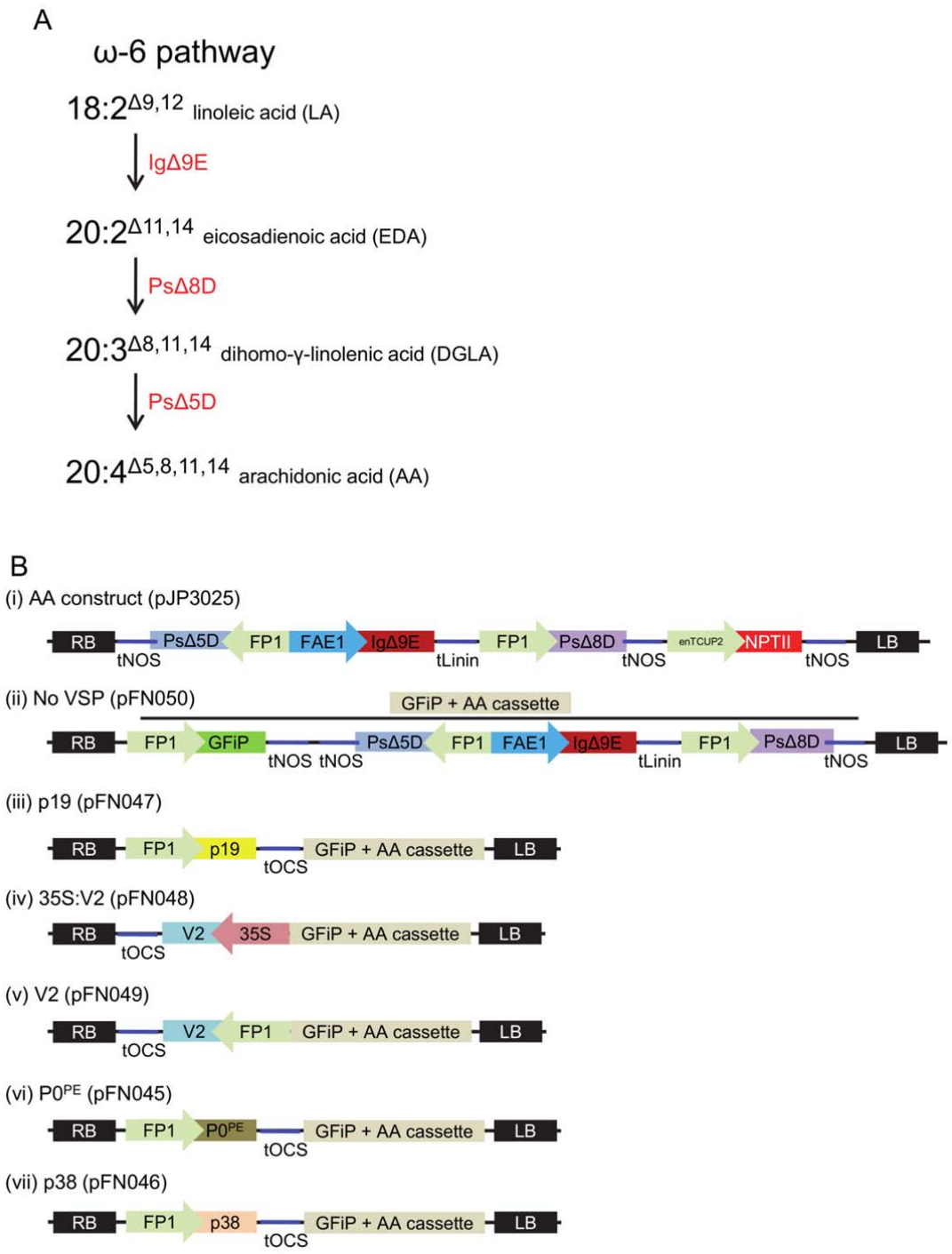

Figure 3.5. Design of constructs containing a three-gene pathway for biosynthesis of AA (20:4) in seed oil.

A. A schematic of enzymes involved in the biosynthesis of 20:4 via the ω-6 pathway using 18:2 (LA) as the starting substrate.

B. A schematic of the construct maps designed for stable transformation of *A.thaliana*. **(i)** The construct pJP3025 consisted of the *IgΔ9E* driven by the *A.thaliana* FAE1 promoter, *PsΔ8D* and *PsΔ5D* driven by the

B.napus truncated napin FP1 promoter. **(ii)** The addition of GFiP to pJP3010 generated pFN050. **(iii-vii)** Addition of a VSP to pFN050 generated pFN047, pFN048, pFN049, pFN045 and pFN046. Abbreviations are: RB, right border; tOCS, *A.tumefaciens* octopine synthase terminator; 35S, CaMV 35S promoter; GFiP, intronic GFP reporter; tNOS, *A.tumefaciens* nopaline synthase terminator (polyadenylation signal); PsΔ5D, *Pavlova salina* Δ5-desaturase; IgΔ9E, *Isochrysis galbana* Δ9-elongase; tLinin, *Linum usitatissimum* conlinin2 terminator; PsΔ8D, *P.salina* Δ8-desaturase; enTCUP2, enhanced tobacco cryptic promoter 2; NPTII, neomycin phosphotransferase II selectable marker; LB, left border.

3.2.6 The performance of the AA constructs with silencing of **NbFAD7** *in transient leaf assay*

Prior to stably transforming *A.thaliana*, the AA constructs were transiently expressed in *N.benthamiana* leaves to test the activity of the various genes. The seed-specific promoters were activated with the addition of 35S:LEC2 as previously described. The flux of 18:2 is low in *N.benthamiana* leaves due to efficient desaturation of 18:2 to 18:3 by NbFAD7 (Chapter 2, Fig 2.12A). To ensure maximal levels of substrate 18:2 would be available for the AA pathway, *NbFAD7* was silenced with hpNbFAD7.

Leaves were infiltrated with combinations of V2 (pCW197) (Fig 3.1A), LEC2, hpNbFAD7 and the AA constructs. Leaves were harvested 5 dpi and total leaf lipids extracted as FAME. The activation of seed-specific promoters were initially confirmed visually by the presence of GFP in the leaves. The result of one representative construct (pFN050) is presented in Figure 3.6.

Very low amounts of 20:2, 20:3 and 20:4-FAME (0.2%, 0.1% and 0.1% respectively) were detected in leaves infiltrated with pFN050 and LEC2 only. The addition of V2 (pCW197), as a separate construct, increased the levels of new fatty acids 20:2-, 20:3- and 20:4-FAME to 0.4%, 0.8% and 1.6%. The enzymes of the AA pathway are also able to produce ω-3 fatty acids by using 18:3 (ω-3) as the starting substrate, so 0.7% of EPA (20:5n3) was also measured. Increasing the flux of 18:2 into the pathway by silencing *NbFAD7* produced 0.8% of 20:2-, 2.0% of 20:3- and 3.7% of 20:4-FAME. It was expected that silencing of *NbFAD7* and the subsequent reduction in levels of 18:3 would result in reduced levels of 20:5n3, but the level of 20:5n3 more than doubled to 1.3% in leaves silenced for NbFAD7 activity (Fig 3.6). These experiments provide another example of the shunting of endogenous metabolites into engineered pathways – in this instance an increase in 20:4 was observed.

The efficiencies of the enzymes in the transient assay were also calculated. These calculations indicated that the conversion efficiency of substrate into product for each step of the pathway catalysed by IgΔ9E, PsΔ8D and PsΔ5D was 20%, 85% and 65%, respectively. Similar efficiencies of conversion at each step of the pathway were measured in leaves infiltrated with or without hpNbFAD7. The biochemistry of the leaf system revealed that the IgΔ9E is the bottleneck in the pathway, converting 18:2 to 20:2.

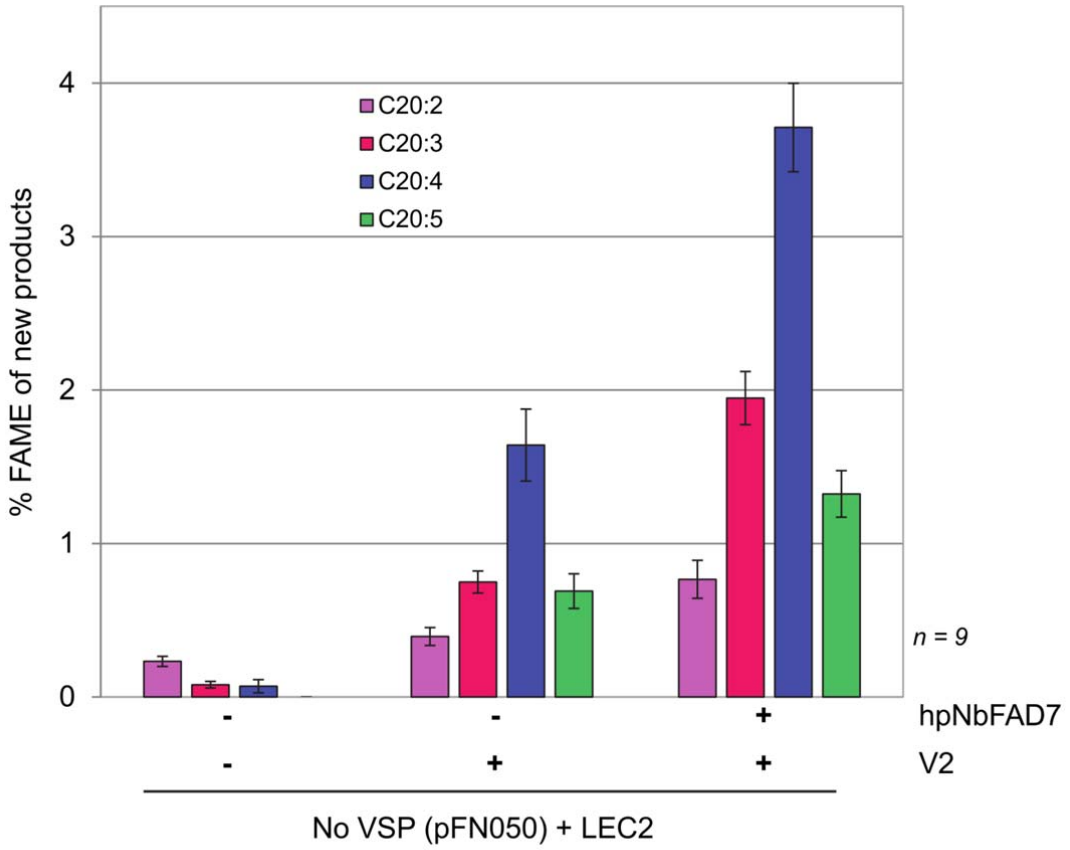

Figure 3.6. Transient metabolic engineering of *N.benthamiana* leaves for biosynthesis of AA.

Leaves infiltrated with combinations of 'No VSP' AA construct (pFN050), V2, LEC2 and hpNbFAD7. Leaves were harvested 5 dpi and total leaf lipids extracted as FAME. The relative percentages of new fatty acids presented including the ω-3 and ω-6 products. Means for each infiltration treatment calculated and error bars are the standard errors of the mean calculated for 9 leaf samples.

3.2.7 Generation, propagation and standardised metabolite analyses of five generations of transgenic **A.thaliana** *spanning over two years*

To test the hypothesis that the use of VSP is able to enhance and stabilise the production of LCPUFA in oilseeds over several generations, T-DNA binary constructs combining the AA pathway and various VSPs (Figure 3.5B) were transformed into *A.thaliana* genotype MC49. This genotype is a *fad3/fae1* double mutant containing high levels of 18:2 in seed oil (Zhou et al., 2006). MC49 contains very low levels of 18:3 (<1%), avoiding the parallel ω-3 pathway for the synthesis of EPA in the seed. Plants were transformed using floral dipping techniques (Clough and Bent, 1998) and transformants were selected based on kanamycin resistance. Plants were grown to maturity and phenotypic and metabolite analysis of the events indicated that the expression of VSPs did not have a negative effect on the development and transgene expression in *A.thaliana*. T2 lines were therefore propagated for another three generations to collect T5 seeds.

Six kanamycin-resistant seedlings from each T2 event were transferred to soil to generate T2 plants, annotated as pFN0XX-YY-ZZ-AA-BB to represent the construct number used for the transformation and the seeds collected from the subsequent generations (construct number and XX=T1, YY=T2 seeds, ZZ=T3 seeds, AA=T4 seeds and BB=T5 seeds). The T3 seeds were harvested, seed lipids extracted as FAME and lipid profiles analysed. Based on FAME profile, six kanamycin-positive seedlings were taken to T4 and subsequently to T5. In order to avoid bias in selection of seedlings, the selected progeny were based on the relative percentage of AA measured in the respective parent line – the selected range included lines that had high, medium and low levels of AA in the seed.

The processes of initial transformation to generate a large transgenic population and then growing their progenies for five generations occurred over a two-year period. Each generation of plants were grown in controlled conditions with defined day lengths and temperature controls. FW10-23 is the elite T3 control line generated by Petrie et al. (2012a) – during this previous study, FW10-23 was the only elite event that produced ~20% of AA in T3 *A.thaliana* seed. Therefore, to monitor deviations in sample preparation and the sensitivity of analytical instruments, FAME was extracted from seeds of FW10-23 and analysed in every batch of transgenic *A.thaliana* during the two-year period. This FW10-23 control was accompanied by the use of fresh lipid standards with each FAME analysis

conducted. Statistical analyses were performed on the FAME profile of FW10-23 collected during the two-year period of data collection and there were no statistically significant differences over the two-year period of analysis (data not shown). These studies were required to ensure that all lipid analyses conducted during this time could be cross-referenced and standardised.

Pathway	Construct	Individual T1 events	Events taken to T5
AA+GFiP	pFN050	24	23
AA+GFiP+P0^{PE}	pFN045	10	5
AA+GFiP+p38	pFN046	16	14
AA+GFiP+p19	pFN047	39	32
AA+GFiP+35S:V2	pFN048	8	6
AA+GFiP+V2	pFN049	26	21

Table 3.1. Summary of the various AA constructs used for transformation of *A.thaliana*.

This table summarises the generation of independent transgenic events for each vector construct. *A.thaliana* was transformed with these vectors and a large number of independent events were generated. Each data point for parent and descendent was preserved and graphed, generating progeny plots compiled in Figure 3.7.

3.2.8 Visualisation and analysis of the levels of AA and intermediates in five generations of transgenic A.thaliana

In order to study the effect of seed-specific expression of VSPs on the AA pathway, it was our intention to progress all T2 events to T5 – this resulted in a large number of transgenic plants. The transformation of *A.thaliana* with the AA constructs generated over 100 independent transgenic events and over 3000 lipid analyses in the two-year period. In order to better visualise these large datasets, this chapter uses two different data visualisation techniques.

The first visualisation method is referred to as the "progeny plots" (Fig 3.7) – these represent the performances of parents and progenies of each independent transgenic event across subsequent generations. The progeny plots are one method of illustrating the basis of selecting transgenic events to be taken through to subsequent generations. The progeny plots also illustrate that minimal bias existed in the selection of transformed events and that elite events were not selected preferably. Figure 3.7 contains progeny plots for all transgenic events, excluding those created with pFN045 construct.

A second visualisation tool used is known as “box-whisker plots” – these overlay and summarise large datasets and data points, illustrated as a scatter of ‘jittered’ points (Spitzer et al., 2014). In box-whisker plots, the median defines the level of the metabolite that splits the given range of data points in half, such that half are above the median and half below. The upper and lower edges of the box-whisker plot represent the first and third quartiles, while the ‘whiskers’ represent the 10^{th} and 90^{th} percentiles (interquartile range). Data points lying outside of the whiskers are considered outliers and are plotted individually as black dots. Box-whisker plots are considered a more robust method to summarise large populations of data, especially those that display a wide range of values (Spitzer et al., 2014). Box-whisker plots are displayed for the various populations spanning T2 to T5 generations for the intermediate metabolite 20:2 (Fig 3.8) and the final metabolite 20:4 (Fig 3.9). A final box-whisker plot that summarises the levels of 20:4 measured in various T5 events is shown in Figure 3.10. The box-whisker plot analysis for another intermediate metabolite, 20:3, (Appendix Fig A) is not reported in detail due to the relatively minor changes that occurred in five generations.

Figures 3.7, 3.8, 3.9 and 3.10 are used to illustrate the results that are presented in the following sub-sections.

3.2.8.1 T2 population

There were 24 pFN050 T2 kanamycin-positive seedlings and 23 of these survived to produce T3 seeds (Table 3.1, Fig 3.7A). The segregation analysis of the T2 seedlings revealed that only three of the events were considered high copy number insertions (pFN050-01, pFN050-02 and pFN050-07) based on the lack of null segregants in the T2 generation (Appendix Table B). However the levels of 20:4 in these events were low (10.6%, 8.2% and 9.8%, respectively), suggesting that high copy number events did not necessarily result in elevated levels of transgenic metabolites.

There were 16 pFN046 kanamycin-positive seedlings and 14 of these survived to generate T2 seeds (Table 3.1, Fig 3.7B). Null segregants were observed in all T2 events, suggesting that the chances of high copy number insertions were less in this population (Appendix Table B). The highest level of 20:4 (13.1%) was measured in pFN46-10, with 12% of null segregants.

Transformation of *A.thaliana* with the pFN045 generated very few T2 events (Table 3.1). A high number of pFN045 seedlings turned yellow a few days after germination, suggesting that seed-specific expression of $P0^{PE}$ is highly potent. This was also observed in Col-0 plants that were transformed with $P0^{PE}$ gene driven by the FP1 promoter (Fig 3.1). In the segregation analysis it was impossible to discriminate between the null segregants and the aborted $P0^{PE}$ expressing seedlings, therefore copy number analyses remain inconclusive. Due to the seed-lethal effect of $P0^{PE}$, only 5 of 10 T1 seedlings survived, resulting in a small population of $P0^{PE}$ transgenic plants (Table 3.1) and for this reason the progeny plots for pFN045 events are not included. The low recovery rate of kanamycin-positive seedlings also suggested that a number of transformed embryos might have aborted earlier due to toxicity of $P0^{PE}$. Furthermore based on the presence of 20:2 and 20:3 and absence of 20:4, the PsΔ5D activity was absent in pFN045-08 event (Fig 3.7). Due to the small size of the population and the potency of $P0^{PE}$, it was not possible to assess the effect of $P0^{PE}$ on the performance of the transgenic pathway in five generations. The $P0^{PE}$ results are therefore not explored any further in this chapter.

There were 39 kanamycin-positive T1 events expressing the pFN047 construct, although only 32 of these independents events survived and were progressed through to T5 (Table 3.1, Fig 3.7C). There were three events which produced the highest level of 20:4 in T2 seed – pFN047-04 with 14.8% 20:4, pFN047-08 with 17.8% 20:4 and pFN047-39 with 19.6% 20:4. The percentages of kanamycin-positive seedlings were 94%, 80% and 100%, respectively (Appendix Table B). The segregation analysis suggested that these events were high copy number events.

A large number of transformants were created with the pFN049 construct (Table 3.1, Fig 3.7D) – there were 26 kanamycin-positive seedlings and 21 of these were taken to T5. The metabolite data revealed that PsΔ5D activity was missing in pFN049-26, resulting in exclusion of this line from further analysis. The level of 20:4 was very high in two of the T2 events, pFN049-17 and pFN049-21, containing 19.4% and 18.5% 20:4 (Fig 3.7D). Segregation analysis revealed that both of these events were high copy number events with 0 and 4% null segregants observed (Appendix Table B).

There were 8 kanamycin-positive seedlings that were expressing pFN048 (Table 3.1, Fig 3.7E). Six of these plants were propagated through to T5 generation and progeny plots for the 20:4 content are displayed in Figure 3.7E. Interestingly, the progeny of these 6 T2 events have very high levels (~20%) of 20:4 (Fig 3.7E).

A number of kanamycin-resistant seedlings that were not expressing the three genes to produce 20:4 in the seed were also identified in each transgenic population. Only two (pFN047-09 and pFN049-09) were taken to T5 as negative control plants and others (pFN048-08 and pFN046-11) were excluded from the study.

The T2 FAME results revealed that the seeds of a number of VSP lines contained equivalent levels of 20:4 measured in FW10-23, a T3 line. These lines included pFN047-08, pFN047-39, pFN049-17 and pFN049-21 with 17.8%, 19.6%, 19.4% and 18.5% 20:4, respectively. The highest level of 20:4 measured in a pFN050 line was 15.0% (pFN050-17). The total new products in pFN050-07, pFN050-15, pFN050-17, pFN050-19, pFN050-23, pFN047-39, pFN049-17, pFN049-21 and pFN046-10 were approximately equivalent to total new products measured in FW10-23, but pFN050-17, pFN047-39, pFN049-17 and pFN049-21 contained relatively high levels of 20:4 and the others contained high levels of intermediates.

The pFN047 and pFN049 populations contained T2 seeds with a more dispersed 20:4 plot (Fig 3.9). The 20:4 median was relatively similar for pFN050, pFN047 and pFN049 populations (Fig 3.9), but was significantly lower for the pFN046 population. The lowest and highest levels of 20:4 measured in pFN047 and pFN049 events were 5.6% and 19.6% respectively, while levels in pFN050 and pFN046 events were 5.0% and 15.0% (Fig 3.9).

The box-whisker plot analysis of 20:2-FAME extracted from T2 seeds revealed that the pFN050 population contained the highest level of 20:2 (Fig 3.8). The lowest and highest relative percentages of 20:2 in the pFN050 population were 3.1% and 12.9%. There were four pFN050 lines that contained more than 10% 20:2. The level of 20:2 ranged from 4.5% to 9.3% in the pFN046 population and from 1.9% to 8.2% in the pFN047 and pFN049 populations.

3.2.8.2 T3 population

As previously described, 6 seedlings from each independent T2 event were taken to T3. The T3 populations were therefore relatively larger and the levels of 20:2 and 20:4 measured showed a wider spread for all representative constructs (Fig 3.8, Fig 3.9). The lowest and highest levels of 20:2 in the pFN049 population were 1.4% (pFN049-16-4) and 8.0% (pFN049-01-02)(Fig 3.8). The lowest and highest levels of 20:2 in the pFN047 population were 2.5% (pFN047-20-07) and 7.8% (pFN047-27-03). The lowest and highest levels of 20:2 in the pFN050 population were 2.7% (pFN050-21-03) and 18.2% (pFN050-23-03). The relative percentage of 20:2 measured in the parent of pFN050-23-03 was 11.1% and a dramatic increase was observed in the level of intermediate in T3 seeds. The lowest and highest levels of 20:2 in the pFN046 population were 2.4% (pFN046-05-06) and 17.0% (pFN046-07-03). Similarly, the parent of pFN046-05 contained 10.0% 20:2 in T2 seeds. A number of pFN050 and pFN046 independent T2 events produced T3 progeny that contained >10% 20:2 (Fig 3.8).

The most striking result obtained during T3 seed-oil analysis was that line pFN047-26-03 contained 39.4% of 20:4 (Fig 3.9). The T2 segregation analysis of this event yielded 59% survival rate with a number of seeds that did not germinate. Six of the T2 seedlings were taken to T3, however only three survived. The T3 seeds of one progeny, pFN047-26-03, contained 39.4% 20:4 and the seed of the other progeny contained ~12% 20:4. Apart from this unusual occurrence, another four pFN047 independent T2 events generated T3 progeny

that contained ~20% 20:4. Another pFN047 event that contained 8.3% 20:4 in T2 produced T3 progeny containing 3.8% 20:4, which was the lowest level of 20:4 measured in the pFN047 T3 population. The other five progeny of this particular event contained >10% 20:4 in T3. There were a number of other lines that contained <10% 20:4 in the pFN047 and pFN049 populations, however the 20:4 medians of the mentioned populations were significantly higher than the 20:4 median of pFN050 and pFN046 populations (Fig 3.9). The box-whisker plot analysis of the T3 populations also showed that the VSP lines produced more elite events. The pFN048 population was relatively small, however there were a number of lines that contained >15% 20:4. The highest levels of 20:4 measured in the pFN050 and pFN046 lines were 19.7% (pFN050-09-02) and 16.5% (pFN046-03-03). The 20:4 medians overall in T3 populations, when compared to their T2 parents, had decreased in the pFN050 and pFN046 populations and increased in the pFN047 and pFN049 populations.

3.2.8.3 T4 population

Another six seedlings were selected from T3 events, as shown in the progeny plots (Fig 3.7), to produce T4 seeds. The FAME analysis of T4 seeds revealed that the medians for both 20:2 and 20:4 were significantly different for the VSP and No VSP lines (Fig 3.8, Fig 3.9). The 20:2 medians for the pFN050 and pFN046 populations were significantly higher than those for pFN047 and pFN049 populations. Interestingly, the levels of 20:2 in all T4 populations were more spread, suggesting that the relative percentage of 20:2 increased in all populations. The pFN049 population was more compact however, with the lowest median for 20:2. There were very few lines that contained ~10% 20:2 in the pFN047 and pFN049 populations, however one third of the pFN050 population contained >10% 20:2. There were a number of pFN050 and pFN046 lines that contained ~20% of 20:2 and in which the level of 20:4 had significantly decreased (Fig 3.8).

The 20:4 median of T4 increased in all populations when compared to T3. The 20:4 median of pFN050 increased to ~11%, however the increases in the pFN047 and pFN049 populations were comparatively larger at ~14% (Fig 3.9). The 20:4 median of pFN049 population was slightly higher than pFN047 in T3, but became equal for both populations in T4. The lowest level of 20:4 measured in pFN047 and pFN049 lines was ~7%, which was significantly higher than ~1% contained in a number of pFN050 and pFN046 lines (Fig 3.9).

In order to analyse 20:4 in T4 seeds, a number of pFN047-26 seeds from each of the T3 lines were germinated and the seedlings grown to maturity. There were null segregants among the T3 seedlings. A progeny from each of the other two T3 lines also produced seeds that contained ~38% 20:4. The remainder of the T4 lines contained 10–18% 20:4. A number of T4 events of pFN047-26 that had contained low levels of 20:4 in T3 segregated out to produce ~39% of 20:4 in T4 – these lines remained as outliers and did not have an effect on the parameters of the box-whisker plot analysis for the pFN047 population. Another line pFN047-39 stopped segregating in T4 and the relative percentage of 20:4 dropped to ~13%.

3.2.8.4 T5 population

The box-whisker plot analysis of the T5 populations revealed that the relative percentage of 20:2 (Fig 3.8) was higher in pFN050 population compared to pFN047, pFN048 and pFN049. The T4 pFN046 lines that contained ~20% of 20:2 produced T5 seeds that contained relatively lower levels of 20:2 (<15%) and <1% of 20:3 and 20:4 were also measured (Fig 3.8). A higher number of pFN050 lines contained >15% of 20:2 (Fig 3.8), while the pFN049 population contained the lowest median and most compact spread of 20:2 compared to the other T5 populations. Very few pFN047 lines also contained >10% 20:2, however these were treated as outliers compared to the level of 20:2 measured in majority of 'p19' lines.

There was no change in the 20:4 median of the pFN050 population (~10%), but the 20:4 median significantly increased in the pFN047 (~16%) and pFN049 (~15%) populations (Fig 3.9). There were a number of pFN047 lines that contained <10% of 20:4, however all pFN049 lines contained >10% (Fig 3.9). A higher number of pFN047 and pFN049 lines contained >20% 20:4.

A combination of the progeny plots (Fig 3.7) and the box-whisker plot analysis (Fig 3.8, Fig 3.9, Fig 3.10) of the five generations revealed that generally the levels of intermediate (20:2) decreased and 20:4 increased, although in most pFN050 and pFN046 populations the intermediates increased and 20:4 decreased.

The progeny plots of three pFN050 events (pFN050-01, pFN050-02 and pFN050-05) revealed that the levels of 20:4 increased with each generation, including in the last generation analysed (Fig 3.7A). In the remaining 20 events, the level of 20:4 either did not change or dropped over the five generations. The highest level of 20:4 (20.2%) was measured in one of

pFN050-02 T5 progeny (Fig 3.7A). Overall, there was an increase in the amount of 20:4 in T2 and T3 but levels dropped in T4 and T5 (Fig 3.7A).

The majority of pFN046 events had relatively low amounts of 20:4 and the progeny plots (Fig 3.7B) revealed that 20:4 started declining in T5 in all events except for the progeny of pFN046-01 (17.8% 20:4 measured in T5 seed).

A number of T4 progeny of pFN047-26 containing lower levels of 20:4 lines were taken to T5 to assess their segregation (Fig 3.7C). The metabolite data have shown that a number of T4 progeny containing low levels of 20:4 segregated to produce ~38% 20:4 in the T5 seed. The metabolite data and segregation analysis have revealed that pFN047-26 was a multi-copy event and progeny of this event contained exceptionally high levels of 20:4. The pFN047-08 lines segregated in T4 and the level of 20:4 increased in a number of T5 progeny to >20%. Overall, the progenies of 11 out of 32 pFN047 independent T2 events produced seeds that contained >20% 20:4. The progeny and box-whisker plots of pFN047 population show that 20:4 increases in majority of the lines and stabilises in T5, and that there was a slight decline in 20:4 observed in a number of T5 lines (Fig 3.7C).

The progeny of the pFN049-21 event segregated in T4 and T5 as well. The level of 20:4 did not drop in the T5 progeny of pFN049-17 and pFN049-21 (Fig 3.7D), compared to the T5 progeny of pFN047-39 (Fig 3.7C) and pFN050-07 (Fig 3.7A) where 20:4 dropped over time. The generational study of pFN049 population revealed overall that 20:4 levels were relatively consistent in T3-T5 progenies of majority of the V2 events and that there was a slight decline observed in the level of 20:4 in a number of T5 events.

Although only a small number of pFN048 were traced through five generations, these events were generally high accumulators of 20:4. The progeny plots of three T2 events have shown that the level of 20:4 continued to rise in T5 (Fig 3.7E). Segregation analysis of these events also suggested that they stopped segregating in T3, while the other three events showed a decline in level of 20:4 over time.

A number of the FW10-23 T3 seeds were also germinated and ten plants were grown to collect T4 seeds. Although FW10-23 lines were a generation behind they were grown as controls with the remainder of the T5 populations. The FAME analysis of the T4 seeds showed a dramatic increase in the 20:2 levels and decrease in the 20:4 levels (Fig 3.10). As

previously mentioned, the T3 event was a single copy homozygous event. The segregation and FAME analyses of FW10-23 T4 seeds did not show segregation, however the level of transgenic metabolites had dropped.

A

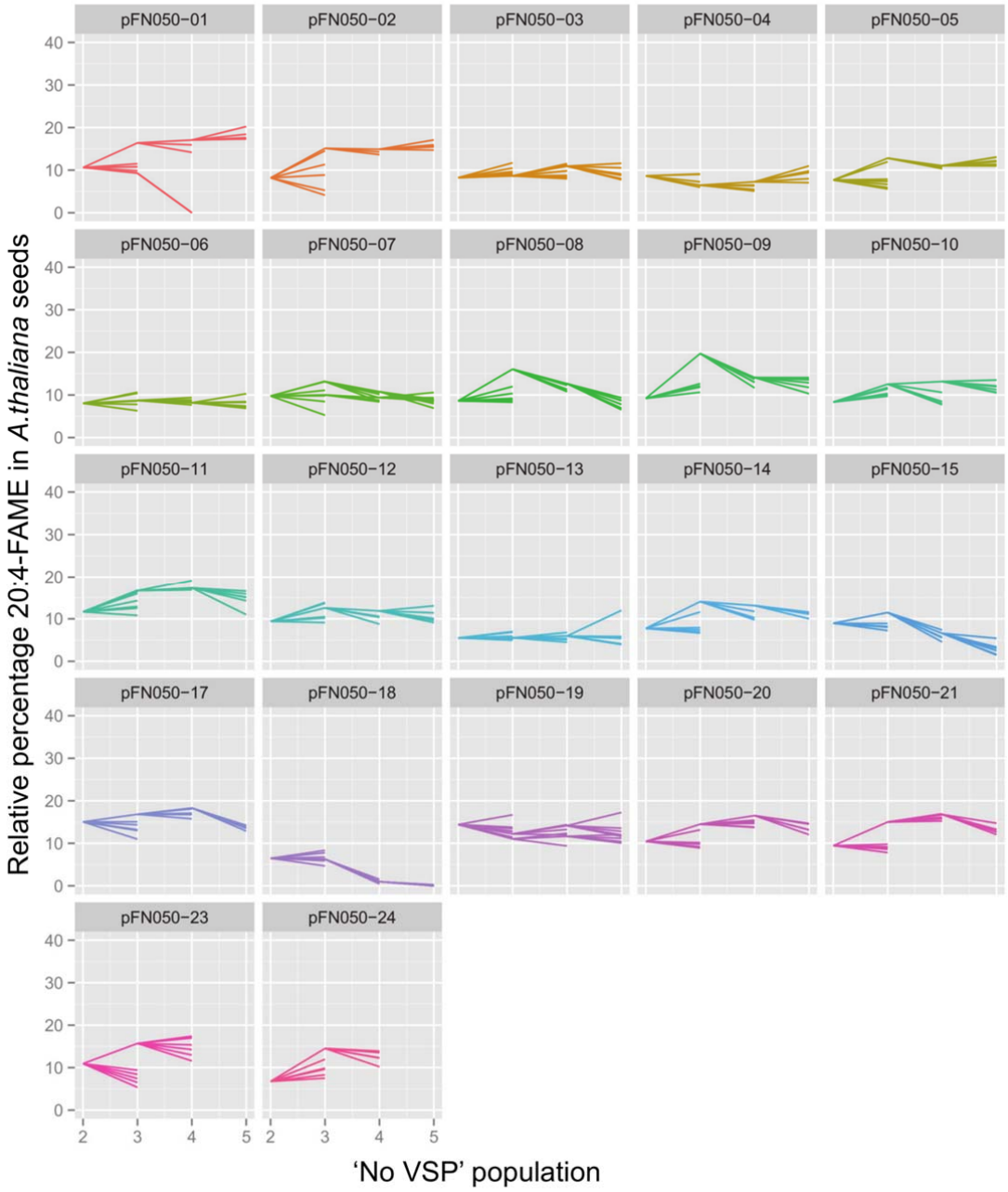
pFN050−01
pFN050−02
pFN050−03
pFN050−04
pFN050−05
pFN050−06
pFN050−07
pFN050−08
pFN050−09
pFN050−10
pFN050−11
pFN050−12
pFN050−13
pFN050−14
pFN050−15
pFN050−17
pFN050−18
pFN050−19
pFN050−20
pFN050−21
pFN050−23
pFN050−24
0
10
20
30
40
2
3
4
5
Relative percentage 20:4-FAME in A.thaliana seeds
'No VSP' population

B

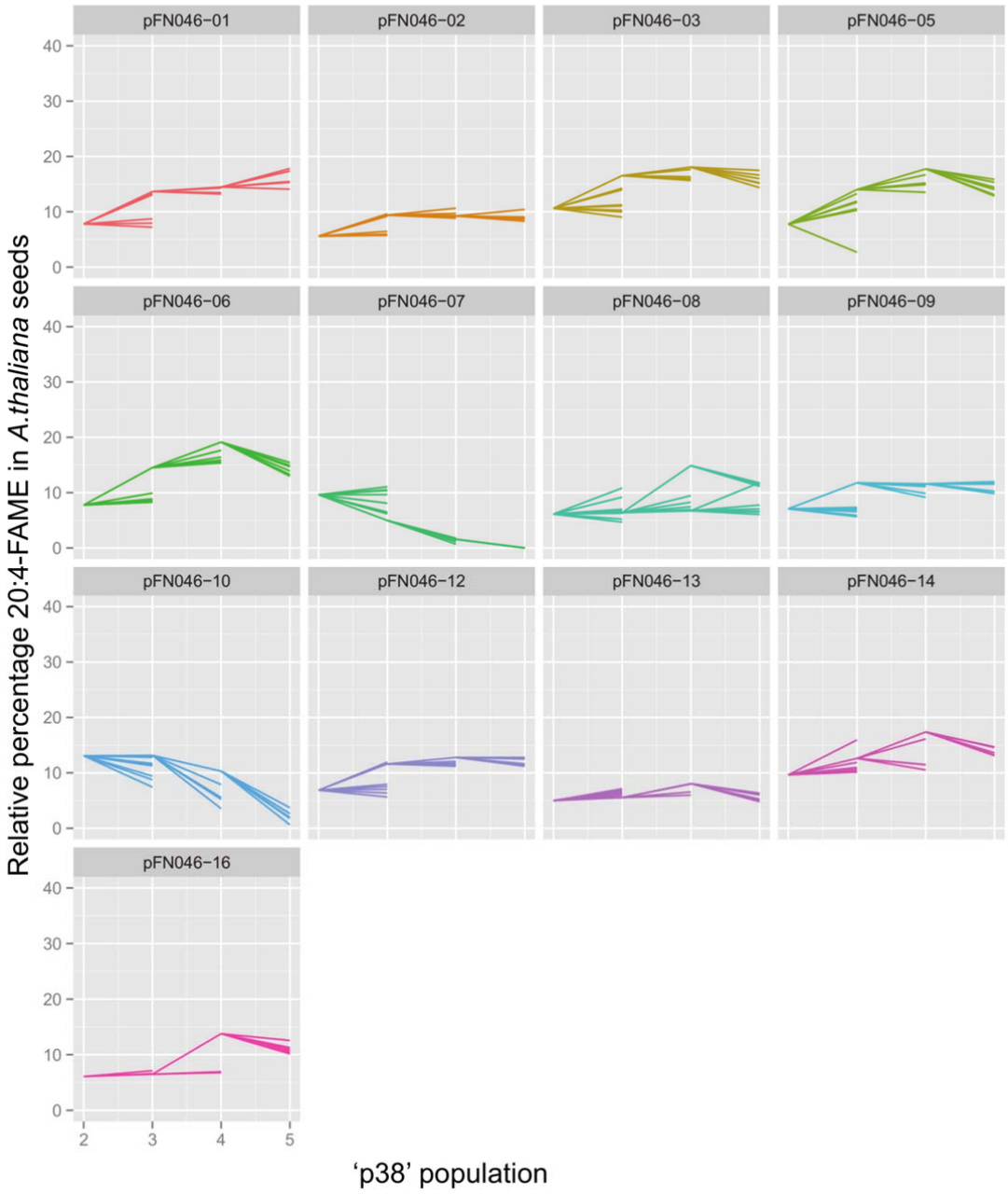
pFN046-01
pFN046-02
pFN046-03
pFN046-05
pFN046-06
pFN046-07
pFN046-08
pFN046-09
pFN046-10
pFN046-12
pFN046-13
pFN046-14
pFN046-16
0
10
20
30
40
2
3
4
5
Relative percentage 20:4-FAME in A.thaliana seeds
'p38' population

C

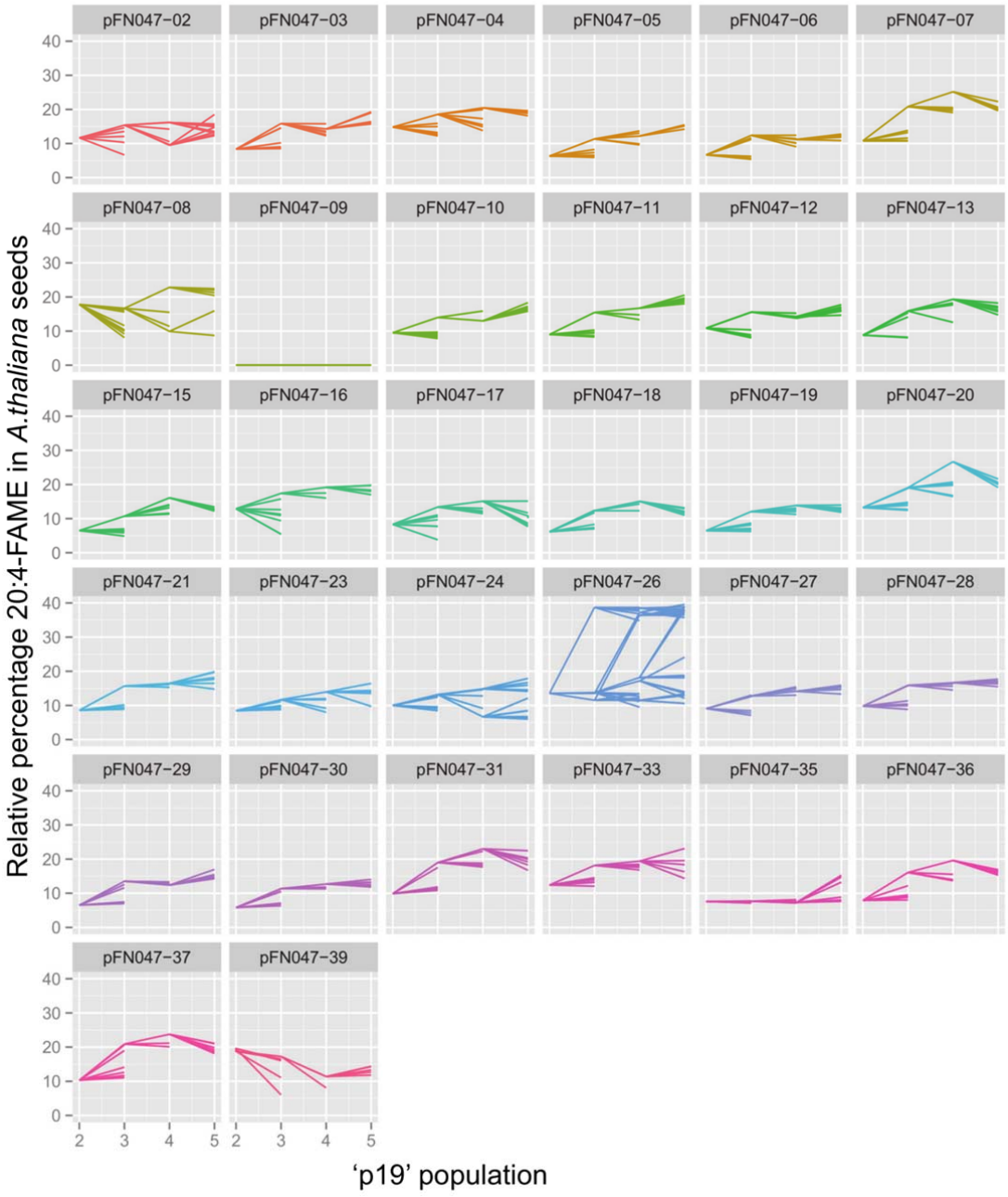
pFN047−02
pFN047−03
pFN047−04
pFN047−05
pFN047−06
pFN047−07
pFN047−08
pFN047−09
pFN047−10
pFN047−11
pFN047−12
pFN047−13
pFN047−15
pFN047−16
pFN047−17
pFN047−18
pFN047−19
pFN047−20
pFN047−21
pFN047−23
pFN047−24
pFN047−26
pFN047−27
pFN047−28
pFN047−29
pFN047−30
pFN047−31
pFN047−33
pFN047−35
pFN047−36
pFN047−37
pFN047−39
0
10
20
30
40
2
3
4
5
Relative percentage 20:4-FAME in A.thaliana seeds
'p19' population

D

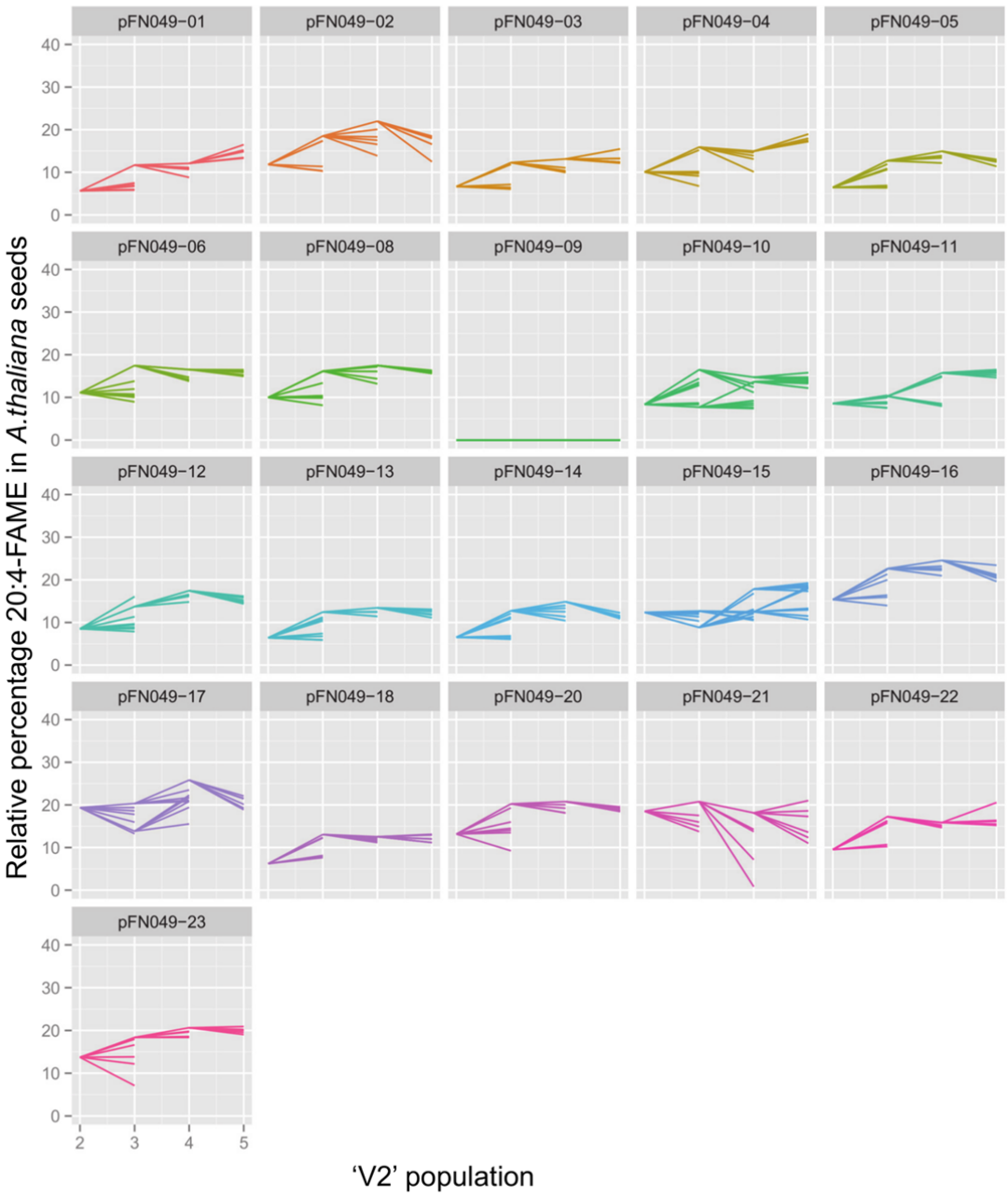
pFN049-01
pFN049-02
pFN049-03
pFN049-04
pFN049-05
pFN049-06
pFN049-08
pFN049-09
pFN049-10
pFN049-11
pFN049-12
pFN049-13
pFN049-14
pFN049-15
pFN049-16
pFN049-17
pFN049-18
pFN049-20
pFN049-21
pFN049-22
pFN049-23
0
10
20
30
40
2
3
4
5
Relative percentage 20:4-FAME in A.thaliana seeds
'V2' population

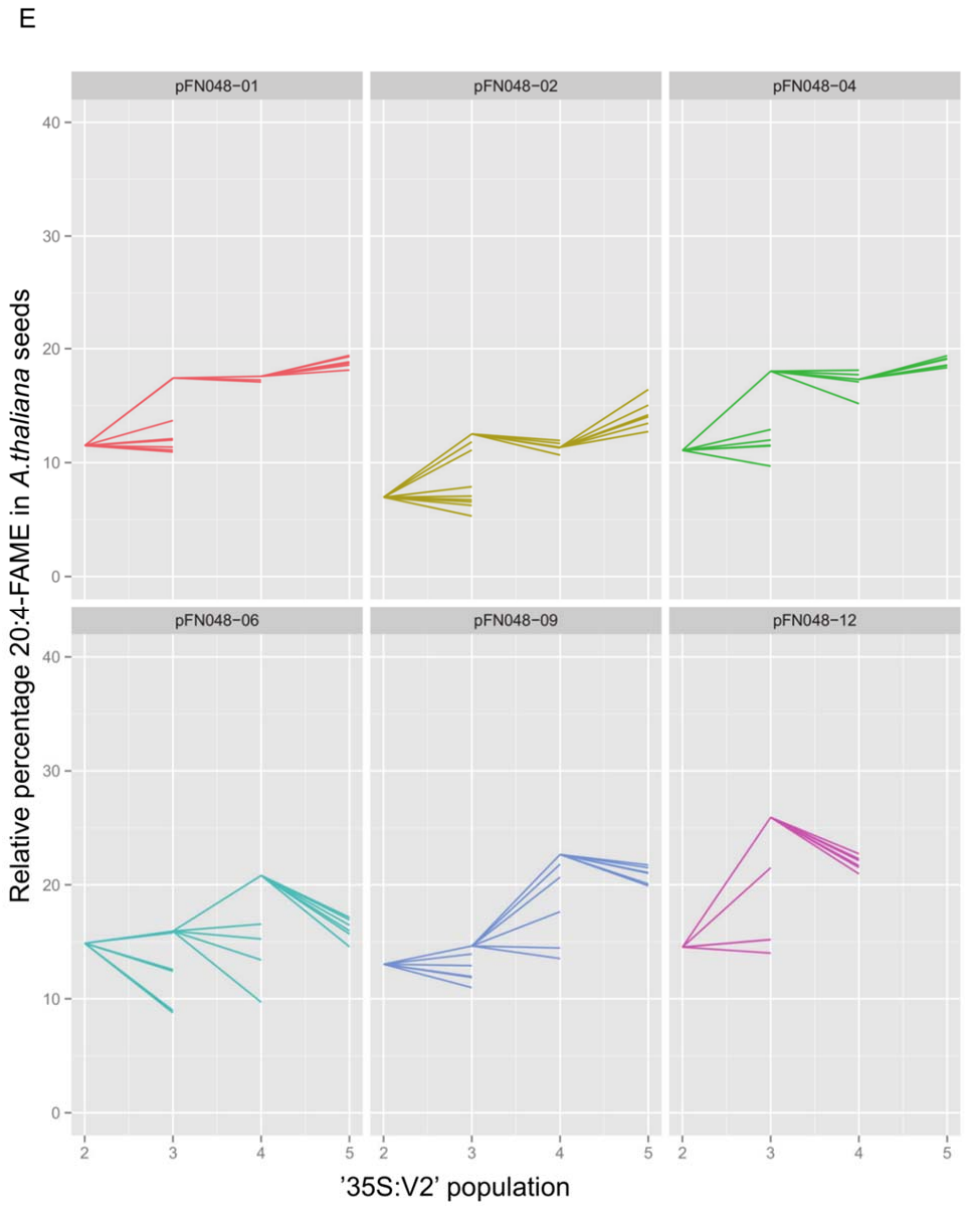

Figure 3.7. The progeny plots for the various transgenic populations of *A.thaliana* connecting T2 events to their respective progeny in T3, T4 and T5.

A. The progeny plots of lines expressing the AA+GFiP (pFN050, 'No VSP' population).

B. The progeny plots of lines expressing the AA+GFiP+p38 (pFN046, 'p38' population).

C. The progeny plots of lines expressing the AA+GFiP+p19 (pFN047, 'p19' population).

D. The progeny plots of lines expressing the AA+GFiP+V2 (pFN049, 'V2 population).

E. The progeny plots of lines expressing the AA+GFiP+35S:V2 (pFN048, '35S:V2' population).

Note: pFN0XX-XX refers to the construct and the subsequent T2 event.

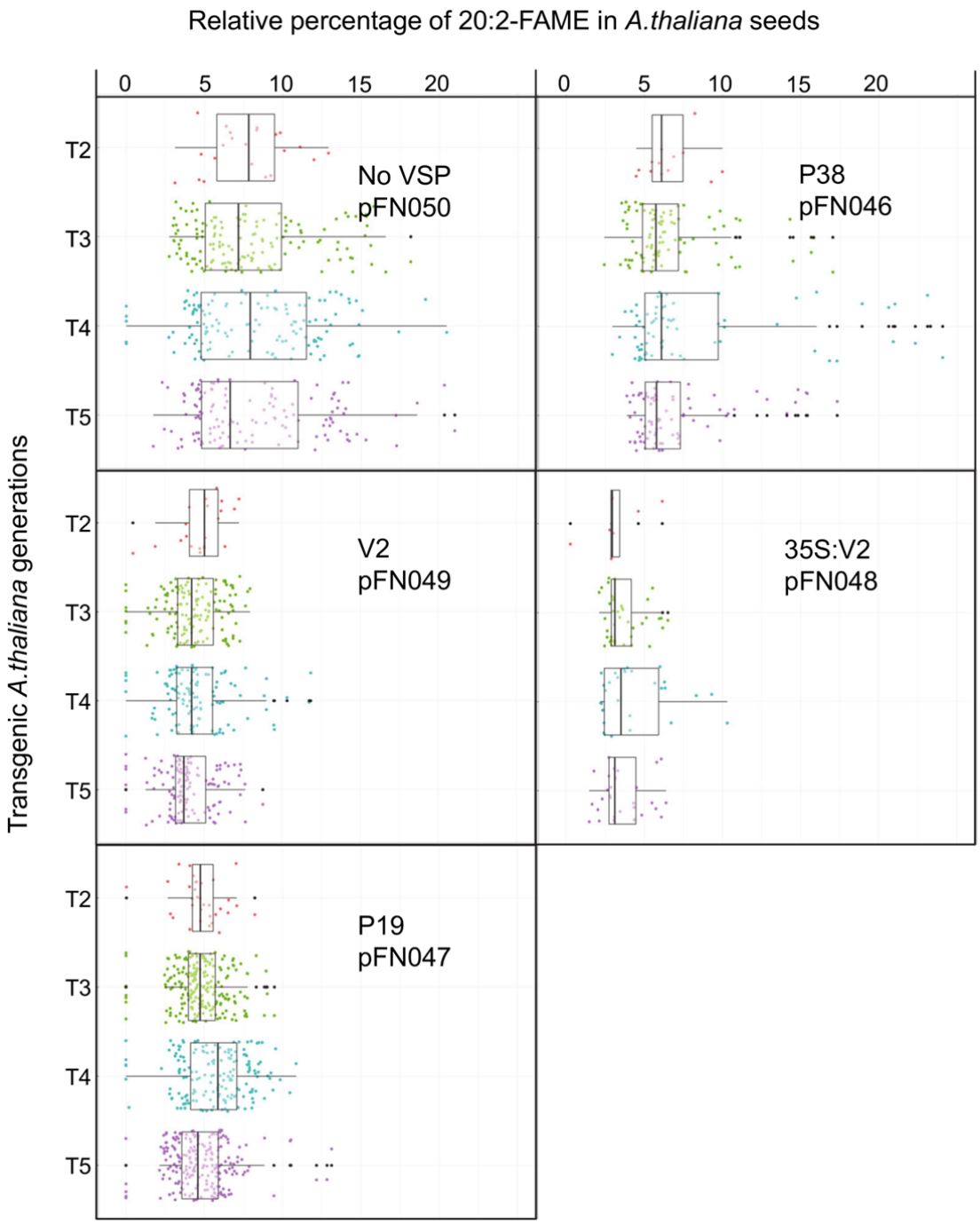

Figure 3.8. Relative percentages of 20:2-FAME extracted from T2–T5 seeds of transgenic *A.thaliana*.

Box-whisker plot analysis of a large population of transgenic *A.thaliana* expressing the constructs described in Figure 3.5B. Relative percentage of 20:2 is shown and dot points refer to independent transformation events in T2 and their respective progenies in T3–T5.

Box-whisker plot analysis: The boundary of the box closest to zero indicates the 25th percentile, a line within the box marks the median, and the boundary of the box farthest from zero indicates the 75th percentile. Whiskers (error bars) above and below the box indicate the 90th and 10th percentiles. Points outside of the whiskers are not included in the calculation of quartiles.

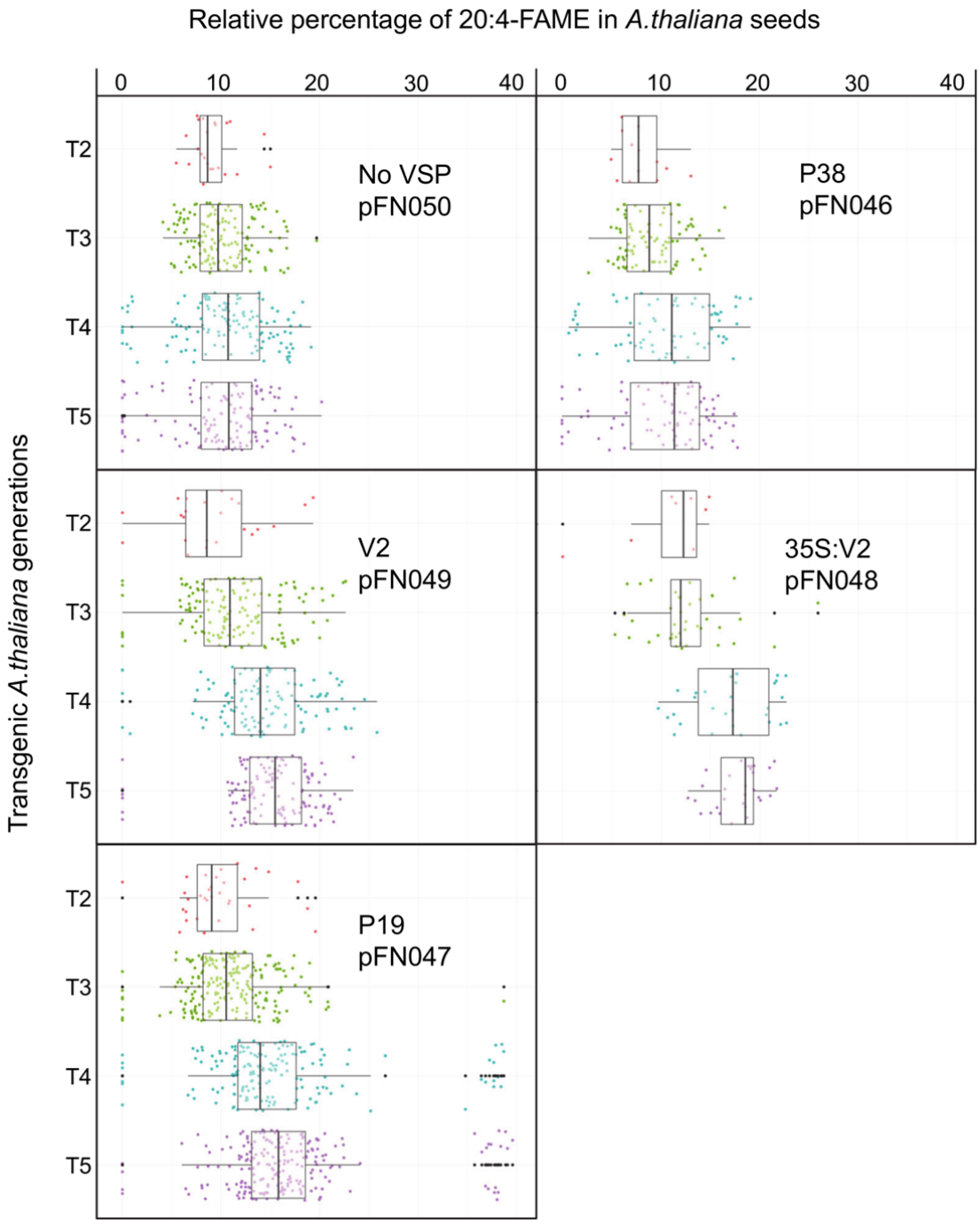

Figure 3.9. Relative percentages of 20:4-FAME extracted from T2–T5 seeds of transgenic *A.thaliana*.

Box-whisker plot analysis of a large population of transgenic *A.thaliana* expressing the constructs described in Figure 3.5B. Relative percentage of 20:4 is shown and dot points refer to independent transformation events in T2 and their respective progenies in T3–T5.

Box-whisker plot analysis: The boundary of the box closest to zero indicates the 25th percentile, a line within the box marks the median, and the boundary of the box farthest from zero indicates the 75th percentile. Whiskers (error bars) above and below the box indicate the 90th and 10th percentiles. Points outside of the whiskers are not included in the calculation of quartiles.

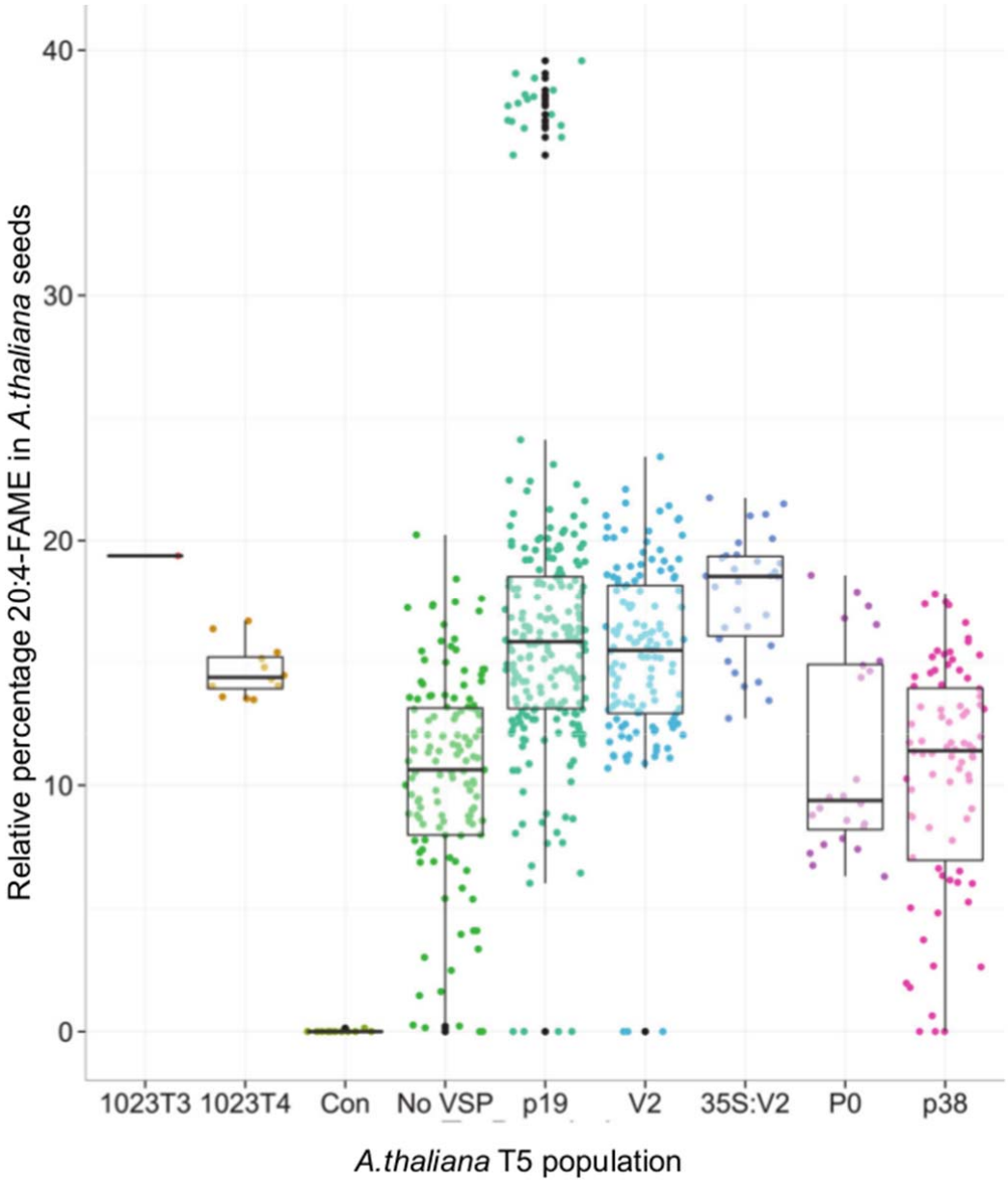

Figure 3.10. Relative percentages of 20:4-FAME extracted from T5 seeds of transgenic *A.thaliana*.

Box-whisker plot analysis of a large population of transgenic *A.thaliana* expressing the constructs described in Figure 3.5B. Relative percentage of 20:4 measured in T5 seeds and each line represented as a dot point. Abbreviations are: 1023T3, FW10-23 T3; 1023T4, progeny of FW10-23 in T4; Con, MC49 transformed with GFiP construct.

Box-whisker plot analysis: The boundary of the box closest to zero indicates the 25th percentile, a line within the box marks the median, and the boundary of the box farthest from zero indicates the 75th percentile. Whiskers (error bars) above and below the box indicate the 90th and 10th percentiles. Points outside of the whiskers are not included in the calculation of quartiles.

3.2.9 The effect of high levels of 20:4 on total seed oil and seed germination rates

Various phenotypic characteristics were measured in seeds containing varying amounts of 20:4. In early generations, it was observed that seeds with high levels of 20:4 were smaller than wild-type MC49 seeds. In a number of experiments, seeds containing high levels of 20:4 took longer to germinate and some seeds were not able to germinate at all. Slow germination rates and small seed phenotypes were observed in a number of lines, independent of the presence or absence of a functional VSP. This indicated that these effects were not related to the seed-specific expression of a VSP but rather to the content of 20:4 and related LCPUFA. This problem was investigated further by quantifying seed oil in several 20:4 events with levels of 20:4 ranging from low to very high.

A number of T4 p19 lines were selected for oil extraction based on the relative percentage of 20:4 measured in their seeds. Figure 3.11A shows the total oil content extracted from a known mass of seeds for each T4 line and oil measured as a percentage of seed mass. The wild-type MC49, GFiP expressing MC49 and pFN047-09-01-03 (null segregant) seeds contained 33%, 32% and 34% of oil, respectively, indicating that transgenic processes themselves did not affect these seed oil phenotypes at the T4 generation. The seeds of pFN026-03-08 containing ~38% of 20:4 contained only 10% total oil – this dramatic decrease equates to 70% reduction in oil from the wild-type seeds to 38% 20:4 seeds. Another line, pFN047-07-03-03, containing 25% 20:4 had 22% oil in the seed, which represented a 34% decrease in total seed oil. The seeds containing low amounts of 20:4, such as pFN047-19-07-06 with 13% 20:4, which contained 31% oil in the seed, a 6% decrease in total seed oil. The line pFN047-33-03-04 contained 18.5% 20:4 with 28% oil in the seed. The analysis of the relative percentage of 20:4 and oil content indicated a negative correlation overall (Fig 3.11A).

The effects of various levels of 20:4 on germination rates were investigated using progeny of pFN047-26-03 and compared to T2 seedlings of pFN050-23 (Fig 3.11B). These two events contained 38% and 11% 20:4 respectively. There were no phenotypic or germination rate differences between wild-type MC49 and the progeny of pFN050-23. The seedlings of pFN047-26-03 and pFN050-23 seeds were photographed 30 days after germination. The images of kanamycin-resistant seedlings indicated that seeds with high levels of 20:4 germinated at a slower rate (Fig 3.11B). The roots of 38% 20:4 seeds appeared first and

seeds germinated in full after six or seven days after imbibition. The size and morphology of leaves of a number of pFN047-26-03 seedlings were comparatively similar to pFN050-23 seedlings. The majority of pFN050-23 seeds germinated on MS media (supplemented with sucrose), however only half of 38% 20:4 seeds germinated on the same MS media. Only few pFN047-26-03 germinated on soil.

The seed-coat colour of events producing high levels of 20:4 was also darker compared to wild-type MC49 seeds. This dark colour phenotype was observed in FW10-23 seeds and more prominent in several AA+VSP lines. It was observed that the higher level of 20:4 in the seed resulted in darker seed-coat colour – the ~38% 20:4 progeny of pFN047-26 had the darkest seed-coat colour (data not shown). The cause behind this phenotype was not investigated any further.

The observations during this study have revealed that high levels of LCPUFA are responsible for reduced oil content in the seed, small seed size, germination problems and darker seed-coat colour.

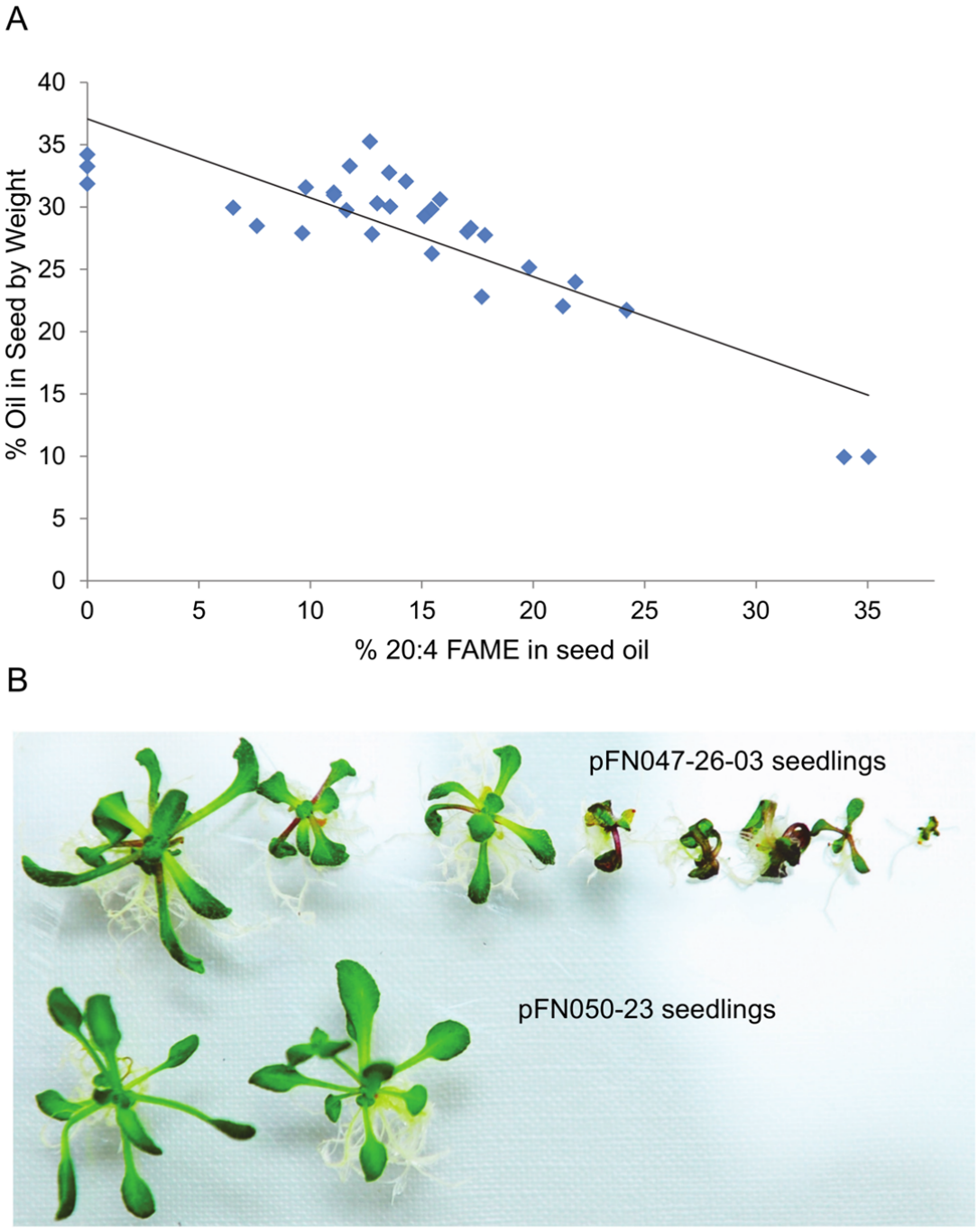

Figure 3.11. The effect of high 20:4 on the accumulation of oil (TAG) in the seed and germination rate.

A. Total oil extracted from T4 transgenic *A.thaliana* lines expressing pFN047. Independent lines analysed were selected based on the varied levels of 20:4 to determine a relationship between seed oil and relative percentage of 20:4. Oil also extracted from wild-type MC49 and MC49 expressing GFiP seeds as controls.

B. The phenotypic comparison between pFN047-26-3 and pFN050-23 seedlings. The sizes and leaf shapes of pFN047-26-03 seedlings (T3, ~38% 20:4) compared to pFN050-23 (T2, 11% 20:4) seedlings. Seedlings photographed 30 days after imbibition.

3.2.10 Comparison of 20:4 in half cotyledons of transgenic **B.napus** *expressing the various AA constructs*

Previous sections in this chapter have indicated that the seed-specific expression of V2 and p19 is tolerated in *A.thaliana* and also enhances the accumulation of 20:4 in seed oil. These encouraging results in *A.thaliana* suggested that the transformation of *B.napus* with similar vectors was warranted. The three-gene metabolic pathway for the production of AA, including either V2 (pFN049) or p19 (pFN047), was used to transform *B.napus* and assess the effect of the selected VSPs on development of *B.napus* and the level of 20:4 in the seed. Previous literature has shown that transformation of *B.napus* with the AA pathway (pJP3025) resulted in ~9% 20:4 in T1 seed oil (single seed analysis) (Petrie et al., 2012a). The aim was therefore to transform *B.napus* with the AA+GFiP+VSP constructs and measure the relative percentage of 20:4 in various generations of transgenic *B.napus*.

The elite control line of *B.napus* (CT108-03) expressing the three-gene construct to produce 20:4 in the seed was kindly donated by Dr Srinivas Belide. Petrie et al. (2012a) reported the FAME profile of T1 seeds of this event. The *B.napus* germplasm used for transformation was Oscar, referred to as the wild-type control. Constructs pFN047 (AA+GFiP+p19) and pFN049 (AA+GFiP+V2) (previously described in Figure 3.5B) were used to transform *B.napus* using tissue culture transformation techniques (see the Methods section in this chapter). Unlike *A.thaliana,* large populations of independently-transformed events of *B.napus* are difficult to generate – I would like to thank Dr Srinivas Belide for his efforts to generate transgenic *B.napus* lines. *B.napus* is transformed via a tissue culture method that generates T1 seed after approximately 4 months.

Approximately 15 independent events were generated using constructs pFN047 and pFN049. Each of these independent events generated many hundreds of seeds and total FAME was extracted from 100 mg pooled seeds of T1 *B.napus* seeds. The highest level of 20:4 measured in the pooled seeds was 3.41%. Oscar contains ~11% 18:3n3 so the AA pathway enzymes were also able to produce significant amounts of the ω-3 LCPUFA – the fatty acids with ‘n6’ and ‘n3’ represent the ω-6 and ω-3 fatty acids. This analysis was conducted on all independent events and the events containing the highest levels of 20:4 were selected for further study. Three independent events expressing pFN049 and two independent events expressing pFN047 were selected to grow to the next generation. Seeds

from these elite events were germinated on wet filter paper and the 20:4 content of cotyledon tissue (small tip of cotyledon) from each seedling was used for FAME analysis to accurately screen for null segregants. Materials containing 20:4 were propagated into mature plants.

The FAME analysis of the pooled T3 seeds revealed that the relative percentage of 20:4n6 ranged between 2.1% and 5.9% (Table 3.2). Comparatively, the pFN049 lines contained a higher level of 20:4n6 than the pFN047 lines. The FAME analysis also revealed that a high amount of 20:2n6 was not desaturated by PsΔ8D, as the analysed lines contained 9.7–11.4% 20:2n6 (Table 3.2). Surprisingly, the level of 20:3n3 (first intermediate of the ω-3 pathway) ranged between 5.8% and 7.5% (Table 3.2). The lines also contained 0.5–1.4% 20:5n3. The line that contained the highest level of 20:4 was a pFN049 line (pFN049-02-02) containing 5.9% 20:4n6, 1.3% 20:5n3 and 25.6% total new products (Table 3.2).

In order to compare the effect of V2 and p19 on plant phenotype and performance of the AA pathway, a number of T2 seeds were germinated to grow T3 plants. This included elite lines from the pFN049 and pFN047 populations, CT108-03 and Oscar as negative control. A large number of seeds were germinated and FAME extracted from their half cotyledons. The cotyledons containing high levels of 20:4 were put on soil to produce T3 plants. The dot plot (Fig 3.12) shows that the cotyledons contained varying levels of transgenic metabolites. The cotyledon of a pFN049 line contained 16.7% 20:4 and 34.6% total new product (Fig 3.12) – this line contained the highest level of 20:4 and total new products, however the seedling did not survive once it was transferred to soil. Another twenty seeds of the same parent line were germinated, however none contained such high levels of transgenic metabolites.

The CT108-03 cotyledons contained ~5.5% 20:4 and ~16% total new products while the majority of the pFN049 and pFN047 lines contained comparatively higher levels of the ω-6 and ω-3 LCPUFA (Fig 3.12).

The phenotypes of the T3 VSP lines and T2 No VSP line were compared (Fig 3.13). The seeds of the wild-type, No VSP and VSP events were germinated and seedlings transferred to soil on the same day. This comparison revealed that a number of the plants expressing the AA pathway had different leaf morphology, including increased number of smaller leaves in the pFN049 line (pFN049-02-02-23) (Fig 3.13A) that contained a high level of 20:4 (7.0%) and total new products (27.7%) in T3 seeds. However the leaves of pFN049 line that contained

7.3% 20:4 (pFN049-14-01-03) were relatively similar to Oscar. These two pFN049 lines contained the highest level of 20:4 (~7%) and total new products in the seed (~28%) (Table 3.3). The seeds of the No VSP line CT108-03-04 contained 6.4% 20:4 and 19.2% total new products (Table 3.3), but the plant took longer to flower and contained more leaves than Oscar (Fig 3.13A). The pFN049 and pFN047 lines contained 20–28% total new products, higher than the total new products in the elite No VSP line (Table 3.3).

Similar to *A.thaliana*, the seeds of high LCPUFA lines were smaller and took longer than Oscar to germinate. This phenotype was not observed in the other pFN049 lines, suggesting that this phenotype was due to the high levels of 20:4 and not the seed-specific expression of V2. CT108-03-04 (No VSP), pFN047-11-03-10, pFN049-02-02-23 and pFN049-14-01-03 contained 19.2%, 22.0%, 27.7% and 27.8% of total new products in the seed (Table 3.3) – these lines took longer to flower compared to Oscar and majority of the VSP events (Fig 3.13). pFN047-08-03-06 and pFN049-14-01-09 flowered at the same time as and looked relatively similar to Oscar (Fig 3.13A). These lines contained 5.0% and 6.3% of 20:4 in seed-oil (Table 3.3). Another two lines, pFN049-02-06-05 and pFN047-11-03-04, matured at a faster rate than Oscar (Fig 3.13B). These lines flowered and produced a higher number of siliques, and their T4 seeds contained 6.0% and 7.0% of 20:4, respectively. The images of mature plants compared to the levels of transgenic metabolites measured in the seed have suggested that intermediate levels of LCPUFA are tolerated in *B.napus*. The seed-specific expression of V2 and p19 did not reveal major phenotypic changes.

The level of the metabolites in the parallel ω-3 pathway revealed that a significant amount of 20:3n3 was not desaturated to produce high levels of 20:5n3 (Table 3.3). Overall, the metabolite analyses in several generations of *B.napus* revealed that the efficiency of PsΔ8d in converting its ω-3 and ω-6 substrates was significantly lower than in *A.thaliana*.

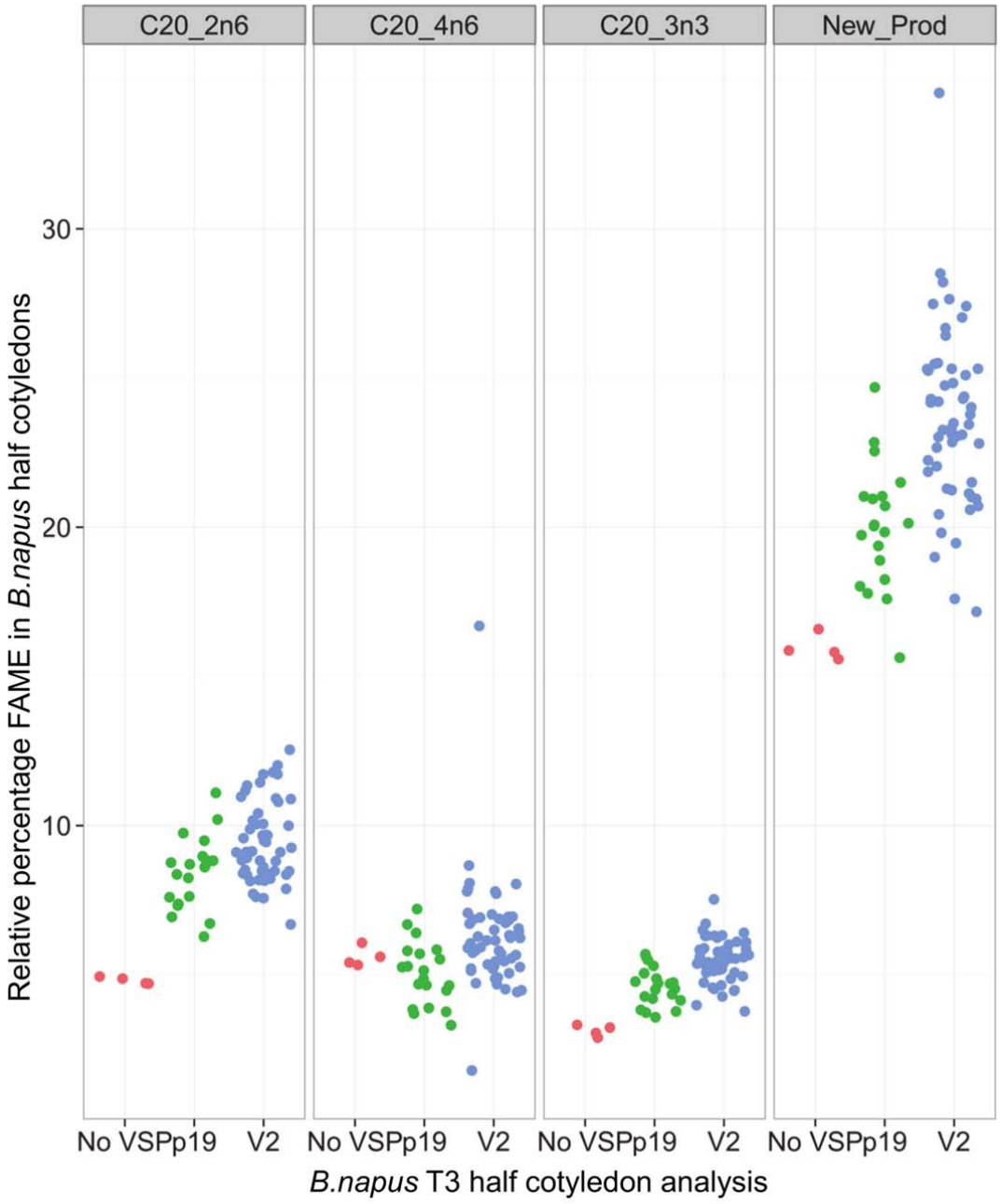

Figure 3.12. FAME extracted from half cotyledon of T3 *B.napus* seedlings.

Relative percentage FAME extracted from half cotyledon of T3 transgenic *B.napus* expressing pFN047 and pFN049. Abbreviations: p19 and V2 refer to lines expressing pFN047 and pFN049 respectively; No VSP refers to the T3 elite event of pJP3025; 20_2n6, 20:2 ω-6; 20_4n6, 20:4 ω-6; 20_3n3, 20:3 ω-3; New_Prod, total new products of the transgenic pathway.

Lines	C18:1	C18:2	C18:3	C20:2n6	C20:3n6	C20:4n6	C20:3n3	C20:5n3	New_Prod
Oscar	61.07	19.70	8.50	0.00	0.00	0.00	0.00	0.00	0.00
pFN047-08-03	53.64	7.89	4.17	9.70	1.55	4.02	6.70	1.02	23.00
pFN047-11-02	54.31	9.12	4.77	10.16	1.65	3.17	5.81	0.79	21.57
pFN047-11-03	54.43	7.87	3.60	9.92	1.50	4.31	5.81	1.09	22.63
pFN047-11-07	52.53	8.88	4.29	10.02	1.79	3.97	6.18	1.02	22.99
pFN049-02-02	49.29	9.76	4.66	11.00	1.38	5.87	6.01	1.32	25.58
pFN049-02-06	50.26	9.26	4.45	11.05	1.33	5.59	5.95	1.22	25.14
pFN049-02-12	50.00	9.26	4.38	11.12	1.26	5.65	5.79	1.21	25.04
pFN049-12-01	51.27	8.40	4.27	10.34	1.29	4.57	7.08	1.40	24.68
pFN049-12-02	57.51	7.43	3.43	10.31	0.97	2.06	6.29	0.46	20.08
pFN049-12-07	52.11	8.00	4.52	9.68	1.35	3.93	7.50	1.29	23.75
pFN049-14-01	48.08	9.50	5.01	11.37	1.29	4.88	6.79	1.27	25.60
pFN049-14-02	49.49	10.15	5.90	9.91	1.46	3.23	6.93	0.85	22.37
pFN049-14-11	51.47	8.98	4.56	9.74	1.62	3.98	6.28	1.05	22.66

Table 3.2. Relative percentage FAME extracted from T3 seeds of transgenic *B.napus*.

Total FAME extracted from 100 mg pooled T3 seeds of *B.napus* expressing the constructs pFN047 and pFN049, as outlined in Fig 3.5B. Total FAME also extracted from seeds of a wild-type control (Oscar).

Lines	C18:1	C18:2	C18:3	C20:2n6	C20:3n6	C20:4n6	C20:3n3	C20:5n3	New_Prod
Oscar	57.83	22.11	11.82	0.00	0.00	0.00	0.00	0.00	0.00
CT108-03-04	59.72	7.71	3.67	6.84	0.71	6.43	3.59	1.60	19.17
pFN047-08-03-06	53.26	9.78	5.91	9.64	1.39	4.95	5.02	1.16	22.17
pFN047-11-03-04	52.36	10.27	6.53	6.94	1.54	7.00	4.49	2.07	22.04
pFN047-11-03-10	56.43	9.03	4.91	7.93	1.18	5.27	4.23	1.42	20.04
pFN049-02-02-12	52.75	11.16	5.06	9.77	1.33	5.18	3.90	0.92	21.10
pFN049-02-02-23	43.81	10.85	7.03	11.15	1.14	7.03	6.41	1.92	27.66
pFN049-02-06-05	49.89	10.66	5.82	10.34	1.22	6.03	5.05	1.38	24.02
pFN049-14-01-03	44.07	10.31	6.89	10.38	1.27	7.34	6.49	2.28	27.76
pFN049-14-01-09	49.75	10.39	6.70	8.40	1.33	6.26	5.44	1.89	23.32

Table 3.3. Relative percentage FAME extracted from T4 seeds of transgenic *B.napus*.

Total FAME extracted from 100 mg pooled T4 seeds of *B.napus* expressing the constructs pFN047 and pFN049 as outlined in Fig 3.5B. Total FAME also extracted from seeds of a control T3 line expressing pJP3025 (CT108) as well as wild-type control (Oscar).

A


Oscar
CT108-03-04
pFN047-08-03-06
pFN047-11-03-10
pFN049-02-02-12


Oscar
pFN049-02-02-23
pFN049-14-01-03
pFN049-14-01-09

B

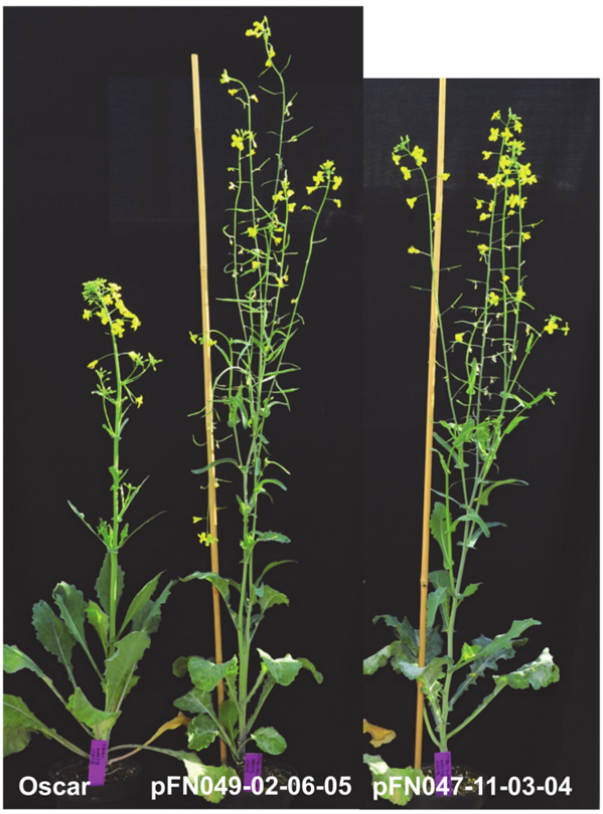

Figure 3.13. Phenotypes of mature *B.napus* plants expressing the AA pathway compared to plants co-expressing the AA pathway with a VSP.

Panels **A–B**. Phenotypic comparison of mature wild-type *B.napus* (Oscar) with transgenic *B.napus* expressing the constructs pJP3025 (No VSP control, T2 plant CT108-03-04), pFN047 (p19, T3 plants) and pFN049 (V2, T3 plants). Seeds were germinated and transferred to soil on the same day. Plants were photographed 45 days after germination.

3.3 Discussion

This chapter outlined a novel approach to enhance the overexpression of multi-gene transgenic pathways in oilseeds in both the model plant *A.thaliana* and the crop plant *B.napus*. The co-expression of V2 or p19 enhanced the performance of the transgenic pathway, resulting in higher levels of AA in the oilseeds of both *A.thaliana* and *B.napus*. This study highlights that *A.thaliana* has a higher metabolic potential for the production of AA with an upper threshold approaching 40% of the oil profile. In contrast, *B.napus* only reached 7% AA due to a metabolic bottleneck that resulted in the accumulation of intermediates of the pathway.

In this study, considerable effort was invested in generating independent transgenic events and maintaining and tracking the performance of these transgenic events for five generations. It is common practice in the metabolic engineering of plants to generate a large population of transgenic events and to continually select for elite lines and discard underperforming lines, however in this study a range of 'poor', 'medium', and 'good' performing lines were maintained for five generations. This performance was based on the relative percentage of the transgenic metabolites extracted from pooled seeds of each independent event. This broad selection criterion was used to generate a large population of transgenic events, rather than only focusing on a few elite events. It is evident from the metabolite analysis that the seed-specific expressions of V2 and p19 were able to enhance the performance of transgenic pathway in the majority of transgenic events in a population.

3.3.1 The effect of expression of several different VSPs in A.thaliana

A number of viruses encode for VSPs to disrupt sRNA biogenesis in plants (Incarbone and Dunoyer, 2013) and sRNAs are critical for a range of processes in plants, including development (Vaucheret, 2006) and defence mechanisms (Incarbone and Dunoyer, 2013). The current study revealed that the effect of a number of VSPs is tolerated in *A.thaliana* when expressed exclusively during oil synthesis in seed development. The VSPs selected for this study included p19, V2, $P0^{PE}$ and p38. The constitutive expression of both p19 and $P0^{PE}$ have been shown to cause major developmental defects in *A.thaliana* (Dunoyer et al., 2004; Fusaro et al., 2012) – in this study, these VSPs were expressed with the FP1 promoter to coincide with oil synthesis during seed development. This study also showed that the expression of p19 and V2 with the FP1 promoter avoided detrimental effects that would

otherwise have been expected if these genes were expressed during embryogenesis. The FP1 promoter has a peak of expression after critical events during embryogenesis (Le et al., 2010) and it is commonly used for genetic engineering of oilseed crops and *A.thaliana* (Stalberg et al., 1993). A Western Blot analysis of tissue from *A.thaliana* plants expressing FP1:GFiP was used to confirm that the activity of the FP1 promoter was limited to the seed.

Previous studies have shown that *A.thaliana* expressing p38 under a constitutive promoter (35S) did not exhibit developmental abnormalities (Dunoyer et al., 2004). It has also been shown that constitutive expression of p38 inhibited co-suppression of GFP in transient assay (Azevedo et al., 2010). This study investigated seed-specific expression of p38, however no phenotypic changes were observed. The effect of constitutive expression of V2 has not been studied previously, therefore V2 was expressed with both the FP1 and the 35S promoters. In order to compare the phenotypic changes caused by the stable expression of VSPs in *A.thaliana*, a control binary construct driving the seed-specific expression of GFiP was also prepared. The GFiP gene was reconstructed to include an intron in the middle of the GFP gene and various signals were added to allow secretion of the protein from the plant cell – these changes allow GFP to be easily visualised in the mature seed.

Plants which were stably transformed with VSPs expressed during oil synthesis in seed development were able to germinate and grow to maturation relatively similar to the wild-type plants. These plants were also capable of producing viable seeds. V2 was also tolerated in *A.thaliana* when expressed with the 35S promoter – the CaMV 35S promoter is known to have low levels of expression during seed development and during important stages of embryogenesis.

A range of phenotypes were displayed in the cotyledons of transgenic *A.thaliana* seedlings of the Col-0 ecotype expressing the selected VSPs . The phenotypic observations revealed that the seed-specific expression of $P0^{PE}$ and p19 resulted in 'ballerina like' and 'dog-ear like' cotyledons. This phenotype was obvious in the Col-0 and MC49 ecotypes of *A.thaliana*, while the seedlings expressing V2 with either the FP1 or 35S promoter looked similar to the wild-type plants. Although the V2 events contained wild-type-like cotyledons, the majority of these events had short roots. In order to confirm the short root phenotype, a large number of VSP events were germinated and then grown on vertical plates to assess the length of the roots. The experiments were repeated in two consecutive generations and

root length suggested that the V2-expressing events contained short roots and that the expression of 35S:V2 and FP1:V2 resulted in disruption of a developmental pathway associated with root development. In controlled growth conditions, the plants matured at the same rate as the control wild-type and GFiP-expressing plants, suggesting that the short roots did not have an effect on plant growth. The molecular mechanism behind this phenotype was not studied. Seedlings of *B.napus* and another ecotype of *A.thaliana* (MC49) expressing pFN048 and pFN049 did not have short roots, suggesting that the 'short root' phenotype was specific to Col-0 ecotype of *A.thaliana*.

The aim of seed-specific expression of the VSPs was to assist in metabolic engineering of lipid pathways in the seed – it was therefore essential that the seed-specific expression of the selected VSPs did not have a major effect on the oil profile and total oil of the seed. The total oil analysis revealed that the seeds of p19-expressing events contained relatively lower amounts of oil than the wild-type seeds. However, changes in the oil profile were observed in all transgenic events, including the seeds of lines that were expressing FP1:GFiP. This study therefore concludes that the process of transgenesis (expression of GFiP only) produced some changes in the lipid profile, but there were no other significant changes in the lipid profile due to the further inclusion of VSPs. These changes in lipid profile were not investigated any further, but it is possible that the secreted GFP protein interacts with the lipid desaturation pathways, a process that has not been described.

There were 200 individual *A.thaliana* transgenic events expressing the various VSP constructs which were grown through to T5. It is plausible that limiting the expression of VSPs to during oil synthesis in the seed avoided major developmental defects in *A.thaliana*. The results presented in this chapter are also the first to report the stable transformation of *A.thaliana* with V2 and the phenotypes associated with seed-specific and constitutive expression of V2 in *A.thaliana*. Overall, these results have shown that the expression of V2 and other selected VSPs is tolerated in the seed of *A.thaliana*.

3.3.2 Determining a suitable transgenic pathway to monitor the effect of VSPs on transgene performance over five generations

To investigate the effect of the previously mentioned VSPs on transgene performance, it was critical to determine a suitable transgenic pathway. The design of the study required that the transgenic pathway contain the following features:

- The pathway should have a suitable dynamic range, such that poorly performing events can be easily discriminated from 'elite' events
- A multi-step metabolic pathway to convert a relatively simple endogenous substrate into more elaborate metabolites with potential commercial application
- The pathway should produce transgenic metabolites that are easily detectable using simple analytical techniques.

The production of LCPUFA in the seed is consistent with the above parameters, therefore the selection of the transgenic pathway included biosynthesis of ω-3 and ω-6 LCPUFA in the seed. A DHA-producing pathway was initially chosen for the study, comprising five sequential steps using linolenic acid (18:3n3) as the starting substrate in the seed. The stable transformation of *A.thaliana* with the DHA constructs produced a very low number of transgenic events. During the genetic transformation and analysis of the positive events, it became obvious that the design of the construct was not ideal. There were five FP1 promoters and the gene cassettes were placed in one direction (a simple linear design), which may have compromised the insertion and stability of the transgenes (Petrie et al., 2010; Petrie et al., 2012b). Although the production of DHA has gained commercial interest, it was difficult to generate multiple transgenic *A.thaliana* plants with the use of the five-gene transgenic pathway. Furthermore, the transgenic plants only produced low levels of DHA, making the selection of poor and elite events difficult to analyse.

An alternative metabolic pathway, for the production of AA, was therefore investigated. The design of this pathway involved three transgenes to synthesise an ω-6 LCPUFA, AA, using linoleic acid (18:2n6) as the substrate. MC49 was used for stable transformation with the AA pathway, an ecotype of *A.thaliana* containing high levels of 18:2 and very low levels of 18:3 due to mutations in *fad3* and *fae1* genes. The transgenic plants expressing the AA pathway contained a wider dynamic range of AA in *A.thaliana* seeds, spanning between 5% and 20%

(Petrie et al., 2012a). The AA pathway contained a lower number of transgenes than the DHA pathway and also avoided the use of the same promoter to drive all transgenes.

Recently the re-configuration of the DHA construct involving changes in the choice of promoters and placement of the genes resulted in higher levels (~15%) of DHA in *A.thaliana* seeds (Petrie et al., 2012b). This result also indicated that reconfiguring multi-gene constructs for improving pathway performance in plants is a difficult process.

3.3.3 Transient expression of the AA constructs in N.benthamiana *leaves*

The simultaneous silencing and overexpression technique introduced in Chapter 2 was also assessed with the AA pathway. *N.benthamiana* leaves contain high amounts of 18:3 and it was possible to silence *NbFAD7* and overexpress the AA pathway to replicate the seed system. The results have shown that silencing of *NbFAD7* resulted in doubling the levels of AA produced in the leaf. The endogenous metabolite was successfully shunted into the assembly of the AA pathway. Interestingly, due to the presence of 18:3n3, a parallel pathway was also taking place which resulted in relatively high levels of the ω-3 LCPUFA, EPA (20:5). The silencing of *NbFAD7* was expected to result in dramatic changes in the levels of 20:4 and 20:5 but this was not observed. The results suggested that the transgenic enzymes were very selective in utilising 18:3n3 as substrate. These results also suggested that transgenic modification of a high 18:3 oilseed crop with the AA pathway could be expected to result in high levels of 20:5 in seed oil.

3.3.4 The production and monitoring of transgenic A.thaliana *over five generations*

The stable transformation of *A.thaliana* with the AA constructs generated a large number of transgenic events. This study generated progeny plots that assisted in tracking the performance of the AA pathway in independent lines over five generations. The comparison of the performance of the transgenes was not easily determined by comparing the progeny plots of the different populations. However the box-whisker plot analyses of the pathway intermediates and AA have shown that the populations co-expressing V2 or p19 performed relatively better than the populations without these VSPs. These methods of presenting the data allowed a global view of the influence of a particular VSP on AA biosynthesis in *A.thaliana* and *B.napus* oilseeds.

The gradual increase in the levels of 20:2 that occurred in five generations was indicative of transgene silencing in all populations, although this increase was higher in the pFN046 and pFN050 populations. The pFN047 and pFN049 populations contained low levels of intermediates and high levels of AA throughout the five generations. In the later generations, the level of intermediates also increased slightly in a number of pFN049 and pFN047 lines, however molecular analysis was not conducted to confirm that these lines contained the VSP part of the T-DNA insert. The VSP was placed next to the right border in the AA constructs and it is possible that the VSP part of the T-DNA was not inserted into the genome of *A.thaliana*. The pFN047 and pFN049 populations were relatively large and the comparisons suggest that the pFN049 population performed marginally better than the pFN047 population.

pFN048 was a very small population but there were many elite events that contained ~20% of AA in T5 seeds. It is possible that high expressing lines may not have survived due to lethality of V2 expressed with a 35S promoter. More importantly, the results have shown that constitutive expression of V2 is tolerated in *A.thaliana* and it is plausible that T-DNA not exclusively designed for modification of oilseed may also benefit from the co-expression of 35S:V2.

The progeny plots and box-whisker plots revealed that the pFN046 population was a poorly-performing transgenic population compared to other VSP-containing and pFN050 plants. This suggests that p38 was not able to inhibit co-suppression of the transgenes. It was expected that expression of p38 might inhibit methylation-driven silencing of the transgenic pathway, however this was not observed. It is also possible that the p38 gene cassette in pFN046 construct encoded for a dysfunctional protein.

3.3.5 Molecular basis of VSP enhancement on transgenic performance in oilseeds

Transgenes may either fail or perform as elite events for reasons that remain obscure. The thorough metabolite analysis of the large transgenic population conducted during this study indicated that the co-expression of V2 or p19 enhanced the levels of transgenic metabolites in five generations. An exhaustive molecular analysis of transgenic events was not conducted in this thesis. However, given the large body of evidence regarding the interference of VSP in sRNA biogenesis, it seems plausible that sRNA pathways are involved in restricting transgene performance in oilseeds.

Segregation analysis is a relatively simple form of molecular analysis that indicates the number of independent loci in which transgenes have inserted. The independent T2 events were grown to T5 and segregation analyses have shown that a number of high copy number events contained high levels of AA, which reduced over the generations as the successive progenies segregated out (for example pFN047-39, a p19 event). The early generations showed a correlation between the inserted transgene copy number and the levels of transgenic metabolites. In later generations, when the events stopped segregating, it is possible that a number of AA events were multi-copy events, which became homozygous in all loci. Previous reports have shown that transgenes may be present in a genome at numerous locations, however high transgene insertion events may be more prone to transgenic silencing than single copy events (Schubert et al., 2004).

It is also possible that parts of the T-DNA may have been inserted in multiple locations in the genome. It is expected that Southern Blot analysis or Droplet Digital PCR techniques to probe the presence of every transgene might assist in determining the true copy number of every transgene in the genome of *A.thaliana*. Furthermore, the silencing of the transgenes in the pFN050 and pFN046 populations may have been due to the sRNA-driven methylation of transgenes. The promoters (FP1) and terminators (NOS) were used for a number of the genes in the constructs and it is possible that these became the target of transgene silencing. Investigating the methylation marks on these regions may assist in confirming the molecular basis behind the silencing of the transgenes.

Both p19 and V2 interfere with the plant's RNA silencing machinery in very different ways, however both were able to enhance the performance of the AA pathway. The function of p19 is well studied and can be expected to inhibit silencing of transgenes by stopping the 21nt sRNA targeting the respective transgenes. However, the other size class of sRNA targeting the transgenes would not have been stopped by p19 and some silencing can be observed. The function of V2 is to disrupt assembly of RDR6 and SGS3 by facilitating the production of secondary siRNAs in order to amplify the silencing signal targeting the transgenes. Therefore, as the V2 expressing lines may contain the primary siRNA targeting the transgenes, some silencing would be observed in these lines as well. It would be interesting to extract the V2 protein from oilseeds expressing AA pathways and to

determine if there are other protein bodies bound to V2. These purification assays could be greatly facilitated by the availability of a suitable antibody against V2 (see Chapter 4).

3.3.6 Shortcomings of construct design

The original AA construct that consisted of the three genes encoding for *IgΔ9E*, *PsΔ8D* and *PsΔ5D* avoided the placement of the FP1 promoters and NOS terminators in close proximity. A Linin terminator was used in between the two NOS terminators and *IgΔ9E* was driven by *FAE1* promoter, which was placed between the *PsΔ8D* and *PsΔ5D* genes. However the addition of *GFiP* and various VSPs increased the number of FP1 promoters and NOS terminators in the construct. FP1:GFiP cassette contained a NOS terminator which was placed next to the NOS terminator of FP1:PsΔ5D – it is plausible that the placement of the NOS terminators were not ideal. The terminators are very strong and it was assumed that transcriptional read-through (formation of hairpin-like structures) would not occur. The FP1 promoters of *GFiP* and *PsΔ5D* were running into each other and in the event that transcriptional read-through occurred, the hairpin structure may include the NOS terminator and FP1 promoter. Processing of the hairpin would then result in sRNA-driven silencing of all FP1 promoters and NOS terminators. Transcription of *PsΔ8D* and *PsΔ5D* was terminated by the NOS terminator and in the pFN050 and pFN046 populations, the metabolites corresponding to the activities of the respective enzymes suggested that *PsΔ8D* and *PsΔ5D* were silenced prior to *IgΔ9E*. It was also unfortunate that *PsΔ8D* and *PsΔ5D* were driven by the FP1 promoter. It is thus unclear if the targeted silencing of the NOS terminator or the FP1 promoter resulted in silencing of the respective genes.

The addition of FP1:p19, FP1:V2, FP1:p38 and FP1:P0^{PE} added an extra FP1 promoter to the construct. The promoter of *V2* was placed back to back with the FP1 promoter of *GFiP* (Fig 3.5) which may have encouraged RNA silencing, although no molecular analysis was performed to detect sRNA targeting the FP1 promoters. It is also possible that the *FAE1* promoter is better than FP1.

Despite the shortcomings in the multi-gene transgene design, it is typical of metabolic engineering that numerous gene cassettes are stacked onto one relatively short stretch of DNA. Although improvements in construct design can be made by testing promoters, terminators and orientation of cassettes, these generally require empirical testing similar to that demonstrated in this chapter. This chapter demonstrates that the use of VSP is able to

improve the performance of a genetic construct using a rational strategy – reliant on blocking host sRNA pathways that presumably target the transgenes of interest.

3.3.7 38% AA in A.thaliana *seeds*

A progeny of pFN047-26 segregated out to produce ~38% AA and ~41% total new products in the seed. This study is the first to report such high levels of LCPUFA in an oilseed. It was also interesting that a number of pFN047-26 progeny contained low levels of AA in T2 and T3, but T4 produced progeny that contained ~38% AA. Similarly, a number of low AA-containing T4 parents produced 38% AA T5 progeny. The segregation pattern of pFN047-26 alone is not sufficient to confidently assign a transgene copy number to the respective T3, T4 and T5 progenies of pFN047-26. Further molecular analysis is required to better understand the segregation behaviour of this line. The segregation pattern does however confirm that pFN047-26 was initially a multi-copy event.

The events that contained super high levels of AA also showed other phenotypic changes, including darker seed-coat colour and smaller seed size. The darker seed-coat colour was not investigated further to determine its molecular basis. The smaller seed may have been due to accumulation of large amounts of LCPUFA affecting other lipid biosynthesis pathways. The smaller seeds and reduced availability of oil also had an effect on the germination rate of the super high AA containing events. These results suggested that *A.thaliana* seeds may not be well-suited for the use of AA during germination. The seeds were unable to germinate on soil with normal conditions – the nutrients of MS media (supplemented with sucrose) were essential for germination of these lines. Studying the fatty acid profile of germinating *A.thaliana* seeds containing varied levels of LCPUFA has shown that the LCPUFA are not readily-consumed for energy production unlike other native fatty acids (personal communication Pushkar Shrestha, 2013). It is also possible that the germination rates of 38% AA lines were affected due to reduced levels of lipids in the seed.

Quantification of total oil measured as TAG confirmed that an increase in AA levels in the seed resulted in a decrease in total oil. It is plausible that the *A.thaliana* lipid-handling enzymes are inefficient in processing high levels of LCPUFA into TAG, resulting in reduced amounts of TAG. Furthermore, moderate levels of LCPUFA do not have an adverse effect on seed size, oil content and germination rate. There is a trade-off between oil content and the amount of LCPUFA product in that oil – for instance, a seed with 30% AA in the oil profile

may be of reduced value to the producer due to the substantial reduction in oil content. Therefore the relationship between fatty acid composition of an oil and oil content are important factors to consider in commercial production scenarios.

Recently, Nykiforuk et al. (2012) reported transgenic *C.tinctorius* plants with 70% γ-linolenic acid (GLA, 18:3n6) in seed oil. GLA is an unusual ω-6 PUFA that serves as a precursor for a number of metabolic pathways in humans. Nykiforuk et al. (2012) reported that the 70% GLA plants were rather similar to the wild-type plants and that the LPCAT, PLA2 or PDAT/CPT/PDCT pathways were responsible for such efficient removal of GLA from PC and subsequent assembly into TAG. They also indicated that the rapid acyl exchange between PC and CoA pools can occur in *C.tinctorius,* however it was not clear if LPCAT and or PLA2 was responsible for the exchange. These results suggest that the lipid-handling enzymes of *C.tinctorius* are able to handle large amounts of unusual fatty acids, unlike *A.thaliana* and *B.napus*.

Reports have also shown that the synthesis of unusual fatty acids in the seed of several plants poses bottlenecks for other metabolic pathways, such as accumulation of oil. A recent paper illustrates the difficulty of assembling unusual fatty acids into TAG (Bates et al., 2014). The expression of a *R.communis FAH12* (fatty acid Δ12-hydroxylase) in *A.thaliana* seed for the synthesis of ricinoleic acid resulted in very low amounts of ricinoleic acid in seed oil (Broun and Somerville, 1997). The presence of ricinoleic acid in membrane phospholipids also presented bottlenecks for other native metabolic processes and overall seed oil reduced by 50% (Bates et al., 2014). In *R.communis,* >80% ricinoleic acid is present in seed oil due to the presence of specialised PDAT gene that preferentially transfers ricinoliec acid from phospholipids into oil (Kim et al., 2011). Furthermore, engineering *A.thaliana* with a combination of *RcPDAT* and *RcFAH12* resulted in an increased level of ricinoleic acid in seed oil (Kim et al., 2011). Bates et al. (2014) have also shown that inefficient glycerolipid synthesis in the ER is detected in plants, resulting in posttranscriptional down regulation of fatty acid synthesis in the plastid. This report implied that specialised accumulation pathways may be needed for the unusual fatty acids to be efficiently assembled into oil without creating penalties in oil content. These reports suggest that other specialised lipid-handling enzymes are required to engineer oilseed crops for the synthesis of LCPUFA in oil without the adverse effects on oil content and seed germination.

3.3.8 Metabolic engineering of B.napus *with the AA pathway co-expressed with V2 and p19*

The stable transformation of *B.napus* assisted in studying the effects of the seed-specific expression of V2 and p19 on the development of *B.napus* and performance of the transgenes over four generations. The results have shown that the expression of V2 and p19 was tolerated in *B.napus* and these plants did not have developmental abnormalities when compared with wild-type and No VSP expressing transgenic plants. There were a higher number of VSP-independent elite events that produced higher levels of ω-3 and ω-6 LCPUFA than in the No VSP elite events generated by Petrie et al. (2012a).

The results have also shown that *B.napus* accumulated a higher amount of intermediates of the AA pathway in seed oil. Although the VSP expressing plants did not contain very high levels of AA, the levels of total new products were higher in VSP expressing plants than in the control No VSP event. Overall, the expression of V2 and p19 resulted in elite events with approximately 30% LCPUFA, although the final end point was an intermediate and not AA in *B.napus*.

3.3.9 Comparing lipid fluxes in N.benthamiana *leaves,* A.thaliana *seeds and* B.napus *seeds*

It was interesting that the enzymes of the AA pathway behaved differently in *N.benthamiana* leaves and seeds of *A.thaliana* and *B.napus*. However, the major bottleneck observed in all three systems was due to desaturation by PsΔ8D. It was not clear whether the PsΔ8D was performing poorly in desaturating 20:2 or if other enzymes were competing for 20:2 and reducing its availability for PsΔ8D. The FAME analysis of *B.napus* and *A.thaliana* seeds expressing the various AA constructs showed that the levels of 20:2 were relatively higher than 20:4 in *B.napus* than in *A.thaliana*. It was assumed that PsΔ8D and PsΔ5D are membrane-bound desaturases which catalyse desaturation of fatty acids on the PC fraction, however no biochemical analyses were performed to confirm that PsΔ8D catalysed the desaturation of 20:2n6 and 20:3n3 on the PC head group.

The accumulation of the intermediate 20:2 in *B.napus* is interesting in comparison to *A.thaliana,* where this metabolic pathway continued to the AA endpoint. As elongation precedes desaturation, there is an assumed shuffling of metabolites from the CoA pool (for

elongation) back to the PC pool (for desaturation). It therefore seems that *B.napus*, which accumulates the elongation product 20:2, may be less metabolically capable than *A.thaliana* to move 20:2 from the CoA pool into the PC pool. This shuffling step could occur via *de novo* PC synthesis or directly via LPCAT activity. By either route, it seems that *B.napus* is less able than *A.thaliana* to move 20:2 from the CoA pool to the PC membranes. It is important to appreciate that *B.napus* is principally evolved in the generation of erucic acid (22:1), which requires two rounds of elongation in the CoA pool, while *A.thaliana* requires only one round of elongation for the production of gondoic acid (20:1). Perhaps there are subtle differences in the biochemistry of acyl shuffling in these closely-related plants that affect the production of AA.

Head group analysis of *N.benthamiana* leaves expressing IgΔ9E indicated that elongated products such as 20:2 were readily found on the PC membrane fractions, suggesting a ready movement of these lipids between soluble and membrane fractions. It is also plausible that other enzymes in *A.thaliana* and *B.napus* selectively remove 20:2 from PC – for example, PDAT activity (Bates et al., 2014) may transfer 20:2-PC into seed oil. Although *B.napus* and *A.thaliana* are both Brassicaceae, biochemistry of the lipid assembly pathways of the two are possibly different. Chapter 2 discussed the activity of LPCAT and other enzymes that might be involved in rapid exchange of acyl groups between the PC and the CoA lipid pools – the current results suggest that the set of enzymes involved in these processes in *N.benthamiana*, *A.thaliana* and *B.napus* are slightly different and result in different metabolic bottlenecks.

Overall, the observations during this study suggested that the biochemistries of the three plant species are very different in transportation of LCPUFA between the PC and CoA lipid pools. More detailed analysis of the materials generated in this study will be required to accurately determine the metabolic capability of leaf and oilseed tissues.

3.4 Conclusions

In conclusion, this study revealed that the seed-specific expression of V2 and p19 enhanced the performance of the AA pathway in *A.thaliana* and *B.napus*. These improvements were most evident in the T4 and T5 generations. Although the V2 and p19 *B.napus* lines did not contain very high levels of AA, the total new products were relatively more than the total new products extracted from the line not expressing a VSP. A higher number of elite events were generated with the pFN047 and pFN049 constructs than with the other constructs in both *A.thaliana* and *B.napus*. The generational study of the *A.thaliana* and *B.napus* transgenic events showed that VSPs are able to protect transgenes, possibly by avoiding sRNA-driven silencing pathways of the plant. The techniques used for measuring the lipid profile of seeds in each transgenic population were an indirect way of measuring transgene performance. The metabolites of the AA pathway provided strong evidence that seed-specific expression of V2 and p19 enhanced transgene performance without causing drastic developmental defects in model and crop plants.

This study also showed that the three systems used for the expression of the AA pathway have different biochemistries – LCPUFAs are handled differently in leaves of *N.benthamiana* and seeds of *A.thaliana* and *B.napus*. The introduction of VSPs assisted in enhancement of transgene performance, however bottlenecks (such as reduced amounts of oil in the seed and varied germination rates) were caused due to high levels of ω-3 and ω-6 LCPUFA.

3.5 Future work

This study provided a very detailed investigation of the performance of a transgenic pathway in five generations of *A.thaliana*. Although the level of AA did not decline in populations co-expressing the AA pathway with V2 or p19, the molecular basis of this phenomenon was not investigated. The following experiments may assist in investigating the molecular mechanism behind the inhibition of transgene silencing in V2 and p19 populations:

- Methylation analysis of the transgenic pathway – this analysis would clarify the silencing mechanisms adopted by the plant to silence the transgenes. The methylation studies of the entire genome may also determine if the methylation of the transgenes also carried on to silencing of the nearby endogenes.
- Expression analysis of each transgene – it is possible that parts of the T-DNA were inserted in the genome in slightly different ratios.
- Droplet Digital PCR analysis of transgene copy number – this analysis would determine whether high copy number events were targeted, triggering the silencing pathway sooner than the single copy events. Designing primers for amplification of all three transgenes may also determine if parts of the T-DNA were inserted in multiple locations in the genome. The presence of those genes inserted in more than one location might also trigger early silencing of the respective genes.
- Engineering the super high AA transgenic *A.thaliana* events with lipid-handling genes that are able to assemble AA into seed oil – this may require biochemical analysis involving various different DGAT and PDAT genes to assess which candidates are able to efficiently assemble LCPUFA into TAG.
- Engineering the super high AA transgenic *A.thaliana* events with lipases that are able to assist in production of energy during seed germination.
- Exposing the VSP expressing lines to several different pathogens to investigate if VSPs have compromised the defence of the plant.
- sRNA deep sequencing of a representative line from each 'No VSP', 'p19' and 'V2' populations to determine the sRNA populations generated against the transgenes.

This future work can be expected to enhance our current understanding of transgene behaviour in plants. Consequently, this knowledge could be applied to producing transgenic

events that are immune to RNA silencing pathways of the plant. The metabolic engineering of lipid pathways may further assist in generating lines that contain high levels of ω-3 and ω-6 LCPUFA with fewer effects on seed oil and germination.

3.6 Methods

3.6.1 Molecular cloning – Preparation of constructs

The fatty acid biosynthesis genes encoding the *Isochrysis galbana* Δ9-elongase (*IgΔ9E*) and the *Pavlova salina* Δ8-desaturase (*PsΔ8D*) and Δ5-desaturases (*PsΔ5D*) and the bacterial selection marker were obtained on a single DNA fragment from pJP3010 by digestion with *Pme*I and *Avr*II, giving rise to a 9560 bp fragment (Petrie et al., 2012a). The *IgΔ9E* coding region on this fragment was joined to an *A.thaliana* FAE1 promoter and a conlinin transcription termination/polyadenylation region (LuCnl2-3'). The desaturase coding regions were each joined to a truncated napin FP1 promoter (pBnFP1) and a *nos*3' transcription termination/polyadenylation region. The three fatty acid biosynthesis genes on this fragment were oriented and spaced in the same manner as in pJP107 (Petrie et al., 2012a) and encoded the same proteins as pJP107. The DNA fragment also comprised a FP1:GFiP:*nos*3' gene from pCW141 (WO2010/057246) which encoded a green fluorescent protein (GFP).

pCW162, pCW163 and pCW164 were digested with SwaI (blunt end) followed by gel clean-up. The linearised DNA was digested with AvrII and the fragment containing FP1:GFiP, FP1:VSP and bacterial selection marker was isolated from gel. pJP3010 was digested with PmeI (blunt end) and AvrII. The selection of the restriction enzyme cuts ensured that the two fragments were able to ligate in one direction. The 9560 bp of pJP3010 and ~8000 bp fragment of the VSP constructs were ligated (T4 DNA Ligase – Promega) and electroporated into DH5α. Positive colonies were confirmed by PCR and cultured overnight for vector mini-prep. Consequently, pFN045, pFN046 and pFN047 were prepared containing AA with either one of $P0^{PE}$, p38 or p19, respectively. Vectors were confirmed by restriction enzyme digestion. The pFN049 (V2) construct was prepared by digesting the FP1:$P0^{PE}$ fragment from pFN045 and ligating the backbone vector to FP1:V2. pCW195 and pCW197, containing FP1:V2 and 35S:V2 respectively, were digested with SacI and pFN045 was digested with AhdI. T4 DNA polymerase (Promega) was added to the restriction enzyme mixture (according to Promega protocol) to blunt the ends of digested fragments, which were then ligated. The constructs pFN048 and pFN049 were confirmed by PCR and restriction enzyme digestions. The digested pFN045 backbone without the FP1:$P0^{PE}$ was re-cirularised with DNA ligase to form pFN050 (No VSP) construct. Each of the VSPs was cloned under the expression

control of the FP1 promoter and *OCS*3' transcription termination/polyadenylation region. The only exception is in pFN048 construct, where the V2 coding region was under the control of the constitutive CaMV 35S promoter. The VSP gene in each case was within the T-DNA region of the constructs, adjacent to the right border of the T-DNA. Each of the six constructs comprised an *NPT*II selectable marker gene within the T-DNA and adjacent to the left border of the T-DNA. All of the constructs had an *RK2* origin of replication for maintenance of the plasmids in *A.tumefaciens*. The newly prepared vectors were electroporated into GV3101 strain of *A.tumefaciens* for transient assay and stable transformation of *A.thaliana*.

3.6.2 Transformation of A.thaliana *with the VSP and AA constructs*

To transform the genotype MC49 of *A.thaliana*, a *fad3/fae1* double mutant with high linoleic acid levels in its seed lipid, plants were treated by the floral dip method (Clough and Bent, 1998). The constructs were transformed into *A.tumefaciens* strain GV3101 for the transfer of T-DNA. The treated plants were grown to maturity and T1 seeds harvested from them were plated on MS media containing kanamycin, in order to select for transformed T1 plants. Screening for GFP expression in the seed was also used as a visual marker for transformed T1 seeds. The seedlings that survived on MS media containing 50 mgL^{-1} of kanamycin or which were obtained from GFP-positive seeds were transferred to soil and grown to maturity for T2 seeds.

3.6.3 Segregation analysis and plant growth conditions

Segregation analysis was also carried out for each individual event by growing 60-70 seeds from each event on MS media containing 50 mgL^{-1} of kanamycin. Six positive seedlings from each event were transferred to soil and grown to maturity.

Plants were grown with a 8/16 hr (light/dark) photoperiod in 24^{o}C. The *A.thaliana* plants generated during this study were grown in the same growth room with unchanged conditions throughout the two-year period.

3.6.4 Transformation of B.napus *using tissue culture*

The transformation of *B.napus* with the various AA constructs was performed by Dr Srinivas Belide's team at CSIRO Plant Industry. The following protocol was used by Belide team for transformation of *B.napus*:

B.napus (cultivar Oscar) seeds were sterilised using chlorine gas, as described by Kereszt et al. (2007). Sterilised seeds were germinated on half-strength MS media (Murashige and Skoog, 1962) with 0.8% agar, pH 5.8 and grown at 24°C under fluorescent lighting (50 µE/m2s) with a 16/8 hr (light/dark) photoperiod for 6–7 days. Cotyledonary petioles with 2–4 mm stalk were aseptically isolated from seedlings and used as explants. *A.tumefaciens* strain AGL1 was transformed with all the binary plasmids, namely pJP3025, pFN047 and pFN049.

Cultures were inoculated using single colonies (fresh plates) in 10 mL of LB medium with appropriate antibiotics and grown overnight at 28^{o}C with agitation of 150 rpm. The bacterial cells were put through centrifugation at 4000 rpm for 5 mins, washed with MS media (2% sucrose), re-suspended in 10 mL of MS media (2% sucrose) and grown for 4 hours with the addition of appropriate antibiotics and 100 µM acetosyringone (Belide et al., 2011). Two hours prior to infection, spermidine was added to a final concentration of 1.5 mM and the final density of the bacteria adjusted to $OD_{600\ nm}$ = 0.4 with fresh MS media (2% sucrose).

Freshly-isolated cotyledonary petioles were infected with 20 mL of *A.tumefaciens* culture(s) for 6 minutes. The petioles were then blotted on sterile filter paper to remove excess *A.tumefaciens* and transferred to co-cultivation media (MS with 1 mgL^{-1} TDZ, 0.1 mgL^{-1} NAA, 100 µM acetosyringone supplemented with 50 mgL^{-1} L-cysteine, 15 mgL^{-1} ascorbic acid and 250 mgL^{-1} MES). All plates were sealed with micropore tape and incubated in the dark at 24^{o}C for 48 hrs. The co-cultivated explants (cotyledonary petioles) were transferred to pre-selection media (MS with 1 mgL^{-1} TDZ, 0.1 mgL^{-1} NAA, 3 mgL^{-1} AgNO3, 250 mgL^{-1} cefotaxime and 50 mgL^{-1} timentin) and cultured for 4–5 days at 24^{o}C with a 16/8 hr (light/dark) photoperiod. The explants were then transferred to selection media (MS with 1 mgL^{-1} TDZ, 0.1 mgL^{-1} NAA, 3 mgL^{-1} AgNO3, 250 mgL^{-1} cefotaxime and 50 mgL^{-1} timentin and 40 mgL^{-1} kanamycin) and cultured for 4 weeks at 24^{o}C with 16/8 hr (light/dark) photoperiod. Explants with green callus were transferred to shoot regeneration media (MS media with 0.5 mgL^{-1} Kinetin, 3 mgL^{-1} AgNO3, 250 mgL^{-1} cefotaxime, 50 mgL^{-1} timentin and 40 mgL^{-1} kanamycin) and cultured for another 2 weeks. Small regenerating shoot buds were transferred to hormone free MS media (MS with 3 mgL^{-1} AgNO3, 250 mgL^{-1} cefotaxime, 50 mgL^{-1} timentin and 40 mgL^{-1} kanamycin) and cultured for another 2–3 weeks.

Potential transgenic shoots (>1.5 cm) were isolated and subcultured on MS media with increased concentration of kanamycin (50 mgL^{-1} kanamycin, 0.5 mgL^{-1} GA3, 3 mgL^{-1} AgNO3, 250 mgL^{-1} cefotaxime and 50 mgL^{-1} timentin) for another 2–3 weeks. Surviving shoots were transferred to root induction media (MS media with 50 mgL^{-1} kanamycin, 0.5 mgL^{-1}, NAA, 3 mgL^{-1} AgNO3, 250 mgL^{-1} cefotaxime and 50 mgL^{-1} timentin) and cultured for 2–3 weeks. Transgenic plants were then transferred to glasshouse and established on soil. Plants were grown under a photoperiod of 16/8 hrs (light/dark) at 22±2°C.

3.6.5 Lipid analyses

The methods for various different lipid analyses performed during this study were conducted in consultation with Dr Pushkar Shrestha. Approximately 100 pooled seeds of transgenic *A.thaliana* were taken from each transformed plant for the determination of seed lipid composition. Lipids were extracted with 750 µl of MeOH:HCl:DCM (dichloromethane) (10:1:1) containing 2 µg of internal standard (17:0). Samples were heated at 80^{o}C for 2 hrs. After cooling, 300 µl of MQ water and 500 µl of Hexane:DCM (4:1) was added to each sample, which was then vortexed and layers allowed to separate. In most cases it was not necessary to centrifuge. The top organic layer was extracted into a clean vial and evaporated under N_2 gas, and FAME eluted in 200 µl of hexane. The GC machine described in Chapter 2 was used for the analysis of samples (Wood et al., 2009). Each run included a freshly diluted NuCheck 411 standard, which was used for normalisation of FAME profiles. For the quantification of oil, 100 mg of seeds were weighed using a sensitive balance. The addition of a known amount of internal standard (17:0-TAG) and seed mass were used to calculate amount of oil/mg of seed.

The lipid analyses of *B.napus* seeds were performed. 100 mg of seeds were weighed and total lipids extracted using the Bligh & Dyer method (Bligh and Dyer, 1959) with slight modifications. The seeds were homogenised in 300 µl MeOH and 600 µl of $CHCl_3$ using tissue lyser. 90 µl of the homogenate was transferred to a 2 mL Agilent vial. The liquid contents of the sample were evaporated under N_2 gas. 750 µl of MeOH:HCl:DCM (10:1:1) and 10 µg of internal standard (17:0) added to each sample and heated for 2 hrs at 80^{o}C. After cooling the samples to room temperature, 300 µl of 0.1 % NaCl solution and 600 µl of Hexane:DCM (4:1) was added to each sample, vortexed and the top organic layer transferred to a clean vial. The sample was eluted in 600 µl of hexane.

The lipid analysis of the half cotyledon of *B.napus* involved harvest of half cotyledon – the cotyledons were harvested before they turned green. 750 µl of MeOH:HCl:DCM (10:1:1) and 10 µg of internal standard (17:0) was added directly to each cotyledon sample and heated for 2 hrs at 80^{o}C. After cooling the samples to room temperature, 300 µl of 0.1 % NaCl solution and 500 µl of Hexane:DCM (4:1) was added to each sample, vortexed and the top organic layer transferred to a clean vial. The transferred phase was evaporated under N_2 gas and FAME eluted in 500 µl of hexane. FAME was analysed as previously described (Wood et al., 2009).

3.6.6 Generation of progeny plots and box-whisker plots using R

The data presentation plots using R Studio (open source software available at http://www.rstudio.com/) were prepared with the assistance of Dr Alex Whan. Refer to instructions online for the use of R studio.

Prior to loading data files the following packages were run:

- reshape2
- ggplot2
- lattice

The command lines run in R Studio in order to generate representative progeny plots, box-whisker plots and dot-plots are given in the following section.

3.6.6.1 Progeny plot using csv file named V2F.csv

```
V2F <- read.csv("V2F.csv")
names(V2F)
progeny_dat <- function(raw.dat, variable, ID, Generation) {
 raw.dat$Parents <- sub("(.+)-[0-9]+$", "\\1", raw.dat[,ID])
 raw.dat$Parents[-grep("-", raw.dat$Parents)] <- NA
 raw.dat$Event <- sub("([a-zA-Z0-9]+\\-[0-9]{2}).+", "\\1", raw.dat[,ID])
 holder <- data.frame(Parent = sub("(.+)-[0-9]+$", "\\1", raw.dat[,ID]), Line = raw.dat[,ID])
 holder$Parent[-grep("-", raw.dat$Parents)] <- NA
 holder2 <- merge(holder, raw.dat[,c(variable, ID)], by.x = "Parent", by.y = ID)
 index <- grep(variable, names(holder2))
 names(holder2)[index] <- paste0(names(holder2)[index], "_Parent")
```

```
 clean.dat <- merge(raw.dat, holder2, all = T)
 dat.m <- melt(clean.dat[,c(ID, variable, Generation, "Event", "Parent", names(holder2)[index])])
 dat.m$gen <- as.numeric(sub("T", "", dat.m[,Generation]))
 dat.m$gen[grep("Parent", dat.m$variable)] <- dat.m$gen[grep("Parent", dat.m$variable)]-1
 dat.m$gen[dat.m$gen == 1] <- NA
 p <- ggplot(dat.m, aes(gen, value))
 p <- p + geom_line(aes_string(group=ID, colour = "Event"))
 return(list(plot = p, data = dat.m))
}
V2F.f <- progeny_dat(V2F, "C20_4", "Line", "Generation")
V2F.f$plot+ facet_wrap(~Event)+labs(x="V2 Generations",y="Relative % 20:4-FAME in A.thaliana seed")+scale_y_continuous(limits=c(0,40))
V2F.pl <- V2E.f$data
```

3.6.6.2 Plotting box-whisker plot for csv file named T5.csv

```
df1<-read.csv("T5.csv")
str(df1)
df2<-melt(df1)
str(df2)
df2$Population<-ordered(df2$Population,levels=c("1023T3","1023T4","Con","No VSP","p19","V2","35S:V2","P0","p38"))
p1<-ggplot(df2,aes(Population,value))+geom_point(position="jitter",aes(colour=variable))+facet_wrap(facets="variable")
p1
p2<-ggplot(df2[df2$variable%in%c("C20_4"),],aes(Population,value))+geom_point(position="jitter",aes(colour=Population),size=2)+facet_wrap(nrow=1,facets="variable")+theme_bw(base_size = 20)+scale_y_continuous(limits=c(0,40))
p2<-p2+labs(x="T5 Population",y="Relative % FAME in A.thaliana seed")
p2
p3<-p2+geom_boxplot(alpha=0.5)
p3
```

3.6.6.3 Plotting dot plot for csv file named Canola T2 Seedlings.csv

```
df1<-read.csv("Canola T2 Seedlings.csv")

str(df1)

df2<-melt(df1)

str(df2)

df2$Population<-ordered(df2$Population,levels=c("p19","V2"))

p1<-
ggplot(df2,aes(Population,value))+geom_point(position="jitter",aes(colour=variable))+facet
_wrap(facets="variable")

p1

p2<-
ggplot(df2[df2$variable%in%c("C20_2n6","C20_4n6","C20_3n3","New_Prod"),],aes(Populat
ion,value))+geom_point(position="jitter",aes(colour=Population),size=3)+facet_wrap(nrow=
1,facets="variable")+theme_bw(base_size = 20)

p2<-p2+labs(x="B.napus T2 population",y="Relative % FAME in B.napus half cotyledon")

p2
```

3.6.7 Other analyses

Western blot and transient assays were also performed, as previously described in Chapter 2.

Chapter 4 Characterisation of the V2 protein

4.1 Introduction

The results presented in previous chapters showed that V2 allowed simultaneous overexpression of transgenes and silencing of endogenes in the transient assay as well as prolonged overexpression of a transgenic pathway in five generations of transgenic *A.thalina*. A deep understanding of the effect of V2 on the silencing machinery of the plant may therefore further assist in enhanced metabolic engineering of plants. Existing reports have shown that V2 disrupts the RDR6- and SGS3-driven RNA silencing pathways (Glick et al., 2008). This chapter investigates the role of V2 in suppressing the RNA silencing mechanisms of the plant by addressing the following questions:

- Does V2 have an effect on the processing of hpRNA and amiRNA in *A.thaliana*?
- What techniques are best suited in quantifying V2 protein?

4.2 Results

4.2.1 The effect of V2 on the processing of hpRNA targeting the activity of Chalcone synthase in A.thaliana

Based on literature findings and results presented in Chapters 2 and 3, a key assumption has been made that V2 does not interfere with the processing of hpRNA when stably transformed in *A.thaliana*. To test this hypothesis, a transgenic *A.thaliana* Col-0 line expressing a hpRNA targeting chalcone synthase (CHS) activity, referred to as hpAtCHS, (Wesley et al., 2001) was selected for super transformation with V2. The seeds of the hpAtCHS line have a transparent seed coat (referred to as white in this chapter). The hairpin against *CHS* is driven by the CaMV 35S promoter, therefore a binary construct of V2 driven by the CaMV 35S promoter, referred to as 35S:V2 (pCW197), was used for super transformation of the hpAtCHS line. This line was also super transformed with p19 driven by the FP1 promoter, referred to as FP1:p19 (pCW164), to generate a number of control transformants. Based on literature findings and results presented in previous chapters, this study hypothesised that the expression of 35S:V2 and FP1:p19 does not interfere with silencing effect of hpAtCHS.

The super transformation of hpAtCHS with 35S:V2 construct generated 20 T1 events. No brown seeds were observed during T1 selection – this is because seed coats are derived from transgenic maternal material not assessable in T1 generation. These independent events were then propagated to generate T2 seeds. The 35S:V2 T2 events generated a mix of seed coat colours ranging between white (hpAtCHS) and brown (wild-type Col-0). Table 4.1 presents a list of the independent events and the associated seed coat colours. The super transformation events produced seeds that were white (25%), light brown (15%), brown (55%) and mix of both colours (5%). The seeds of control T2 events (hpAtCHS/FP1:p19) appeared white (Table 4.1).

Line	Seed-coat colour
hpCHS	White
FP1:p19-01	White
FP1:p19-02	White
FP1:p19-03	White
FP1:p19-04	White
35S:V2-01	Light brown
35S:V2-02	Brown
35S:V2-03	Light brown
35S:V2-04	Brown
35S:V2-05	Brown
35S:V2-06	White
35S:V2-07	Brown
35S:V2-08	White
35S:V2-09	Brown
35S:V2-10	Brown
35S:V2-11	Brown
35S:V2-12	Brown
35S:V2-13	White
35S:V2-14	Mix of white and brown
35S:V2-15	White
35S:V2-16	Light brown
35S:V2-17	Brown
35S:V2-18	Brown
35S:V2-19	White
35S:V2-20	Brown

Table 4.1. The effect of constitutive expression of V2 on the seed coat colour of *A.thaliana* expressing hpAtCHS.

A.thaliana plants silenced for CHS activity were super transformed with 35S:V2 resulting in a number of seed colours outlined in this table. hpAtCHS plants were also super transformed with FP1:p19 to produce a number of control lines where the seed coat colour was not affected.

4.2.2 The effect of V2 and p19 on a polycistronic artificial miRNA stably transformed in A.thaliana

The unexpected finding that V2 interfered with the processing of hpAtCHS in *A.thaliana* prompted me to investigate the effect of V2 on the processing of a polycistronic artificial miRNA (amiRNA). Plants process hpRNA and miRNA in different ways (Eamens et al., 2008) and this study hypothesised that V2 has no effect on the efficiency of amiRNA in silencing the targeted gene(s).

A transgenic line of *A.thaliana* expressing a polycistronic amiRNA was used to study the effect of V2 on the amiRNA. The polycistronic amiRNA was designed to target and silence *AtFATB*, *AtFAD2* and *AtFAE1* (Belide et al., 2014). The *Oryza sativa* gene encoding for miR395 was cloned and the first three stem loops were modified to contain 21mer sequences to silence three lipid biosynthesis genes (Belide et al., 2014). The modified gene (stem loop with 21mer targeting either *AtFATB*, *AtFAD2* or *AtFAE1*) was inserted into the binary vector FP1-pORE04 (the original pORE04 vector modified to contain the FP1 promoter) for seed specific silencing of *AtFATB*, *AtFAD2* and *AtFAE1* (Belide et al., 2014). Refer to (Belide et al., 2012)) for a detailed explanation of how the 21mer sequences were selected for effective silencing of *AtFATB*, *AtFAD2* and *AtFAE1*. The schematic of the construct consisting of amiRNA is shown in Figure 4.2A (Belide et al., 2014). The resulting vector was referred to as pJP1094 and it contained the *NPTII* plant selection maker. The Col-0 ecotype of *A.thaliana* was transformed with pJP1094 and the resulting stable, single copy homozygous line was referred to as HX-13. HX-13 seeds contained relatively decreased levels of 16:0, 18:2 and 20:1 compared to the wild-type Col-0 seeds. The T3 progeny of HX-13 was kindly donated by Dr Srinivas Belide for this study.

HX-13 was super transformed with FP1:V2 (pFN059), 35S:V2 (pFN058) and FP1:p19 (pCW164). The V2 and p19 binary constructs contained a FP1:GFP cassette and T1 super transformed events were selected using the GFP expression in T1 seeds (Fig 4.1B). A relatively large population of events was selected and taken to T2 – their respective seeds were photographed for GFP expression (Fig 4.1C) and analysed for changes in the fatty acid profile of seed oil (Fig 4.1D). It was expected that p19 driven by the FP1 promoter would reduce the efficiency of the amiRNAs in targeting the endogenes. There were 11, 10 and 11

independent transformation events that were generated for the FP1:p19, 35S:V2 and FP1:V2 constructs respectively.

The control HX-13 seeds had no GFP expression (Fig 4.1C, i) while the T2 VSP-expressing seeds showed a varying level of GFP expression (Fig 4.1C, ii–iv). The GFP expression in seeds was scored out of 3, where 0 referred to seeds expressing no GFP and 3 to seeds showing the highest level of GFP expression (Fig 4.1C, 4.1D). Events that did not express GFP were treated as HX-13 controls. In a number of cases, the lipid data coincided with the GFP expression, suggesting that high GFP-expressing lines also showed an impairment in silencing efficiency of the amiRNAs (Fig 4.1D). A number of high GFP-expressing lines contained very small seeds (Fig 4.1C, iv).

The HX-13 seeds contained 6.9%, 65.6% and 11.4% of 16:0, 18:1 and 20:1 respectively, compared to 8.6%, 14.8% and 17.8% measured in Col-0 seeds. Seed-specific expression of p19 resulted in an increase in 16:0- and 20:1-FAME and a decrease in 18:1-FAME, confirming that p19 was inhibiting the miRNAs from silencing the endogenes. The levels of 16:0, 18:1 and 20:1 measured in the seeds of FP1:p19 super transformants were similar to the levels measured in Col-0 seeds. There were three FP1:p19 lines that showed the highest levels of GFP expression and their seeds were smaller in size.

For simplicity of data presentation, the remainder of the observations are based on the changes measured in 18:1 levels. HX-13 and Col-0 contained 65.4% and 14.8% of 18:1 respectively. The lowest level of 18:1 (20.0%) was measured in FP1:p19-09 line, while the highest level (40.9%) was measured in FP1:p19-10 line. FP1:V2-03, FP1:V2-07 and FP1:V2-09 contained 43.0%, 43.4% and 35.6% of 18:1, similar to the levels measured in FP1:p19-10 line. The lowest level of 18:1 measured in 35S:V2 lines was 46.7%. There were ten V2 lines that contained >59% of 18:1, relatively close to the original HX-13 line. Expression of V2 did have an effect on the efficiency of amiRNAs, however the effect was not as evident as observed in the p19 events. Furthermore, no high GFP-expressing lines were scored in the V2 population.

A

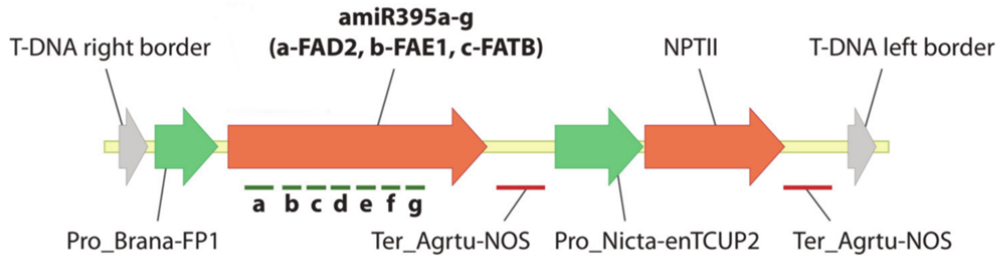
amiR395a-g
(a-FAD2, b-FAE1, c-FATB)
T-DNA right border
NPTII
T-DNA left border
a b c d e f g
Pro_Brana-FP1
Ter_Agrtu-NOS
Pro_Nicta-enTCUP2
Ter_Agrtu-NOS

B

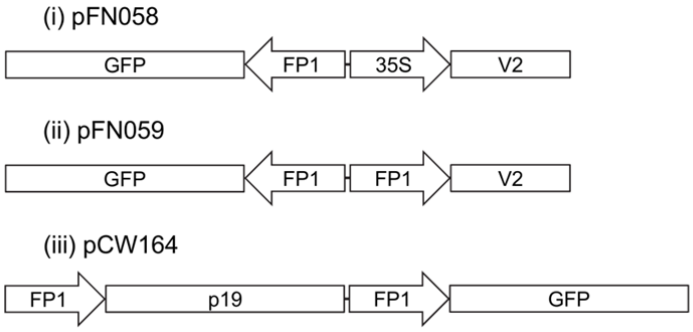
(i) pFN058
GFP
FP1
35S
V2
(ii) pFN059
GFP
FP1
FP1
V2
(iii) pCW164
FP1
p19
FP1
GFP

C

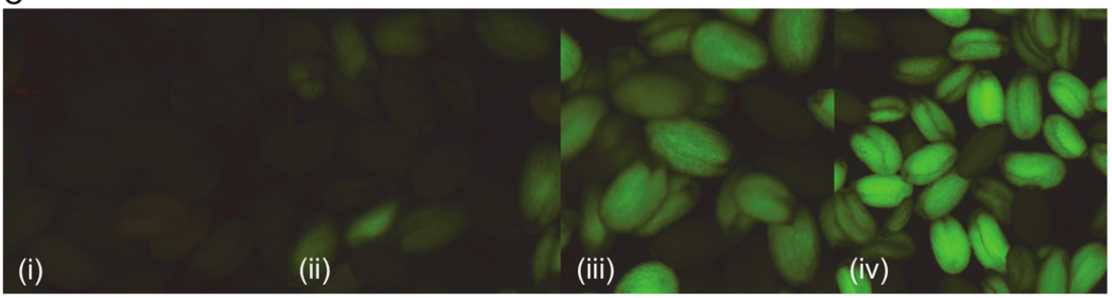
(i)
(ii)
(iii)
(iv)

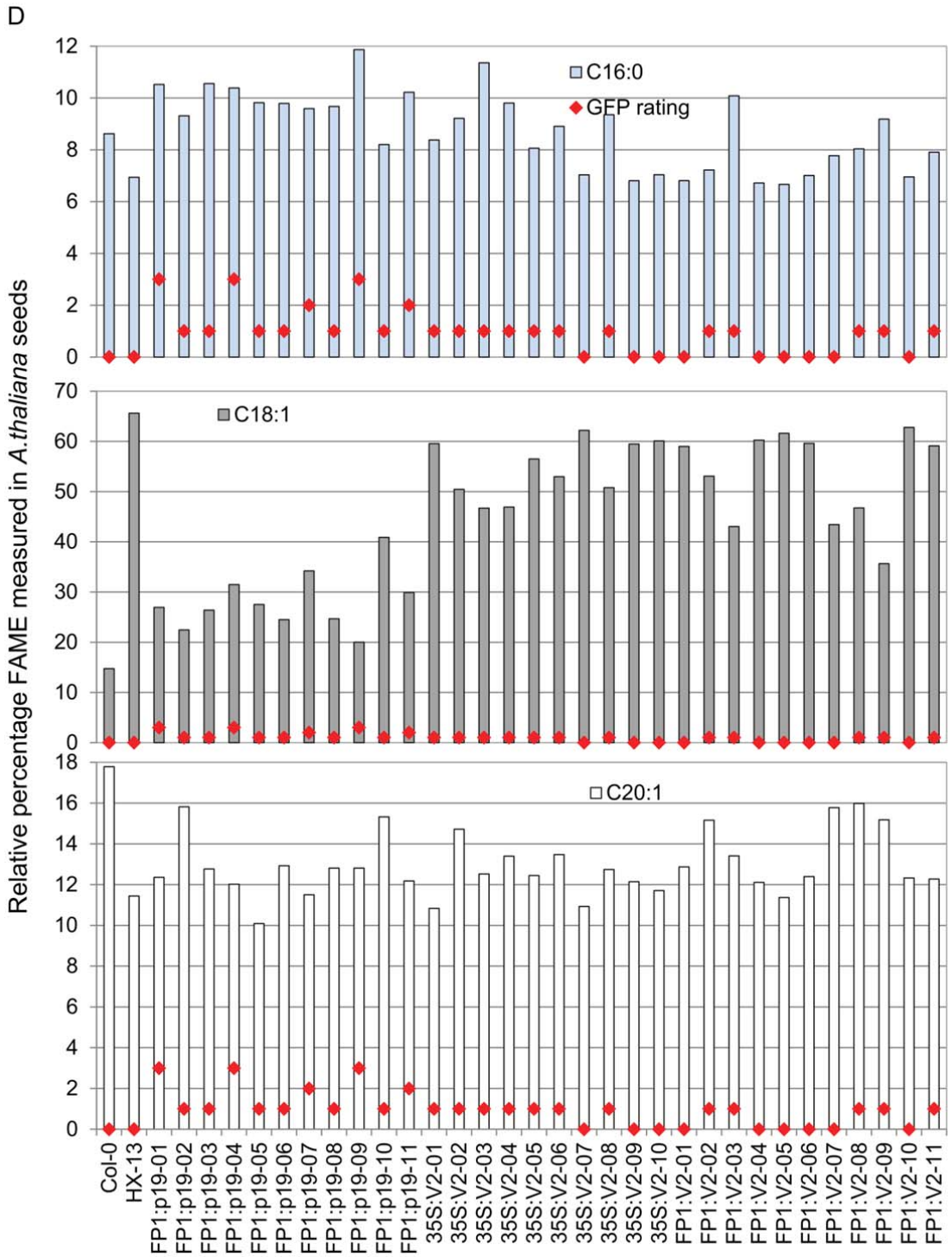

Figure 4.1. The effect of V2 and p19 on the processing of a polycistronic miRNA targeting three endogenes in *A.thaliana*.

A. Schematic of the T-DNA of the polycistronic amiRNA construct, adopted from Belide *et al*. (2014). The *Oryza sativa* gene encoding for miR395 was cloned and the first three stem loops were modified to contain 21mer

sequences targeting: *AtFATB*, *AtFAD2* or *AtFAE1* (Belide et al., 2014). amiRNA was driven by the FP1 promoter and terminated by NOS terminator.

B. Schematic of T-DNA binary constructs containing the VSPs V2 and p19 prepared for stable transformation of *A.thaliana*. The constructs were used for super transformation of *A.thaliana* expressing a polycistronic amiRNA driven by the FP1 promoter targeting *AtFATB*, *AtFAD2* and *AtFAE1*. GFP driven by the FP1 promoter was added to the constructs to act as visual marker and aid in selection of super transformants.

C. Images of T2 *A.thaliana* seeds expressing the polycistronic amiRNA, GFP and a VSP. The images: (i) Col-0 seeds expressing amiRNA, HX-13 (ii, iii) a mix of GFP and non-GFP seeds, (iv) high expressing GFP line.

D. The 16:0-, 18:1- and 20:1-FAME extracted from T2 seeds of *A.thaliana* expressing the amiRNA with p19 or V2.

4.2.3 Assessing the suppressor activity of V2 and p19 tagged with 6xHA

Results in this chapter show that V2 might have had an effect on the efficacy of hpRNA and amiRNAs in targeting endogenes in *A.thaliana*. It is also possible that the V2 transgene was silenced, which could be determined by quantification of the V2 protein in the super transformation events, however there are no commercially-generated antibodies against V2.

Previous work has shown that a HA tag fused to the C-terminus of p19 did not have an effect on its suppressor activity (Chapman et al., 2004). In this study, the stop codon of both V2 and p19 were removed and their C-termini were fused to 6xHA tag. The genes were driven by the CaMV 35S promoter in a binary construct (Fig 4.2A).

The suppressor activities of V2 and p19 were tested by infiltrating *N.benthamiana* leaves with combinations of V2-HA, p19-HA, GFP, hpGFP, V2 and p19. A representative leaf was photographed for 6 consecutive dpi and tissue was extracted at 4 dpi for total protein analysis. The images (Fig 4.2B) show 5 dpi that V2 enabled higher GFP overexpression than V2-HA (confirmed by Western blot analysis using anti-GFP antibodies; Fig 4.2D), but the difference was relatively small. Similarly, the images comparing the effects of p19 and p19-HA on the overexpression of GFP have shown 5 dpi that the accumulation of GFP was less in the spot infiltrated with GFP and p19-HA compared to the spot infiltrated with GFP and p19 (Fig 4.2C), and that GFP is silenced by the hpGFP in the spot infiltrated with p19-HA (Fig 4.2C). These results suggest that the addition of 6xHA to V2 and p19 does not impair the suppressor activity of the VSPs in leaves for up to 4 dpi, but that a difference becomes obvious at 5 dpi. The leaf spot infiltrated with p19-HA, GFP and hpGFP showed that GFP was silenced (Fig 4.2C) – Western blot analysis (using anti-GFP antibodies; Fig 4.2D) of infiltrated leaf tissue confirmed this observation.

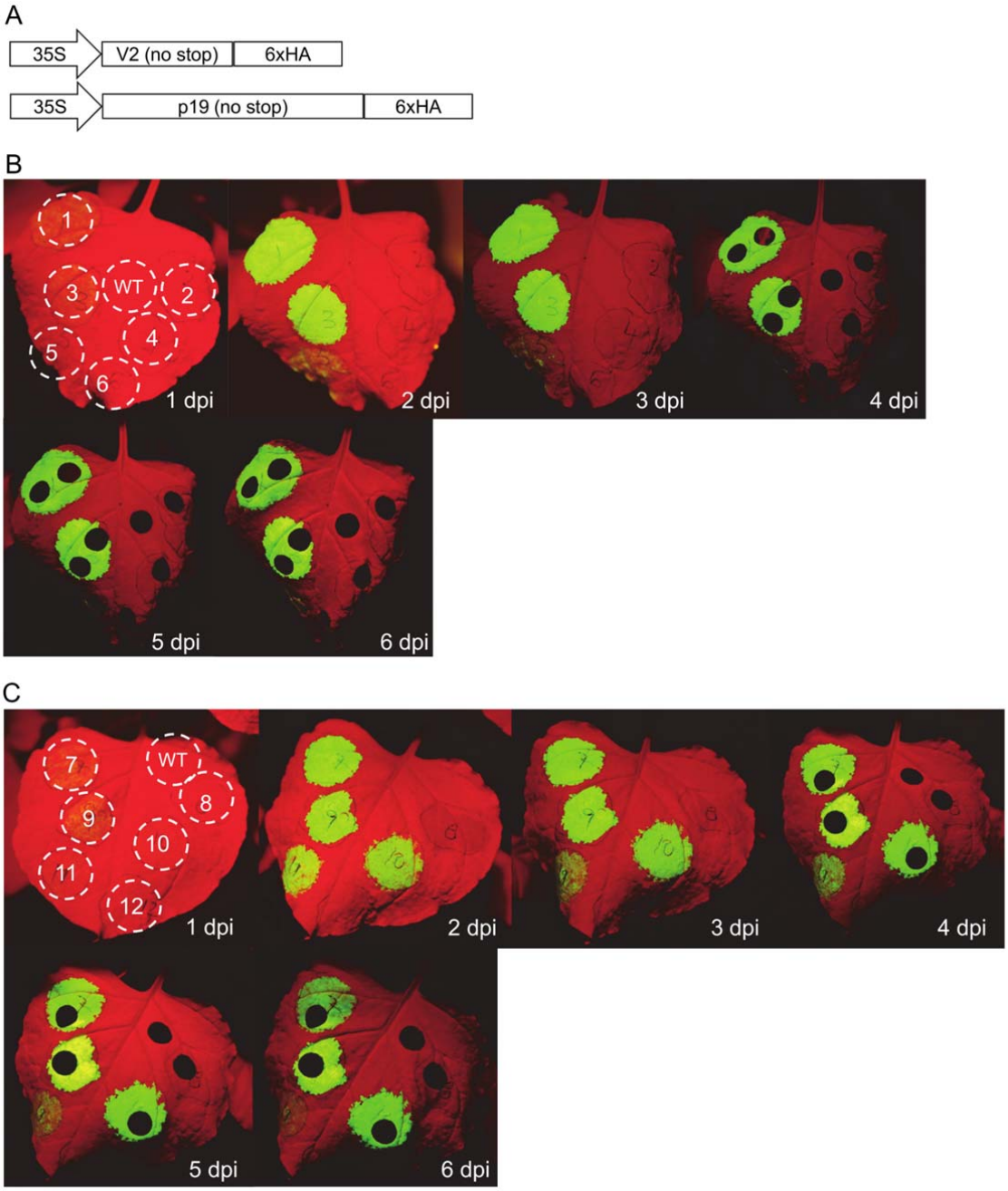
A
35S
V2 (no stop)
6xHA
35S
p19 (no stop)
6xHA
B
1
WT
2
3
4
5
6
1 dpi
2 dpi
3 dpi
4 dpi
5 dpi
6 dpi
C
7
WT
8
9
10
11
12
1 dpi
2 dpi
3 dpi
4 dpi
5 dpi
6 dpi

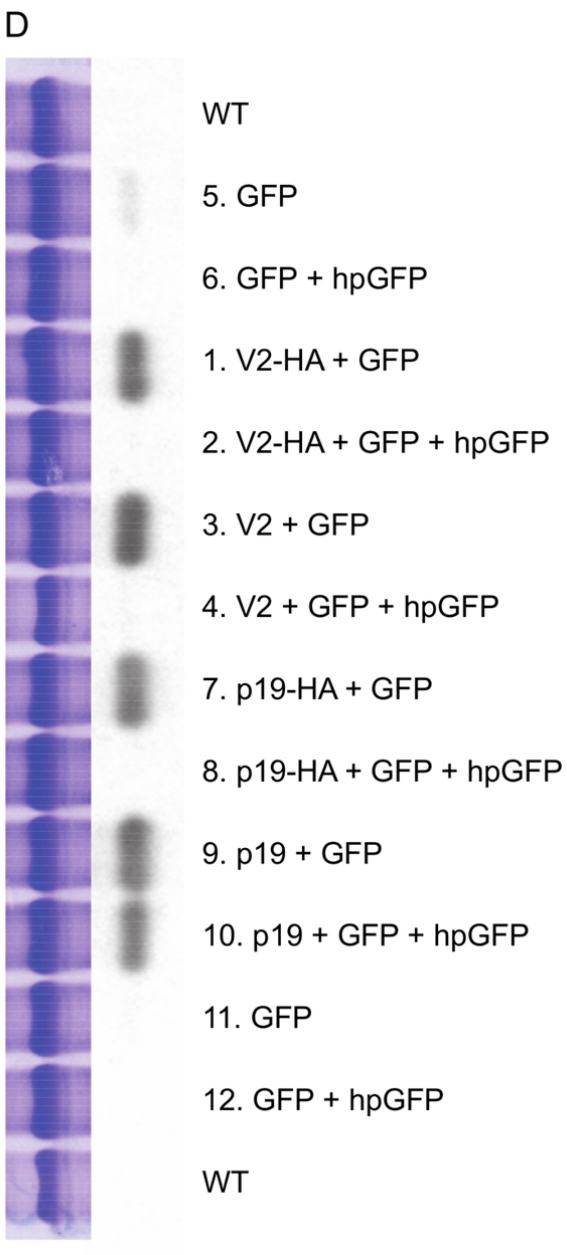

Figure 4.2. The protein analysis of HA epitope tagged V2 and p19.

A. Schematic of T-DNA binary constructs prepared for leaf expression of the V2 and p19 containing a 6xHA epitope tag. Genes were driven by the CaMV 35S promoter.

B–C. Time course of GFP expression in *N.benthamiana* leaves infiltrated with combinations of GFP, hpGFP, V2, p19, V2-HA and p19-HA. Images show one representative leaf photographed daily 1–6 dpi, and the first image is used to indicate the placement of infiltration treatments.

D. Western blot analysis of total protein extracted from leaves shown in **B** and **C**.

B–C. The numbers on each dotted circle correspond to the infiltration treatment. The infiltration treatment number recognises the corresponding infiltrated leaf tissue used for Western blot.

4.2.4 Analysis of polyclonal antibodies generated for recognition of V2 protein

Previous results (section 4.2.3) showed that fusing a HA tag to the C-terminus of V2 impairs its suppressive activity and that a polyclonal antiserum specific for V2 would greatly aid further experiments to characterise its actions and interactions. For this reason, V2 antigen for antibody production was generated in bacteria using the expression vector pET14-b. The V2 ORF was then fused to a His tag at its N-terminus and a 6xHA epitope tag at its C-terminus (Fig 4.3A) and the construct transformed into Rosetta 2(DE3) cells. These cells were grown for 16 hrs in 10 mL of media. The media contained components that auto-induced the cells after a certain period of time (Overnight Express Autoinduction System, Novagen). The cells were pelleted by centrifugation and then lysed using BugBuster® Protein Extraction Reagent. The V2 protein is insoluble in BugBuster solution, so the soluble proteins were removed in several washes with BugBuster. The V2 protein was then injected into a rabbit (by staff at the South Australian Health & Medical Research Institute, Veterinary Services) and 50 mL of serum was collected 11 weeks after the first injection.

To test whether antibodies in the serum from the rabbit were able to specifically detect V2 protein in a plant system, they were used on total protein that had been extracted from *N.benthamiana* leaves transiently expressing V2. Leaves were infiltrated with combinations of V2, p19 and GFP and their total proteins were extracted 4 dpi and analysed by Western blot. Polyclonal antibodies against p19 (from a commercial source) were also used as a control. The ~25 kDa p19 protein and ~20 kDa V2 protein were readily detected by their respective antisera and neither serum gave other-sized bands (Fig 4.3B) – this shows that the anti-V2 antiserum is very specific and contains few or no antibodies that react non-specifically with *N.benthamiana* leaf proteins.

This serum will be a very useful tool for further work but unfortunately was not produced in time to be further used in the present study.

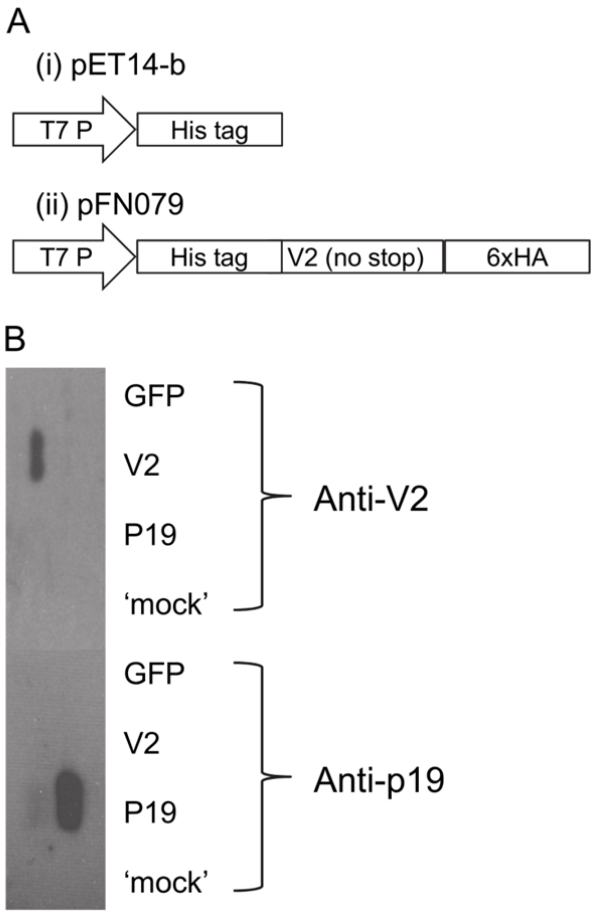

Figure 4.3. Detection of V2 protein using antibodies against V2.

A. Schematic of bacterial expression construct containing V2 fused with His and 6xHA epitope tags. The bacterial expression vector pET14-b was used for modification.

B. Western blot analysis of transient expression of V2 in *N.benthamiana* leaves. Leaves were infiltrated with combinations of V2, p19 and GFP. Leaf tissue harvested 4 dpi for total protein extraction. 'Mock' refers to leaf tissue infiltrated with empty AGL1 cells.

4.3 Discussion

The results presented in this chapter are preliminary molecular analyses to enhance the current understanding of the function of V2 in disrupting the RNA silencing pathways in plants. The results presented in Chapter 2 showed that V2 allowed simultaneous overexpression of transgenes and silencing of endogenes – based on these results it was proposed that V2 does not inhibit hpRNA- and amiRNA-driven silencing of genes in stably transformed *A.thaliana*. Some of the results presented in this chapter were expected regarding the effect of V2 on the processing of hpRNA and amiRNA in *A.thaliana* and these merit repeating for further investigation. The production of a polyclonal antibody for quantification of V2 protein in transgenic materials was also described, but was not generated in time to utilise fully.

4.3.1 The effect of V2 on the processing of a hpRNA and amiRNAs targeting various endogenes in A.thaliana

V2 has been proposed to disrupt the SGS3- and RDR6-driven production of secondary siRNA (Incarbone and Dunoyer, 2013). However, hpRNA and miRNA are not processed via this pathway (Eamens et al., 2008). The results in this chapter showed that the efficiency of hpAtCHS and amiRNAs reduced in lines super transformed with V2 – this may have been due to the co-suppression of the promoters driving V2, hpAtCHS and amiRNA.

This study generated a number of negative and positive control events by super transforming the hpAtCHS and HX-13 lines with FP1:p19. The hpAtCHS is a transgenic *A.thaliana* line that lacks CHS activity and displaying a transparent seed coat. Previous reports have shown that super transformation of hpAtCHS line with 35S:p19 resulted in events that produced dark seed coat colour (Dunoyer et al., 2004). The results in this chapter showed that the seed-specific expression of p19 did not impair the silencing efficacy of hpAtCHS and generated a number of negative controls to compare with the V2 super transformation events. Interestingly, constitutive expression of V2 in hpAtCHS resulted in a range of seed coat colours.

The polycistronic amiRNA in the HX-13 lines is driven by the FP1 promoter and super transformation with FP1:p19 resulted in inhibition of amiRNAs activity. The amiRNAs were designed to produce 21 nt miRNAs (Belide et al., 2014) and p19 was expected to bind to the

majority of amiRNAs (Silhavy et al., 2002), preventing them from loading into RISC. Interestingly, amiRNAs was less effective in a number of V2 lines as well. The FAME analysis of the transgenic seeds showed that the expression of V2 did not completely disrupt the silencing of endongenes driven by the polycistronic amiRNA.

The V2 results could be explained by considering silencing of the 35S promoters driving the hpAtCHS and V2 in the super transformation events – the introduction of a second T-DNA containing a 35S promoter into hpAtCHS perhaps resulted in silencing of the 35S promoter, driving both the hpRNA and V2. Daxinger et al. (2008) reported that the introduction of a second 35S promoter to *A.thaliana* already expressing a transgene driven by a 35S promoter resulted in methylation of the 35S promoters. The V2 constructs introduced into HX-13 contained at least one FP1 promoter (driving GFiP and V2) and this may have resulted in methylation of the FP1 promoters and a subsequent reduction in the silencing efficiency of the amiRNAs. This suggests that the super transformation events with reduced activity of hpAtCHS and amiRNA should contain very low levels of V2 protein, therefore a number of experiments were designed to quantify V2 in various transgenic lines.

4.3.2 The fusion of HA epitope tag to the C-terminus of V2

The most straight-forward technique to quantify V2 was based on fusing the HA epitope tag to V2 and using commercially-available antibodies against HA. However the results presented in this chapter showed that V2 lost its suppressive ability after HA was fused to its C-terminus. The addition of the HA tag to the C-terminus of p19 also changed the suppressive behaviour of p19 and, surprisingly, the new version of p19 inhibited co-suppression of GFP while allowing processing of hpGFP to silence to GFP. p19 could not stop all of the siRNAs from a hpGFP, but was able to bind to small amount of siRNAs for sense co-suppression of GFP before the amplification of the signal via the RDR6/SGS3 pathway. In effect, adding the HA to p19 rendered it about as effective as V2, in that it was not stopping majority of the siRNA generated by hpGFP, however it was still able to allow overexpression of transgenes by inhibiting transitivity. Another construct was prepared by fusing the HA tag to the N-terminus of p19, however, the suppressive behaviour of HA-p19 and p19-HA were equivalent in the transient leaf assay. Overall, these results showed that the addition of an epitope tag was not the ideal technique in quantifying V2 protein.

4.3.3 Production of polyclonal antibodies against V2

The next step to quantify V2 protein was based on generating antibodies against V2. A bacterial expression construct was prepared to generate antigen for downstream production of antibodies against V2. The polyclonal antibodies were able to recognise V2 in total protein extracted from *N.benthamiana* leaf tissue transiently transformed with V2. The analysis showed that this can be used as a tool to assist in unravelling the suppressive behaviour of V2. However, due to time constraints, no further analyses were performed.

4.4 Conclusion

In conclusion, the results presented in this chapter have shown that the polyclonal antibodies produced against V2 are able to assist in quantifying V2 protein in super transformed hpAtCHS and HX-13 lines. It is expected that future *in vivo* molecular and proteomic analyses of V2 protein may also result in discovery of other structures to which V2 binds during viral infection.

4.5 Future work

Future work may involve the following:

- Quantifying V2 protein in super transformed hpAtCHS and HX-13 lines to validate that the reduction in the efficiency of silencing molecules (hpRNA and amiRNAs) is due to methylation driven silencing of the transgenes.
- Preparation of antibodies against V2 may allow characterisation of V2 and the structures that interact or bind to V2. This *in vivo* analysis is expected to involve transient expression of V2 in *N.benthamiana* leaves and extraction of total protein 4 dpi. The total proteins would be separated using size exclusion chromatography. Western Blot analysis using antibodies against V2 would determine the size of the V2 protein complex (Wood et al., 2006). The information and antibodies could be used to pull down the V2 complex. The use of proteomic and sRNA deep sequencing techniques may further assist in determining structures that bind to V2.
- Verlaan *et al.* (2013) recently reported that wild tomato lines resistant to TYLCV encode for two alleles (*Ty-1* and *Ty-3*) that are highly homologous to *AtRDR3*, *AtRDR4* and *AtRDR5*. These alleles were discovered in *S.chilense*. It is postulated that Ty-1 and Ty-3 are substitutes of RDR6 and that the VSPs encoded by TYLCV do not interact with Ty-1 and Ty-3. A simple analysis to validate that V2 does not interact with Ty-1 and Ty-3 would involve transient overexpression of V2, GFP, Ty-1 and Ty-3 in *N.benthamiana* leaves. It is expected that Ty-1 and Ty-3 would substitute for the lost activity of NbRDR6 and allow co-suppression of GFP. A BLAST search of the *N.benthamiana* transcriptome may also assist in determining if AtRDR3, AtRDR4 and AtRDR5 homologs are expressed in *N.benthamiana* leaves.
- Lam *et al.* (2012) reported that SGS3 and RDR1 were involved in regulation of wax biosynthesis. SGS3 and RDR1 are involved in down-regulation of a key gene involved in wax biosynthesis in *A.thaliana*. It is possible that the wax content of stems of *A.thaliana* plants expressing V2 with the 35S promoter is different to the wild-type levels. Therefore, quantification of wax in the 35S:V2 and wild-type *A.thaliana* plants may confirm that V2 inhibits a SGS3 regulated pathway.

4.6 Methods

4.6.1 Preparation of plasmids

The two constructs containing a HA epitope tag, pFN053 (V2-HA) and pFN054 (p19-HA), were prepared by amplifying the V2 and p19 genes from pCW197 and pCW196, respectively. The entire coding regions of V2 and p19 were amplified excluding the stop codon. The fragments were placed into the TOPO cloning vector (pENTR/D-TOPO, Invitrogen™ life technologies) according to the manufacturer's protocol. LR Clonase II Enzyme Mix (Invitrogen™ life technologies) was used to set up a reaction between the TOPO vectors (pFN051 and pFN052) and pCH313 (contained 6xHA epitope tag) according to the manufacturer's protocol. The resulting constructs were electroporated into GV3101 strain of *A.tumefaciens* for infiltrations into *N.benthamiana* leaves. A third HA-p19 construct was also prepared by preparing a PCR product of 6xHA with a start codon and NotI flanking ends. HA was cloned from pFN053 using the Sense primer TTTTGCGGCCGCCGATTCGAGATGTATCCTTA and the Antisense primer TTTTGCGGCCGCCCCCGCGTATCCGGGCACGT. The PCR purified fragment was cloned into pGEM-T Easy vector and digested with NotI. This fragment was then ligated into the NotI digested pCW087 backbone vector (TOPO vector containing p19 open reading frame) generating pFN055. LR Clonase II Enzyme Mix (Invitrogen™ life technologies) was used to set up a reaction between pFN055 and pXRZ393 to generate HA-p19 vector (pFN056).

The two constructs prepared for super transformation of HX-13 lines were pFN058 (35S:V2) and pFN059 (FP1:V2). These were prepared by cloning the FP1:GFiP cassette from pCW141 into pCW197 and pCW195.

The construct prepared for bacterial expression of His-V2-HA required amplification of V2-HA from pFN053 with the Sense primer TTTCATATGTGGGATCCACTTCTAAATGA and Antisense primer TTTCTCGAGTCACCCCGCGTATCCGGGCA. The fragment ends contained NdeI and XhoI flanking ends. The fragment and the bacterial expression vector (pET14-b) were digested with NdeI and XhoI and ligated using T4 DNA Ligase (Promega) to generate pFN079 (His-V2-HA). The resulting construct was heat-shocked into Rosetta 2(DE3) (Novagen) according to the manufacturer's protocol.

4.6.2 Bacterial expression

10 mL of overnight express media (Overnight Express™ Autoinduction System 1, Novagen) was inoculated with Rosetta 2(DE3) cells harbouring pFN079 and the culture was grown overnight. 2 mL of turbid culture was centrifuged at 13000 *g* for 3 mins. Supernatant was discarded and another 2 mL of culture was added and centrifuged at 13000 *g* for 3 mins. This step was repeated until a large pellet remained from 10 mL of culture. The pellet was suspended in 900 µL of BugBuster (BugBuster® Protein Extraction Reagent). The slurry was left at RT for 20 mins and centrifuged at 13000 *g* for 3 mins. The supernatant was transferred to another tube and 600 µL of Bugbuster was added to the pellet and incubated at RT for 20 mins. The slurry was centrifuged at 13000 *g* for 3 mins and supernatant transferred to another tube. The pellet was re-suspended in 1 mL of BugBuster and incubated at RT for 10 mins. The slurry centrifuged at 13000 *g* for 3 mins and supernatant transferred to another tube. The pellet was dried in 20 mins using rotavap. The pellet weighed ~4 mg.

A speckle of the dry protein was re-suspended in 100 µL of 4% SDS. 100 µL of each supernatant recovered from the clean-up steps were also resuspended in in 100 µL of 4% SDS. The mixture was heated to 70^{o}C for 10 mins. 1X volume of 2X loading buffer was added to the mix and heated at 70^{o}C for 10 mins. The mix was then centrifuged at 13000 *g* for 3 mins and loaded on SDS-PAGE gel.

Chapter 5 Summary

5.1 General summaries

Since the commercialisation of genetically modified (GM) crops in 1996, a cumulative 1.5 billion hectares of land have been cultivated with GM crops in 2013 (James, 2013). This large increase is due to the benefits of GM crops, such as pest resistance and nutritional and industrial values. Genetic engineering of oil crops for the synthesis of novel fatty acids that have nutritional value (for example LCPUFA) or industrial value (for example DHSA) has great potential to enhance the breadth, quality and sustainability of agriculture. However, the production of a successful GM crop has many hurdles to overcome. The lipid biosynthesis pathways in plants are complex with a great deal of intra- and inter-pathway regulation. To rapidly capture and test the spectrum of possibilities for new oils and profiles that are now possible through transgenesis, with modified and non-host enzymes, requires a faster means of investigation than by stable transformation and conventional breeding. Also newly introduced transgenes can be unstable and lose their efficacy as the plant perceives them as foreign and shuts them down. The primary aims of this study were to develop a system for rapid manipulation of lipid biosynthesis and to investigate ways of maintaining transgene expression over time.

5.2 The transient modification of lipid pathways in *N.benthamiana* leaves

Various ways were found to enhance the transient assay in *N.benthamiana* leaves, facilitating elaborate modifications of lipid pathways to be achieved. These included the use of an alternative VSP, V2, which permits simultaneous hpRNA driven silencing of endogenes and overexpression of transgenes. The agro-infiltration assay was optimised by determining the size of hpRNA required for maximal gene silencing. The design of hpRNA constructs was validated for targeting multiple members of a gene family or to specifically target one gene. Transient silencing of endogenes was shown to be efficient with much lower concentrations of *A.tumefaciens* than commonly used, and while co-expression of a non-specific hpRNA allows overexpression of transgenes, co-infiltration of the transgene with a V2 construct gives maximal overexpression. The assay conditions described in this thesis are ideal for assembly of transgenic pathways for metabolic engineering of lipid pathways.

Other important aspects of this study included the discovery and characterisation of the *NbFAD2* gene family in *N.benthamiana*. Two of the family members (*NbFAD2.1* and *NbFAD2.2*) were effectively silenced with a long hpRNA (hpNbFAD2) targeting the conserved regions of *NbFAD2*. However comparing the lipid profile of leaves silenced with hpNbFAD2 with those silenced by hpRNA targeting the 3'UTR regions of *NbFAD2.1* and *NbFAD2.2* points towards the existence of a third NbFAD2. The hpRNA-mediated silencing techniques were applied to transient silencing of a number of other lipid modifying enzymes (NbSAD1, NbFAD3, NbFAD6 and NbFAD7). The leaf lipid profiles were in concordance with mutant studies in *A.thaliana*, although slight changes were observed in leaf lipid profile after the transient silencing of NbFATA, NbFATB, NbTGD1, NbLPCAT, NbGPAT and NbLPAAT.

The silencing of lipid-handling enzymes was combined with the assembly of transgenic pathways to trace the flux of transgenic metabolites. Silencing of *NbFAD2* was combined with the overexpression of GhCPFAS, AtFAE1 and AtDGAT1. High levels of 18:1 were shunted into a transgenic pathway for the synthesis of DHSA, a cyclopropanated fatty acid. This is the first study to report that GhCPFAS is able to convert leaf 18:1 into DHSA. It also shows that DHSA is readily available in the CoA pool, allowing AtDGAT1 to transfer DHSA into leaf oil and AtFAE1 to elongate it to eDHSA. These experiments showed that *N.benthamiana* leaves can be engineered to synthesise high levels of novel fatty acids. Furthermore, the system also showed the rapid movement and modification of fatty acids between the PC and CoA lipid pools. Identification of the *N.benthamiana* enzyme(s) responsible for the transfer of DHSA into the CoA pool would be of great benefit so that oilseed crops might be engineered to produce high levels of DHSA in seed oil.

Another transgenic system, involved the overexpression of IgΔ9E, was used to trace the flux of elongated products in different lipid fractions of the leaf cell. This revealed that large amounts of the IgΔ9E-elongated products were replacing PC lipids. This may have been due to leaf lipid handling enzymes that are efficient and selective for transferring LCPUFA between the CoA and PC lipid pools. The discovery of these enzymes is expected to assist in metabolic engineering of oilseed crops with exceptionally high levels of LCPUFA in oil.

5.3 Enhanced transgene expression in *A.thaliana* and *B.napus*

The major breakthrough presented in this thesis is that seed-specific expression of VSPs is able to enhance transgene overexpression. Seed-specific expression of V2 and p19 was combined with a three-gene transgenic pathway to synthesise arachidonic acid in the seed of *A.thaliana* and *B.napus*. The generational metabolite studies have indirectly shown that V2 and p19 were able to inhibit co-suppression-driven silencing of transgenes in both oilseeds. Large populations of transgenic lines created with the AA constructs showed that the lines expressing V2 or p19 performed relatively better for five generations compared to lines without a VSP. More importantly, a decreasing trend was obvious in the No VSP population, while the transgenic metabolites increased in the V2 and p19 populations.

Overall, the results showed that LCPUFA-handling enzymes in *A.thaliana* are very different to the ones active in *B.napus* during oil synthesis in the seed. However the p19 and V2 *B.napus* lines contained the highest level of total new products, suggesting that the addition of these genes is very beneficial in increasing levels of transgene product.

Chapter 6 Materials and Methods

6.1 Buffers and reagents used in this study

All media and solutions listed below were made in the appropriate volume in autoclaved MQ water and buffers were autoclaved unless otherwise stated.

Ampicillan (50 mg/mL, final volume = 20 mL, not autoclaved, filter sterilised)

- Ampicillin 1 g

Blotting buffer (pH 8.3, final volume = 1 L)

- Tris Base 3.02 g
- Glycine 14.4 g
- 99% Ethanol 200 mL

Dipping media (final volume = 1 L, not autoclaved)

- Sucrose 100 g
- Silwet 200 µL
- Acetosyringone (1 M) 1 mL
- Infiltration media 1 L

Gel Loading buffer 6X (final volume = 100 mL, not autoclaved)

- Sucrose (40% w/v) 40 g
- Bromophenol Blue (0.25% w/v) 250 mg
- TE Buffer, pH 8 50 mL

I-block (0.2%, final volume = 50 mL, heat required, not autoclaved)

- Skim milk powder 2.5 g
- TBST (fresh 1X solution) 50 mL

Infiltration media (pH 5.7 with 1 M NaOH, final volume = 1 L)

- MES (final concentration of 5 mM) 1 g
- MgSO4 ($MgSO_4.3H_2O$) (final concentration of 5 mM) 0.9 g

Kanamycin (50 mg/mL, final volume = 20 mL, not autoclaved, filter sterilised)

- Kanamycin 1 g

Luria-Bertani medium (LB), pH 7	
• Bacto-tryptone	1% (w/v)
• yeast extract	0.5% (w/v)
• NaCl	1% (w/v)
MS Macro 20X	
• NH_4NO3	33 g
• $CaCl_2.2H_2O$	8.8 g
• KNO_3	38 g
• $MgSO_4.7H_2O$	7.4 g
• KH_2PO_4	3.4 g
MS Micro (100X, 500 mL)	
• H_3BO_3	3.11 g
• $MnSO_4.4H_2O$	11.15 g
• $ZnSO_4.7H_2O$	4.3 g
• KI	415 mg
• $Na_2MoO_4.2H_2O$	125 mg
• $CuSO_4.5H_2O$	12.5 mg
• $CoCl_2.6H_2O$	12.5 g
MS iron (20 mM, 500 mL)	
• $FeCl_3.6H_2O$	2.7 g
MS EDTA (200X, 500 mL)	
• Na_2EDTA	3.36
MS Vitamins (100X, 100 mL)	
• Nicotinic acid	5 mg
• Pyridoxine	5 mg
• Thiamine HCl	1 mg
• Glycine	20 mg

Murashige and Skoog (MS) plant growth medium (pH 5.8, final volume = 1 L)

- Sucrose 20 g
- Myo Inositol 100 mg
- MS Macro 20X 50 mL
- MS Micro 100X 1 mL
- MS Iron 5 mL
- MS EDTA 5 mL
- MS Vitamins 10 mL
- Agar (Sigma, A7921) 8.4 g

Protein treatment buffer (2X, final volume = 1 mL, not autoclaved)

- 1 M Tris-Cl, pH 6.8 0.125 mL
- 10% SDS, 0.35 M 0.4 mL
- Glycerol 0.2 mL
- DTT (this should be added just prior to use) 31 mg
- dH2O To make 1 mL final
- Bromophenol Blue 0.02 g

Rifampicin (25 mg/mL, dissolved in AR methanol, final volume = 20 mL, not autoclaved, filter sterilised)

- Rifampicin 500 mg

Running buffer (10X, final volume = 1 L)

- Tris base 30.3 g
- Glycine 144 g
- SDS 10 g

SDS (10%, final volume = 400 mL)

- SDS powder (wear a mask when weighing) 40 g
- MQ H_2O (heated to 50^{o}C to dissolve SDS) 400 mL

Seed sterilisation solution (20% bleach, final volume = 100 mL, not autoclaved)

- Premium White King Bleach 20 L

Spectinomycin (50 mg/mL, final volume = 20 mL, not autoclaved, filter sterilised)

- Spectinomycin 1 g

TBS Buffer (10X, pH 7.4, final volume = 1 L)

- Tris base — 12.1 g
- NaCl — 87 g
- HCl — For pH adjustment

TBST (1X, final volume = 1 L, not autoclaved)

- TBS Buffer (10X, pH 7.4) — 100 mL
- Tween 20 — 5 mL

TE buffer (pH 8.0, final volume = 1 L)

- Tris-HCl buffer (100mM, pH 8.0) — 100.0 mL
- EDTA (0.5M, pH 8.0) — 2 mL

Timentin (200 mg/mL, final volume = 15 mL, not autoclaved, filter setrilised)

- Timentin — 3.1 g

Tris-borate buffer (TBE, 10X, final volume = 1 L, not autoclaved)

- Tris base — 54.0 g
- Boric base — 27.5 g
- EDTA (0.5M, pH 8.0) — 20 mL

Tris-HCl buffer (concentration = 100 mM, pH 8.0, final volume = 1 L)

- Tris base — 12.1 g

pH adjusted to 8.0 with concentrated HCl

Tris-HCl (concentration = 1 M, pH 6.8, final volume = 100 mL)

- Tris base — 12.10 g
- Conc. HCl — To adjust pH
- MQ H_2O — To final volume

Tris-HCl (concentration = 1.5 M, pH 8.8, final volume = 100 mL)

- Tris base — 17.17 g
- Conc. HCl — To adjust pH
- MQ H_2O — To final volume

6.2 General molecular biology techniques

6.2.1 Polymerase chain reaction (PCR)

A 10 µl PCR reaction mix was prepared using ThermoPol Taq DNA polymerase (NEB) with 200 µM dNTPs, 200 nM of each oligonucleotide primer and sufficient amounts of template or bacterial cells suspended in water. Thermal cycling was performed in a Mastercycler (Eppendorf) with an initial denaturation at 95°C for 2 minutes, 35 cycles of 94°C for 30 sec, 58°C (adjusted for each oligonucleotide primer pair) for 30 sec, 72°C for 1 min per kb of DNA, and a final extension of 5 mins at 72°C. In some cases a 'touch down' PCR was run where a high annealing temperature was used for the first PCR cycle following by a decrease of 0.5^{o}C in the consecutive 9 cycles. The remainder of the cycles (20–25) were run at 5^{o}C lower than the initial annealing temperature. Primers were designed using Vector NTI® software (Life Technologies™).

6.2.2 Agarose gel electrophoresis

For the detection and separation of 500 bp to 5 kb fragments of DNA a 1% agarose gel was prepared by melting agarose (Biotechnology grade, Amresco) in 1 x Tris Borate EDTA (TBE) buffer. Prior to gel casting 100 µg/L ethidium bromide (AppliChem) was added to the mix. DNA samples were mixed with gel loading buffer and electrophoresed in 1 x TBE typically at 100 V for 30–40 mins. DNA bands were visualised and photographed in a GelDoc XR imaging system (BioRad). For isolation of DNA fragment, gel piece was cut on a blue light box.

6.2.3 Molecular cloning of vectors in E.coli

In a number of cases the DNA fragments of interest were digested from other vectors. Restriction enzymes obtained from New England Biolabs (NEB) or Fermentas were used in the recommended concentrations and in the provided buffers. In most cases high fidelity restriction enzymes were used to reduce incubation times. The recommended incubation temperatures and times were used to ensure complete digestion of DNA fragments. Digested fragments were gel isolated and purified using a QIAquick Gel Extraction prior to ligation reactions.

PCR amplicons generated with the *PfuUltra*™ II Fusion HS DNA Polymerase (Agilent Technologies Inc.) using the recommended thermocycling conditions were recovered and cloned into pGEM-T Easy cloning vector (Promega) or directly into other cloning vectors. The

PCR amplicon generally contained A-tails to for direct ligation into pGEM-T Easy vector or the amplicon ends were designed to complement a restriction enzyme cut in the backbone vector. Klenow enzyme (2.5 U) was used for blunting of DNA fragements and SAP (1 U) to dephosphorylate the blunted ends.

Ligations were performed using 0.5 µL of T4 DNA ligase (Promega) in a 10 µl reaction mix and incubated overnight at 4^{o}C. Ligations were incubated for 2 hrs at room temperature when the rapid ligation buffer was used. In most cases a 3:1 molar ratio of insert:vector backbone was used. Ligated vectors were recovered by electroporation of DH5α (*E.coli* strain) and selected on LB media containing appropriate antibiotics. Colonies harbouring the desired vectors were screened by PCR. LB broth cultures were inoculated with the positive colony and incubated overnight in 5 mL volumes at 37^{o}C.

QIAprep Spin Miniprep Kit (QIAGEN) was used for the isolation of vector DNA from 4 mL *E.coli*. A further restriction enzyme digestion of the vector was used to verify the purified vector. A 0.75 mL *E.coli* culture of the verified vector was combined with 0.75 mL of glycerol and stored in -80^{o}C.

Various different regions of vectors were subsequently sequenced using BigDye chemistry and verified to match the sequence of the fragment in Vector NTI.

6.2.4 Electroporation of vectors into A.tumefaciens

The selected binary vectors were electroporated into either AGL1 or GV3101 strains of *A.tumefaciens*. Transformed colonies were recovered on LB media supplemented with rifampicin (25 mgL^{-1}) in addition to a selective agent corresponding to the resistance gene in the binary vector (Kanamycin 50 mgL^{-1} or Spectinomycin 100 mgL^{-1}) at 28°C overnight. Two recovered colonies were selected for inoculation of 5 mL LB broth, grown for 24 hrs (GV3101) or 48 hrs (AGL1) in 28^{o}C with shaking. 1 mL of this culture was combined with 1 mL of 50% glycerol and stored at -80°C for future work. The remaining culture was used for infiltration of *N.benthamiana* leaves.

6.2.5 Antibiotics

Antibiotics were prepared in sterile MQ water and filter sterilised using acrodisc (0.2 µm supor membrane). 18 mL syringe (slip lock fitting, Terumo) and 18 or 20 gauge needle

(Terumo) were used for the sterilisation process. Rifampicin was prepared in methanol. Aliquots of the stocks were stored in -20^{o}C.

6.3 Cultivars and plant growth conditions

Unless otherwise stated, Col-0 and MC49 were used in all *A.thaliana* related experiments. Seeds were sterilised in 20% bleach solution (Premium White King Bleach). Sterilisation process: seeds were shaken in 20% bleach solution for 20 mins, shaken in MQ water for 20 mins, the washing process in MQ water repeated 3 times. Upon completion, seeds were aseptically spread out onto 150 mm MS agar plates, which were stratified for 48 hours at 4^{o}C. Plates were then transferred to a controlled environment chamber (21^{o}C with 16 hrs light at 150 µmole/m2/sec and 8 hrs dark). In most cases, the antibiotic positive seedlings were counted to assist in segregation analysis of the respective line. Generally, three weeks after germination plant seedlings were either planted to soil under the same conditions described for germination of the seedlings. Seeds were sown on moist Plugger Custom soil mix (Debco).

6.3.1 Stable transformation of A.thaliana

10–15 *A.thaliana* plants (ecotype Col-0 and MC49) were grown on soil in 30 mm wide pots. The plants were grown until most plants were flowering and excess mature flowers were removed. 100 mL cultures of the desired *A.tumefaciens* harbouring vectors were grown for 24 hrs (GV3101) or 48 hrs (AGL1). Saturated *A.tumefaciens* cultures were centrifuged at 2000 *g* for 5 mins and resuspended in 400 mL dipping media. Unopened flower buds were dipped in this suspension and plants were wrapped in plastic cling-film overnight (Clough and Bent, 1998). Plants were then grown for another 4 weeks, dried and seeds collected.

6.3.2 Selection of positive transformants

Majority of the binary constructs contained the NPTII selection marker. The selection was performed on MS media supplemented with 50 mgL^{-1} kanamycin and 100 mgL^{-1} Timentin (to control bacterial growth).

6.3.3 GFP Imaging

Transgenic *A.thaliana* seeds were assessed for GFP expression under a stereo fluorescence microscope with heGFP filter set (SteREO Lumar V12, Zeiss, Germany).

6.4 *A.tumefaciens* infiltrations and *N.benthamiana* growth conditions

A.tumefaciens strains either AGL1 or GV3101 harbouring each binary vector was grown overnight at 28°C in LB broth supplemented with the appropriate antibiotics. Turbid cultures were supplemented with 100 µM acetosyringone and grown for a further 2 hrs. Cultures were centrifuged (4000 *g* for 5 min at room temperature) and gently resuspended in ~2 mL of infiltration buffer supplemented with 100 µM acetosyringone. A final combination of cultures was prepared so that each *A.tumefaciens* construct equalled $OD_{600\ nm}$ 0.2 unless otherwise stated. The final mixture of *A.tumefaciens* cells referred to as a 'treatment' was infiltrated by the gentle squeezing of cultures from a 1 mL syringe barrel into the underside of fully-expanded leaves of 5–6 weeks old *N.benthamiana* plants. Mock control refers to leaf tissue infiltrated with *A.tumefaciens* cultures containing no binary vector unless otherwise stated.

N.benthamiana seeds were germinated on Debco seedling mix supplemented with Osmocotte Exact Mini slow release fertiliser (2 g fertiliser per litre of soil). Two-week-old seedlings were transferred into new pots to contain one seedling per pot. Debco Custom Plugger mix 222 was used and supplemented with 1.5 g of Osmocotte Exact mini per litre of soil. Plants were housed in a 24°C plant growth room with overhead lighting using 9:15 light:dark cycle, where the light intensity was 250 µmol at the leaf surface. Typically only two leaves per plant (each wider than ~12 cm) were used for infiltrations with non-ideal leaves (too old or too young) removed from the plant 1 day prior to the infiltration. Prior to infiltrations, leaves were marked with treatment codes either by following a pre-designed randomisation of infiltration treatments over pre-conceived "spots" on the leaf or by visually randomising the codes on the leaves. Infiltrated areas of leaves, commonly 3–4 cm in diameter for oil quantification and ~1.5 cm for total FAME profile analysis, were either circled by a permanent marker or identified by the GFP fluorescent signal using a hand-held NightSea (NightSea, Bedford, MA, USA) illumination system. Infiltrated leaves were generally harvested 4–5 days dpi. A video outlining the plant growth room and infiltration procedure used in this study can be found at http://www.youtube.com/watch?v=DhtZ0E6edcQ.

6.5 Western blot analysis

A 1 cm^2 disc of infiltrated *N.benthamiana* leaves or 50 mg of *A.thaliana* tissue types were used for denaturing and protein extraction. Leaf samples were directly ground in 1 mL of 2X protein extraction buffer. Proteins were separated using SDS-PAGE.

In most cases 15 mL of 10-12% resolving gel was prepared:

Reagents	12% Resolving Gel
Acrylamide (40%)	4.5 mL
1.5 M Tris-Cl pH 8.8	3.45 mL
10% SDS	0.15 mL
H_2O	6.75 mL
10% AMPS	0.15 mL
TEMED	6 µL
Total	15 mL

10% freash AMPS was prepared by dissolving 0.05 g of solid AMPS in 0.5 mL of MQ H_2O.

5% stacking gel was prepared as follows:

Reagents	5% Stacking Gel
Acrylamide (40%)	625 µL
1 M Tris-Cl pH 6.8	625 µL
10% SDS	50 µL
H_2O	3.15 mL
10% AMPS	50 µL
TEMED	5 µL
Total	5 mL

The leaf samples ground in protein extraction buffer were heated at 95^oC for 5 mins and centrifuged at 10000 *g* for 10 mins (or at 13000 *g* for 3 mins). After centrifugation, the supernatant was not transferred to a new tube and loaded on the gel.

The gel running apparatus was filled with 1X running buffer. The wells were loaded with up to 15 µL of sample. The electrophoresis was performed at 80 V for 10 mins followed by 200 V for 50 mins.

Blotting was through semidry transfer. Gels were placed in blotting buffer to ensure gel do not dry out. Meanwhile six pieces of filter paper and one piece of PVDF membrane (millipore Immobilon-P Transfer membranes, 0.45 µm PVDF – membrane very expensive) were cut to the size of the gel (6.6 cm X 8.6 cm) per gel. PVDF membrane requires hydrating in 100% ethanol. Once hydrated, the ethanol is washed off with blotting buffer. The filter membranes were also soaked in blotting buffer. A stack of 3 layers of filter paper, PVDF membrane, gel and three pieces of filter membrane was placed on the semi-dry transfer cell. The transfer is completed by operated the power pack at 150 mA for 45 minutes for one gel.

The probing of the selected proteins required: PVDF membrane is soaked in 100% ethanol for 1 min. Ethanol is washed with distilled water a few times and rehydrate for ~3 mins. The membrane is washed in generous amount of TBST twice. Membrane is blocked in 5% skim milk in TBST for ~1 hr slow mixing. 2 µL of primary antibody was then added to 10 mLs 5% skim milk in TBST solution (anti-GFP monoclonal antibody 1:5000 dilution, Clontech), poured on the membrane and shaken at moderate speed for 1 hr. The blot is washed with TBST for 1 hr. The membrane is then shaken in 5% skim milk in TBST with 2 µL of secondary antibody (goat anti-mouse HRP 1:5000 dilution, Promega) for 1 hr. The membrane is washed with 1 L of 1XTBST buffer. Chemiluminescence as per NEN instructions.

Coomassie blue staining of total proteins in a duplicate gel was used as an indication of protein loading between samples.

6.6 GC analysis and FAME standards

GC was performed using an Agilent Technologies 6890N GC (Palo Alto, California, USA) equipped with a non-polar Equity™-1 fused silica capillary column (15 m x 0.1 mm i.d., 0.1 µm film thickness), an FID, a split/splitless injector and an Agilent Technologies 7683 Series autosampler and injector using helium as the carrier gas. Samples were injected in splitless mode at an oven temperature of 120°C and after injection the oven temperature was raised to 201°C at 10°Cmin^{-1} and finally to 270°C and held for 20 min. Peaks were quantified with Agilent Technologies ChemStation software (Rev B.03.01 (317), Palo Alto, California, USA).

Peak responses were similar for the fatty acids of authentic Nu-Check GLC standard-411 (Nu-Check Prep Inc, MN, USA) which contains equal proportions of 31 different fatty acid methyl esters, including 18:1, 18:2 and 20:1. Slight variations of peak responses among peaks were balanced by multiplying the peak areas by normalization factors of each peak. The proportion of each fatty acid in total fatty acids was calculated on the basis of individual and total peaks areas of the fatty acids.

During sample preparation an additional internal control, 17:0 free fatty acid or 17:0-TAG was added to samples. The 17:0 peaks measured in each sample determined the quality of FAME preparation in a batch.

6.7 Vectors used in this study

Vectors	Features	Reference
GhCPFAS	The ORF of *GhCPFAS* cloned into pXRZ393, in a binary vector.	Dr Shoko Okada
hpNbLPCAT	637 bp mid region of *NbLPCAT1* cloned into pHG12.	Dr Craig Wood
pCW141 pOPAL_seed	GFiP gene driven by the FP1 promoter in a binary vector.	Dr Craig Wood
pCW162 $P0^{PE}$_seed	GFiP and $P0^{PE}$ genes driven by the FP1 promoter in a binary vector.	Dr Craig Wood
pCW163 p38_seed	GFiP and p38 genes driven by the FP1 promoter in a binary vector.	Dr Craig Wood
pCW164 p19_seed	GFiP and p19 genes driven by the FP1 promoter in a binary vector.	Dr Craig Wood
pCW195 V2_seed	V2 gene driven by the FP1 promoter in a binary vector.	Dr Craig Wood
pCW196 p19_35S	P19 gene driven by the *CaMV* 35S promoter in a binary vector.	Dr Craig Wood
pCW197 V2_35S	V2 gene driven by the *CaMV* 35S promoter in a binary vector.	Dr Craig Wood
pCW483_FAE1 with intron	AtFAE1 gene driven by the *CaMV* 35S promoter. An intron cloned into the middle region of AtFAE1 for cloning purposes.	Dr Craig Wood
pCW609_hpNbFAD2.1 3'UTR (300e)	300 bp fragment targeting the 3'UTR region of *NbFAD2.1* was cloned into pHG12	Dr Craig Wood
pENTR/D-TOPO	A cloning strategy used for directionally cloning blunt-end PCR product into a vector for entry into the Gateway® System.	Life technologies
pET-14b	Bacterial expression vector containing his tag	Novagen
pFN012_DHA 35S:V2	35S:V2 and FP1:GFiP were cloned into pJP3057.	This study

pFN014_DHA FP1:V2	FP1:V2 and FP1:GFiP were cloned into pJP3057.	This study
pFN016_DHA FP1:p19	FP1:p19 and FP1:GFiP were cloned into pJP3057.	This study
pFN033_hpNbFAD2	660 bp region of *NbFAD2.1* cloned into pHG12.	This study
pFN043_hpPetuniaFAD2	600 bp region of petunia FAD2 was amplified and cloned into pHG12.	This study
pFN045_AA & FP1:P0^{PE}	A seed specific binary vector containing FP1:GFiP, FP1:P0^{PE} cassettes and three genes for the biosynthesis of AA in the seed.	This study
pFN046_AA & FP1:p38	A seed specific binary vector containing FP1:GFiP, FP1:p38 cassettes and three genes for the biosynthesis of AA in the seed.	This study
pFN047_AA & FP1:p19	A seed specific binary vector containing FP1:GFiP, FP1:p19 cassettes and three genes for the biosynthesis of AA in the seed.	This study
pFN048_AA & 35S:V2	A seed specific binary vector containing FP1:GFiP, 35S:V2 cassettes and three genes for the biosynthesis of AA in the seed.	This study
pFN049_AA & FP1:V2	A seed specific binary vector containing FP1:GFiP, FP1:V2 cassettes and three genes for the biosynthesis of AA in the seed.	This study
pFN050_AA	A seed specific binary vector containing three genes for the biosynthesis of AA in the seed.	This study
pFN053_V2-HA	The stop codon from V2 was removed and it was fused to 6XHA tag. Both genes were driven by the *CaMV* 35S promoter cloned into pXRZ393.	This study
pFN054_p19-HA	The stop codon from p19 was removed and it was fused to 6XHA tag. Both genes were driven by the *CaMV* 35S promoter cloned into pXRZ393.	This study

pFN056_HA-p19	6xHA tag fused to the N-terminus of p19 and cloned into pXRZ393.	This study
pFN058_35S:V2	GFiP driven by the FP1 promoter was cloned into pCW197.	This study
pFN059_FP1:V2	GFiP driven by the FP1 promoter was cloned into pCW195.	This study
pFN070_hpRNA300a	300 bp intronic region of *NbFAD2.1* cloned into pHG12.	This study
pFN071_hpRNA300b	300 bp region of *NbFAD2.1* cloned into pHG12.	This study
pFN072_hpNbFAD2-300	300 bp region of *NbFAD2.1* cloned into pHG12.	This study
pFN073_hpRNA300d	300 bp region of *NbFAD2.1* cloned into pHG12.	This study
pFN078_hpNbFAD2.2 3'UTR	370 bp of 3'UTR region of *NbFAD2.1* cloned into pHG12.	This study
pFN079_His-V2-HA	The stop codon of V2 removed and the sequence combined with 6XHA sequence containing a stop codon. The combination cloned into pET-14b for bacterial expression of the protein. The His tag was present in the pET-14b vector which was cloned in frame with V2-HA.	This study
pFN083_hpNbFAD3	689 bp region of *NbFAD3* cloned into pHG12.	This study
pFN084_hpNbFAD7	647 bp region of *NbFAD7* cloned into pHG12.	This study
pFN085_hpNbFATB	652 bp region of *NbFATB* cloned into pHG12.	This study
pFN088_NbFAD2.1 yeast	The ORF of *NbFAD2.1* (1152 bp) cloned into yeast expression vector, pYES2.	This study
pFN089_NbFAD2.2 yeast	The ORF of *NbFAD2.2* (1203 bp) cloned into yeast expression vector, pYES2.	This study
pFN091_hpNbFAD6	677 bp region of *NbFAD6* cloned into pHG12.	This study
pFN094_hpNbFATA	841 bp region of *NbFATA1* cloned into pHG12.	This study

pFN095_hpNbSAD1	700 bp region of *NbSAD1* cloned into pHG12.	This study
pFN101_hpNbGPAT9	502 bp region of *NbGPAT9* cloned into pHG12.	This study
pFN104_hpNbLPAAT4	400 bp region of *NbLPAAT4* cloned into pHG12.	This study
pFN105_hpNbLPAAT6	400 bp region of *NbLPAAT6* cloned into pHG12.	This study
pGEM-T Easy	Cloning vector	Promega
pHELLSGATE8 & pHELLSGATE12	Getway cloning construct used to prepare hpRNA molecules (Helliwell and Waterhouse, 2003).	Dr Chris Helliwell & Professor Peter Waerhouse
pJP1094	Polycistronic amiRNA targeting *AtFATB*, *AtFAD2* and *AtFAE1*	Drs Srinivas Belide & James Petrie
pJP2602	The coding sequence of IgΔ9E was cloned into 35S-pORE4 to yield pJP2062.	Dr James Petrie
pJP3010	pORE backbone containing three gene cassettes for FAE1:IgΔ9E, FP1:PsΔ8D and FP1:PsΔ5D (Petrie et al., 2012a).	Dr James Petrie
pJP3057	pORE backbone containing five gene cassettes for FP1:PcΔ6E, FP1:MsΔ6D, FP1:PsΔ4D and FP1:PsΔ5D and FP1:PcΔ5E (Petrie et al., 2010)	Dr James Petrie
pUQ214_GFP	Cytoplasmic GFP driven by the 35S promoter in a binary expression vector (Brosnan et al., 2007b).	Professor Peter Waterhouse
pUQ218_hpGFP	GF specific hpRNA targeting GFP (Brosnan et al., 2007b).	Professor Peter Waterhouse
pXRZ393	35S binary overexpression vector prepared for cloning of gene fragments.	Dr Xue-Rong Zhou
pXRZ603	The ORF of *AtDGAT1* cloned into pXRZ393 (Wood et al., 2009).	Dr Xue-Rong Zhou

Table 6.1. List of vectors used in this study.

A comprehensive list of vectors used in this study with associated references.

Appendices

sRNA Size class	0 bp mismatches	3 bp mismatches
NbFAD2.1 ORF		
20sfw	208839 (13.05%)	256917 (16.05%)
20srev	174190 (10.88%)	209532 (13.09%)
21sfw	1170681 (15.26%)	1428945 (18.63%)
21srev	1128803 (14.72%)	1379805 (17.99%)
22sfw	943303 (12.56%)	1168521 (15.56%)
22srev	866550 (11.54%)	1094555 (14.58%)
23sfw	116594 (7.47%)	165412 (10.60%)
23srev	199388 (6.37%)	152748 (9.79%)
24sfw	340748 (8.23%)	426908 (10.32%)
24srev	323150 (7.81%)	413347 (9.99%)
NbFAD2.2 ORF		
20sfw	32 (0.00%)	67959 (4.25%)
20srev	45 (0.00%)	72032 (4.50%)
21sfw	141 (0.00%)	239927 (3.13%)
21srev	180 (0.00%)	376824 (4.91%)
22sfw	64 (0.00%)	179390 (2.39%)
22srev	90 (0.00%)	333369 (4.44%)
23sfw	5 (0.00%)	27847 (1.79%)
23srev	4 (0.00%)	25994 (1.67%)
24sfw	11 (0.00%)	80016 (1.93%)
24srev	12 (0.00%)	67349 (1.63%)

Appendix Table A. Number of sRNA deep sequencing reads aligning to *NbFAD2.1* and *NbFAD2.2*.

The sRNA size classes were aligned onto the forward (fw) and reverse (rev) strands of *NbFAD2.1* and *NbFAD2.2*.

T2 Events	% of transgenic seedlings	T2 Events2	% of transgenic seedlings	T2 Events4	% of transgenic seedlings
pFN050-01	100	pFN047-16	92	pFN049-20	84
pFN050-02	100	pFN047-17	70	pFN049-21	94
pFN050-03	83	pFN047-18	83	pFN049-22	65
pFN050-04	none recorded	pFN047-19	67	pFN049-23	85
pFN050-05	83	pFN047-20	88	pFN049-24	none recorded
pFN050-06	none recorded	pFN047-21	75	pFN049-25	73
pFN050-07	100	pFN047-23	73	pFN049-26	80
pFN050-08	70	pFN047-24	78	pFN048-01	79
pFN050-09	82	pFN047-26	59	pFN048-02	83
pFN050-10	65	pFN047-27	78	pFN048-04	77
pFN050-11	80	pFN047-28	73	pFN048-06	93
pFN050-12	67	pFN047-29	83	pFN048-08	No AA – not grown
pFN050-13	79	pFN047-30	58	pFN048-09	72
pFN050-14	80	pFN047-31	73	pFN048-11	93
pFN050-15	86	pFN047-33	65	pFN048-12	86
pFN050-17	100	pFN047-35	79	pFN045-01	38
pFN050-18	83	pFN047-36	88	pFN045-04	55
pFN050-19	73	pFN047-37	69	pFN045-06	69
pFN050-20	77	pFN047-39	100	pFN045-08	100
pFN050-21	84	pFN049-01	76	pFN045-09	73
pFN050-22	80	pFN049-02	75	pFN046-01	77
pFN050-23	98	pFN049-03	79	pFN046-02	82
pFN050-24	78	pFN049-04	80	pFN046-03	82
pFN047-02	94	pFN049-05	77	pFN046-05	74
pFN047-03	72	pFN049-06	none recorded	pFN046-06	71
pFN047-04	93	pFN049-08	76	pFN046-07	93
pFN047-05	60	pFN049-09	No AA – 78	pFN046-08	78
pFN047-06	74	pFN049-10	69	pFN046-09	86
pFN047-07	74	pFN049-11	85	pFN046-10	88
pFN047-08	80	pFN049-12	61	pFN046-11	No AA – not grown
pFN047-09	No AA–74	pFN049-13	80	pFN046-12	69
pFN047-10	75	pFN049-14	79	pFN046-13	64
pFN047-11	71	pFN049-15	70	pFN046-14	80
pFN047-12	74	pFN049-16	72	pFN046-16	81
pFN047-13	75	pFN049-17	100		
pFN047-15	74	pFN049-18	80		

Appendix Table B. Segregation analysis of T2 *A.thaliana* seedlings expressing various AA constructs.

The segregation analysis of the *A.thaliana* T2 population of seedlings expressing the AA constructs outlined in Fig 3.5B. The percentages of T2 seedlings that survived on media containing 50 mgL^{-1} of kanamycin were calculated.

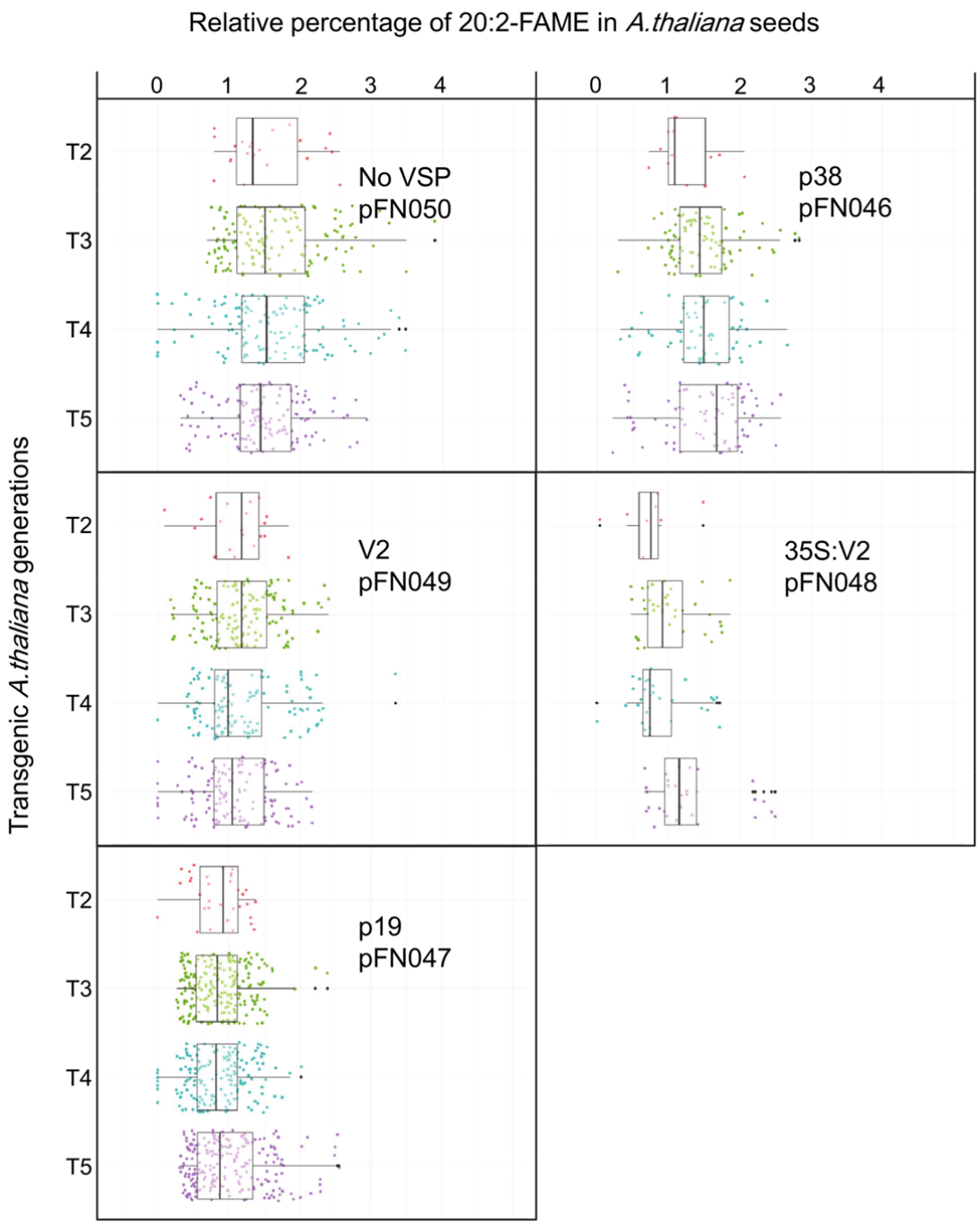

Appendix Figure A. Relative percentage of 20:3-FAME extracted from T3–T5 seeds of transgenic *A.thaliana*.

Box-plot analysis of a large population of transgenic *A.thaliana* expressing the constructs described in Fig 3.5B. Relative percentage of 20:3 is shown and dot points refer to the T3–T5 progeny of independent T2 events.

Box-whisker plot analysis: The boundary of the box closest to zero indicates the 25th percentile, a line within the box marks the median, and the boundary of the box farthest from zero indicates the 75th percentile. Whiskers (error bars) above and below the box indicate the 90th and 10th percentiles. Points outside of the whiskers are not included in the calculation of quartiles.

Bibliography

Andrews, J., and Keegstra, K. (1983). Acyl-CoA Synthetase is located in the outer membrane and Acyl-CoA Thioesterase in the inner membrane of pea chloroplast envelopes. Plant Physiology *72*, 735-740.

Astier-Manifacier, S., and Cornuet, P. (1971). RNA-dependent RNA polymerase in Chinese cabbage. Biochimica et biophysica acta *232*, 484-493.

Azevedo, J., Garcia, D., Pontier, D., Ohnesorge, S., Yu, A., Garcia, S., Braun, L., Bergdoll, M., Hakimi, M.A., Lagrange, T.*, et al.* (2010). Argonaute quenching and global changes in Dicer homeostasis caused by a pathogen-encoded GW repeat protein. Genes & Development *24*, 904-915.

Badami, R.C., and Patil, K.B. (1980). Structure and occurrence of unusual fatty acids in minor seed oils. Prog Lipid Res *19*, 119-153.

Bafor, M., Smith, M.A., Jonsson, L., Stobart, K., and Stymne, S. (1991). Ricinoleic acid biosynthesis and triacylglycerol assembly in microsomal preparations from developing castor-bean (Ricinus communis) endosperm. The Biochemical journal *280 (Pt 2)*, 507-514.

Bao, X., Katz, S., Pollard, M., and Ohlrogge, J. (2002). Carbocyclic fatty acids in plants: Biochemical and molecular genetic characterization of cyclopropane fatty acid synthesis of Sterculia foetida. Proceedings of the National Academy of Sciences *99*, 7172-7177.

Bao, X., Thelen, J.J., Bonaventure, G., and Ohlrogge, J.B. (2003). Characterization of Cyclopropane Fatty-acid Synthase from Sterculia foetida. Journal of Biological Chemistry *278*, 12846-12853.

Bar-Ziv, A., Levy, Y., Hak, H., Mett, A., Belausov, E., Citovsky, V., and Gafni, Y. (2012). The tomato yellow leaf curl virus (TYLCV) V2 protein interacts with the host papain-like cysteine protease CYP1. Plant signaling & behavior *7*, 983-989.

Bartel, D.P. (2004). MicroRNAs: genomics, biogenesis, mechanism, and function. Cell *116*, 281-297.

Bateman, A. (2002). The SGS3 protein involved in PTGS finds a family. BMC Bioinformatics *3*, 21.

Bates, P.D., Durrett, T.P., Ohlrogge, J.B., and Pollard, M. (2009). Analysis of acyl fluxes through multiple pathways of triacylglycerol synthesis in developing soybean embryos. Plant Physiology *150*, 55-72.

Bates, P.D., Fatihi, A., Snapp, A.R., Carlsson, A.S., Browse, J., and Lu, C. (2012). Acyl editing and headgroup exchange are the major mechanisms that direct polyunsaturated fatty acid flux into triacylglycerols. Plant Physiol *160*, 1530-1539.

Bates, P.D., Johnson, S.R., Cao, X., Li, J., Nam, J.-W., Jaworski, J.G., Ohlrogge, J.B., and Browse, J. (2014). Fatty acid synthesis is inhibited by inefficient utilization of unusual fatty acids for glycerolipid assembly. Proceedings of the National Academy of Sciences.

Bates, P.D., Ohlrogge, J.B., and Pollard, M. (2007). Incorporation of newly synthesized fatty acids into cytosolic glycerolipids in pea leaves occurs via acyl editing. J Biol Chem *282*, 31206-31216.

Bates, P.D., Stymne, S., and Ohlrogge, J. (2013). Biochemical pathways in seed oil synthesis. Current Opinion in Plant Biology *16*, 358-364.

Baud, S., and Lepiniec, L. (2010). Physiological and developmental regulation of seed oil production. Prog Lipid Res *49*, 235-249.

Baulcombe, D.C. (2004). RNA silencing in plants. Nature *431*, 356-363.

Baulcombe, D.C. (2007). Amplified silencing. Science *315*, 199-200.

Beclin, C., Boutet, S., Waterhouse, P., and Vaucheret, H. (2002). A branched pathway for transgene-induced RNA silencing in plants. Current biology : CB *12*, 684-688.

Belide, S., Hac, L., Singh, S.P., Green, A.G., and Wood, C.C. (2011). Agrobacterium-mediated transformation of safflower and the efficient recovery of transgenic plants via grafting. Plant Methods *7*, 12.

Belide, S., Petrie, J.R., Shrestha, P., Fahim, M., Liu, Q., Wood, C., and Singh, S.P. (2014). Multi-gene silencing using a single polycistronic artificial miRNA.

Belide, S., Petrie, J.R., Shrestha, P., and Singh, S.P. (2012). Modification of seed oil composition in Arabidopsis by artificial microRNA-mediated gene silencing. Frontiers in Plant Science *3*.

Benning, C. (2009). Mechanisms of lipid transport involved in organelle biogenesis in plant cells. Annual Review of Cell and Developmental Biology *25*, 71-91.

Bernstein, E., Caudy, A.A., Hammond, S.M., and Hannon, G.J. (2001). Role for a bidentate ribonuclease in the initiation step of RNA interference. Nature *409*, 363-366.

Blevins, T., Rajeswaran, R., Shivaprasad, P.V., Beknazariants, D., Si-Ammour, A., Park, H.-S., Vazquez, F., Robertson, D., Meins, F., Hohn, T*., et al.* (2006). Four plant Dicers mediate viral small RNA biogenesis and DNA virus induced silencing. Nucleic Acids Research *34*, 6233-6246.

Bligh, E., and Dyer, W. (1959). A rapid method of total lipid extraction and purification. Canadian Journal of Biochemistry and Physiology *37*, 911-917.

Block, M.A., Dorne, A.J., Joyard, J., and Douce, R. (1983). Preparation and characterization of membrane fractions enriched in outer and inner envelope membranes from spinach chloroplasts. II. Biochemical characterization. J Biol Chem *258*, 13281-13286.

Bombarely, A., Rosli, H.G., Vrebalov, J., Moffett, P., Mueller, L.A., and Martin, G.B. (2012). A draft genome sequence of Nicotiana benthamiana to enhance molecular plant-microbe biology research. Molecular Plant-Microbe Interactions *25*, 1523-1530.

Bonaventure, G., Bao, X., Ohlrogge, J., and Pollard, M. (2004). Metabolic responses to the reduction in palmitate caused by disruption of the FATB gene in Arabidopsis. Plant Physiology *135*, 1269-1279.

Bonaventure, G., Salas, J.J., Pollard, M.R., and Ohlrogge, J.B. (2003). Disruption of the FATB gene in Arabidopsis demonstrates an essential role of saturated fatty acids in plant growth. The Plant Cell Online *15*, 1020-1033.

Bortolamiol, D., Pazhouhandeh, M., Marrocco, K., Genschik, P., and Ziegler-Graff, V. (2007). The Polerovirus F box protein P0 targets ARGONAUTE1 to suppress RNA silencing. Current biology : CB *17*, 1615-1621.

Brenna, J.T., Salem, N., Jr., Sinclair, A.J., and Cunnane, S.C. (2009). alpha-Linolenic acid supplementation and conversion to n-3 long-chain polyunsaturated fatty acids in humans. Prostaglandins, leukotrienes, and essential fatty acids *80*, 85-91.

Brigneti, G., Voinnet, O., Li, W.-X., Ji, L.-H., Ding, S.-W., and Baulcombe, D.C. (1998). Viral pathogenicity determinants are suppressors of transgene silencing in Nicotiana benthamiana. EMBO J *17*, 6739-6746.

Brosnan, C.A., Mitter, N., Christie, M., Smith, N.A., Waterhouse, P.M., and Carroll, B.J. (2007a). Nuclear gene silencing directs reception of long-distance mRNA silencing in Arabidopsis. P Natl Acad Sci USA *104*, 14741-14746.

Brosnan, C.A., Mitter, N., Christie, M., Smith, N.A., Waterhouse, P.M., and Carroll, B.J. (2007b). Nuclear gene silencing directs reception of long-distance mRNA silencing in Arabidopsis. Proceedings of the National Academy of Sciences *104*, 14741-14746.

Broun, P., and Somerville, C. (1997). Accumulation of ricinoleic, lesquerolic, and densipolic acids in seeds of transgenic Arabidopsis plants that express a fatty acyl hydroxylase cDNA from castor bean. Plant Physiol *113*, 933-942.

Browse, J., McConn, M., James, D., Jr., and Miquel, M. (1993). Mutants of Arabidopsis deficient in the synthesis of alpha-linolenate. Biochemical and genetic characterization of the endoplasmic reticulum linoleoyl desaturase. J Biol Chem *268*, 16345-16351.

Browse, J., and Somerville, C. (1991). Glycerolipid Synthesis: Biochemistry and Regulation. Annual Review of Plant Physiology and Plant Molecular Biology *42*, 467-506.

Browse, J., Warwick, N., Somerville, C.R., and Slack, C.R. (1986). Fluxes through the prokaryotic and eukaryotic pathways of lipid synthesis in the '16:3' plant Arabidopsis thaliana. The Biochemical journal *235*, 25-31.

Burgyan, J., and Havelda, Z. (2011). Viral suppressors of RNA silencing. Trends Plant Sci *16*, 265-272.

Cahoon, E.B., Damude, H., Hitz, W., Kinney, A., Kolar, C., and Liu, Z.-B. (2004). Production of very long chain polyunsaturated fatty acids in oilseed plants (US).

Cao, S., Zhou, X.-R., Wood, C., Green, A., Singh, S., Liu, L., and Liu, Q. (2013). A large and functionally diverse family of Fad2 genes in safflower (Carthamus tinctorius L.). BMC Plant Biology *13*, 5.

Carlson, S.E., Werkman, S.H., Peeples, J.M., Cooke, R.J., and Tolley, E.A. (1993). Arachidonic acid status correlates with first year growth in preterm infants. Proceedings of the National Academy of Sciences of the United States of America *90*, 1073-1077.

Carman, G.M., and Han, G.-S. (2009). Phosphatidic Acid Phosphatase, a key enzyme in the regulation of lipid synthesis. Journal of Biological Chemistry *284*, 2593-2597.

Castilho, A., Strasser, R., Stadlmann, J., Grass, J., Jez, J., Gattinger, P., Kunert, R., Quendler, H., Pabst, M., Leonard, R*., et al.* (2010). In planta protein sialylation through overexpression of the respective mammalian pathway. J Biol Chem *285*, 15923-15930.

Cernac, A., and Benning, C. (2004). WRINKLED1 encodes an AP2/EREB domain protein involved in the control of storage compound biosynthesis in Arabidopsis. Plant J *40*, 575-585.

Chapman, E.J., and Carrington, J.C. (2007). Specialization and evolution of endogenous small RNA pathways. Nat Rev Genet *8*, 884-896.

Chapman, E.J., Prokhnevsky, A.I., Gopinath, K., Dolja, V.V., and Carrington, J.C. (2004). Viral RNA silencing suppressors inhibit the microRNA pathway at an intermediate step. Genes & Development *18*, 1179-1186.

Chapman, K.D., and Ohlrogge, J.B. (2012). Compartmentation of triacylglycerol accumulation in plants. J Biol Chem *287*, 2288-2294.

Chapman, S., Kavanagh, T., and Baulcombe, D. (1992). Potato virus X as a vector for gene expression in plants. Plant J *2*, 549-557.

Clemente, T.E., and Cahoon, E.B. (2009). Soybean oil: Genetic approaches for modification of functionality and total content. Plant Physiology *151*, 1030-1040.

Clough, S., and Bent, A. (1998). Floral dip: a simplified method for Agrobacterium-mediated transformation of Arabidopsis thaliana. Plant J *16*, 735 - 743.

Coutu, C., Brandle, J., Brown, D., Brown, K., Miki, B., Simmonds, J., and Hegedus, D.D. (2007). pORE: a modular binary vector series suited for both monocot and dicot plant transformation. Transgenic Research *16*, 771-781.

Curaba, J., and Chen, X. (2008). Biochemical activities of Arabidopsis RNA-dependent RNA Polymerase 6. J Biol Chem *283*, 3059-3066.

Czosnek, H., and Laterrot, H. (1997). A worldwide survey of tomato yellow leaf curl viruses. Archives of virology *142*, 1391-1406.

Dahlqvist, A., Ståhl, U., Lenman, M., Banas, A., Lee, M., Sandager, L., Ronne, H., and Stymne, S. (2000). Phospholipid:diacylglycerol acyltransferase: An enzyme that catalyzes the acyl-CoA-independent formation of triacylglycerol in yeast and plants. Proceedings of the National Academy of Sciences *97*, 6487-6492.

Daxinger, L., Hunter, B., Sheikh, M., Jauvion, V., Gasciolli, V., Vaucheret, H., Matzke, M., and Furner, I. (2008). Unexpected silencing effects from T-DNA tags in Arabidopsis. Trends in plant science *13*, 4-6.

Deleris, A., Gallego-Bartolome, J., Bao, J., Kasschau, K.D., Carrington, J.C., and Voinnet, O. (2006). Hierarchical action and inhibition of plant Dicer-Like proteins in antiviral defense. Science *313*, 68-71.

Diaz-Pendon, J.A., Li, F., Li, W.-X., and Ding, S.-W. (2007). Suppression of antiviral silencing by Cucumber mosaic virus 2b protein in Arabidopsis is associated with drastically reduced accumulation of three classes of viral small interfering RNAs. The Plant Cell Online *19*, 2053-2063.

Ding, S.W. (2010). RNA-based antiviral immunity. Nature reviews Immunology *10*, 632-644.

Ding, S.W., and Voinnet, O. (2007). Antiviral immunity directed by small RNAs. Cell *130*, 413-426.

Doan, T.T.P., Domergue, F., Fournier, A.E., Vishwanath, S.J., Rowland, O., Moreau, P., Wood, C.C., Carlsson, A.S., Hamberg, M., and Hofvander, P. (2012). Biochemical characterization of a chloroplast localized fatty acid reductase from Arabidopsis thaliana. Biochimica et Biophysica Acta (BBA) - Molecular and Cell Biology of Lipids *1821*, 1244-1255.

Donaire, L., Barajas, D., Martínez-García, B., Martínez-Priego, L., Pagán, I., and Llave, C. (2008). Structural and genetic requirements for the biogenesis of Tobacco rattle virus-derived small interfering RNAs. Journal of Virology *82*, 5167-5177.

Dong, L., Liu, M., Fang, Y.Y., Zhao, J.H., He, X.F., Ying, X.B., Zhang, Y.Y., Xie, Q., Chua, N.H., and Guo, H.S. (2011). DRD1-Pol V-dependent self-silencing of an exogenous silencer restricts the non-cell autonomous silencing of an endogenous target gene. Plant J *68*, 633-645.

Dong, X., van Wezel, R., Stanley, J., and Hong, Y. (2003). Functional characterization of the nuclear localization signal for a suppressor of posttranscriptional gene silencing. Journal of Virology *77*, 7026-7033.

Dörmann, P., and Benning, C. (2002). Galactolipids rule in seed plants. Trends in Plant Science *7*, 112-118.

Dorne, A.J., Joyard, J., Block, M.A., and Douce, R. (1985). Localization of phosphatidylcholine in outer envelope membrane of spinach chloroplasts. The Journal of Cell Biology *100*, 1690-1697.

Dunoyer, P., Lecellier, C.-H., Parizotto, E.A., Himber, C., and Voinnet, O. (2004). Probing the microRNA and small interfering RNA pathways with virus-encoded suppressors of RNA silencing. The Plant Cell Online *16*, 1235-1250.

Dunoyer, P., Schott, G., Himber, C., Meyer, D., Takeda, A., Carrington, J.C., and Voinnet, O. (2010). Small RNA duplexes function as mobile silencing signals between plant cells. Science *328*, 912-916.

Eamens, A., Wang, M.-B., Smith, N.A., and Waterhouse, P.M. (2008). RNA silencing in plants: Yesterday, today, and tomorrow. Plant Physiol *147*, 456-468.

Eastmond, P.J., Quettier, A.-L., Kroon, J.T.M., Craddock, C., Adams, N., and Slabas, A.R. (2010). PHOSPHATIDIC ACID PHOSPHOHYDROLASE1 and 2 regulate phospholipid synthesis at the endoplasmic reticulum in Arabidopsis. The Plant Cell Online *22*, 2796-2811.

Elmayan, T., Adenot, X., Gissot, L., Lauressergues, D., Gy, I., and Vaucheret, H. (2009). A neomorphic sgs3 allele stabilizing miRNA cleavage products reveals that SGS3 acts as a homodimer. FEBS Journal *276*, 835-844.

Elmayan, T., Balzergue, S., Béon, F., Bourdon, V., Daubremet, J., Guénet, Y., Mourrain, P., Palauqui, J.-C., Vernhettes, S., Vialle, T.*, et al.* (1998). Arabidopsis mutants impaired in cosuppression. The Plant Cell Online *10*, 1747-1757.

Elmayan, T., and Vaucheret, H. (1996). Expression of single copies of a strongly expressed 35S transgene can be silenced post-transcriptionally. The Plant Journal *9*, 787-797.

Ferrer-Orta, C., Arias, A., Escarmis, C., and Verdaguer, N. (2006). A comparison of viral RNA-dependent RNA polymerases. Curr Opin Struct Biol *16*, 27-34.

Fire, A., Xu, S., Montgomery, M.K., Kostas, S.A., Driver, S.E., and Mello, C.C. (1998). Potent and specific genetic interference by double-stranded RNA in Caenorhabditis elegans. Nature *391*, 806-811.

Fukunaga, R., and Doudna, J.A. (2009). dsRNA with 5′ overhangs contributes to endogenous and antiviral RNA silencing pathways in plants. EMBO J *28*, 545-555.

Fusaro, A.F., Correa, R.L., Nakasugi, K., Jackson, C., Kawchuk, L., Vaslin, M.F.S., and Waterhouse, P.M. (2012). The Enamovirus P0 protein is a silencing suppressor which inhibits local and systemic RNA silencing through AGO1 degradation. Virology *426*, 178-187.

Garabagi, F., Gilbert, E., Loos, A., McLean, M.D., and Hall, J.C. (2012). Utility of the P19 suppressor of gene-silencing protein for production of therapeutic antibodies in Nicotiana expression hosts. Plant Biotechnol J *10*, 1118-1128.

Garcia-Ruiz, H., Takeda, A., Chapman, E.J., Sullivan, C.M., Fahlgren, N., Brempelis, K.J., and Carrington, J.C. (2010). Arabidopsis RNA-dependent RNA polymerases and dicer-like proteins in antiviral defense and small interfering RNA biogenesis during Turnip Mosaic Virus infection. Plant Cell *22*, 481-496.

Gaydou, E.M., Ralaimanarivo, A., and Bianchini, J.P. (1993). Cyclopropanoic fatty acids of litchi (Litchi chinensis) seed oil. A reinvestigation. Journal of Agricultural and Food Chemistry *41*, 886-890.

Gibellini, F., and Smith, T.K. (2010). The Kennedy pathway—De novo synthesis of phosphatidylethanolamine and phosphatidylcholine. IUBMB Life *62*, 414-428.

Gidda, S.K., Shockey, J.M., Rothstein, S.J., Dyer, J.M., and Mullen, R.T. (2009). Arabidopsis thaliana GPAT8 and GPAT9 are localized to the ER and possess distinct ER retrieval signals: functional divergence of the dilysine ER

retrieval motif in plant cells. Plant physiology and biochemistry : PPB / Societe francaise de physiologie vegetale *47*, 867-879.

Giner, A., Lakatos, L., Garcia-Chapa, M., Lopez-Moya, J.J., and Burgyan, J. (2010). Viral protein inhibits RISC activity by argonaute binding through conserved WG/GW motifs. PLoS Pathog *6*, e1000996.

Glick, E., Zrachya, A., Levy, Y., Mett, A., Gidoni, D., Belausov, E., Citovsky, V., and Gafni, Y. (2008). Interaction with host SGS3 is required for suppression of RNA silencing by tomato yellow leaf curl virus V2 protein. Proceedings of the National Academy of Sciences *105*, 157-161.

Gonzalez, I., Martinez, L., Rakitina, D.V., Lewsey, M.G., Atencio, F.A., Llave, C., Kalinina, N.O., Carr, J.P., Palukaitis, P., and Canto, T. (2010). Cucumber mosaic virus 2b protein subcellular targets and interactions: their significance to RNA silencing suppressor activity. Molecular plant-microbe interactions : MPMI *23*, 294-303.

Goodin, M.M., Zaitlin, D., Naidu, R.A., and Lommel, S.A. (2008). Nicotiana benthamiana: Its history and future as a model for plant–pathogen interactions. Molecular Plant-Microbe Interactions *21*, 1015-1026.

Gordon, K.H., and Waterhouse, P.M. (2007). RNAi for insect-proof plants. Nat Biotechnol *25*, 1231-1232.

Grogan, D.W., and Cronan, J.E., Jr. (1984). Cloning and manipulation of the Escherichia coli cyclopropane fatty acid synthase gene: physiological aspects of enzyme overproduction. Journal of bacteriology *158*, 286-295.

Grogan, D.W., and Cronan, J.E., Jr. (1997). Cyclopropane ring formation in membrane lipids of bacteria. Microbiology and molecular biology reviews : MMBR *61*, 429-441.

Haas, G., Azevedo, J., Moissiard, G., Geldreich, A., Himber, C., Bureau, M., Fukuhara, T., Keller, M., and Voinnet, O. (2008). Nuclear import of CaMV P6 is required for infection and suppression of the RNA silencing factor DRB4. EMBO J *27*, 2102-2112.

Hagan, N.D., Spencer, D., Moore, A.E., and Higgins, T.J.V. (2003). Changes in methylation during progressive transcriptional silencing in transgenic subterranean clover. Plant Biotechnology Journal *1*, 479-490.

Hamilton, A.J., and Baulcombe, D.C. (1999). A species of small antisense RNA in posttranscriptional gene silencing in plants. Science *286*, 950-952.

Harada, J.J. (2001). Role of Arabidopsis LEAFY COTYLEDON genes in seed development. Journal of Plant Physiology *158*, 405-409.

He, X., Turner, C., Chen, G.Q., Lin, J.T., and McKeon, T.A. (2004). Cloning and characterization of a cDNA encoding diacylglycerol acyltransferase from castor bean. Lipids *39*, 311-318.

Helliwell, C., and Waterhouse, P. (2003). Constructs and methods for high-throughput gene silencing in plants. Methods (San Diego, Calif) *30*, 289-295.

Helliwell, C., Wesley, S., Wielopolska, A., and Waterhouse, P. (2002). High-throughput vectors for efficient gene silencing in plants. Functional Plant Biology *29*, 1217-1225.

Heppard, E.P., Kinney, A.J., Stecca, K.L., and Miao, G.H. (1996). Developmental and growth temperature regulation of two different microsomal omega-6 desaturase genes in soybeans. Plant Physiol *110*, 311-319.

Hildebrand, J.G., and Law, J.H. (1964). Fatty Acid Distribution in Bacterial Phospholipids. The Specificity of the Cyclopropane Synthetase Reaction*. Biochemistry *3*, 1304-1308.

Himber, C., Dunoyer, P., Moissiard, G., Ritzenthaler, C., and Voinnet, O. (2003). Transitivity-dependent and -independent cell-to-cell movement of RNA silencing. EMBO J *22*, 4523-4533.

Hobbs, S.L., Kpodar, P., and DeLong, C.M. (1990). The effect of T-DNA copy number, position and methylation on reporter gene expression in tobacco transformants. Plant Mol Biol *15*, 851-864.

Hobbs, S.L., Warkentin, T.D., and DeLong, C.M. (1993). Transgene copy number can be positively or negatively associated with transgene expression. Plant Mol Biol *21*, 17-26.

Honda, A., Mizumoto, K., and Ishihama, A. (1986). RNA polymerase of influenza virus. Dinucleotide-primed initiation of transcription at specific positions on viral RNA. Journal of Biological Chemistry *261*, 5987-5991.

Horn, M.E.T., and Waterhouse, P.M. (2010). Rapid match-searching for gene silencing assessment. Bioinformatics *26*, 1932-1937.

Hsieh, Y.-C., Omarov, R.T., and Scholthof, H.B. (2009). Diverse and newly recognized effects associated with short interfering RNA binding site modifications on the Tomato bushy stunt virus p19 silencing suppressor. Journal of Virology *83*, 2188-2200.

Huang, C.-c., Smith, C.V., Glickman, M.S., Jacobs, W.R., and Sacchettini, J.C. (2002). Crystal structures of mycolic acid cyclopropane synthases from Mycobacterium tuberculosis. Journal of Biological Chemistry *277*, 11559-11569.

Hutvagner, G., and Simard, M.J. (2008). Argonaute proteins: key players in RNA silencing. Nature reviews Molecular cell biology *9*, 22-32.

Iba, K., Gibson, S., Nishiuchi, T., Fuse, T., Nishimura, M., Arondel, V., Hugly, S., and Somerville, C. (1993). A gene encoding a chloroplast omega-3 fatty acid desaturase complements alterations in fatty acid desaturation and chloroplast copy number of the fad7 mutant of Arabidopsis thaliana. Journal of Biological Chemistry *268*, 24099-24105.

Ichihara, K.i., Mae, K., Sano, Y., and Tanaka, K. (1995). 1-Acylglycerophosphocholine O-acyltransferase in maturing safflower seeds. Planta *196*, 551-557.

Incarbone, M., and Dunoyer, P. (2013). RNA silencing and its suppression: novel insights from in planta analyses. Trends in Plant Science.

Jacobsen, S.E., Running, M.P., and Meyerowitz, E.M. (1999). Disruption of an RNA helicase/RNAse III gene in Arabidopsis causes unregulated cell division in floral meristems. Development *126*, 5231-5243.

James, C. (2013). Global status of commercialized Biotech/GM Crops: 2013. ISAAA: Ithaca, NY.

Jauvion, V., Rivard, M., Bouteiller, N., Elmayan, T., and Vaucheret, H. (2012). RDR2 partially antagonizes the production of RDR6-dependent siRNA in sense transgene-mediated PTGS. PLoS One *7*, e29785.

Jin, H. (2008). Endogenous small RNAs and antibacterial immunity in plants. FEBS Letters *582*, 2679-2684.

Jones, L., Hamilton, A.J., Voinnet, O., Thomas, C.L., Maule, A.J., and Baulcombe, D.C. (1999). RNA-DNA interactions and DNA methylation in post-transcriptional gene silencing. Plant Cell *11*, 2291-2301.

Jouannet, V., Moreno, A.B., Elmayan, T., Vaucheret, H., Crespi, M.D., and Maizel, A. (2012). Cytoplasmic Arabidopsis AGO7 accumulates in membrane-associated siRNA bodies and is required for ta-siRNA biogenesis. EMBO J *31*, 1704-1713.

Jovel, J., Walker, M., and Sanfacon, H. (2011). Salicylic acid-dependent restriction of Tomato ringspot virus spread in tobacco is accompanied by a hypersensitive response, local RNA silencing, and moderate systemic resistance. Molecular plant-microbe interactions : MPMI *24*, 706-718.

Jovel, J., Walker, M., and Sanfaçon, H. (2007). Recovery of Nicotiana benthamiana plants from a necrotic response induced by a nepovirus is associated with RNA silencing but not with reduced virus titer. Journal of Virology *81*, 12285-12297.

Kereszt, A., Li, D., Indrasumunar, A., Nguyen, C.D., Nontachaiyapoom, S., Kinkema, M., and Gresshoff, P.M. (2007). Agrobacterium rhizogenes-mediated transformation of soybean to study root biology. Nature protocols *2*, 948-952.

Kheyr-Pour, A., Bendahmane, M., Matzeit, V., Accotto, G.P., Crespi, S., and Gronenborn, B. (1991). Tomato yellow leaf curl virus from Sardinia is a whitefly-transmitted monopartite geminivirus. Nucleic Acids Research *19*, 6763-6769.

Kim, H.U., Lee, K.R., Go, Y.S., Jung, J.H., Suh, M.C., and Kim, J.B. (2011). Endoplasmic reticulum-located PDAT1-2 from castor bean enhances hydroxy fatty acid accumulation in transgenic plants. Plant & cell physiology *52*, 983-993.

Kirsch, C., Hahlbrock, K., and Somssich, I.E. (1997). Rapid and transient induction of a parsley microsomal delta 12 fatty acid desaturase mRNA by fungal elicitor. Plant Physiol *115*, 283-289.

Koletzko, B., Baker, S., Cleghorn, G., Neto, U.F., Gopalan, S., Hernell, O., Hock, Q.S., Jirapinyo, P., Lonnerdal, B., Pencharz, P.*, et al.* (2005). Global standard for the composition of infant formula: Recommendations of an ESPGHAN coordinated international expert group. Journal of Pediatric Gastroenterology and Nutrition *41*, 584-599.

Koo, A.J.K., Ohlrogge, J.B., and Pollard, M. (2004). On the export of fatty acids from the chloroplast. Journal of Biological Chemistry *279*, 16101-16110.

Kumagai, M.H., Donson, J., della-Cioppa, G., Harvey, D., Hanley, K., and Grill, L.K. (1995). Cytoplasmic inhibition of carotenoid biosynthesis with virus-derived RNA. Proceedings of the National Academy of Sciences *92*, 1679-1683.

Kunst, L., Taylor, D.C., and Underhill, E.W. (1992). Fatty acid elongation in developing seeds of Arbidopsis thaliana. Plant Physiol Biochem *30*, 425-434.

Lager, I., Lindberg Yilmaz, J., Zhou, X.-R., Jasieniecka, K., Kazachkov, M., Wang, P., Zou, J., Weselake, R., Smith, M.A., Bayon, S.*, et al.* (2013). Plant Acyl-CoA:lysophosphatidylcholine acyltransferases (LPCATs) have different specificities in their forward and reverse reactions. Journal of Biological Chemistry.

Lakatos, L., Szittya, G., Silhavy, D., and Burgyan, J. (2004). Molecular mechanism of RNA silencing suppression mediated by p19 protein of tombusviruses. EMBO J *23*, 876-884.

Lam, P., Zhao, L., McFarlane, H.E., Aiga, M., Lam, V., Hooker, T.S., and Kunst, L. (2012). RDR1 and SGS3, components of RNA-mediated gene silencing, are required for the regulation of cuticular wax biosynthesis in developing inflorescence stems of Arabidopsis. Plant Physiology *159*, 1385-1395.

Law, J.A., and Jacobsen, S.E. (2010). Establishing, maintaining and modifying DNA methylation patterns in plants and animals. Nat Rev Genet *11*, 204-220.

Le, B.H., Cheng, C., Bui, A.Q., Wagmaister, J.A., Henry, K.F., Pelletier, J., Kwong, L., Belmonte, M., Kirkbride, R., Horvath, S.*, et al.* (2010). Global analysis of gene activity during Arabidopsis seed development and identification of seed-specific transcription factors. Proceedings of the National Academy of Sciences *107*, 8063-8070.

Lee, R.C., Feinbaum, R.L., and Ambros, V. (1993). The C. elegans heterochronic gene lin-4 encodes small RNAs with antisense complementarity to lin-14. Cell *75*, 843-854.

Leonard, A.E., Bobik, E.G., Dorado, J., Kroeger, P.E., Chuang, L.T., Thurmond, J.M., Parker-Barnes, J.M., Das, T., Huang, Y.S., and Mukerji, P. (2000). Cloning of a human cDNA encoding a novel enzyme involved in the elongation of long-chain polyunsaturated fatty acids. The Biochemical journal *350 Pt 3*, 765-770.

Li-Beisson, Y., Shorrosh, B., Beisson, F., Andersson, M.X., Arondel, V., Bates, P.D., Baud, S., Bird, D., DeBono, A., Durrett, T.P.*, et al.* (2013). Acyl-Lipid Metabolism. The Arabidopsis Book, e0161.

Lightner, J., James, D.W., Dooner, H.K., and Browse, J. (1994). Altered body morphology is caused by increased stearate levels in a mutant of Arabidopsis. The Plant Journal *6*, 401-412.

Lindbo, J.A., Silva-Rosales, L., Proebsting, W.M., and Dougherty, W.G. (1993). Induction of a highly specific antiviral state in transgenic plants: Implications for regulation of gene expression and virus resistance. Plant Cell *5*, 1749-1759.

Liu, D., Shi, L., Han, C., Yu, J., Li, D., and Zhang, Y. (2012). Validation of reference genes for gene expression studies in virus-infected *Nicotiana benthamiana* using quantitative real-time PCR. PLoS ONE *7*, e46451.

Lombardi, R., Circelli, P., Villani, M.E., Buriani, G., Nardi, L., Coppola, V., Bianco, L., Benvenuto, E., Donini, M., and Marusic, C. (2009). High-level HIV-1 Nef transient expression in Nicotiana benthamiana using the P19 gene silencing suppressor protein of Artichoke Mottled Crinckle Virus. BMC biotechnology *9*, 96.

Maisonneuve, S., Bessoule, J.J., Lessire, R., Delseny, M., and Roscoe, T.J. (2010). Expression of rapeseed microsomal lysophosphatidic acid acyltransferase isozymes enhances seed oil content in Arabidopsis. Plant Physiol *152*, 670-684.

Manavella, P.A., Koenig, D., and Weigel, D. (2012). Plant secondary siRNA production determined by microRNA-duplex structure. Proceedings of the National Academy of Sciences of the United States of America *109*, 2461-2466.

Margis, R., Fusaro, A.F., Smith, N.A., Curtin, S.J., Watson, J.M., Finnegan, E.J., and Waterhouse, P.M. (2006). The evolution and diversification of Dicers in plants. FEBS Lett *580*, 2442-2450.

Marker, S., Le Mouël, A., Meyer, E., and Simon, M. (2010). Distinct RNA-dependent RNA polymerases are required for RNAi triggered by double-stranded RNA versus truncated transgenes in Paramecium tetraurelia. Nucleic Acids Research *38*, 4092-4107.

McConn, M., Hugly, S., Browse, J., and Somerville, C. (1994). A Mutation at the fad8 locus of Arabidopsis identifies a second chloroplast [omega]-3 desaturase. Plant Physiol *106*, 1609-1614.

Mehrshahi, P., Stefano, G., Andaloro, J.M., Brandizzi, F., Froehlich, J.E., and DellaPenna, D. (2013). Transorganellar complementation redefines the biochemical continuity of endoplasmic reticulum and chloroplasts. Proceedings of the National Academy of Sciences *110*, 12126-12131.

Mikkelsen, M.D., Olsen, C.E., and Halkier, B.A. (2010). Production of the cancer-preventive glucoraphanin in tobacco. Molecular plant *3*, 751-759.

Millar, A.A., and Kunst, L. (1997). Very-long-chain fatty acid biosynthesis is controlled through the expression and specificity of the condensing enzyme. The Plant Journal *12*, 121-131.

Miquel, M., and Browse, J. (1992). Arabidopsis mutants deficient in polyunsaturated fatty acid synthesis. Biochemical and genetic characterization of a plant oleoyl-phosphatidylcholine desaturase. Journal of Biological Chemistry *267*, 1502-1509.

Mlotshwa, S., Pruss, G.J., Peragine, A., Endres, M.W., Li, J., Chen, X., Poethig, R.S., Bowman, L.H., and Vance, V. (2008). DICER-LIKE2 plays a primary role in transitive silencing of transgenes in Arabidopsis. PLoS ONE *3*, e1755.

Mongrand, S., Bessoule, J.-J., Cabantous, F., and Cassagne, C. (1998). The C16:3\C18:3 fatty acid balance in photosynthetic tissues from 468 plant species. Phytochemistry *49*, 1049-1064.

Montgomery, T.A., Howell, M.D., Cuperus, J.T., Li, D., Hansen, J.E., Alexander, A.L., Chapman, E.J., Fahlgren, N., Allen, E., and Carrington, J.C. (2008). Specificity of ARGONAUTE7-miR390 Interaction and Dual Functionality in TAS3 Trans-Acting siRNA Formation. Cell *133*, 128-141.

Moss, E.G. (2002). MicroRNAs: Hidden in the genome. Current Biology *12*, R138-R140.

Mourrain, P., Béclin, C., Elmayan, T., Feuerbach, F., Godon, C., Morel, J.-B., Jouette, D., Lacombe, A.-M., Nikic, S., Picault, N*., et al.* (2000). Arabidopsis SGS2 and SGS3 genes are required for posttranscriptional gene silencing and natural virus resistance. Cell *101*, 533-542.

Murashige, T., and Skoog, F. (1962). A revised medium for rapid growth and bio assays with Tobacco tissue cultures. Physiologia Plantarum *15*, 473-497.

Muthan, B., Roston, R.L., Froehlich, J.E., and Benning, C. (2013). Probing Arabidopsis chloroplast diacylglycerol pools by selectively targeting bacterial diacylglycerol kinase to suborganellar membranes. Plant Physiology.

Naim, F., Nakasugi, K., Crowhurst, R.N., Hilario, E., Zwart, A.B., Hellens, R.P., Taylor, J.M., Waterhouse, P.M., and Wood, C.C. (2012). Advanced engineering of lipid metabolism in Nicotiana benthamiana using a draft genome and the V2 viral silencing-suppressor protein. PLoS ONE *7*, e52717.

Nakamura, Y., Koizumi, R., Shui, G., Shimojima, M., Wenk, M.R., Ito, T., and Ohta, H. (2009). Arabidopsis lipins mediate eukaryotic pathway of lipid metabolism and cope critically with phosphate starvation. Proceedings of the National Academy of Sciences *106*, 20978-20983.

Nakasugi, K., Crowhurst, R.N., Bally, J., Wood, C.C., Hellens, R.P., and Waterhouse, P.M. (2013). Transcriptome sequence assembly and analysis of RNA silencing genes of Nicotiana benthamiana. PLoS ONE *8*, e59534.

Napier, J.A. (2007). The production of unusual fatty acids in transgenic plants. Annu Rev Plant Biol *58*, 295 - 319.

Napier, J.A., Michaelson, L.V., and Stobart, A.K. (1999). Plant desaturases: harvesting the fat of the land. Curr Opin Plant Biol *2*, 123-127.

Napoli, C., Lemieux, C., and Jorgensen, R. (1990). Introduction of a chimeric chalcone synthase gene into petunia results in reversible co-suppression of homologous genes in trans. Plant Cell *2*, 279-289.

Navot, N., Pichersky, E., Zeidan, M., Zamir, D., and Czosnek, H. (1991). Tomato yellow leaf curl virus: A whitefly-transmitted geminivirus with a single genomic component. Virology *185*, 151-161.

Needleman, P., Turk, J., Jakschik, B.A., Morrison, A.R., and Lefkowith, J.B. (1986). Arachidonic acid metabolism. Annual review of biochemistry *55*, 69-102.

Nykiforuk, C., Shewmaker, C., Harry, I., Yurchenko, O., Zhang, M., Reed, C., Oinam, G., Zaplachinski, S., Fidantsef, A., Boothe, J.*, et al.* (2012). High level accumulation of gamma linolenic acid (C18:3) in transgenic safflower (*Carthamus tinctorius*) seeds. Transgenic Res *21*, 367-381.

Ohlrogge, J.B., and Browse, J. (1995). Lipid biosynthesis. The Plant Cell Online *7*, 957-970.

Ohlrogge, J.B., Kuhn, D.N., and Stumpf, P.K. (1979). Subcellular localization of acyl carrier protein in leaf protoplasts of Spinacia oleracea. Proceedings of the National Academy of Sciences *76*, 1194-1198.

Okuley, J., Lightner, J., Feldmann, K., Yadav, N., Lark, E., and Browse, J. (1994a). Arabidopsis FAD2 gene encodes the enzyme that is essential for polyunsaturated lipid synthesis. The Plant Cell Online *6*, 147-158.

Okuley, J., Lightner, J., Feldmann, K., Yadav, N., Lark, E., and Browse, J. (1994b). Arabidopsis FAD2 gene encodes the enzyme that is essential for polyunsaturated lipid synthesis. Plant Cell *6*, 147-158.

Palauqui, J.C., Elmayan, T., Pollien, J.M., and Vaucheret, H. (1997). Systemic acquired silencing: transgene-specific post-transcriptional silencing is transmitted by grafting from silenced stocks to non-silenced scions. EMBO J *16*, 4738-4745.

Park, W., Li, J., Song, R., Messing, J., and Chen, X. (2002). CARPEL FACTORY, a Dicer Homolog, and HEN1, a Novel Protein, Act in microRNA Metabolism in Arabidopsis thaliana. Current Biology *12*, 1484-1495.

Parthibane, V., Rajakumari, S., Venkateshwari, V., Iyappan, R., and Rajasekharan, R. (2012). Oleosin is bifunctional enzyme that has both monoacylglycerol acyltransferase and phospholipase activities. Journal of Biological Chemistry *287*, 1946-1954.

Petrie, J.R., Shrestha, P., Belide, S., Mansour, M.P., Liu, Q., Horne, J., Nichols, P.D., and Singh, S.P. (2012a). Transgenic production of arachidonic acid in oilseeds. Transgenic Res *21*, 139-147.

Petrie, J.R., Shrestha, P., Liu, Q., Mansour, M.P., Wood, C.C., Zhou, X.-R., Nichols, P., Green, A., and Singh, S.P. (2010). Rapid expression of transgenes driven by seed-specific constructs in leaf tissue: DHA production. Plant Methods *6*, 8.

Petrie, J.R., Shrestha, P., Zhou, X.-R., Mansour, M.P., Liu, Q., Belide, S., Nichols, P.D., and Singh, S.P. (2012b). Metabolic engineering plant seeds with fish oil-like levels of DHA. PLoS ONE *7*, e49165.

Petrie, J.R., and Singh, S.P. (2011). Expanding the docosahexaenoic acid food web for sustainable production: engineering lower plant pathways into higher plants. AoB plants *2011*, plr011.

Preisig, C.L., and Kuć, J.A. (1988). Metabolism by potato tuber of arachidonic acid, an elicitor of hypersensitive resistance. Physiological and Molecular Plant Pathology *32*, 77-88.

Qi, B., Beaudoin, F., Fraser, T., Stobart, A.K., Napier, J.A., and Lazarus, C.M. (2002). Identification of a cDNA encoding a novel C18-Δ9 polyunsaturated fatty acid-specific elongating activity from the docosahexaenoic acid (DHA)-producing microalga, Isochrysis galbana. FEBS Letters *510*, 159-165.

Qi, B., Fraser, T., Mugford, S., Dobson, G., Sayanova, O., Butler, J., Napier, J.A., Stobart, A.K., and Lazarus, C.M. (2004). Production of very long chain polyunsaturated omega-3 and omega-6 fatty acids in plants. Nat Biotechnol *22*, 739-745.

Qu, F., Ye, X., Hou, G., Sato, S., Clemente, T.E., and Morris, T.J. (2005). RDR6 has a broad-spectrum but temperature-dependent antiviral defense role in Nicotiana benthamiana. Journal of Virology *79*, 15209-15217.

Qu, F., Ye, X., and Morris, T.J. (2008). Arabidopsis DRB4, AGO1, AGO7, and RDR6 participate in a DCL4-initiated antiviral RNA silencing pathway negatively regulated by DCL1. Proceedings of the National Academy of Sciences of the United States of America *105*, 14732-14737.

Ralaimanarivo, A., Gaydou, E., and Bianchini, J.-P. (1982). Fatty acid composition of seed oils from six Adansonia species with particular reference to cyclopropane and cyclopropene acids. Lipids *17*, 1-10.

Robert, S., Singh, S., Zhou, X., Petrie, J., Blackburn, S., Mansour, M., Nichols, P., Liu, Q., and Green, S. (2005). Metabolic engineering of Arabidopsis to produce nutritionally important DHA in seed oil. Funct Plant Biol *32*, 473 - 479.

Roughan, P.G., Holland, R., and Slack, C.R. (1980). The role of chloroplasts and microsomal fractions in polar-lipid synthesis from [1-14C]acetate by cell-free preparations from spinach (Spinacia oleracea) leaves. The Biochemical journal *188*, 17-24.

Roughan, P.G., and Slack, C.R. (1982). Cellular organization of glycerolipid metabolism. Annual Review of Plant Physiology *33*, 97-132.

Routaboul, J.M., Benning, C., Bechtold, N., Caboche, M., and Lepiniec, L. (1999). The TAG1 locus of Arabidopsis encodes for a diacylglycerol acyltransferase. Plant physiology and biochemistry : PPB / Societe francaise de physiologie vegetale *37*, 831-840.

Ruiz-Ferrer, V., and Voinnet, O. (2009). Roles of plant small RNAs in biotic stress responses. Annu Rev Plant Biol *60*, 485-510.

Ruxton, C.H., Reed, S.C., Simpson, M.J., and Millington, K.J. (2004). The health benefits of omega-3 polyunsaturated fatty acids: a review of the evidence. Journal of human nutrition and dietetics : the official journal of the British Dietetic Association *17*, 449-459.

Sakurada, K., Iwase, H., Takatori, T., Nagao, M., Nakajima, M., Niijima, H., Matsuda, Y., and Kobayashi, M. (1999). Identification of cis-9,10-methylenehexadecanoic acid in submitochondrial particles of bovine heart. Biochimica et biophysica acta *1437*, 214-222.

Sato, S., Xing, A., Ye, X., Schweiger, B., Kinney, A., Graef, G., and Clemente, T. (2004). Production of γ-linolenic acid and stearidonic acid in seeds of marker-free transgenic Soybean 11. Crop Sci *44*, 646-652.

Schiebel, W., Haas, B., Marinković, S., Klanner, A., and Sänger, H.L. (1993). RNA-directed RNA polymerase from tomato leaves. II. Catalytic in vitro properties. Journal of Biological Chemistry *268*, 11858-11867.

Schott, G., Mari-Ordonez, A., Himber, C., Alioua, A., Voinnet, O., and Dunoyer, P. (2012). Differential effects of viral silencing suppressors on siRNA and miRNA loading support the existence of two distinct cellular pools of ARGONAUTE1. EMBO J *31*, 2553-2565.

Schubert, D., Lechtenberg, B., Forsbach, A., Gils, M., Bahadur, S., and Schmidt, R. (2004). Silencing in Arabidopsis T-DNA transformants: The predominant role of a gene-specific RNA sensing mechanism versus position effects. Plant Cell *16*, 2561-2572.

Schwach, F., Vaistij, F.E., Jones, L., and Baulcombe, D.C. (2005). An RNA-dependent RNA polymerase prevents meristem invasion by potato virus X and is required for the activity but not the production of a systemic silencing signal. Plant Physiol *138*, 1842-1852.

Shanklin, J., and Cahoon, E.B. (1998). Desaturation and related modifications of fatty acids. Annual Review of Plant Physiology and Plant Molecular Biology *49*, 611-641.

Sharma, P., and Ikegami, M. (2010). Tomato leaf curl Java virus V2 protein is a determinant of virulence, hypersensitive response and suppression of posttranscriptional gene silencing. Virology *396*, 85-93.

Shockey, J.M., Gidda, S.K., Chapital, D.C., Kuan, J.-C., Dhanoa, P.K., Bland, J.M., Rothstein, S.J., Mullen, R.T., and Dyer, J.M. (2006). Tung tree DGAT1 and DGAT2 have nonredundant functions in triacylglycerol biosynthesis and are localized to different subdomains of the endoplasmic reticulum. The Plant Cell Online *18*, 2294-2313.

Sijen, T., Fleenor, J., Simmer, F., Thijssen, K.L., Parrish, S., Timmons, L., Plasterk, R.H., and Fire, A. (2001). On the role of RNA amplification in dsRNA-triggered gene silencing. Cell *107*, 465-476.

Sijen, T., Wellink, J., Hiriart, J.B., and Van Kammen, A. (1996). RNA-mediated virus resistance: Role of repeated transgenes and delineation of targeted regions. The Plant Cell Online *8*, 2277-2294.

Silhavy, D., Molnar, A., Lucioli, A., Szittya, G., Hornyik, C., Tavazza, M., and Burgyan, J. (2002). A viral protein suppresses RNA silencing and binds silencing-generated, 21- to 25-nucleotide double-stranded RNAs. EMBO J *21*, 3070-3080.

Siloto, R.M.P., Findlay, K., Lopez-Villalobos, A., Yeung, E.C., Nykiforuk, C.L., and Moloney, M.M. (2006). The accumulation of oleosins determines the size of seed oilbodies in arabidopsis. The Plant Cell Online *18*, 1961-1974.

Slack, C.R., Roughan, P.G., and Balasingham, N. (1978). Labelling of glycerolipids in the cotyledons of developing oilseeds by [1-14C] acetate and [2-3H] glycerol. The Biochemical journal *170*, 421-433.

Sledzinski, T., Mika, A., Stepnowski, P., Proczko-Markuszewska, M., Kaska, L., Stefaniak, T., and Swierczynski, J. (2013). Identification of cyclopropaneoctanoic Acid 2-hexyl in human adipose tissue and serum. Lipids *48*, 839-848.

Smith, C.J.S., Watson, C.F., Bird, C.R., Ray, J., Schuch, W., and Grierson, D. (1990). Expression of a truncated tomato polygalacturonase gene inhibits expression of the endogenous gene in transgenic plants. Molec Gen Genet *224*, 477-481.

Smith, L.M., Pontes, O., Searle, I., Yelina, N., Yousafzai, F.K., Herr, A.J., Pikaard, C.S., and Baulcombe, D.C. (2007). An SNF2 protein associated with nuclear RNA silencing and the spread of a silencing signal between cells in Arabidopsis. Plant Cell *19*, 1507-1521.

Smith, M.A., Jonsson, L., Stymne, S., and Stobart, K. (1992). Evidence for cytochrome b5 as an electron donor in ricinoleic acid biosynthesis in microsomal preparations from developing castor bean (Ricinus communis L.). Biochem J *287*, 141-144.

Spitzer, M., Wildenhain, J., Rappsilber, J., and Tyers, M. (2014). BoxPlotR: a web tool for generation of box plots. Nat Meth *11*, 2.

Spychalla, J.P., Kinney, A.J., and Browse, J. (1997). Identification of an animal omega-3 fatty acid desaturase by heterologous expression in Arabidopsis. Proceedings of the National Academy of Sciences of the United States of America *94*, 1142-1147.

Stalberg, K., Ellerstrom, M., Josefsson, L.G., and Rask, L. (1993). Deletion analysis of a 2S seed storage protein promoter of Brassica napus in transgenic tobacco. Plant Molecular Biology *23*, 671-683.

Stoutjesdijk, P.A., Singh, S.P., Liu, Q., Hurlstone, C.J., Waterhouse, P.A., and Green, A.G. (2002). hpRNA-mediated targeting of the Arabidopsis FAD2 gene gives highly efficient and stable silencing. Plant Physiology *129*, 1723-1731.

Stymne, S., and Stobart, A.K. (1984). Evidence for the reversibility of the acyl-CoA-lysophosphatidylcholine acyltransferase in microsomal preparations from developing safflower (Cathamus Tinctorius L) cotyledons and rat-liver. Biochem J *223*, 305-314.

Taylor, F.R., and Cronan, J.E.J. (1979). Cyclopropane fatty acid synthase of Escherichia coli. Stabilization, purification, and interaction with phospholipid vesicles. Biochemistry *18*, 3292-3300.

Thomas, C.L., Jones, L., Baulcombe, D.C., and Maule, A.J. (2001). Size constraints for targeting post-transcriptional gene silencing and for RNA-directed methylation in Nicotiana benthamiana using a potato virus X vector. Plant J *25*, 417-425.

Tzen, J., Cao, Y., Laurent, P., Ratnayake, C., and Huang, A. (1993). Lipids, proteins, and structure of seed oil bodies from diverse species. Plant Physiol *101*, 267-276.

Vaistij, F.E., Jones, L., and Baulcombe, D.C. (2002). Spreading of RNA targeting and DNA methylation in RNA silencing requires transcription of the target gene and a putative RNA-dependent RNA polymerase. Plant Cell *14*, 857-867.

Van Blokland, R., Van der Geest, N., Mol, J.N.M., and Kooter, J.M. (1994). Transgene-mediated suppression of chalcone synthase expression in Petunia hybrida results from an increase in RNA turnover. The Plant Journal *6*, 861-877.

van der Krol, A.R., Mur, L.A., Beld, M., Mol, J.N., and Stuitje, A.R. (1990). Flavonoid genes in petunia: addition of a limited number of gene copies may lead to a suppression of gene expression. The Plant Cell Online *2*, 291-299.

van Herpen, T.W.J.M., Cankar, K., Nogueira, M., Bosch, D., Bouwmeester, H.J., and Beekwilder, J. (2010). *Nicotiana benthamiana* as a production platform for artemisinin precursors. PLoS ONE *5*, e14222.

van Wezel, R., Dong, X., Liu, H., Tien, P., Stanley, J., and Hong, Y. (2002). Mutation of three cysteine residues in Tomato yellow leaf curl virus-China C2 protein causes dysfunction in pathogenesis and posttranscriptional gene silencing suppression. Molecular Plant-Microbe Interactions *15*, 203-208.

Vanhercke, T., Wood, C.C., Stymne, S., Singh, S.P., and Green, A.G. (2013). Metabolic engineering of plant oils and waxes for use as industrial feedstocks. Plant Biotechnology Journal *11*, 197-210.

Vargason, J.M., Szittya, G., Burgyán, J., and Hall, T.M.T. (2003). Size selective recognition of siRNA by an RNA silencing suppressor. Cell *115*, 799-811.

Vaucheret, H. (2005). MicroRNA-dependent trans-acting siRNA production. Sci STKE *2005*, pe43-.

Vaucheret, H. (2006). Post-transcriptional small RNA pathways in plants: mechanisms and regulations. Genes & Development *20*, 759-771.

Vaucheret, H. (2008). Plant ARGONAUTES. Trends in plant science *13*, 350-358.

Vaucheret, H., Béclin, C., Elmayan, T., Feuerbach, F., Godon, C., Morel, J.-B., Mourrain, P., Palauqui, J.-C., and Vernhettes, S. (1998). Transgene-induced gene silencing in plants. The Plant Journal *16*, 651-659.

Vaucheret, H., Palauqui, J.-C., Elmayan, T., and Moffatt, B. (1995). Molecular and genetic analysis of nitrite reductase co-suppression in transgenic tobacco plants. Molec Gen Genet *248*, 311-317.

Vazquez, F., Vaucheret, H., Rajagopalan, R., Lepers, C., Gasciolli, V., Mallory, A.C., Hilbert, J.-L., Bartel, D.P., and Crété, P. (2004). Endogenous trans-Acting siRNAs Regulate the Accumulation of Arabidopsis mRNAs. Molecular Cell *16*, 69-79.

Verlaan, M.G., Hutton, S.F., Ibrahem, R.M., Kormelink, R., Visser, R.G.F., Scott, J.W., Edwards, J.D., and Bai, Y. (2013). The Tomato yellow leaf curl virus resistance genes are allelic and code for DFDGD-class RNA–dependent RNA polymerases. PLoS Genetics *9*, e1003399.

Vickery, J.R. (1980). The fatty acid composition of seed oils from ten plant families with particular reference to cyclopropene and dihydrosterculic acids. J Am Oil Chem Soc *57*, 87-91.

Vickery, J.R., Whitfield, F.B., Ford, G.L., and Kennett, B.H. (1984). The fatty acid composition of gymnospermae seed and leaf oils. J Am Oil Chem Soc *61*, 573-575.

Voinnet, O. (2009). Origin, biogenesis, and activity of plant microRNAs. Cell *136*, 669-687.

Voinnet, O., and Baulcombe, D.C. (1997). Systemic signalling in gene silencing. Nature *389*, 553.

Voinnet, O., Rivas, S., Mestre, P., and Baulcombe, D. (2003). An enhanced transient expression system in plants based on suppression of gene silencing by the p19 protein of tomato bushy stunt virus. The Plant Journal *33*, 949-956.

Wallis, J.G., and Browse, J. (1999). The Δ8-desaturase of Euglena gracilis: An alternate pathway for synthesis of 20-carbon polyunsaturated fatty acids. Archives for Biochemistry and Biophysics *365*, 307-316.

Wallis, J.G., and Browse, J. (2002). Mutants of Arabidopsis reveal many roles for membrane lipids. Progress in Lipid Research *41*, 254-278.

Wang, A.Y., Grogan, D.W., and Cronan, J.E., Jr. (1992). Cyclopropane fatty acid synthase of Escherichia coli: deduced amino acid sequence, purification, and studies of the enzyme active site. Biochemistry *31*, 11020-11028.

Wang, L.P., Shen, W.Y., Kazachkov, M., Chen, G.Q., Chen, Q.L., Carlsson, A.S., Stymne, S., Weselake, R.J., and Zou, J.T. (2012). Metabolic interactions between the Lands Cycle and the Kennedy Pathway of gycerolipid snthesis in Arabidopsis dveloping seeds. Plant Cell *24*, 4652-4669.

Wang, X.-B., Jovel, J., Udomporn, P., Wang, Y., Wu, Q., Li, W.-X., Gasciolli, V., Vaucheret, H., and Ding, S.-W. (2011). The 21-nucleotide, but not 22-nucleotide, viral secondary small interfering RNAs direct potent antiviral defense by two cooperative argonautes in *Arabidopsis thaliana*. The Plant Cell Online *23*, 1625-1638.

Wang, X.-B., Wu, Q., Ito, T., Cillo, F., Li, W.-X., Chen, X., Yu, J.-L., and Ding, S.-W. (2010). RNAi-mediated viral immunity requires amplification of virus-derived siRNAs in Arabidopsis thaliana. Proceedings of the National Academy of Sciences *107*, 484-489.

Wang, Z., and Benning, C. (2012). Chloroplast lipid synthesis and lipid trafficking through ER-plastid membrane contact sites. Biochem Soc Trans *40*, 457-463.

Wartig, L., Kheyr-Pour, A., Noris, E., De Kouchkovsky, F.ß., Jouanneau, F.ß., Gronenborn, B., and Jupin, I. (1997). Genetic analysis of the monopartite Tomato yellow leaf curl geminivirus: Roles of V1, V2, and C2 ORFs in viral pathogenesis. Virology *228*, 132-140.

Waterhouse, P.M., Graham, M.W., and Wang, M.-B. (1998). Virus resistance and gene silencing in plants can be induced by simultaneous expression of sense and antisense RNA. Proceedings of the National Academy of Sciences *95*, 13959-13964.

Wesley, S.V., Helliwell, C.A., Smith, N.A., Wang, M., Rouse, D.T., Liu, Q., Gooding, P.S., Singh, S.P., Abbott, D., Stoutjesdijk, P.A*., et al.* (2001). Construct design for efficient, effective and high-throughput gene silencing in plants. The Plant Journal *27*, 581-590.

Williams, J.P., Imperial, V., Khan, M.U., and Hodson, J.N. (2000). The role of phosphatidylcholine in fatty acid exchange and desaturation in Brassica napus L. leaves. The Biochemical journal *349*, 127-133.

Winichayakul, S., Scott, R.W., Roldan, M., Hatier, J.H., Livingston, S., Cookson, R., Curran, A.C., and Roberts, N.J. (2013). In vivo packaging of triacylglycerols enhances Arabidopsis leaf biomass and energy density. Plant Physiol *162*, 626-639.

Wood, C.C., Petrie, J.R., Shrestha, P., Mansour, M.P., Nichols, P.D., Green, A.G., and Singh, S.P. (2009). A leaf-based assay using interchangeable design principles to rapidly assemble multistep recombinant pathways. Plant Biotechnology Journal *7*, 914-924.

Wood, C.C., Robertson, M., Tanner, G., Peacock, W.J., Dennis, E.S., and Helliwell, C.A. (2006). The Arabidopsis thaliana vernalization response requires a polycomb-like protein complex that also includes VERNALIZATION INSENSITIVE 3. Proceedings of the National Academy of Sciences *103*, 14631-14636.

Worley, C., Ling, R., and Callis, J. (1998). Engineering in vivo instability of firefly luciferase and Escherichia coli β-glucuronidase in higher plants using recognition elements from the ubiquitin pathway. Plant Molecular Biology *37*, 337-347.

Wu, G., Truksa, M., Datla, N., Vrinten, P., Bauer, J., Zank, T., Cirpus, P., Heinz, E., and Qui, X. (2005). Stepwise engineering to produce high yields of very long-chain polyunsaturated fatty acids in plants. Nat Biotechnol *23*, 1013 - 1017.

Xu, C., Fan, J., Cornish, A.J., and Benning, C. (2008). Lipid trafficking between the endoplasmic reticulum and the plastid in Arabidopsis requires the extraplastidic TGD4 protein. The Plant Cell Online *20*, 2190-2204.

Xu, C., Fan, J., Froehlich, J.E., Awai, K., and Benning, C. (2005). Mutation of the TGD1 chloroplast envelope protein affects phosphatidate metabolism in Arabidopsis. The Plant Cell *17*, 3094-3110.

Yang, M., Zheng, G., Zhang, F., and Xu, Y. (2006a). FAD2-silencing has pleiotropic effect on polar lipids of leaves and varied effect in different organs of transgenic tobacco. Plant Science *170*, 170-177.

Yang, S.J., Carter, S.A., Cole, A.B., Cheng, N.H., and Nelson, R.S. (2004). A natural variant of a host RNA-dependent RNA polymerase is associated with increased susceptibility to viruses by Nicotiana benthamiana. Proceedings of the National Academy of Sciences of the United States of America *101*, 6297-6302.

Yang, Z., Ebright, Y.W., Yu, B., and Chen, X. (2006b). HEN1 recognizes 21–24 nt small RNA duplexes and deposits a methyl group onto the 2′ OH of the 3′ terminal nucleotide. Nucleic Acids Research *34*, 667-675.

Ye, K., Malinina, L., and Patel, D.J. (2003). Recognition of small interfering RNA by a viral suppressor of RNA silencing. Nature *426*, 874-878.

Ying, X.-B., Dong, L., Zhu, H., Duan, C.-G., Du, Q.-S., Lv, D.-Q., Fang, Y.-Y., Garcia, J.A., Fang, R.-X., and Guo, H.-S. (2010). RNA-dependent RNA polymerase 1 from *Nicotiana tabacum* suppresses RNA silencing and enhances viral infection in *Nicotiana benthamiana*. The Plant Cell Online *22*, 1358-1372.

Yoshikawa, M., Iki, T., Tsutsui, Y., Miyashita, K., Poethig, R.S., Habu, Y., and Ishikawa, M. (2013). 3' fragment of miR173-programmed RISC-cleaved RNA is protected from degradation in a complex with RISC and SGS3. Proceedings of the National Academy of Sciences of the United States of America *110*, 4117-4122.

Yu, B., Yang, Z., Li, J., Minakhina, S., Yang, M., Padgett, R.W., Steward, R., and Chen, X. (2005). Methylation as a crucial step in plant microRNA biogenesis. Science *307*, 932-935.

Yu, X.-H., Rawat, R., and Shanklin, J. (2011). Characterization and analysis of the cotton cyclopropane fatty acid synthase family and their contribution to cyclopropane fatty acid synthesis. BMC Plant Biology *11*, 97.

Zamore, P.D., Tuschl, T., Sharp, P.A., and Bartel, D.P. (2000). RNAi: Double-stranded RNA directs the ATP-dependent cleavage of mRNA at 21 to 23 nucleotide intervals. Cell *101*, 25-33.

Zhang, J., Liu, H., Sun, J., Li, B., Zhu, Q., Chen, S., and Zhang, H. (2012). Arabidopsis fatty acid desaturase FAD2 is required for salt tolerance during seed germination and early seedling growth. PLoS One *7*, e30355.

Zhao, D., and Song, G.-q. High-throughput sequencing as an effective approach in profiling small RNAs derived from a hairpin RNA expression vector in woody plants. Plant Science.

Zhou, X., Singh, S., Liu, Q., and Green, A. (2006). Combined transgenic expression of Δ12-desaturase and Δ12-epoxygenase in high linoleic acid seeds leads to increased accumulation of vernolic acid. Functional Plant Biology *33*, 585-592.

Zrachya, A., Glick, E., Levy, Y., Arazi, T., Citovsky, V., and Gafni, Y. (2007). Suppressor of RNA silencing encoded by Tomato yellow leaf curl virus-Israel. Virology *358*, 159-165.